RADON AS A TOOL IN GEOPHYSICAL RESEARCH

Asta Gregorič

Doctoral Dissertation
Jožef Stefan International Postgraduate School
Ljubljana, Slovenia, March 2013

Evaluation Board:

Prof. Dr. Ivan Kobal, Chairman, Jožef Stefan Institute, Jamova cesta 39, 1000 Ljubljana, retired

Prof. Dr. Aleksander Zidanšek, Member, Jožef Stefan International Postgraduate School, Jamova cesta 39, 1000 Ljubljana

Assist. Prof. Dr. Boris Zmazek, Member, Gimnazija Ptuj, Volkmerjeva cesta 15, 2250 Ptuj

Prof. Dr. Sašo Džeroski, Member, Jožef Stefan Institute, Jamova cesta 39, 1000 Ljubljana

MEDNARODNA PODIPLOMSKA ŠOLA JOŽEFA STEFANA
JOŽEF STEFAN INTERNATIONAL POSTGRADUATE SCHOOL

Asta Gregorič

RADON AS A TOOL IN GEOPHYSICAL RESEARCH

Doctoral Dissertation

RADON KOT ORODJE V GEOFIZIKALNIH RAZISKAVAH

Doktorska disertacija

Supervisor: Assoc. Prof. Dr. Janja Vaupotič

Ljubljana, Slovenia, March 2013

Index

Abstract

Radon (^{222}Rn, half-life 3.82 days) is a natural radioactive noble gas which originates from the radioactive decay of radium (^{226}Ra) in the Earth's crust. It is a known hazard to humans, due to its radioactivity. Moreover, radon can also be used as a versatile tool in geophysical research. In order to use radon as a reliable tracer for different geophysical processes, good knowledge of its transport mechanisms and about the parameters influencing its exhalation to the atmosphere is of special importance.

In this doctoral thesis, radon transport characteristics in different environments and spatial and temporal variations of radon levels are presented and discussed. The use of radon as an earthquake precursor is highlighted and special attention is devoted to the effects of hydrometeorological parameters on radon concentration in soil gas and to methods for identifying anomalies in radon concentration caused by seismic activity.

The spatial distribution of radon levels in soil gas was studied in the area of the Ravne fault and on a fly ash pile. The obtained results showed high spatial variability, which was (within the same lithological type) mainly controlled by various levels of rock and soil permeability. Radon concentrations and radon exhalation rates, measured at five profiles perpendicular and parallel to the Ravne fault, were in the range of 0.9–32.9 kBq m^{-3} and 1.1–41.9 mBq m^{-2} s^{-1}, respectively. The concentration of radon in fly ash was in the range of 0.3–46.9 kBq m^{-3}. The radon exhalation rate was 24 mBq m^{-2} s^{-1} on the part of the pile covered with grass and 37 mBq m^{-2} s^{-1} on the part with trees and bushes.

The temporal fluctuation of radon levels in connection to seismic activity was studied in the thermal waters at Bled and Hotavlje. Several anomalies were identified which might have been caused by geophysical processes preceding earthquakes. Furthermore, different responses of radon fluctuation to seismic activity were observed at these two measurement locations, which indicates a strong dependence on the geological characteristics of the aquifer. The average radon concentration was 10.5 ± 2.1 kBq m^{-3} at Bled (October 2005 to September 2007) and 197 ± 121 kBq m^{-3}at Hotavlje (October 2005 to June 2008).

Four different approaches for differentiating between radon anomalies caused by seismic activity and those caused solely by hydrometeorological parameters were compared in order to determine their efficiency. Among these, machine learning methods were shown to have a great advantage and potential.

Since karst caves represent a boundary layer between the Earth's crust and the atmosphere, they are often used for scientific research. The temporal and spatial variability of radon concentration and its transport characteristics were studied on the basis of continuous measurements of radon concentration at four locations in Postojna Cave, namely Lepe Jame (Beautiful Caves), the lowest point, Velika Gora (Great Mountain) and Pisani Rov (Gaily Coloured Corridor). Special attention was devoted to the use of radon as a tracer for cave ventilation. Radon concentrations measured at three measurement locations in the tourist part of Postojna Cave (Lepe Jame, the lowest point and Velika Gora) were in the range of 0.2–1 kBq m^{-3} and 3–10 kBq m^{-3}, in winter and summer, respectively. On the other hand, significantly higher radon levels were observed in the dead-end passage Pisani Rov, with radon levels in summer reaching up to

45 kBq m^{-3}, comparable to the highest concentrations measured in karst caves worldwide. The most important parameter governing ventilation and thus radon levels in the cave was found to be the outside air temperature. Two major ventilation regimes were identified, namely a summer and a winter one. A model for predicting radon concentration on the basis of outside air temperature was developed for the Velika Gora measurement location. Besides the temperature gradients between the cave and the outside air, an important influence on the spatial distribution of radon levels was found to be the geomorphology of cave passages, as well as the spatial variability of radon exhalation from rock surfaces and cave sediments.

Povzetek

Radon (^{222}Rn, razpolovni čas 3,82 dni) je naraven radioaktiven žlahten plin, ki nastaja z radioaktivnim razpadom iz radija (^{226}Ra) v zemeljski skorji. Poleg škodljivega vpliva sevanja na zdravje ljudi lahko radon uporabljamo kot orodje v geofizikalnih raziskavah. Pri uporabi radona kot sledila različnih geofizikalnih procesov je zelo pomembno dobro poznavanje mehanizmov transporta radona in parametrov, ki vplivajo na hitrost izhajanja radona iz zemeljske skorje v ozračje (ekshalacija).

V doktorskem delu sem raziskovala značilnosti transporta radona v različnih okoljih ter prostorske in časovne spremembe koncentracije radona. Predstavila sem uporabo radona kot znanilca potresov s posebnim poudarkom na vplivu hidrometeoroloških dejavnikov na koncentracije radona v talnem zraku in na metodah določanja anomalij v koncentraciji radona, povzročenih s seizmično aktivnostjo.

Prostorsko porazdelitev koncentracije radona v talnem zraku sem študirala na območju Ravenskega preloma in na odlagališču elektrofiltrskega pepela. Dobljeni rezultati odražajo precejšnje prostorsko nihanje koncentracije radona, ki je v okviru določene litološke enote odvisna predvsem od stopnje prepustnosti kamnin in zemljin. V petih profilih, prečno in vzporedno s prelomom, smo izmerili koncentracije radona v območju 0,9–32,9 kBq m^{-3} in hitrost ekshalacije radona v območju 1,1–41,9 mBq m^{-2} s^{-1}. V elektrofiltrskem pepelu smo izmerili koncentracijo radona v območju 0,3–46,9 kBq m^{-3}, hitrost ekshalacije pa 24 mBq m^{-2} s^{-1} na s travo poraščenem delu odlagališča in 37 mBq m^{-2} s^{-1} na delu, kjer odlagališče poraščajo drevesa in grmičevje.

Časovno nihanje koncentracije radona v povezavi s seizmično aktivnostjo sem študirala v termalni vodi na Bledu in v Hotavljah. V časovni vrsti koncentracije radona sem določila anomalije, ki bi lahko bile posledica geofizikalnih procesov, ki spremljajo dogajanja pred potresi. Za obravnavani lokaciji je značilno različno odzivanje koncentracije radona v vodi na potresno aktivnost, kar kaže na močno odvisnost koncentracij od geoloških značilnosti vodonosnika. Na Bledu smo izmerili povprečno koncentracijo radona v termalni vodi 10,5 ± 2,1 kBq m^{-3} (oktober 2005 do september 2007), v Hotavljah pa 197 ± 121 kBq m^{-3} (oktober 2005 do junij 2008).

Predstavila in primerjala sem štiri metode ločevanja pravih anomalij v časovni vrsti koncentracije radona, povzročenih s potresno aktivnostjo od navideznih anomalij, ki so posledica hidrometeoroloških vplivov. Kot zelo učinkovite so se izkazale metode strojnega učenja.

Glede na poseben položaj kraških jam na meji med zemeljsko skorjo in atmosfero so te pogosto predmet znanstvenih raziskav. Na osnovi kontinuirnih meritev koncentracije radona, na štirih mestih v Postojnski jami (Lepe jame, najnižja točka, Velika gora in Pisani rov) sem študirala prostorsko porazdelitev in časovne spremembe koncentracije radona v jamskem zraku. Posebno pozornost sem namenila uporabi radona kot sledila za prezračevanje jame. Na treh merilnih mestih v turističnem delu Postojnske jame so bile koncentracije radona pozimi v območju 0,2–1 kBq m^{-3}, poleti pa v območju 3–10 kBq m^{-3}. Precej višje koncentracije radona smo izmerili v slepem rovu, imenovanem Pisani rov, kjer poleti doseže koncentracija radona vrednosti do 45 kBq m^{-3}, ki so primerljive z najvišjimi izmerjenimi koncentracijami radona v kraških jamah po

svetu. Ugotovila sem, da ima največji vpliv na prezračevanje in posledično koncentracije radona v jami, temperatura zunanjega zraka. Določila sem dva glavna režima prezračevanja in sicer poletni in zimski režim. Za merilno lokacijo Velika gora sem izdelala model za napovedovanje koncentracije radona na osnovi temperature zunanjega zraka. Poleg temperaturnih razlik med zunanjim in jamskim zrakom na prostorsko porazdelitev koncentracij radona v jami pomembno vplivata tudi geomorfologija jamskih rovov in prostorska porazdelitev ekshalacije radona iz jamskih sten in sedimentov.

Abbreviations

A	=	radioisotope activity concentration
C_{out}	=	radon concentration in the outside air
C_{Ra}	=	radium concentration
C_{Rn}	=	radon concentration
C_{Rn}^{a}	=	radon concentration in gas phase
C_{Rn}^{w}	=	radon concentration in water
D	=	"bulk" diffusion coefficient
D_e	=	effective diffusion coefficient
D_m	=	molecular diffusion coefficient
f_{em}	=	emanation fraction
J^{d}	=	radon activity diffusive flux density
J_s^{a}	=	radon activity advective flux density per unit of air-filled pore area of soil
J_s^{d}	=	radon activity diffusive flux density per unit of air-filled pore area of soil
K	=	soil permeability matrix
K_T	=	partition coefficient of radon between water and gas phase
L	=	length of diffusion inside a crystal lattice
m	=	fraction of saturation
masl	=	meters above sea level
M_L	=	local magnitude
M_W	=	moment magnitude
N	=	number concentration of atoms
p	=	total porosity
p_e	=	effective porosity
R	=	recoil distance of radon atom
R	=	correlation coefficient
R^2	=	coefficient of determination
R_D	=	strain radius of an earthquake
RnDP	=	radon decay products
S	=	surface area of the cave gallery
$t_{1/2}$	=	half-life of radioisotope
T_{cave}	=	cave air temperature
T_{out}	=	outside air temperature
V	=	volume of the cave gallery

Φ	=	radon exhalation rate
λ	=	radon decay constant
μ	=	viscosity
v	=	superficial velocity factor
v_c	=	cave ventilation rate
ρ_s	=	density of the soil grains
τ	=	residence time

1 Introduction

The research of natural processes and interactions in the solid Earth and its fluid envelopes is jointed under the common interdisciplinary scientific field of geophysics, which refers to different geological applications as well as the hydrological cycle and fluid dynamics. Geophysics is applied to societal needs, such as mineral resources and their sustainable extraction, geohazard research to reduce the risks posed to human communities, and environmental protection.

Gases in the geosphere, jointed under the common term "geogas", are of special concern from the view of geophysics, as they are able to carry information about geophysical processes from deeper parts of the Earth's crust to the surface, where we are able to monitor their spatial and temporal fluctuations. Therefore, the knowledge of their origin and the influence of different parameters on their transport to the surface is of great importance.

A component of geogas that deserves special attention is radon (^{222}Rn), due to its unique characteristics. Besides its radioactivity, which makes detection much easier, it is also a noble gas and thus chemically inert. The relatively short half-life of radon also makes it a useful tool for investigation of the dynamics of several processes (in the lithosphere, hydrosphere and atmosphere).

In order to properly address the question of radon transport in different environments and its use as a tool in geophysical research, basic physical and chemical characteristics of radon will first be presented. Later on, different processes that influence radon transport will be highlighted and finally the research done in the field of radon as an earthquake precursor and radon in caves will be presented.

1.1 Natural radioactivity and radon

Radioactivity is everywhere in our environment. Ionising radiation can have artificial or natural origins. Naturally occurring radionuclides in the Earth's crust are the major source of external gamma radiation. These are ^{40}K and several members of the ^{232}Th, ^{235}U and ^{238}U natural radioactive decay chains, among which ^{40}K contributes 13.8 %, ^{232}Th 14 % and ^{226}Ra 55.8 % to the worldwide average of the terrestrial gamma dose rate of 60 nGy h^{-1} (UNSCEAR, 2000). In addition, alpha transformation of radium generates three isotopes (originating from three natural decay chains) of radioactive noble gas radon, from which ^{222}Rn (radon) is the most abundant. Their appearance in the ambient air, accompanied by their short-lived decay products, contributes more than half to the effective dose a member of the general public receives from all natural radioactive sources on the worldwide average (UNSCEAR, 2000), and is the second major cause of lung cancer, soon after cigarette smoking (Darby et al., 2005). The concentration of radium as the radon source in soil is one of the crucial datum to estimate radon concentration in soil gas (Jönsson et al., 1999; Kunz et al., 1996), radon potential of the ground on which a building is standing (Friedmann and Gröller, 2010; Kemski et al., 2001; Neznal et al., 1996) and consequently, radon levels in indoor air (Celik et al., 2008; Vaupotič et al., 2002).

The radon hazards do not come primarily from radon itself, but rather from radioactive

products formed in the decay of ^{222}Rn – ^{218}Po (α, half-life $t_{1/2}$ = 3.05 min), ^{214}Pb (β/γ, $t_{1/2}$ = 26.8 min), ^{214}Bi (β/γ, $t_{1/2}$ = 19.7 min) and ^{214}Po (α, $t_{1/2}$ = 164 ns). Radon decay products (RnDP) are also radioactive, but unlike radon, they are atoms of heavy metals and readily attach themselves to aerosols present in the air. The main health problems stem from the inhaling of RnDP, or particles carrying RnDP, and the subsequent loading of the radon decay products in the lung (UNSCEAR, 2000).

1.2 Chemistry and physics of radon

Radon is a unique natural element in being a gas, noble and radioactive in all of its isotopes. Those three properties make it very attractive for environmental and radiation protection studies. The fact of being radioactive allows radon to be measured with accuracy and used as a geophysical tracer for locating buried faults and geological structures, earthquake research, volcanic surveillance and mineral exploration, cave ventilation studies, etc.

^{222}Rn originates in the ^{238}U decay chain and has a half-life of 3.82 days, ^{220}Rn (thoron) is in the ^{232}Th chain with half-life of 55.6 seconds and, ^{219}Rn (actinon) is in the ^{235}U series with its half-life of 3.9 seconds (Figure 1). All are alpha particle emitters. The most important isotope is, by far, ^{222}Rn (hereafter referred as "radon") because its half-life allows it to migrate long enough and travel long distances. The contribution of ^{220}Rn can be relevant in some cases, however ^{219}Rn is largely ignored because of its short half-life and due to very small ^{235}U/^{238}U ratio (Wilkening, 1990).

Radon is a colourless gas with a density of 9.73 kg m^{-3} under standard conditions making it the heaviest gas in nature. The radon atom possesses a stable closed shell electronic configuration which gives it the chemical properties of a noble-gas element. The relatively high solubility of radon in water (230 cm^3 kg^{-1} at 20 °C) accounts for its presence at substantial amounts in certain spring waters (Wilkening, 1990).

1.3 Source of radon – the role of geology

The amounts of radon, thoron and actinon depend primarily upon the concentration of uranium and thorium in the soil and rocks, as long-lived nuclides at the head of each of the natural radioactive decay series. Among them, ^{238}U and ^{232}Th are the most abundant in the Earth's crust.

The immediate radon precursor is radium (^{226}Ra). Radium, with a half-life of 1602 years, is spread widely, particularly in materials which are made from mineral products. The forerunner of radium is uranium (^{238}U), which has a half-life of 4.47×10^9 years (Figure 1). It is present in all types of rocks and soils and therefore in most of the raw materials from which we process final products. The radium content is typically expressed as an activity concentration per unit mass.

The activity concentration of a radioisotope, A, is related to the number concentration of atoms, N, by:

$$A = N\lambda \tag{1}$$

where λ is the radioactive decay constant. The SI unit for activity is the Becquerel (Bq), which for any radioactive element, corresponds to the number of atoms needed to yield a radioactive decay rate of one per second. The radioactive decay constant is related to the half-life, $t_{1/2}$, by:

$$\lambda = \frac{\ln 2}{t_{1/2}} \qquad (2)$$

The radium content in these terms is equivalent to the total production rate of radon in the soil. 1 Bq kg^{-1} of radium content implies a total radon production rate of 1 atom kg^{-1} s^{-1}, corresponding to 0.0076 Bq kg^{-1} h^{-1} for ^{222}Rn.

Because of their particular geologic history (crystallization from magma, metamorphism, weathering), certain types of soil and rock have enhanced concentrations of uranium and, therefore, radium and radon (Table 1). Granite, where uranium is present in accessory minerals, is relatively rich in uranium, whereas basalt is relatively uranium-poor. The average value for rock in Earth's crust is about 36 Bq kg^{-1}. Soils average is about 66 Bq kg^{-1}. Therefore, radon gas is part of our environment and about 80 % of radon in the atmosphere comes from the top layers of ground.

Table 1: *Concentrations of uranium (^{238}U) and thorium (^{232}Th) in rocks and soils* (after Wilkening (1990)).

Rock type		Concentration / Bq kg^{-1} ^{238}U	^{232}Th
Igneous rocks	Basalt	7–10	10–15
	Granite	40	70
Sedimentary rocks	Shale, Sandstone	40	50
	Carbonate rocks	25	8
Continental upper crust (average)		36	44
Soils		66	37

The concentration of the preceding isotopes (^{226}Ra, ^{224}Ra and ^{223}Ra; Figure 1) directly controls the production of radon, thoron and actinon. Radon gas, released to capillaries and pores in the soil and rock, can reach levels of the order of 1000 times that of atmospheric values. The proportion of radon, produced by radium decay that escapes a solid grain or material, is described by the emanation coefficient (Chapter 1.4). Geological soil and subsoil characteristics, like radium and thorium contents of rocks and soils, intergranular and fissure porosity and permeability, location of faults, fracture zones, volcanic pipes, soil gas and ground-water fluxes, control radon activity in soil gas. Concentrations of radon in soil gas vary over many orders of magnitude from place to place and show significant time variations at any given site.

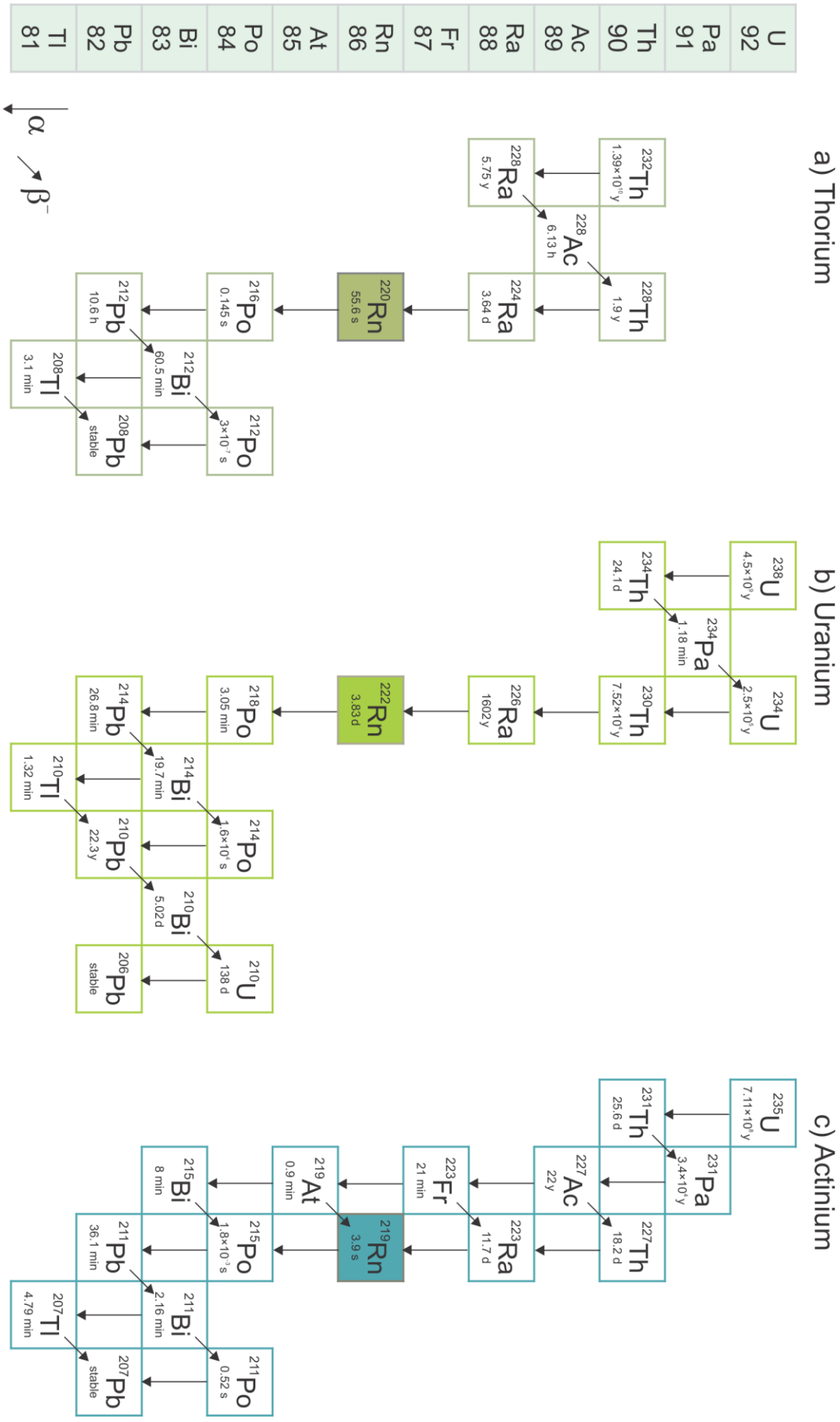

Figure 1: *Radioactive decay chains of* ^{232}Th , ^{238}U *and* ^{235}U.

1.3.1 Physical characteristics of soil

Grain size distribution and porosity

Soils are composed of two fractions. Mineral grains of soils, including small amount of organic matter, form a solid fraction, whereas a void fraction consists of liquid, usually water, and gas. The void fraction is also known as the soil porosity, and the volume fraction of water is called the moisture content. When the moisture content equals to porosity, a soil is saturated.

According to the size distribution of the solid grains, soils can be classified to clay (< 2 μm), silt (2–60 μm), sand (60 μm–2 mm) and gravel (> 2 mm). Clays differ from larger particles, as they are formed by chemical weathering and can, due to their active surfaces and small size, efficiently interact with water and adsorb radioisotopes.

Soil porosities are commonly around 0.5. Clays have higher porosities than sands and poorly sorted soils, having a wide range of grain sizes, may have porosities of 0.3 or less.

Moisture content

The moisture content of a soil can vary over time. Migration of liquid water in the soil pores is controlled by different forces, therefore three components of pore water can be distinguished: "hygroscopic" water is adsorbed on the grain surfaces by electrostatic forces and is particularly important in clays; the "capillary" component of soil water is held in small pores and in a film around the particles by surface tension; "gravitational" water is free to move under the influence of gravity and is the most variable.

Moisture content is a very important factor for radon emanation and migration in soil as discussed in the section 1.4.1 below.

Permeability and width of fractures

Permeability (k) is one of the most important physical characteristics of soils regarding fluid flow and thus radon transport through soil. It is based on the bulk volume flux of a fluid for a given pressure differential, which depends on microscopic properties of soil, such us the size, shape, number and orientation of pores and the moisture content.

The permeability of common soils in the absence of structural pores can span more than 10 orders of magnitude. At the lower end of this range (homogenous clay; $k = 10^{-16}$ m^2), molecular diffusion is the dominant mechanism for radon transport, whereas at the upper end (coarse sand, gravel; $k = 10^{-9}$–10^{-8} m^2), advective flow prevails.

The permeability of soil is dependent on the degree of saturation of the fluid, especially within the large pores. The ration of the effective permeability at a given saturation to the permeability when the saturation is 100 %, is called "relative permeability".

Structural pores, such as fissures and cracks, may significantly influence the effective permeability of soil. Values of crust permeability, as discussed by Manning and Ingebritsen (1999), are of significant level for advective transport (orders of 10^{-20}–10^{-16} m^2). In faulted zones, at a scale of hundreds of meters to kilometers, the permeability is higher than these levels and is much higher at local scale in fractured rocks.

The width of a fracture is the distance, at one given point, between the two rough fractured walls and can be highly variable along the same fracture. Values of fracture aperture at depth vary from 10 to 50 μm for low-permeability argillaceous rocks, to several cm for large fissures in geothermal systems and carbonate (karst) environments (Etiope and Martinelli, 2002). Width of fractures in different types of rocks is presented in Table 2 based on the data from review article by Etiope and Martinelli (2002).

Table 2: *Fracture width in different types of rocks* (after Etiope and Martinelli (2002)).

Type of rock and fault	Fracture width	Comment
- clayey rocks	10–100 μm	
- granite	400–500 μm	
- hydrocarbon-bearing fault planes	order of mm	vertical hydrocarbon migration
- hot dry rock (HDR) geothermal systems	order of mm	vertical hydrocarbon migration
- crystalline bedrock near active faults	order of mm	vertical hydrocarbon migration
- arenaceous rocks	0.2–0.5 mm	Po plain (Italy)
- sandy Quaternary aquifers	0.1–0.2 mm	southern Po plain (Italy)
- Mesozoic carbonates	1–3 mm	over oil reservoirs
- mineral-filled fractures	<50 mm	over oil reservoirs
- granitic basement of the San Andreas Fault zone	>10 mm	at depths of 2000 m
- geothermal systems	1–10 cm	near the surface
- karst	very large joint systems and rock voids, water filled cavernous zones and sinkholes	the largest rock void structures

1.4 Radon emanation properties

The proportion of radon atoms, produced by radium decay that escapes a solid grain or material, is called emanation fraction (f_{em}) (also emanation coefficient or emanation power). During the creation of radon atoms by α-transformation of ^{226}Ra in the Earth's crust, they receive 86 keV recoil energy which enables those being close enough to the grain surface to emanate from the grain into void space, from where they start to migrate through the medium by diffusion and to longer distances by convection/advection, and eventually exhale into the atmosphere and enter the buildings (Etiope and Martinelli, 2002). The recoil distance depends on the density and composition of the material. The range for ^{222}Rn is 20–70 nm in common minerals, 77 nm in water and 53 μm in air (Sakoda et al., 2011). To emanate from a soil or mineral grain into a pore space, the decay must occur within the recoil distance (R) of the grain surface and the radon atom must be ejected in a direction that carries it outward from the solid (Figure 2).

Considering the locations of the end points of the path of the recoiling radon atoms, three fractions of emanation can be distinguished (Nazaroff et al., 1988):

- direct recoil – radon atom is released into a pore space
- indirect recoil – radon atom travels across a pore space and becomes embedded in an adjacent grain and afterwards migrates out of the pocket created by its passage to enter the pore
- diffusion – radon atoms that begin and end their recoil within a single grain, then migrate to the pore through molecular diffusion.

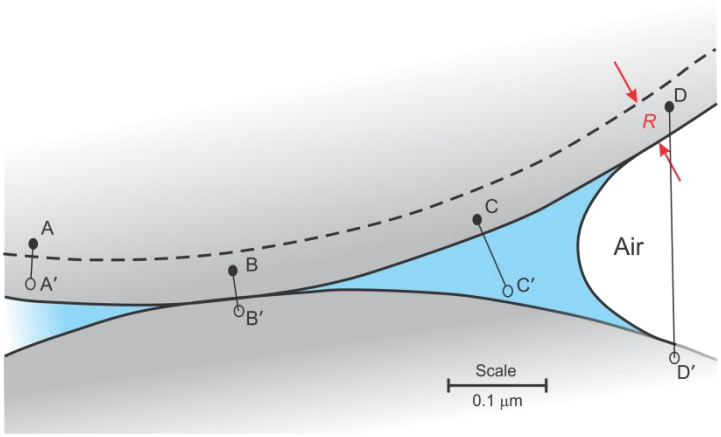

Figure 2: *Schematic representation of emanation process*. A – recoiling radon does not escape the host grain, B – recoil in the adjacent grain, C – recoil into water, leaving radon in pore space, D – recoil into air, leaving radon embedded in adjacent grain. *R* – recoil distance (after Nazaroff (1992)).

The emanation fraction has been comprehensively reviewed by Nazaroff et al. (1992; 1988) and recently by Sakoda et al. (2011). Its values range from 0.05 to 0.7 (UNSCEAR, 2000), with representative values of 0.03 for minerals, 0.13 for rocks, 0.2 for soils, 0.17 for mill tailings and 0.03 for fly ash (Sakoda et al., 2011).

1.4.1 Factors influencing the radon emanation fraction

Large discrepancies have been observed between measured and theoretical emanation fractions, resulting from the effect of radium distribution in soil grains, grain size and shape, moisture content and temperature.

Grain size and radium distribution

Grain size and its shape are two of the important factors that control the soil's emanation fraction because they determine in part how much uranium and radium is near enough to the surface of the soil grain to allow the newly-formed radon to escape into pore spaces. If radium is uniformly distributed throughout the soil or mineral grains and single-grain model is assumed, the radon emanation coefficient is inversely proportional to the grain size (Sakoda et al., 2010a). Expressed in other terms, the radon emanation fraction increases linearly with increasing specific surface area. This model gives the maximum of the radon emanation fraction, because no implantation of radon escaping from the radium-bearing grain into another grain is taken into account (Sakoda et al., 2010a).

Since the calculated emanation fraction was found to be much lower than the measured one, particularly for soil samples, the probability of radon emanation in the case of radium present only on the grain surface was theoretically studied by Morawska and Phillips (1993). The presence of grain coating in which radium is concentrated on the surfaces of soil or mineral grains increases the emanation fraction of soils relative to those in which radium is uniformly distributed throughout the grains. In this case, emanation fraction reaches a constant (saturated) value of 0.5 with increasing grain size. The saturated value is strongly dependent on radium-existing depth from the surface boundary (Sakoda et al., 2010b). More improved models are based on the multiple-grain models incorporating the embedding effect of radon (Sakoda et al., 2010a; Sakoda et al., 2010b).

Clays exhibit high emanation fractions (higher than 0.5) most likely due to radium sorption on clay minerals and iron hydroxides (Miklyaev and Petrova, 2011; Schumann and Gundersen, 1996).

Additional pathways for radon release can be provided by nanopores and pits caused by damage to soil or mineral grains from previous radioactive decays (Sakoda et al., 2011). If a soil or mineral grain is laced with nanopores, the specific surface area of the grain is significantly increased and the radon emanation fraction can be much higher than can be accounted for by escape from the outer surface of the grain alone, particularly for sand-sized and larger grains (Rama and Moore, 1984; Sasaki et al., 2004; Schumann and Gundersen, 1996).

Moisture content

Moisture content has a large impact on the emanation fraction, as demonstrated in several studies (e.g. Barillon et al., 2005; Stranden et al., 1984). First of all, average soil moisture conditions as a function of climate and topography play an important role in soil weathering and development processes, which, in turn, affect the physical and chemical processes of soil and thus radium distribution within soil.

A more direct influence of moisture on radon emanation is that of the thin film of water surrounding soil grains which slows radon atoms, as they are ejected from the soil grain. This effect increases the probability of the radon atom to remain in the pore space rather than embedding in an adjacent soil grain. Therefore, the emanation fraction of completely dehydrated samples (or samples containing only adsorbed water) is low. Subsequent moistening (to moisture content of about 5 % – capillary water) abruptly increases the emanation fraction, becoming insignificant for water contents greater than about 0.3–0.4 of saturation (Bossew, 2003; Miklyaev and Petrova, 2011; Morawska and Phillips, 1993; Nazaroff, 1992; UNSCEAR, 2000). However, regarding the study of

Miklyaev and Petrova (2011) emanation fraction of clays has a stable value, determined by the structure of material at the micro- and even nanolevel, and under natural conditions it is practically independent of changes in the ambient conditions.

Temperature
A rise of temperature has also been found to increase radon emanation fraction (Iskandar et al., 2004; Stranden et al., 1984). Here, the reduction in physical adsorption of radon onto grains and the inner surfaces of grains could play an important role. However, this effect is of minor importance over the range of temperatures common for surface soils.

1.4.2 Radon partitioning in soil pores

Radon atoms in soil are distributed among four states (Nazaroff, 1992):

- bound within the soil grains
- sorbed onto the surface of soil grains (sorbed phase)
- dissolved within water containing in the soil pores (aqueous phase)
- dispersed within the gas contained in the soil pores (gas phase)

Once radon enters the pore space, its partition between the gas and liquid phases depends on the relative volume of water in the pore space and on temperature. Radon partitioning is rapid relative to radon's half-life.

At equilibrium the partitioning of radon between the gas and aqueous phases is described by Henry's law:

$$C_{\mathrm{Rn}}^{\mathrm{w}} = K_{\mathrm{T}} \times C_{\mathrm{Rn}}^{\mathrm{a}} \tag{3}$$

where $C_{\mathrm{Rn}}^{\mathrm{w}}$ represents the radon concentration in water [Bq m^{-3} of water], $C_{\mathrm{Rn}}^{\mathrm{a}}$ radon concentration in gas phase [Bq m^{-3} of pore air], and K_{T} is the Ostwald coefficient – partition coefficient of radon between water and gas, which is a function of temperature (Nazaroff, 1992; UNSCEAR, 2000). The value of K_{T} varies from 0.53 at 0 °C to 0.23 at 25 °C in water and is typically 0.3 at 15 °C (UNSCEAR, 2000).

Taking into account the processes that take control over radon concentration in soil gas, the concentration of radon in the absence of radon transport is described by the following equation (UNSCEAR, 2000):

$$C_{\mathrm{Rn}} = \frac{C_{\mathrm{Ra}} f_{\mathrm{em}} \rho_{\mathrm{s}} (1-p)}{pm((K_{\mathrm{T}}-1)+1)} \tag{4}$$

where C_{Ra} is the concentration of radium in soil [Bq kg^{-1}], f_{em} is the emanation fraction, ρ_{s} is the density of the soil grains [kg m^{-3}], p is the total porosity, m is the fraction of the porosity that is water-filled (fraction of saturation) and K_{T} is the partition coefficient of radon between the air and water phases.

1.5 Radon migration in the Earth's crust

Once radon accumulates in rock pores, either in water or air, it can migrate toward the Earth's surface together with other gases. Gas migration in the Earth's crust is controlled by the relationship between Earth outgassing and geodynamics and it is related to the existence of the gas source itself and preferential routes for degassing, which are in fact zones of enhanced permeability (horizons of more permeable rocks or tectonic discontinuities such as faults and fracture zones) (Etiope and Martinelli, 2002). Driving forces of the fluid flow can change due to tectonic forces (compaction in sedimentary basins, extensional and compressional stresses, etc.) and variations in temperature, pressure, mechanical stresses, chemical reactions and mineral precipitation. All these factors affect fluid transport and thus gas exhalation from the Earth's crust.

Sub-terrestrial fluids can be classified into three main groups according to their reactivity under geothermal conditions, taking into account the main factors controlling the distribution of gases in geothermal discharge (temperature, pressure and the partition coefficients in the distribution of gases between liquids) (Martinelli, 1998):

1. highly active species: H_2O, CO_2, H_2S, NH_3, H_2, N_2
2. CH_4 – upper hydrocarbons are considered to be relatively unaffected by chemical equilibration processes
3. noble gases (He, Rn, etc.) are considered inert or poorly affected by chemical equilibration processes.

Radon ascends towards the surface mainly through cracks or faults on short scale by diffusion (driven by concentration gradients) and, for longer distances, by advection (driven by pressure gradients), dissolved either in water or in carrier gases. Gas movement should be ascribed to the combination of both processes.

1.5.1 Diffusive transport

Diffusion is the process by which a substance is transported from one part of a system to another, in response to variations in its thermodynamic potential. It is the predominant mechanism in interstitial pores and microfractures, where a concentration gradient exists. The molecular diffusion coefficient is a constant of the specific gas and it changes only with temperature, pressure and the physical nature of the substance through which the molecular motion takes place. In the rock pores, this substance is generally water or gas mixture.

The flux density that results from random molecular motion is described by Fick's law, which is for dilute concentration of radon in open air:

$$J^{\mathrm{d}} = -D_{\mathrm{m}} \nabla C_{\mathrm{Rn}} \tag{5}$$

where J^{d} is the radon activity flux density due to diffusion [Bq m^{-2} s^{-1}], D_{m} is the molecular diffusion coefficient [m^2 s^{-1}], C_{Rn} is radon activity concentration [Bq m^{-3}] and ∇ is the concentration gradient [m^{-1}]. The diffusion coefficient of radon in air is 1.2×10^{-5} m^2 s^{-1} and in water 1.37×10^{-9} m^2 s^{-1} (Etiope and Martinelli, 2002; Nazaroff, 1992).

Three different processes can be distinguished (Etiope and Martinelli, 2002):

- "molecular" diffusion of gas in a fluid, D_{m}, which refers to the interaction between diffusing gas and host fluid,
- "interstitional" diffusion of gas in a medium, defined by the effective diffusion coefficient, D_{e}. It describes the diffusion considering the gas molecule motion

through a porous structure,

- "global" diffusion of gas in a medium, defined by the "apparent" (also "true" or "bulk") diffusion coefficient, *D*, which includes the effects of porosity and tortuosity of the medium.

Considering the diffusion of radon through soil pores ("interstitional" diffusion), diffusion coefficient changes due to effects of the solid matrix: the area through which radon may diffuse is reduced and the average path length that radon must traverse is increased. Therefore, effective diffusion coefficient, $D_{e,}$ is used

$$D_e = D_m p_e \tag{6}$$

where p_e [%] corresponds to the effective porosity. The range of D_e in soil is typically 10^{-7}–10^{-5} m^2 s^{-1} (UNSCEAR, 2000). The diffusive flux density of radon activity per unit of air-filled pore area of soil, J_s^d, is written as (Nazaroff, 1992):

$$J_s^d = -D_e \nabla C_{Rn} \tag{7}$$

To describe gas diffusion as a global flux across the bulk of the soil, the "bulk" coefficient *D* must be considered. For soil, an approximate relationship between *D* and D_e exists, which takes into account the soil porosity (p_e):

$$D = D_e p_e \tag{8}$$

Radon may diffuse also inside the crystal lattice. The length of diffusion is defined by

$$L = \left(\frac{D}{\lambda}\right)^{\frac{1}{2}} \tag{9}$$

where: *D* is the diffusion coefficient and λ is the radon decay constant. Migration of radon inside its original crystal due to diffusion is quite limited, as the length of diffusion is 0.7 nm (less than the recoil length) (Martinelli, 1998) and only 5 % of ^{222}Rn is able to reach a distance of 5*L* (*L*–length of diffusion) from its origin.

Experimental results that considered the effect of the volume fraction of water saturation on D_e showed a little effect at low water content (Rogers and Nielson, 1991), since water is predominantly on grain surfaces and in small pores and transport through the larger pores dominates. At high water content, the pores become blocked by water and the diffusion decreases.

Velocity of radon transport in the Earth is quite low ($\leq 10^{-3}$ cm s^{-1}) and radon concentration is reduced by radioactive decay to the background level before even 10 m are traversed (Etiope and Martinelli, 2002; Fleischer, 1981). Therefore, diffusion is important only in capillaries or small-pored rocks.

1.5.2 Advective transport

On the other hand, velocity and space scales of advective movements are much higher than the diffusive ones. Advective transport is driven by pressure gradients, following Darcy's law. Since the forces that drive advective migration act only on gases which occur at sufficient concentrations, a stream of "free gas" is required. The amount of radon itself is, however, too small (orders of 10^{-10} ppm) to form a macroscopic quantity of gas which can react to pressure gradients. Therefore, it must be carried by a macroscopic flow of carrier gases (Kristiansson and Malmqvist, 1982). A gas mixture formed by carrier

gases (e.g. CO_2, CH_4, N_2) and rare gases (e.g. He, Rn) can be referred to as “geogas”.

The "*geogas theory*" was introduced by Kristiansson and Malmqvist (1982) and extensively discussed by Etiope and Martinelli (2002) in order to explain long-distance radon transport and anomalous radon concentrations measured at the ground surface (Mogro-Campero and Fleischer, 1977). This theory includes the following features (Etiope and Martinelli, 2002): microflow of gas, advective multicomponent gas, rapid gas upflow, the bubble flow and matter transport by geogas bubbles.

Advective movement driven by pressure gradient generated by geothermal gradients is called "convection". A normal geothermal gradient of 300 °C km^{-1} is sufficient to activate convection in rocks with a permeability of 10^{-7}–10^{-8} cm for a thickness of a few hundred meters.

For anisotropic permeability of soil, Darcy's law may be written as:

$$v = -\frac{1}{\mu} K \cdot \nabla P \tag{10}$$

where v [m s^{-1}] is the superficial velocity factor (the flow per unit geometrical area defined over a region large relative to individual pores but small relative to the overall dimensions of the soil), μ [Pa s] is the viscosity of the fluid, K is the 3×3 soil permeability matrix and ∇P [Pa m^{-1}] is the pressure gradient. If the intrinsic permeability is constant, permeability matrix is replaced by permeability coefficient k [m^2] (Nazaroff et al., 1988).

Given the superficial air velocity through soil, the advective flux density of radon activity per unit of air-filled pore area, J_s^a [Bq m^{-2} s^{-1}] is expressed by:

$$J_s^a = \frac{C_{Rn} v}{p} \tag{11}$$

Deviations from Darcy's law have been observed at increases of Reynold's number. However, for a typical pressure gradient of 5 Pa m^{-1} and soil permeability less than approximately 10^{-9} m^2 (soils finer than gravel), Darcy's law is expected to hold.

A second assumption is, as in the case of applying Fick's law to porous media, that the pores are large relative to the mean free path of the gas.

1.5.2.1 Advective forms of gas movement

Gas can migrate advectively in several different forms, depending on the condition of the gas-water-rock system. In dry porous or fractured media gas flows through interstitial or fissure space (gas-phase advection), whereas in saturated porous media gas can dissolve and can be then transported in three ways: by groundwater (water-phase advection), it can flow displacing water (gas-phase advection) or it can move in the form of bubble flow by means of buoyancy in aquifers and water-filled fractures. The bubble movement has been theoretically and experimentally recognized as a fast gas migration mechanism governing distribution of carrier and trace gases over wide areas on the Earth’s surface (Etiope and Martinelli, 2002; Vàrhegyi et al., 1992).

1.5.3 The general transport equation

Considering both processes of migration, diffusion and advection, for laminar, steady-state flow through dry, homogeneous and isotropic porous media, the following general transport equation can be written (Etiope and Martinelli, 2002):

$$p_e D_m \frac{d^2 C_{Rn}}{dz^2} - v \frac{dC_{Rn}}{dz} + \alpha - \lambda C_{Rn} = 0 \qquad (12)$$

where α is the generation rate of gas and λC_{Rn} is the rate of removal of radon from the stream due to radioactive decay.

Combining both processes of radon emanation and transport, radon release from soil is maximal, when the soil is moist. In this case small pores are filled with water, thus enhancing radon emanation fraction, whereas radon transport takes place through the larger pores, which are not filled with water. When dry, the soil has greatly reduced emanation fraction and although radon transport is slightly enhanced, the release of radon from soil is decreased. On the other hand, when wet, the permeability and diffusivity are greatly reduced, although radon emanation fraction is slightly higher.

1.6 Geological setting of Slovenia

Slovenia lies on the junction region between the Alps, the Dinarides and the Pannonian basin. This region incorporates the Eastern Alps, Southern Alps, Dinarides, Panonian basin and the Adriatic-Apulian foreland (Placer, 2008; Poljak et al., 2000). The Adriatic-Apulian foreland comprises the larger part of Istria in the south-western corner of Slovenia consisting of rocks of the Adriatic segment of the Adriatic-Dinaric Mesozoic carbonate platform, and the flysch rocks resulting from its degradation (Placer, 2008).

The entire southern part of Slovenia belongs to the Dinarides, characterised by the thrust and nappe structure, consisting mainly of carbonate rocks and sediments resulting from disintegration of the Adriatic-Dinaric carbonate platform: Upper Cretaceous carbonate turbidites, Cretaceous-Palaeocene and Eocene flysch (Placer, 2008). The Southern Alps are palaeogeographically a part of Dinarides. Mesozoic rocks of the Slovenian basin and Upper Triassic rocks of the Julian carbonate platform are exposed within them (Placer, 2008). The Eastern Alps are a geologic-orographic term comprising the complex of Precambrian and Old Palaeozoic high and low grade metamorphic rocks and of Permian and Mesozoic sedimentary rocks north of the Periadriatic fault (Placer, 2008). The Pannonian basin, in the north-eastern part of Slovenia, consists of individual depressions that originated during Palaeogene and Neogene. They are filled with sediments of the Paratethys, deposited on subsided continuations of the Eastern and Southern Alps and Dinarides (Placer, 2008). In addition to the major lithological units described above, also alluvial and glacial deposits, extending along major valleys, have to be considered. In the Ljubljana basin, situated in the central part of Slovenia and in the Krško basin in south-east, the sea and lake sediments prevail.

The most important geologic characteristics influencing radon concentration in soil gas are the lithology and the presence of faults. For this purpose, 8 units have been identified, based on the lithological classification (Figure 3):

- alluvial and glacial deposits (A) represent mainly unconsolidated clastic sediments,
- consolidated clastic sediments (B) are divided into three groups: clastic sediments containing clay (B1), coarse clastic sediments (B2), flysch (B3)
- carbonates (C)
- metamorphic rocks (D)
- sea and lake sediments (E)
- igneous rocks (F)

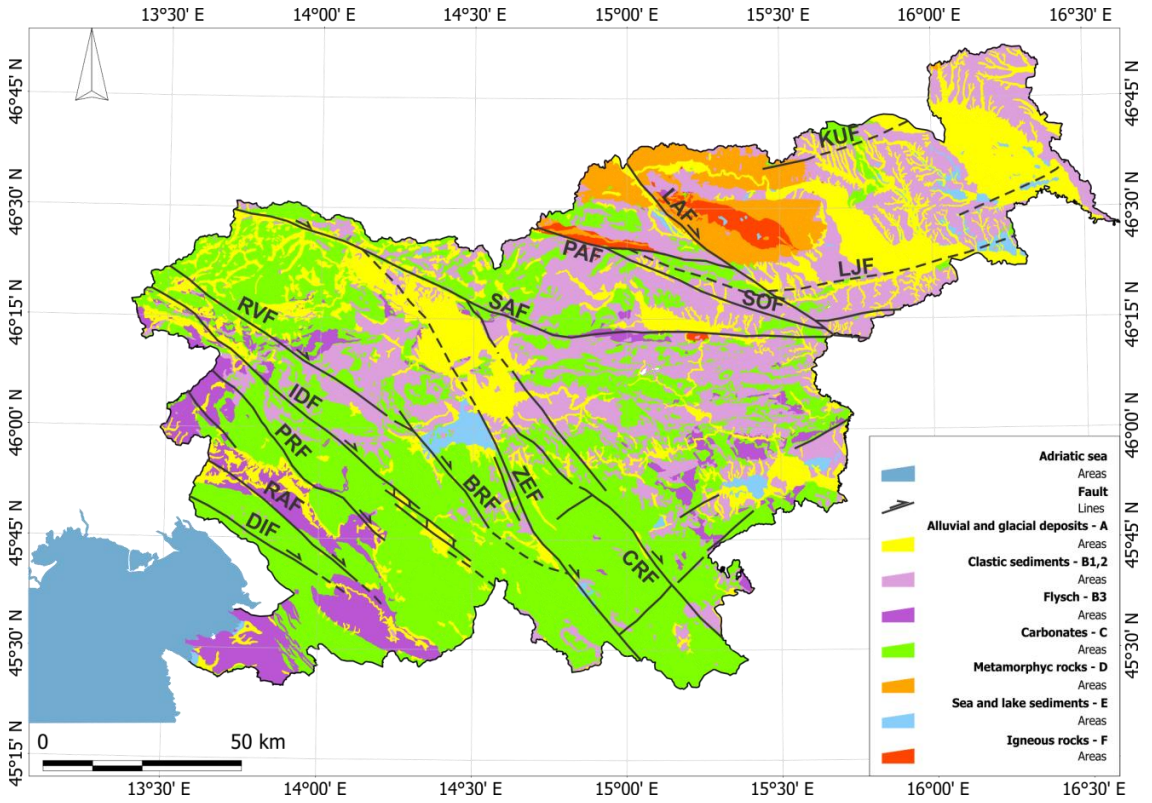

Figure 3: *Lithologic map of Slovenia*. Major faults: RVF – Ravne, IDF – Idrija, PRF – Predjama, RAF – Raša, DIF – Divača, SAF – Sava, BRF – Borovnica, ZEF – Želimlje, CRF – Črnomelj, PAF – Periadriatic, SOF – Šoštanj, LAF – Labot, LJF – Ljutomer, KUF – Kungota (reconstructed from Digital geologic map of Slovenia (GeoZS 1:100000)).

1.6.1 Tectonic and seismic characteristics of Slovenia

Slovenia is tectonically and seismically a highly complex area. The recent structural pattern is a cumulative result of Tethyan evolution, where recent dynamics is determined by the closure of the Tethys and the collision of several lithospheric units. Tisza microplate, Adria microplate and European plate have been amalgamated together during Tertiary time. The seismicity is not concentrated along the primary plate boundary but is rather spread in a broad zone along their deformed rims (Placer, 2008; Poljak et al., 2000; Schmid et al., 2004).

The territory of Slovenia can be considered as one of moderate seismicity. The strongest event known to have happened is the so-called Idrija earthquake of 16 March 1511 (Ribarič, 1979), with the local magnitude (M_L) between 6.8 (Živčić and Cecić, 1998) and 7.2 (Ribarič, 1979). The most pronounced lines of hypocentral concentration are along the Raša (RAF) and the Idrija faults (IDF) in the NW-SE direction (Figure 3) (Poljak et al., 2000).

According to Poljak (2000), the territory of Slovenia can be delineated into five seismogenic areas, i.e. the areas with similar and among themselves differentiable tectonic and seismological characteristics (Figure 4):

1. The Eastern Alps lie north of the PAF and is the least seismically active area. The seismicity is restricted to the upper 20 km of the crust. Recent seismicity is low.
2. The Friuli area occupies the thrust front of the Southern Alps onto the External Dinarides, and is tectonically a highly-deformed area. Its southern border is placed on the thrust front of the Southern Alps towards the External Dinarides. This is the most active zone, with substantial evidence of continuous seismic activity throughout

history. Some of the strongest earthquakes in the entire region are presumed to have occurred inside or at the northern and eastern margins of this region (the so-called 1348 and 1690 Villach events, and the 1511 Idrija event). The most recent seismic sequence occurred in 1976, with the strongest earthquake of $M_L = 6.2$.

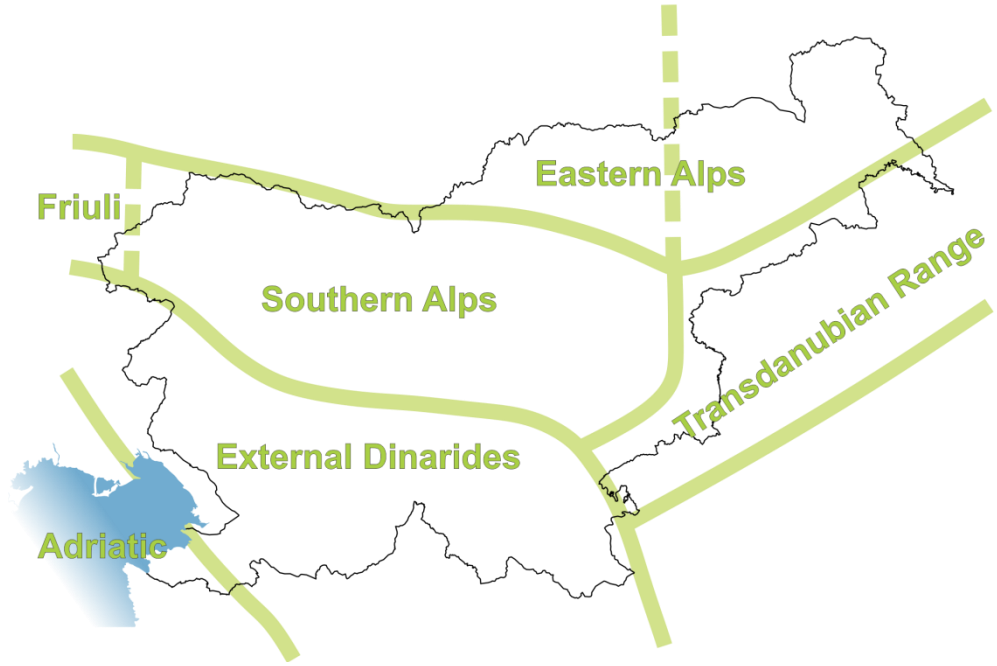

Figure 4: *Seismogenic areas of Slovenia*. (after Poljak et al. (2000)).

3. The Southern Alps in Slovenia encompass the Southern Karavanke, the Julian and the Kamnik-Savinja Alps, and the area of the central Slovenia. The Southern Alps are characterised by regional thrusts from the north to the south and regional faults in a NW-SE direction, with a dextral sense of horizontal displacement. The seismicity of the zone is moderate and rather shallow. The strongest earthquake occurred in 1895 and it damaged the city of Ljubljana ($M_L = 6.1$). The most recent seismic events occurred in the Julian Alps within the Ravne fault zone (RAF, Figure 3 and Figure 12) in 1998 and 2004, with the moment magnitudes (M_W) of 5.6 and 5.2, respectively (Kastelic et al., 2008).
4. The area of Transdanubian Range marks the collision zone between Tisza microplate and the European plate. This area is in Slovenia characterised by folds, faults and thrusts stretching in a NE-SW direction. This zone has been continuously active. The strongest events ($M_L = 6.1$) in 1880 and 1906 happened north of Zagreb.
5. The External Dinarides occupy the southern part of Slovenia. The basic structural characteristic on the External Dinarides is a dense pattern of faults in a NW-SE direction, in addition to the thrusts with the southwestward direction of thrusting. The External Dinarides are characterised by moderate historic and recent seismicity. Hypocenters in the last ten years have been aligned along the Raša (RAF) and Idrija fault (IDF). However the eastern part of the zone has practically no record of historical seismicity.

1.7 Concentration of natural radionuclides in Slovenian soils

Several studies have been conducted regarding natural radioactivity in Slovenia: a systematic radon survey in living and working environment has been conducted in the last two decades (Humar et al., 1992; Vaupotič, 2010). Radium and uranium have been analysed in ground, spring and surface waters (Kobal et al., 1990; Popit et al., 2004; Vaupotič, 2002), and equivalent uranium and equivalent thorium concentrations were determined in soil samples from 30 cm depths at sixty points all over the country (Andjelov and Brajnik, 1996; Brajnik et al., 1992). Recently, ^{40}K, ^{232}Th, ^{238}U, ^{226}Ra and ^{228}Ra were analysed in the *terra rossa* and *eutric cambisol* soil samples from 80 cm depths within regular 25 m × 25 m grid squares at two sites (Vaupotič et al., 2007; Vaupotič et al., 2012).

Table 3: *Basic statistics of natural radionuclides in Slovenian soils*. Values of minimum (min), maximum (max), median, arithmetic mean (AM) and arithmetic standard deviation (ASD) of ^{40}K, ^{232}Th, ^{226}Ra activity concentrations (C_K, C_{Ra}, C_{Ra}) for lithological units: A – alluvial and glacial deposits, B1 – clastic sediments containing clay, B2 – coarse clastic sediments, B3 – flysch, C – carbonates, D – metamorphic rocks, E – sea and lake sediments (Gregorič et al., 2012; Kovács et al., 2013).

	Lith.	Num. of samples	min	max	median	AM	ASD
C_K / Bq kg^{-1}	A	15	256	2383	637	809	579
	B1	18	120	2591	713	889	601
	B2	3	559	832	567	653	155
	B3	6	414	785	602	595	158
	C	24	98	2308	632	801	542
	D	2	713	862	788	788	105
	E	2	303	1098	700	700	562
	total	**70**	**98**	**2591**	**688**	**798**	**519**
C_{Th} / Bq kg^{-1}	A	15	31	126	70	71	26
	B1	18	17	154	85	84	36
	B2	3	65	104	74	81	20
	B3	6	40	68	55	55	12
	C	24	9	169	75	81	40
	D	2	77	83	80	80	4
	E	2	45	66	55	55	14
	total	**70**	**9**	**169**	**74**	**77**	**33**
C_{Ra} / Bq kg^{-1}	A	15	23	102	51	55	23
	B1	18	20	170	51	56	32
	B2	3	42	49	46	46	3
	B3	6	22	42	32	33	8
	C	24	12	269	63	84	62
	D	2	34	43	39	39	6
	E	2	70	75	72	72	3
	total	**70**	**12**	**269**	**48**	**63**	**44**

During a national survey of radon concentration in soil gas (Vaupotič et al., 2008), soil samples were collected in order to upgrade and complete the previous information of natural radionuclides. Soil samples from 70 points were analysed for ^{40}K, ^{232}Th, ^{226}Ra and at 29 points also for ^{234}U and ^{238}U (Gregorič et al., 2012; Kovács et al., 2013). Results are summarised in Table 3 and their distribution with respect to lithological units (Figure 3) also presented as box & whiskers plots in Figure 5. Their spatial distribution is shown in Figure 6. Red areas in Figure 6c, marking areas of radium levels in soil above 200 Bq kg^{-1}, coincide well with the highest radon levels previously found in indoor (Vaupotič, 2010), outdoor air (Vaupotič et al., 2010) and in soil gas (Vaupotič et al., 2008).

Values of ^{40}K on alluvial and glacial deposits (A), on clastic sediments containing clay (B1) and in one sample from carbonate rocks (C) exceed 2000 Bq kg^{-1} (Table 3) and are comparable with the world highest values found in China and Luxemburg (UNSCEAR, 2000). The lowest average concentration of ^{40}K was found on flysch rocks (Table 3, Figure 5a).

The overall arithmetic means of ^{232}Th and ^{226}Ra concentrations was 76.7 ± 33.0 Bq kg^{-1} and 62.7 ± 43.9 Bq kg^{-1}, respectively and are higher than their world averages of 35 Bq kg^{-1} and 30 Bq kg^{-1} (UNSCEAR, 2000). The scattering of concentrations of both ^{232}Th and ^{226}Ra was the widest on carbonates (Table 3, Figure 6b and c), on which also the highest average value for ^{226}Ra was found. Average values for ^{232}Th were the highest on clastic sediments containing clay and on carbonates. The lowest values of all radionuclides were found on flysch rocks.

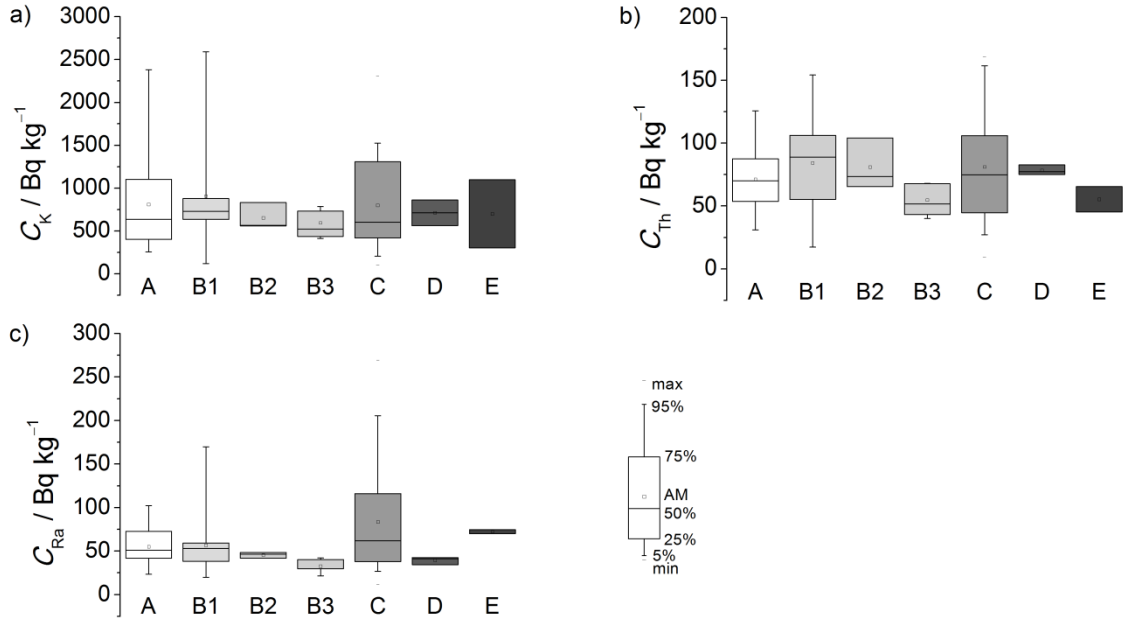

Figure 5: *Box & whiskers diagrams of activity concentration of natural radionuclides in soil at 70 points all over Slovenia with respect to lithology*. a) ^{40}K, b) ^{232}Th, and c) ^{226}Ra. A – alluvial and glacial deposits, B1 – clastic sediments containing clay, B2 – coarse clastic sediments, B3 – flysch, C – carbonates, D – metamorphic rocks, E – sea and lake sediments (Gregorič et al., 2012; Kovács et al., 2013).

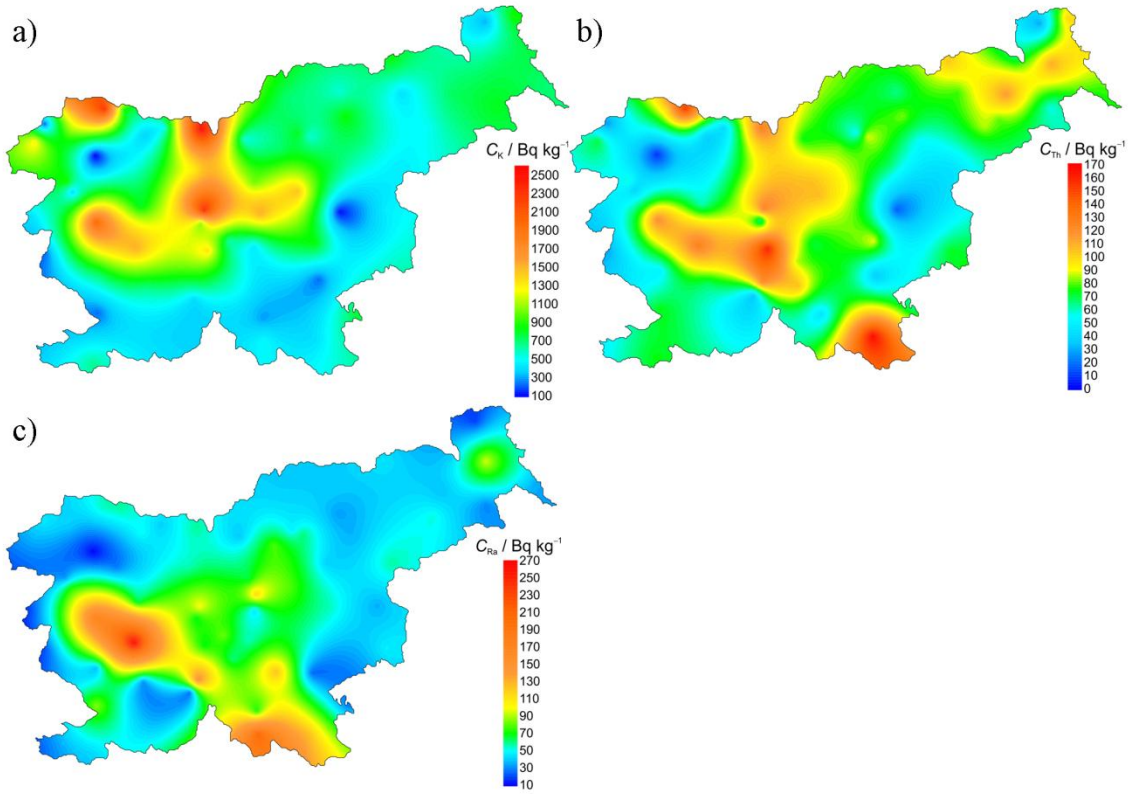

Figure 6: *Spatial distribution of radionuclides in Slovenian soils*. Iso-concentration areas of a) ^{40}K, b) ^{232}Th, and c) ^{226}Ra in soil at 70 points in Slovenia (Gregorič et al., 2012; Kovács et al., 2013).

1.7.1 Radon in soil gas in Slovenia

Soil-gas radon measurements in Slovenia were carried out in summer 2006 and 2007 at seventy locations (Vaupotič et al., 2008) at 80 cm of depth by solid state nuclear track detectors. The results of radon measurements in soil gas are presented in Table 4 and by box & whiskers plot for different lithological units in Figure 7a. Radon levels at alluvial and glacial sediments (A) and clastic sediments containing clay (B1) are similar, with an average value of 37.1 ± 33.2 kBq m^{-3} and 32.4 ± 28.6 kBq m^{-3}, respectively. Only three results were obtained on the unit of coarse clastic sediments (B2), with a slightly higher average of 42.5 ± 27.4 kBq m^{-3}. The lowest radon concentrations were observed on flysch rocks (B3), with an average of 7.5 ± 2.1 kBq m^{-3}, which is consistent with low values of radionuclides on this unit (Figure 5). The highest average value (61.9 ± 55.6 kBq m^{-3}) and the highest scattering were found on carbonate rocks (C). There were only a few locations on metamorphic rocks (D) and sea and lake deposits (E), where relatively low radon concentrations were observed.

An expected positive correlation was found between radon concentration in soil gas and radium concentration in soil (Figure 7b).

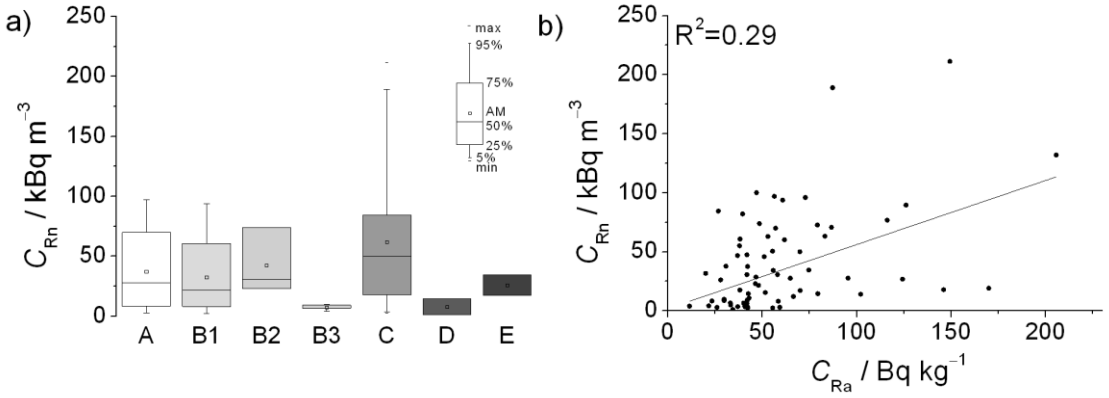

Figure 7: *Radon concentration in soil gas in Slovenia*. a) Box & whisker plot of radon concentration (C_{Rn}) in different lithological units: A – alluvial and glacial deposits, B1 – clastic sediments containing clay, B2 – coarse clastic sediments, B3 – flysch, C – carbonates, D – metamorphic rocks, E – sea and lake sediments (Vaupotič et al., 2008); b) correlation between radon concentration in soil gas (C_{Rn}) and radium concentration in soil (C_{Ra}) (Gregorič et al., 2012; Kovács et al., 2013).

Table 4: *Basic statistics of radon concentration in soil gas in Slovenia.* Values of minimum (min), maximum (max), median, arithmetic mean (AM) and arithmetic standard deviation (ASD) of radon concentration (C_{Rn}) for lithological units: A – alluvial and glacial deposits, B1 – clastic sediments containing clay, B2 – coarse clastic sediments, B3 – flysch, C – carbonates, D – metamorphic rocks, E – sea and lake sediments (Vaupotič et al., 2008).

	Lith.	Num. of samples	min	max	median	AM	ASD
C_{Rn} / kBq m^{-3}	A	15	29	970	277	371	332
	B1	18	24	938	252	324	286
	B2	3	230	739	307	425	274
	B3	6	42	97	78	75	21
	C	24	25	2114	503	619	556
	D	2	11	146	79	79	95
	E	2	172	346	259	259	123
	total	**70**	**11**	**2114**	**251**	**307**	**241**

1.8 Geophysical effects on radon transport

Both mechanisms of radon transport, diffusion and advection, depend on both soil porosity and permeability, which at the same time vary as a function of the stress field (Holub and Brady, 1981). However, as described in the section 1.5.3 above, migration by diffusion is negligible, where a component of advective long-distance transport exists (Etiope and Martinelli, 2002). High permeability of the bedrock and soil in areas of crustal discontinuities, such as fractures and fault zones, promotes intense degassing fluxes, which causes higher soil gas radon concentrations on the ground surface above active fault zones. Although several measurements, experiments and models have been performed, the understanding of the mechanism of radon anomalies and their connection to earthquakes is still inadequate (Chyi et al., 2010; King, 1978; Ramola et al., 1990).

Before an earthquake event stress in the Earth's crust builds up, causing the change in strain field also. Formation of new cracks and pathways under the tectonic stress leads to changes in gas transport and rise of volatiles from the deep layers to the surface. In fact, fluids play a widely recognized role in controlling the strength of crustal fault zones (Hickman et al., 1995). Anomalous changes of radon concentration are closely linked to changes in fluid flow and therefore also to highly permeable areas along fault zones.

Several mechanisms have been proposed, which could explain the relationship between radon anomaly and earthquake. Two models of earthquake precursors are discussed by Mjachkin et al. (1975), with a common principle: at a certain preparation stage a region of many cracks is formed. According to the dilatancy-diffusion model (Martinelli, 1991; Mjachkin et al., 1975), the increase of the tectonic stress causes the extension and opening of favourably oriented cracks in a porous cracked saturated rock. Water flows into the opened cracks, drying the rock near each pore and finally resulting in a decrease of pore pressure in the total earthquake preparation zone. Water from surrounding medium diffuses into the zone. The increased water-rock surface area, due to cracking, leads to an increase in radon transfer from rock matrix to the water. At the end of the diffusion period, the appearance of pore pressure and the increased number of cracks leads to the main rupture.

According to the crack-avalanche model (Mjachkin et al., 1975), the increasing tectonic stress leads to the formation of a cracked focal rock zone, with slowly altering volume and shape. At a certain stage, when the whole focal zone becomes unstable, the cracks quickly concentrate near the fault surface, triggering the main rupture.

An alternate mechanism for earthquake precursory study, based on stress-corrosion theory, was proposed by Anderson and Grew (1977). According to them, the observed radon anomalies are due to slow crack growth controlled by stress corrosion in a rock matrix saturated by ground waters.

King (1978) proposed a compression mechanism for radon release. According to this mechanism, the anomalous high radon release may be due to an increase of crustal compression before an impending earthquake that squeezes out soil gas into the atmosphere at an increasing rate.

Toutain and Baubron (1999) observed that gas transfer within the upper crust is affected by strains less than 10^{-7}, much smaller than those causing earthquakes. According to Dobrovolsky (1979), the radius of the effective precursory manifestation zone depends on the earthquake magnitude and can be calculated using the empirical equation

$$R_{\mathrm{D}} = 10^{0.43 \times M_{\mathrm{L}}} \tag{13}$$

where R_{D} is strain radius in km and M_{L} is the magnitude of the earthquake. Considering

the Earth's crust as anisotropic medium, the above mentioned law can be modified according to the effective sensitivity to impending earthquake. The ideal circle with the theoretical radius can be transformed to an ellipse or characterized by shadow areas where no precursory phenomena are observable due to crustal anisotropy, discontinuities or loose contacts along some faults, which prevent further stress transfer (İnan and Seyis, 2010; Martinelli, 1991).

Although radon anomalies can be studied in soil gas and thermal waters, thermal waters could be much more representative of the geologic environment and could be more reactive to stress/strain changes acting at depth than soil gases. Disadvantage of soil gases lie in weak gas concentrations generally due to the thickness of the sedimentary cover and the high level of atmospheric perturbations (Toutain and Baubron, 1999).

1.8.1 Radon as earthquake precursor

The term earthquake precursor is used to describe a wide variety of geophysical and geochemical phenomena that reportedly precede at least some earthquakes (Cicerone et al., 2009). Observation of these types of phenomena is one of the recent research activities with the aim of reducing the effects of natural hazards. Among different precursors, geochemistry has provided some high-quality signals, since fluid flows in the Earth's crust have a widely recognized role in faulting processes (Hickman et al., 1995). The potential of gas geochemistry in seismo-tectonics has been widely discussed by Toutain and Baubron (1999).

In the late 1960s and early 1970s reports primarily from seismically active countries, such as the former USSR, China, Japan and the USA (Ulomov and Mavashev, 1967; Wakita et al., 1980), indicated that concentrations of radon gas in the Earth apparently changed prior to the occurrences of nearby earthquakes (Lomnitz, 1994). The stress-strain developed within Earth's crust before an earthquake leads to changes in gas transport and rise of volatiles from the deep Earth to the surface (Ghosh et al., 2009; Thomas, 1988), resulting in anomalous changes of radon concentration. The mechanism of observed radon anomalies is still poorly understood, although several of them were proposed (Atkinson, 1980; King, 1978; Lay et al., 1998; Martinelli, 1991). In the past three decades the occurrence of anomalous temporal changes of radon concentrations was studied by several authors in soil gas (King, 1984, 1985; Kuo et al., 2010; Mogro-Campero et al., 1980; Planinić et al., 2001; Ramola et al., 2008; Ramola et al., 1990; Reddy and Nagabhushanam, 2011; Walia et al., 2009a; Walia et al., 2009b; Yang et al., 2005; Zmazek et al., 2005; Zmazek et al., 2002b) and groundwater (Barragán et al., 2008; Favara et al., 2001; Heinicke et al., 2010; Kuo et al., 2006; Ramola, 2010; Singh et al., 1999; Zmazek et al., 2002a; Zmazek et al., 2006). However, radon anomaly is not only controlled by seismic activity, it also changes due to meteorological parameters like soil moisture, rainfall, temperature and barometric pressure (Ghosh et al., 2009; Stranden et al., 1984). This makes it complicated and for small earthquakes often impossible to differentiate the anomalies caused by seismic events from those caused solely by atmospheric changes. Therefore, the application of theoretical and empirical algorithms for removing meteorological effects is necessary (Choubey et al., 2009; Ramola et al., 2008; Ramola et al., 1988; Torkar et al., 2010; Zmazek et al., 2003).

1.8.2 Radon and active faults

The active faults can be classified as normal, inverse or strike-slip faults, depending on the kinematic (compression or extension) mechanism. Faults can occur as single discrete breaks, but where the rock has been repeatedly faulted, or where the rock is especially weak, no discrete break may be evident. Large faults are not discrete surfaces but rather a braided array of slip surfaces encased in a highly fractured and often hydrothermally altered transition or "damage" zone, also called "fault zone". Episodic fracturing and brecciation are followed by cementation and crack healing, leading to cycles of permeability enhancement and reduction along faults (Hickman et al., 1995).

Active faults commonly exhibit anomalously high concentrations of various terrestrially generated gases (Rn, He, Hg, CO_2, etc.) in ground water and soil air (Al-Tamimi and Abumurad, 2001; Baubron et al., 2002; Ioannides et al., 2003; King, 1986; King et al., 1993; Lombardi and Voltattorni, 2010; Richon et al., 2010; Walia et al., 2010), because they act as preferential conduits in the crust. The overall picture emerging from several studies show that an increased radon concentration occurs in the area of active fault zones.

Gas anomalies at active faults may originate from two effects: in "direct leak anomalies" the gas measured corresponds to the deep gas phase; or "secondary anomalies", linked to the different mineralogy and the hydrological behaviour of the fault (Toutain and Baubron, 1999).

Ioannides et al. (2003) concluded that even a small gas velocity, i.e. 10^{-3} cm s^{-1}, can perturb radon concentration at the measuring point by approximately a factor of 2, while higher flows increase radon concentration by more than 4–6 times, depending on the diffusion coefficient. It has been shown (King et al., 1993) that the contrasting permeability in fault gauges and intensely shared zones generate complex geochemical patterns in soil. For the creeping faults, double-peak anomalies of radon concentration have been observed, possibly caused by the low permeability of the fault-gouge materials, sandwiched between two shear zones.

1.8.3 External effects on radon concentration in soil gas and water

Radon concentration in soil gas or water is not only controlled by geophysical parameters, it also changes due to other external effects. Meteorological effects such as soil humidity, rainfall, temperature, barometric pressure and wind, influence the soil gas advection. They also change physical characteristics of soil and rock, thus influencing the rate of radon transport and, consequently, perturbing eventual radon variations caused by geophysical processes originating in deeper parts of the Earth's crust. Shallow soil levels are more affected by changing meteorological conditions than deeper ones. Radon concentrations with no larger variations present are usually observed at depths of 0.8 m, or deeper. Besides the effects of meteorological parameters on radon in soil gas, considerable variations of gas composition of thermal springs have been shown as the result of fluctuations of local hydrologic regime (Klusman and Webster, 1981).

The severe influence of barometric pressure was discussed by several authors, who clearly pointed out an inverse relationship between barometric pressure and radon concentration in soil gas (Chen et al., 1995; Clements and Wilkening, 1974; Klusman and Webster, 1981). A decrease in barometric pressure, with values of other environmental parameters remaining constant, generally causes an increase in radon exhalation from the ground, whereas during periods of rising pressure, air with low radon concentration is forced into the ground, thus diluting radon.

Temperature-related fluctuations of soil gas radon concentration were also proved to

be very important. Klusman and Jaacks (1987) found an inverse relationship between soil temperature and radon concentration. They suggested that lower air temperatures than soil temperatures during the winter months promote upward movement of radon by convection, whereas during the summer, soil temperatures are lower than air temperatures and an inversion layer below the level of sampling reduces upward flux and observed concentration. In general, the behaviour of soil gas migration in different types of soil is seasonally dependent (King and Minissale, 1994; Washington and Rose, 1990).

In systems, where gas movement is driven by diffusion or slow advection processes, radon activity in soil might be controlled by soil moisture and rainfall through the opening of cracks in the surface (Pinault and Baubron, 1996; Toutain and Baubron, 1999). On the other hand, barometric pressure has the main influence on radon concentrations in soils in advective systems, which display generally higher gas flows. However, micro-scale soil heterogeneities in permeability, porosity and lithology, can cause significant heterogeneities in responses of radon concentration to changes of atmospheric parameters (King and Minissale, 1994; Neznal et al., 2004). Numerous and often divergent results of studies related to the effect of external factors on soil gas radon concentration suggest that no general prediction model for excluding meteorological effects can be proposed and studies of radon in soil gas need simultaneous record of meteorological parameters.

1.9 Radon in karst caves

It is well known that high concentrations of radon are common in mines. The existence of similar radiation in underground cavities was found in the 1970s and research of radon concentration in the natural caves has been carried out since then in two directions. The first is the aspect of radiation protection (Duenas et al., 1999; Fernandez et al., 1984; Kávási et al., 2010; Vaupotič, 2008) and the second aspect is that of radon as a tracer for air movement in the cave environment (Cunningham and Larock, 1991; Hakl et al., 1996; Kies and Massen, 1997; Kowalczk and Froelich, 2010; Perrier et al., 2004; Przylibski, 1999).

Minute quantities of uranium (^{238}U) present in limestone (1.3–2.5 ppm) result in relatively high values of radon in karstic caves compared to the outside atmosphere (Cigna, 2005; Gillmore et al., 2002; Hakl et al., 1997) due to low natural ventilation of the underground cavities and a constant emission from surfaces, fractures and drip waters.

In a study of 220 caves around the world, Hakl et al. (1997) reported an annual average radon concentration of 2800 Bq m^{-3}. Probably the highest radon concentration in a karst cave was measured in a Castañar de Ibor cave in Spain (Lario et al., 2006), with an annual mean radon concentration of 32246 Bq m^{-3}.

Radon can be transported from its place of origin by diffusion through the porous rock or advection through fractured rocks. Faults that are usually responsible for the cave formation therefore represent an additional pathway for radon entry into the cave. As discussed in the previous section (1.3.1), very large void systems can exist in the karst environment, representing the preferential path for Earth outgassing. Once a given amount of radon is in the cave, its concentration depends on the cave ventilation and its radioactive decay (Figure 8). Radon concentration in underground cave systems is also characterised by internal mixing of air masses (Perrier and Richon, 2010). According to Wilkening and Watkins (1976) and Perrier et al. (2004), the temporal evolution of radon concentration at a given location in the cave can be described as:

$$\frac{dC_{\mathrm{Rn}}}{dt} = \frac{S}{V}\Phi - \lambda C_{\mathrm{Rn}} - v_{\mathrm{c}}(C_{\mathrm{Rn}} - C_{\mathrm{out}}) \tag{14}$$

where S [m^2] and V [m^3] represent the total area and volume of the cave, Φ [Bq m^{-2} h^{-1}] is the radon exhalation rate from the rock surface, λ [h^{-1}] is ^{222}Rn decay constant (7.56×10^{-3} h^{-1}), v_{c} [h^{-1}] is the cave ventilation rate and C_{out} is radon concentration in the outside air. Note that the radon concentration in the outside air is on the order of tens of Bq m^{-3} and thus negligible in comparison to radon concentration in the cave air.

Cave ventilation has the highest impact on radon concentration in cave air and is further discussed in the section 1.9.1.3.

As the total area and volume of the cave are very hard to determine without exact measurements, the radon source for different locations can be considered separately:

$$\Phi_{\mathrm{ch}} = \frac{S_{\mathrm{ch}}}{V_{\mathrm{ch}}}\Phi \tag{15}$$

where Φ_{ch} [Bq m^{-3} h^{-1}] is the radon source in a specific chamber, S_{ch} [m^2] and V_{ch} [m^3] are, respectively, the surface area and volume of the chamber; and Φ [Bq m^{-2} h^{-1}] represents the radon exhalation rate from the rock surface.

In the case of stable conditions, with no ventilation and no temporal variation in radon concentration in a specific chamber, the radon source can be estimated. In this case

Equation (14) can be transformed to:

$$\Phi_{ch} = \lambda C^{ch}_{Rn-max} \tag{16}$$

where C^{ch}_{Rn-max} [Bq m^{-3}] represents the highest radon concentration in a specific chamber.

Besides ventilation process, also temporal changes in radon source can be observed, caused by changes of moisture content in the fractures and pores (Whittlestone et al., 2003) or by atmospheric pressure variations (e.g. Clements and Wilkening, 1974; Perrier and Richon, 2010). Barometric pumping from the pore space is the effect of atmospheric pressure variation. During pressure drops, radon reach air from the rock unsaturated zone is pumped into the cave atmosphere, where it mixes with the cave air. During the increase of pressure, cave air is pushed into the rock, thus reducing the radon diffusion process from the pore space into the cavity.

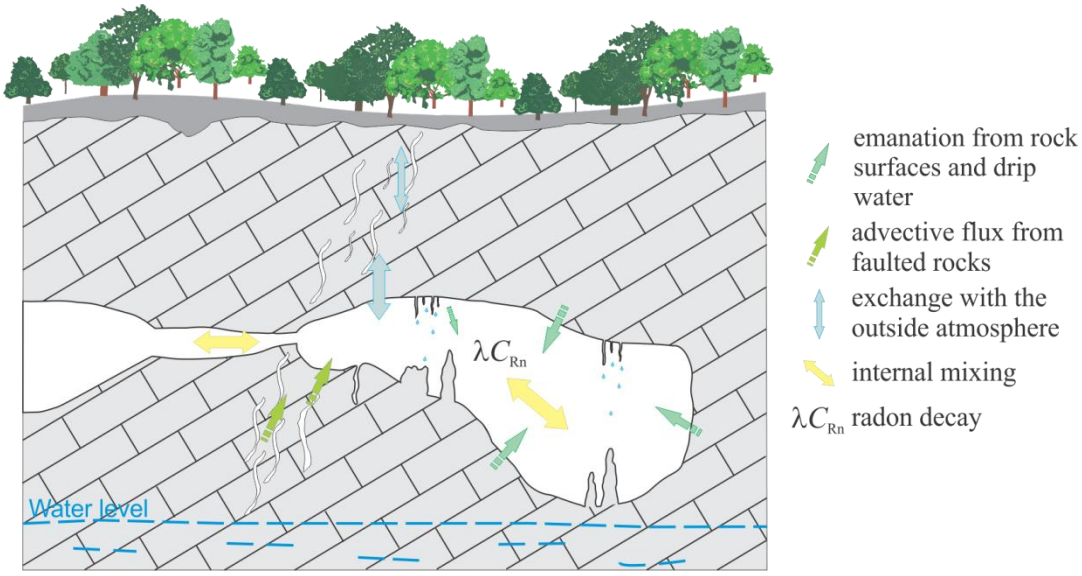

Figure 8: *Simplified representation of radon sources and sinks in a karst cave (cross section).*

1.9.1 Cave microclimate

Cave microclimate is a joint effect of atmospheric environmental processes that take place inside a cave. The karst cave environment is characterised by very high microenvironmental stability with essentially quasi-closed air masses (Badino, 2010) and may be considered stable in comparison to the outside atmosphere. Beyond this apparent stability, however, complex processes occur, which can today be brought to light thanks to advances in measurement techniques, data storage and data processing. All caves should be considered fragile systems, but show caves are particularly at risk because of anthropogenic impact.

Karst systems are limited on their upper part by the outside atmosphere and on their lower part by low permeability bedrock. Two major hydrological subsystems can be distinguished: the vadose (unsaturated) and the phreatic (saturated) zone, both being the subject of karstification processes, leading to the formation of new conduits (Luetscher and Jeannin, 2004).

An understanding of cave microclimate is of great importance when studying the thermodynamics of karst processes, paleoclimate proxies, hydrogeological aspects of speleothems, CO_2 build-up and cave ecosystems (Baldini et al., 2006; Faimon et al.,

2011; Kowalczk and Froelich, 2010; Perrier and Richon, 2010; Spötl et al., 2005; Tremaine et al., 2011). The thermal and moisture characteristics of the cave air (Badino, 2010; De Freitas et al., 1982), as well as the concentration of gases (^{222}Rn, CO_2) (e.g. Cuezva et al., 2011; Fernandez-Cortes et al., 2011; Kowalczk and Froelich, 2010) and aerosols (Bezek et al., 2012) are mainly controlled by the degree of air exchange with the outside environment.

The most important parameter governing dissolution and precipitation processes in carbonate karst is CO_2 (Dreybrodt, 1999), so understanding CO_2 distribution and dynamics in caves is important for paleoclimatic research. The dynamics of CO_2 in caves is governed by the distribution and intensity of its sources and (mainly) advective transport by air currents. The main sources of CO_2 in caves are diffusion from the epikarst, decomposition of organic matter and precipitation of calcite from supersaturated solutions. Many authors therefore include cave ventilation when modelling CO_2 variation over time in order to explain seasonality and trend (Baldini et al., 2008; Fernandez-Cortes et al., 2011; Milanolo and Gabrovšek, 2009; Tanahara et al., 1997).

1.9.1.1 Cave temperature

Underground temperature increases with depth according to geothermal gradient. However, percolating meteoric water in the deep vadose zone, which equilibrates the rock mass with external temperature, is the reason for low cave temperatures. According to Badino (2004), the time scale of climatic fluctuations, which are able to penetrate in the underground, depends on the water and rock thermal capacity, water infiltration rate and rock thickness and ranges from hundreds to thousands of years. Therefore the karst massifs are in thermal equilibrium with "historical" infiltrating fluids (Badino, 2010).

In approximation, cave temperature reflects the local yearly average temperature, under assumption that it is equal to the temperature of surrounding rock, which has basically the temperature of infiltrating water (Badino, 2010). Even so, a number of processes exist that can alter the cave temperature on a seasonal or daily scale and are extensively described by Badino (2010). Cave air temperature is influenced by conductive heat transfer, where temperature at the surface represents the upper boundary and deep geothermal heat flux the lower boundary (Luetscher and Jeannin, 2004). In the systems that are not thermodynamically closed, a temperature gradient exists, with higher temperature in the upper part of the conduit and lower in the bottom. In a closed system, these temperature differences would be wiped out in a short time. Temperature fluctuation is a function of external daily and seasonal temperature variations, carried inside by the inflow of external waters and, secondarily, the inflow of air (Badino, 2010; De Freitas and Schmekal, 2003).

1.9.1.2 Cave humidity, condensation and evaporation

The term "humidity" indicates the water vapour in air. Direction of the vapour gradient between the air and moist surface at any given time period controls the dynamic process of condensation/evaporation. Vapour pressure remains stable at "equilibrium pressure", called also "saturation pressure" (Badino, 2010). Condensation process is very important component of the cave microclimatology, as it plays an important role in the speleothem formation cycle (De Freitas and Schmekal, 2003; Fernandez-Cortes et al., 2006). Perhaps the most important process is that of "condensation corrosion", which occurs where water condensing onto cave walls that are made of soluble rock mineral is undersaturated with respect to the mineral (De Freitas, 2010; De Freitas and Schmekal, 2003).

The humidity of a cave atmosphere is generally at the equilibrium level. Evaporation and condensation occur when the vapour pressure is slightly below or above the

equilibrium level, which is generally connected to the presence of airflow.

1.9.1.3 Cave ventilation

Cave ventilation has been investigated in many caves in connection to its influence on the cave microclimate and sustainable cave management (e.g. Badino, 2010; Cigna, 1968; Faimon et al., 2011; Fairchild et al., 2006). Underground air fluxes are driven by external meteorological conditions, such as atmospheric pressure, temperature and winds.

The time for which atmosphere is retained in a cave is called the residence time (τ, expressed in time units) and the inverse value ($1/\tau$) corresponds to the cave ventilation (ν_c, time^{-1}). Cave ventilation represents the amount of cave air exchanged per time unit. If the cave atmosphere is just pulled back and forth due to an alternating ventilation regime during transitional periods in spring and autumn, there is no air exchange in the deeper parts of the cave. This period can be called a stagnant ventilation period. By contrast, active ventilation is considered in the case of the cave remaining in one ventilation regime for long enough in comparison to the residence time of the cave atmosphere (Faimon et al., 2011).

1.9.1.3.1 Convective ventilation

Convective ventilation is a major mechanism controlling air circulation in caves with more than one entrance at different elevations (Badino, 2010; Cigna, 1968; Hakl et al., 1996; Kowalczk and Froelich, 2010; Wigley, 1967). It is driven by buoyancy force, created by the difference of air density between the external and internal air masses. Internal air density is almost constant, whereas the external is denser during winter and less dense during summer. Therefore, a system with two or more entrances at different altitudes ventilates during the whole season by a so called chimney-effect. When the external temperature is lower than cave temperature, cave air flows from the lower toward the upper entrances and vice versa. The pressure difference (caused by temperature difference) that drives convective ventilation, depends on the difference of the entrance altitudes and on the difference of temperature between the cave and outside air. The velocity of air flux additionally depends on the friction force due to air movement inside the cave, which is a nonlinear function and depends also on the geomorphology of the conduit. It has been shown that air flow is proportional to the square root of temperature difference between the cave and the outside air (Badino, 2010).

1.9.1.3.2 Barometric ventilation

On the other hand so-called barometric ventilation can be very important for caves with large volumes connected by small passages, for caves with one entrance or with extremely small entrances (Badino, 2010; Cigna, 1968; Wigley, 1967). It is driven by the internal-external pressure difference. Therefore, in addition to the outside atmosphere, cave geomorphology plays an important role in cave ventilation. However, this process is relatively weak in the type of caves characteristic for Slovenian karst caves, which are characterised by many cave entrances and relatively small volumes.

1.9.1.3.3 Airflow oscillation

Periodic cave winds have been observed in some cases (Badino, 2010; Cigna, 1968; Faimon et al., 2011; Plummer, 1969), with a period ranging from a few seconds to a few minutes. Such oscillations are broadly interpreted as a resonance phenomenon and depend on the geometry of cave conduits. They could occur for example in the presence of strong winds. However, the high frequency in cave airflows was not discussed yet in detail.

1.9.1.3.4 Implications of cave ventilation

Partial pressure of CO_2 (P_{CO2}) in the cave air, which controls the speleothem growth, is governed mainly by cave ventilation (Faimon et al., 2006; Hakl et al., 1997). If the water P_{CO2} source in the epikarst is considered as invariant (Spötl et al., 2005), only cave ventilation would determine the rate of the speleothem growth. Therefore paleoenvironmental reconstruction based on the study of stalagmites (Banner et al., 2007; Fairchild et al., 2006; Wong et al., 2011) requires detailed information on cave ventilation. Besides controlling P_{CO2}, cave ventilation can disturb paleoproxies also by influencing cave air temperature.

Furthermore, there is a risk connected with artificial changes of cave ventilation by closing or building new ones and thus changing the condition for speleothem growth or even triggering condensational corrosion. This fact makes cave ventilation an important factor, which should be considered in cave conservation studies and sustainable cave management of show caves.

1.9.2 Radon as a tracer for cave ventilation

Radon has often been used as an excellent tracer for air circulation, since it is a noble gas and highly abundant in caves (Cigna, 2003; Cunningham and Larock, 1991; Hakl et al., 1996; Hakl et al., 1997; Kies and Massen, 1997; Kowalczk and Froelich, 2010; Perrier et al., 2004; Przylibski, 1999). Its half-life, suitable for the timescales on which cave ventilation takes place, distinguishes ^{222}Rn from the other two radon isotopes. The ventilation characteristics of a cave can be reflected in the fluctuation of radon concentration as long as the turnover time is shorter than five mean lives of ^{222}Rn (approximately four weeks) (Kowalczk and Froelich, 2010). The pattern of seasonal variation of radon concentration reflects the pattern of circulation of air currents in the underground system. On approaching deeper parts of the karst, radon levels increase and are more stable due to decreasing ventilation rate (Hakl et al., 1997).

Seasonal changes in natural ventilation often cause large temporal variation in radon levels, most commonly characterised by high summer and low winter concentrations (Przylibski, 1999; Szerbin, 1996; Tanahara et al., 1997; Wilkening and Watkins, 1976). Spring and autumn are transitional periods, during which, high variation of radon concentration is expected. Seasonal variation with opposite behaviour, a maximum in winter and minimum in summer, has also been observed in some cases: Moestroff Cave in Luxembourg (Kies and Massen, 1997), Altamira (Lario et al., 2005) and Castañar de Ibor Cave (Lario et al., 2006) in Spain. However, other less common patterns have also been documented, such as maximum concentration during autumn and minimum during summer in the Mammoth Cave, Kentucky (Eheman et al., 1991). Besides seasonal pattern, also diurnal variation of radon concentration has been observed in some cases, particularly during periods of large fluctuation of atmospheric parameters.

1.9.3 Radon concentration in Slovenian caves

In Slovenia karst covers more than 40 % of the area (8700 km^2) with around 10200 registered karst caves. Among them, 21 caves are opened for tourist visits.

Radon concentration is during the last decade measured continuously in two most visited tourist caves in Slovenia, Postojna and Škocjan Caves, in order to estimate doses that tourist guides receive during their working hours.

Radon concentration was measured in 12 show caves by Kobal et al. (1987) in the years from 1978 to 1985. Values of radon concentration vary from cave to cave as well as

along the tourist route in a cave. The highest radon levels were observed in Postojna and Tabor Cave, 2500 and 10000 Bq m^{-3}, respectively. In all other caves, radon levels were less than 1000 Bq m^{-3}. Spatial and temporal distribution of radon levels in the Postojna Cave has been investigated in the year 1987 by grab sampling, using alpha scintillation method (Kobal et al., 1988). Graphical representation of results in shown in Figure 9 and reveals a significant difference in radon levels between winter (Figure 9a) and summer period (Figure 9b).

Postojna Cave, being the longest known cave system in Slovenia for many years (until summer 2012), as well as one of the most visited show caves in Europe, has been a subject of several surveys during the last 15 years. To improve radon dosimetry long-term study of radon and radon decay products was performed (Vaupotič, 2008; Vaupotič et al., 2001). In order to enlighten processes that govern the fraction and distribution of attached and unattached fraction of radon decay products in the cave air, number concentration and size distribution of aerosols in the cave air has been measured recently (Bezek et al., 2012). Relationship between radon concentration and present-day tectonic movement was studied by Šebela et al. (2010). Recently, local characteristics of the Postojna Cave microclimate (Šebela and Turk, 2011) and microbiological studies were conducted (Mulec et al., 2012).

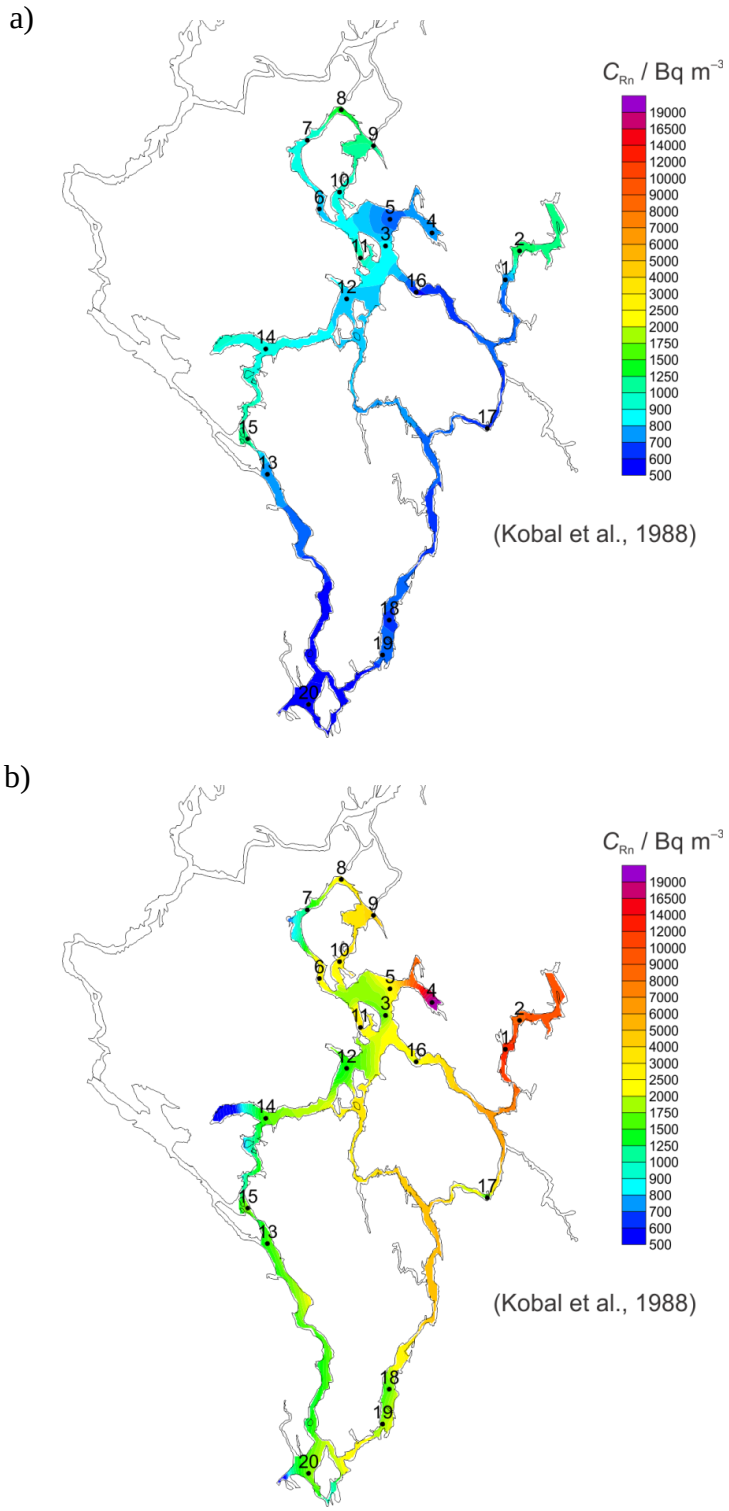

Figure 9: *Spatial distribution of radon concentration in Postojna Cave* (after Kobal et al. (1988)). a) January 1987, b) July 1987. Measurement points: 1 – Pisani Rov before door, 2 – Pisani Rov beyond door, 3 – Nebotičnik, 4 – Čarobni Vrt, 5 – Velika Gora, 6 – near Ruski Most, 7 – Rdeča Dvorana, 8 – end of Lepe Jame, 9 – by Partizan, 10 – the lowest point, 11 – Betlehem, 12 – Koncertna Dvorana, 13 – lower Tartar, 14 – upper Tartar, 15 – Tartar, 16 – railway crossing, 17 – Dvorana Zaves, 18 – Kongresna Dvorana, 19 – entrance above Pivka, 20 – exit.

2 Aims and Hypothesis

Radon, being a geogas component, has a special value in geophysics, as it can be used as a reliable tracer for geophysical processes that take place in deeper parts of the Earth's crust, as well as on the Earth's surface and in the atmosphere. Therefore, knowledge about its sources and the processes governing its transport to the surface is of great importance. In this study, two main aspects of radon as a tool in geophysical research are considered:

a) radon concentration in soil gas and water, radon transport in the Earth's crust and the use of radon as an earthquake precursor – structured into two chapters:
   - radon transport in different environments (Chapter 4.1)
   - radon as a tracer for geophysical processes in the Earth's crust (Chapter 4.2)

b) radon concentration in cave air and its use as a tracer for cave ventilation (Chapter 4.3)

The goals and hypotheses of this thesis are:

a) to study radon transport characteristics in different media through its temporal and/or spatial variations and to assess the contribution of different processes to radon variation. The use of radon gas as an earthquake precursor is evaluated, taking into consideration the role of the geological position of the measurement location and the influence of hydrometeorological conditions. The following hypotheses were considered:

- the effect of geophysical processes on radon fluctuation in soil gas or water is not spatially uniform, but rather depends on the geological characteristics of the measurement location,
- the effect of hydrometeorological parameters on radon concentration in the Earth's crust can be efficiently eliminated by applying different types of analyses in order to detect anomalous patterns of radon concentration, resulting from geophysical processes.

b) to evaluate radon gas as a tracer for cave ventilation, using Postojna Cave as an experimental site. Although the general ventilation characteristics and radon levels of Postojna Cave are already known (and can, to some degree, be estimated from cave morphology and studies performed in other caves worldwide), the direction of airflows and the degree of ventilation in some remote passages remain mainly unknown. An additional aim is to determine and evaluate the contribution of different sources of radon in the cave air. The hypotheses considering radon in the cave are as follows:

- the radon concentration in the cave can be, for a specific location, predicted on the basis of outside atmospheric parameters,
- among all of the atmospheric parameters, the outside temperature is the most important in controlling cave ventilation characteristics and therefore radon levels,
- a time lag exists between outside atmospheric changes and the consequent change of radon concentration in the cave, which is a function of the ventilation rate and the distance from the cave entrance,

- the relationship between radon and carbon dioxide in the cave air can reveal the contribution of different radon sources (contribution of radon from advective and diffusive flux),
- spatial and temporal variation of radon sources is assumed, resulting from exhalation from rock surfaces and sediments, dripping water and cracks.

3 Materials and Methods

3.1 Measurement locations

Measurements of radon concentration were performed in various environments in order to study the behaviour of radon transport, and thus its fluctuation in these environments in relation to changes of geophysical as well as atmospheric parameters. Three different natural environments were selected: soil gas, thermal water and karst caves. In addition, a fly ash deposit (raw industrial material) was considered.

The selection of measurement locations was based on preliminary results and already existing monitoring stations for radon in thermal water and karst caves, whereas in the case of soil gas, the measurement locations were selected according to their geological background. All locations are situated in the western and central parts of Slovenia, as presented in Figure 10:

- the spatial distribution of radon in soil gas was investigated within the Ravne fault zone in NW Slovenia, which is an area of recently increased seismic activity (Chapter 3.1.1),
- the fluctuation of radon concentration in thermal water and soil gas is mainly a result of the joint effect of geophysical and atmospheric parameters. Radon fluctuation with respect to seismic activity was studied in the areas of recent seismic activity in NW Slovenia,
- radon levels in karst caves are mainly governed by the degree of cave ventilation, as well as changes of radon emanation from rock surfaces and exhalation from fractured and faulted rocks, which are in fact influenced by geophysical parameters in the Earth's crust. For this part of the research, the largest Slovenian show cave was selected.

Figure 10: *Map of Slovenia with marked measurement locations*.

3.1.1 Bovec – Ravne fault

Radon concentration in soil gas and radon exhalation rate was measured at 18 points along the Ravne fault in NW Slovenia, grouped in five profiles (Figure 11). Measurement points were selected on the basis of geology and tectonics of the area. However, due to the mountainous morphology, the selection of measurement points was limited to north-western and south-eastern ends of the fault zone, which are accessible by car.

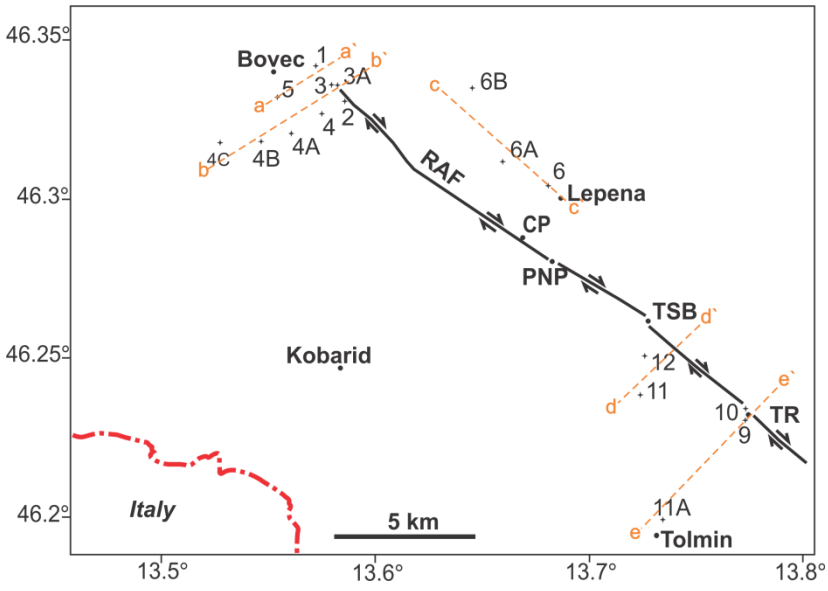

Figure 11: *Ravne fault with marked measurement points and profiles*. RAF – Ravne fault, CP – Čez Potoče, PNP – Planina na Polju, TSB – Tolminka Springs basin and TR – Tolminske Ravne.

Being an active fault zone, responsible for the two most recent strong seismic events in 1998 and 2004, makes this area an interesting research field for studying the influence of tectonic deformation on radon transport in the Earth's crust and its exhalation rate.

The Ravne fault has been studied from the structural point of view by Kastelic et al. (2008). It is an actively propagating NW-SE trending dextral strike-slip fault in the Julian Alps of NW Slovenia. Strike-slip displacements on moderate-steep fault planes are responsible for the recent seismic activity that is confined to shallow crustal levels. The fault is growing by interaction of individual right stepping fault segments and breaching of local transtensional step-over zones. The fault geometry is controlled by the original geometry of the NW–SE trending thrust zone, modified by successive faulting within the fault zone. At epicentral depths, the fault system is accommodating recent strain along newly formed fault planes, whereas in upper parts of the crust, the activity is distributed over a wider deformation zone that includes reactivated brittle thrust faults.

The Bovec basin, at the north-western end of the Ravne fault (Figure 12), is characterised by Triassic and Jurassic carbonates and Cretaceous flysch rocks, covered by fluvio-glacial deposits. The Ravne fault is less exposed to the SE of the Tolminka Springs basin, where it is covered by grass and forested terrain. There is no individual fault planes outcrop between the Tolminka Springs basin and areas SE of Tolminske Ravne. Along that part of the fault trace, the fault exhibits a right-stepping fault segmentation pattern and both segments overstep in the area of Tolminske Ravne.

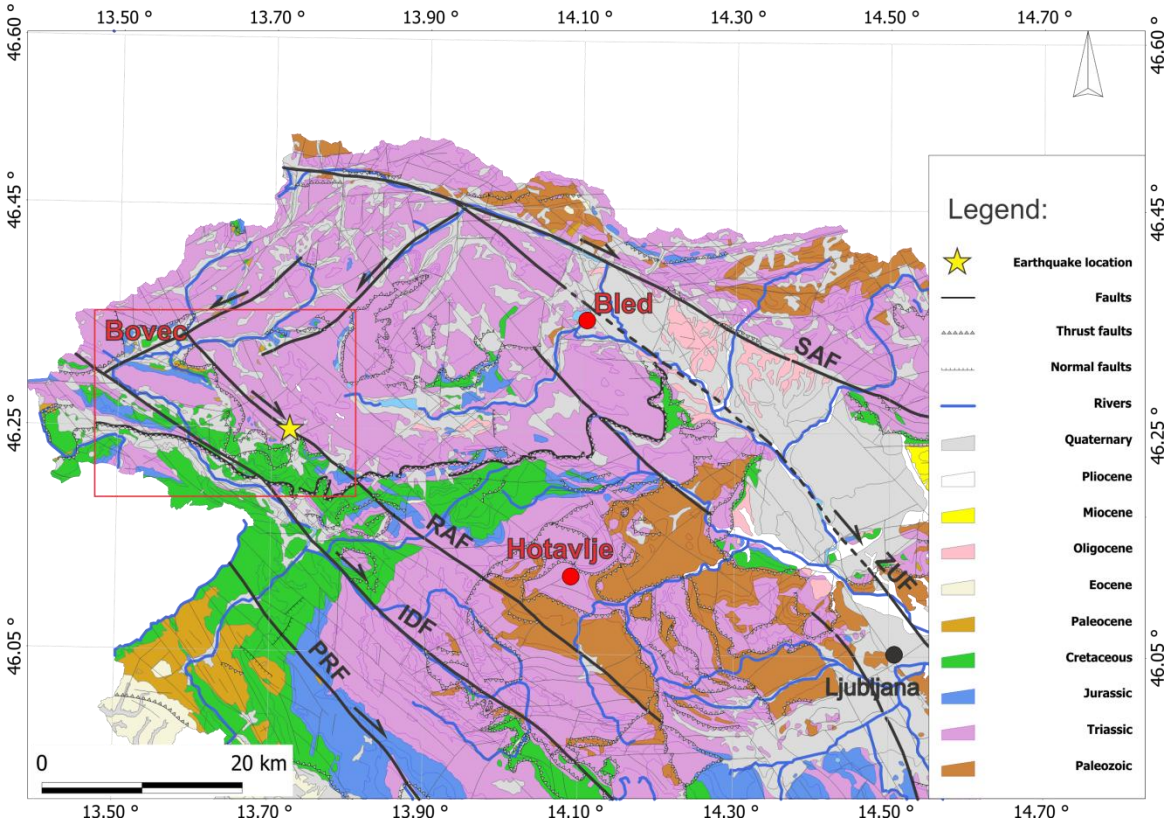

Figure 12: *Geologic map of north-western Slovenia with marked measurement locations*. Rectangle in Bovec region indicates the area of measurement points within the Ravne fault zone (Figure 11). Faults: SAF – Sava, ZUF – Žužemberk, RAF – Ravne, IDF – Idrija, PRF – Predjama. Location of 1998 and 2004 earthquake epicentre is marked with a star.

3.1.2 Thermal water

There are only a few thermal springs in the seismically active area along the Soča river, the closest and most easily accessible ones being at Bled and Hotavlje (Figure 12). In contrast, there are many thermal springs in east Slovenia, but this area exhibits lower seismic activity. Earthquakes that occurred during the time of our research (October 2005–May 2008) and that are inside the range of two lengths of Dobrovolsky radius (R_D, Eq. 13) are indicated in Figure 13.

3.1.2.1 Thermal spring at Bled

The thermal spring at Bled wells on the Bled fault on the eastern side of Lake Bled (46.37N, 14.11E) which belongs to Southern Alps. The Bled fault represents a SW boundary of tectonic depression of Ljubljana and Radovljica, which was formed in Tertiary. Depression is filled by 100 to 500 m deep Tertiary strata (Buser, 1975). Cold meteoric and underground water trickles through fractured carbonate bedrock on the border of depression, where it is warmed due to geothermal gradient. Thermal water then springs from a deep Triassic carbonate reservoir due to convective forces and rises through Oligocene clay and shallower Quaternary lake and glacial sediment. Thermal water is used in the swimming pool of the Toplice Hotel and is characterized by a constant temperature of 21.82 ± 0.01 °C and by active bubbling (Popit et al., 2005).

3.1.2.2 Thermal spring at Hotavlje

The thermal spring at Hotavlje (46.12N, 14.08E) is situated at the bank of a small stream near the Hotavlje village and belongs to the tectonic unit of External Dinarides. Water temperature is constant at 20.22 ± 0.04 °C and wells on the fault in Main dolomite oriented along the valley of Kopačnica (Grad and Ferjančič, 1968). The water is of meteoric origin. Meteoric water trickles through the rocks to deeper layers, where it accumulates and warms up and is then raised again with convective flow through fault zones (Popit, 2004).

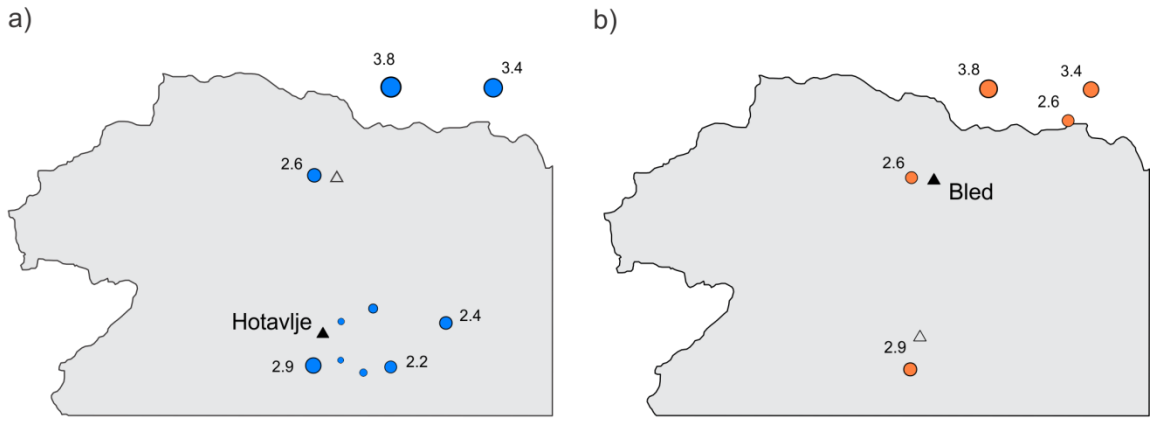

Figure 13: *Earthquakes with an impact on Hotavlje and Bled location from October 2005 to May 2008*. The size of a circle represents the earthquake magnitude (M_L). Only earthquakes with R_D/R ratio of 0.5 are considered.

3.1.3 Karst cave – Postojna Cave

The Postojna Cave, with its 20570 m of known passages (Figure 14), is the second longest of 10000 registered karst caves in Slovenia and one of the most visited show caves in Europe. The river Pivka sinks at the lower entrance to the cave at a height of 511 m above sea level (masl). The entrance to the main, currently dry, passage is situated at 529.5 masl and is 10 m high and 6 m wide. This entrance is also used as a tourist entrance. The cave passages have developed in approximately 800 m of Upper Cretaceous bedded limestone situated between two dextral strike-slip Dinaric faults, Idrija and Predjama Fault (Šebela, 1998; Šebela et al., 2010).

Cave passages are developed in both flanks of the Postojna anticline and follow the strike and dip of the bedding-planes (Čar and Šebela, 1998). They are mostly horizontal, dipping toward the north and northeast (Figure 15). The cave has six known entrances and some less known or unknown connections to the surface, for the most part corrosionally widened fissures. There is no forced ventilation in the cave and air is only exchanged via natural air flow through the numerous cracks, passages and breathing holes (Gams, 1974) connecting the cave with the outside atmosphere.

Mean annual air temperature in Postojna is 8.4 °C with the lowest monthly average – 0.9 °C in January and the highest average 17.7 °C in July. During the last few years, an increase of the mean annual temperature is observed. Average monthly rainfall in Postojna is in the range of 90–170 mm. During the measurement period, a flood occurred from 17 to 21 September 2010, extending over almost the whole of Slovenia. The level of Pivka river just before the sinking point reached 520.4 masl on September 19th. The highest water level in the Postojna Cave system during the flood was 518 m, which is just 2 m lower than the highest observed water level in 1933.

Postojna Cave has been under permanent radon survey since 1995 because of elevated radon concentrations (Kobal et al., 1988; Vaupotič, 2008; Vaupotič et al., 2001). More recently, air temperature and pressure monitoring has been conducted to better understand radon emanations connected with microtectonic displacements of two monitoring sites, Velika Gora and Lepe Jame (Šebela et al., 2010).

All these studies have brought to light the complexity of the Postojna Cave microclimate (Šebela and Turk, 2011), influenced by numerous known and unknown entrances at different levels and the long and highly ramified cave system.

The first location is situated in a narrow fissure in the Lepe Jame (Beautiful Caves) (Figure 14, cross section a-a'), 529 m above the sea level and about 15 m from the route followed by tourists. Because of the large vent hole here, this fissure was artificially widened about 50 years ago in order to create a new passage, but the passage ended in a narrow fissure. Radon concentration was measured continuously at this location during two periods: April 2006–October 2007 and March 2010–October 2012.

The second location is situated at the lowest point of the tourist route (Figure 14, cross section b-b'), at 508 masl, where the passage widens significantly. Measurements of radon concentration have been introduced to this location simultaneously with the research of aerosols in the cave air (Bezek et al., 2012) in March 2011.

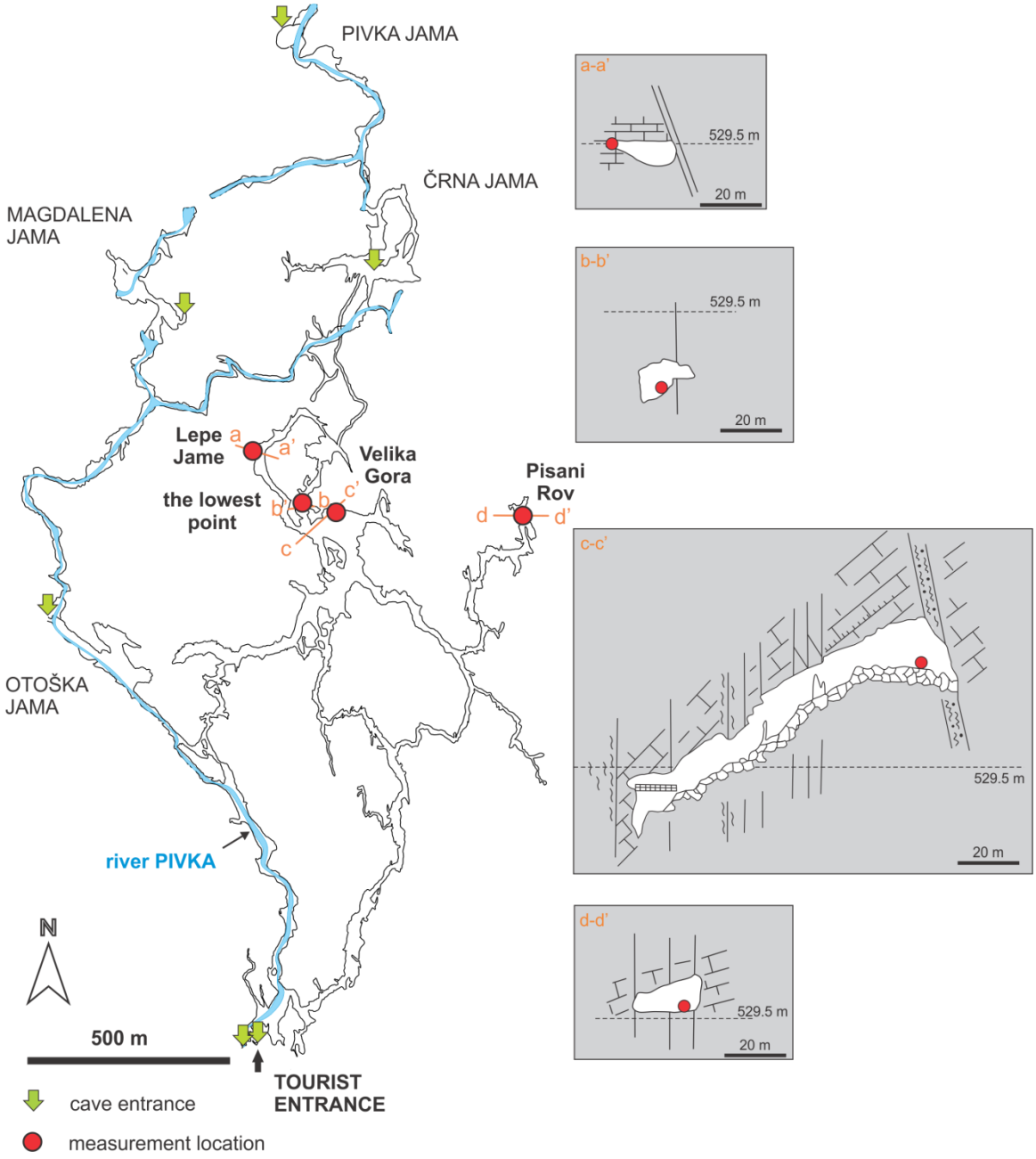

Figure 14: *Ground plan of the Postojna Cave system with marked measurement locations and cross sections.* a-a' (Lepe Jame), b-b' (the lowest point), c-c' (Velika Gora) and d-d' (Pisani Rov) (after Šebela (1998)).

Velika Gora (Great Mountain) is located at the northern edge of the biggest collapse chamber in the cave (Figure 14, cross section c-c') at 561.4 masl with 65 m of the limestone roof and 50 m from a well-used tourist route. Radon was monitored continuously in the Velika Gora chamber from July 2005 to October 2009.

The fourth measurement location (Figure 14, cross section d-d') lies at the end (532 masl) of the 920 m long Pisani Rov (Gaily Coloured Corridor), which deviates from the main passage to the north. This passage is not a part of the tourist route. It terminates below the slopes of a collapse doline where the bottom is filled by sediments at 535 masl (Šebela and Čar, 2000). Along the whole passage, grey loam originating from weathered flysch rocks can be found. The roughly 145 cm thick profile of fluvial sediments situated at the end of Pisani Rov consists of fine-grained sediments (yellowish brown silts to clays

with dark stains in the upper part showing cubic to columnar disintegration with Fe stains on the fractures), covering the collapse boulders and massive flowstone (Zupan Hajna et al., 2008). The deepening of the collapse doline interrupted the continuation of Pisani Rov towards the north (Šebela and Čar, 2000). The smallest thickness of the cave ceiling is about 30 m. Continuous measurements of radon concentration started in this corridor in February 2010 and lasted until October 2012.

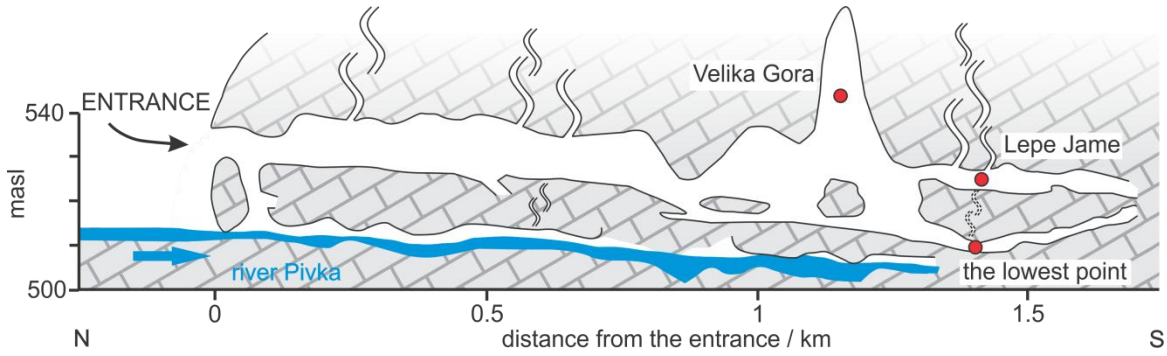

Figure 15: *Longitudinal profile through Postojna Cave with marked measurement locations* (after Gospodarič (1976)).

3.2 Radon measurement techniques

Radon activity can be determined by measuring either the activity of radon itself, the total activity of radon and its decay products (RnDP), the activity of some of RnDP or the gross activity of RnDP. Measurement techniques may be classified according to the principle of analysis, sampling or the duration of measurements.

Regarding the principle of analysis, three types of measurements can be distinguished:

- by the *grab sampling technique*, the instantaneous activity concentration of radon is obtained. Samples of air, soil gas or water are collected and analysed with a proper device, for instance α-scintillation cells, ionisation chambers or semiconductor detectors (Quindós-Poncela et al., 2003; Vaupotič et al., 1992).
- by *continuous monitoring* at a pre-selected frequency, a time series of radon concentration is obtained. Samples are collected and analysed automatically at short time intervals (from several minutes to several hours) over a longer period of time (days or weeks). For this purpose, the following devices are often used (commercial names): Barasol probe, Radon Scout, Radim 5, AlphaGuard and Rad7, RTM 1688 and EQF 3020-2.
- by *integrating measurements*, the average radon activity concentration for the period of exposure is obtained by exposing detectors to radon, either in air, soil gas or water, for a longer period of time (from weeks to months). For these measurements, ion chambers based on electret (Kotrappa et al., 1988) and solid state nuclear track detectors of various manufacturers are used (e.g. Radosys, Gammadata).

Air, soil gas or water may be sampled either actively, by pumping (continuously or at pre-selected intervals) through the detector chamber, or passively, where only radon which diffuses into the detector chamber is measured.

Regarding the duration of measurement, short-term measurements, which last for days or at most a week, and long-term measurements, over weeks and months, can be distinguished (Klein et al., 1995; Nero, 1988; Papastefanou, 2002).

For the purpose of studying the temporal variation of radon levels in karst caves, soil gas or water, continuous measurements are the most appropriate, as they provide an opportunity to observe diurnal variations, as well as variations over a longer time-scale. Therefore, several passive devices for continuous radon measurements have been used, including Barasol probes, Radim 5 and Radon Scout (commercial names). On the other hand, the grab-sampling technique using alpha-scintillation cells was used for the research of the spatial distribution of radon concentration within the Ravne fault zone. This technique is also very useful for preliminary measurements, as it gives reliable results in a relatively short time and in this way represents a helpful tool for choosing the most appropriate location for continuous measurements.

Long-term continuous measurements under real environmental conditions are inevitably subject to extreme conditions, particularly high humidity in caves and soil gas and therefore electronic devices used in field measurements should be robust enough. Besides its corrosive effect, moisture additionally influences the efficiency of radon detection and thus attention should be paid while exposing radon monitors to field conditions.

3.2.1 Grab sampling technique

3.2.1.1 Alpha-scintillation cells

Instantaneous radon activity concentrations can be measured either in indoor air, soil gas or water. For that purpose, air and soil gas are sampled directly into the scintillation cell using a pump, while from water samples, radon is degassed and then transferred into the cell. Two types of scintillation cells have been used for measurements performed within the frame of this thesis: cells manufactured at Jožef Stefan Institute (Kristan and Kobal, 1973; Vaupotič et al., 1992) and the second type, manufactured in Spain (Quindós-Poncela et al., 2003). In both types of scintillation cells, silver-activated zinc sulphide, ZnS(Ag) scintillator is used.

For the purpose of analyses, scintillation cell is placed inside a photomultiplier tube inside a light-tight enclosure three hours after sampling, when secular equilibrium between radon and its decay products has been reached. Light pulses emitted when alpha particles emitted by Rn and RnDP strike the scintillator, are amplified by the photomultiplier tube and then counted with an alpha counter PRM 145 (AMES, Slovenia).

3.2.2 Continuous measurements of radon concentration

3.2.2.1 Barasol probe

Battery-operated Barasol probe (MC-450, Algade, France) is a passive device for continuous measurements of radon concentration. The probe is primarily designed for radon measurements in soil gas and it therefore has a higher lower limit of detection (about 500 Bq m^{-3}) than devices designed for measurements in indoor or outdoor air. It gives radon concentration based on alpha spectrometry of radon decay products (formed from radon that diffuses into the detector active volume) in the energy range of 1.5 MeV to 6 MeV using an implanted solid-state silicon detector. The detector sensitivity is 50 Bq m^{-3} per 1 imp h^{-1} with a sampling frequency of once an hour. It also records temperature and relative barometric pressure. Data are stored in the internal memory at predefined frequency and are periodically transferred to a personal computer.

The advantage of this type of probes is their robustness and high capacity of internal memory and battery, which makes Barasol a very convenient device for long-term measurements under environmental conditions. However, high lower limit of detection restricts its use to environments with high radon concentration.

3.2.2.2 Radim 5 and Radon Scout

Radim 5 (SMM Company, Czech Republic) and Radon Scout (Sarad, Germany) are passive devices for continuous radon measurements, mainly designed for indoor air measurements. Both instruments are battery-operated and have the same principle detection. The activity of radon, diffused into the measuring chamber, is measured via its decay products ^{218}Po and ^{214}Po, electrostatically collected on the surface of a semi-conductor detector.

The measuring range of Radim 5 monitor is from 80 Bq m^{-3} to 50 MBq m^{-3} and the sampling interval is 0.5 or 1 hour. It is intended for extreme conditions, when 100 % humidity or dust environment is expected.

Radon Scout has lower measuring range than Radim 5, from 5 Bq m^{-3} to 10 MBq m^{-3}, with a statistical error lower than 5 %. Additionally, it measures also temperature and relative humidity. Measured data are stored in the internal memory at predefined intervals (1 or 3 hours) and then transferred to a personal computer.

3.3 Databases

Databases included in the research are mostly based on long-term measurements of radon concentration and atmospheric parameters. In the case of thermal water, measurements had already started in the frame of previous research. The same is true for measurements at Velika Gora and Lepe Jame in Postojna Cave. During the progress of the research and temporary results, the need for additional measurements at some crucial points in the cave appeared, in order to be able to interpret the time evolution and fluctuation of radon concentration and thus cave ventilation. However, the radon time series at each location exceeds a period of one year, which is necessary to observe the seasonal behaviour of observed parameters.

As distinguished from other locations, the spatial distribution of radon concentration was highlighted in the case of the Ravne fault zone.

Hourly values of atmospheric parameters (temperature, barometric pressure and relative humidity) and daily height of rainfall for the Postojna region were provided by the Slovenian Environment Agency (Ministry of Agriculture and Environment of the Republic of Slovenia) until November 2010. A data logger DL-180THP (Voltcraft, Germany) was installed in front of the tourist entrance to Postojna Cave in November 2010, and has been continuously recording atmospheric parameters at one hour intervals since then. The list of radon databases included in the thesis is summarised in Table 5.

The location of seismic events and their magnitudes was provided by the Seismology Office of the Slovenian Environment Agency (Ministry of Agriculture and the Environment of the Republic of Slovenia).

In order to improve the knowledge of the Postojna Cave microclimate and cave ventilation in particular, additional parameters (T_{cave} – cave air temperature and CO_2 concentration), were considered beside radon concentrations that were provided by Dr. Stanka Šebela and Dr. Franci Gabrovšek from the Karst Research Institute (Research Centre of the Slovenian Academy of Sciences and Arts).

Table 5: *Summary of databases*.

	Location	Media	Period	Type of measurement	Device
Postojna Cave	Lepe Jame	cave air	04/2006–10/2007	continuous	Radim 5
			03/2010–10/2012	continuous	Radim 5
	the lowest point	cave air	03/2011–10/2012	continuous	Barasol
	Velika Gora	cave air	07/2005–10/2009	continuous	Barasol Radon Scout
	Pisani Rov	cave air	02/2010–10/2012	continuous	Barasol
	Bled	thermal water	10/2005–9/2007	continuous	Barasol
	Hotavlje		10/2005–6/2008	continuous	Barasol
	Bovec – Ravne fault	soil gas	17/8/2008–3/9/2008	grab sampling	alpha scintillation

A complete time series of radon concentration at four measurement locations in the Postojna Cave is presented in Figure 17. The longest uninterrupted time series are obtained using Barasol probe, while missing data in the time series obtained by Radim 5 or Radon Scout are usually caused by device malfunction.

3.4 Uncertainty of radon measurements

Field measurements under real environmental conditions are inevitably subjected to additional sources of uncertainty, compared to laboratory experiments under well-controlled conditions. These additional components of uncertainty, connected to field measurements, mainly arise from sampling technique, unpredictable environmental conditions and approximations and assumptions incorporated in the measurement method and procedure, which are very difficult to evaluate quantitatively.

In field measurements, such as continuous measurements of radon concentration in water, soil gas or cave air, uncertainty related to sampling and transportation of samples is avoided. However, a disadvantage in a sense of accuracy of field measurements is their unreplicability due to the changing values of measured parameters. Therefore, it is even more important to accurately evaluate uncertainties arising from measurement devices, prior to field measurements. Using a calibrated measuring device is a prerequisite to obtain good and reliable measured values. Calibration, as well as intercomparison, enables a laboratory to evaluate their own data obtained with various measuring devices, and to compare their results with those of other laboratories.

Calibration of radon measurement devices owned by Radon Center (Department of Environmental Sciences, Jožef Stefan Institute) is performed regularly either by the company, where the instrument was produced or by exposing a measuring device to known concentration of radon in a radon chamber. IFJ-KR-600 Radon Chamber (Figure 16), located in the Laboratory of Radiometric Expertise at The Henryk Niewodniczański Institute of Nuclear Physics, Polish Academy of Sciences, Kraków, Poland (IFJ-PAN) has been used for calibration and intercomparison of measuring devices (Kozak et al., 2009).

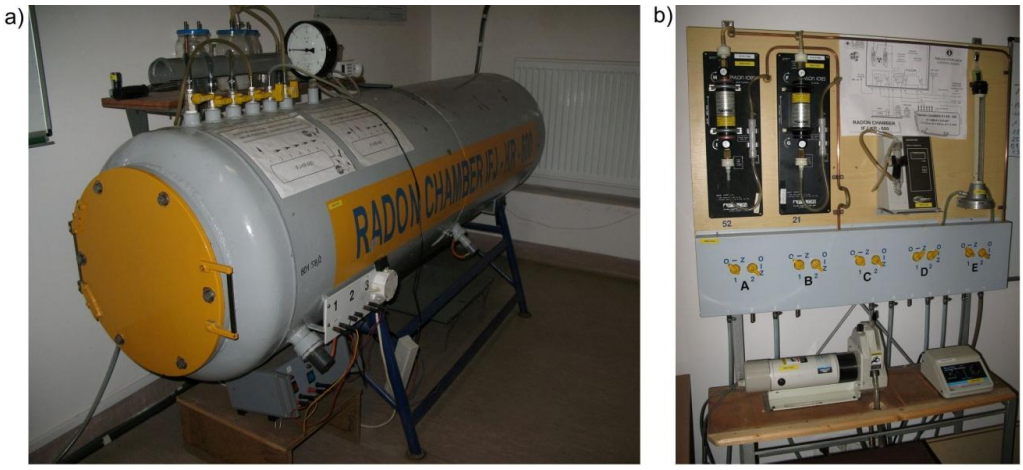

Figure 16: *Radon Chamber IFJ-KR-600.* a) radon chamber, b) control panel.

Traditional methods for the development of ^{222}Rn reference standards are based on the quantitative transfer of the ^{222}Rn produced in a known period of time by a ^{226}Ra standard source, to a suitable chamber operating as the ^{222}Rn detector. The counting efficiency of this detector is obtained from the instrument reading and the known ^{222}Rn activity. The detector is therefore used as a ^{222}Rn reference measurement system (De Felice, 2007). This is a so called "relative standard".

Intercomparison of radon measuring devices and sampling techniques is performed regularly between different laboratories and also within Radon Center between different devices (i.e. Barasol probes, Radon Scout and Radim 5), with AlphaGuard (Saphymo, Germany) used as a reference instrument.

4 Publications

4.1 Radon transport in different environments

While radon is often used as a tracer in different geophysical applications, it is important to understand the processes governing its formation and transport to the Earth's surface. Simultaneously with numerous experimental studies carried out worldwide with the goal of constructing geogenic radon maps of different countries, several theoretical models were applied with the purpose of predicting radon concentration from radium levels in soil gas. However, the Earth's non-homogenous crust and its upper soil layer are responsible for a high level of uncertainty of such applications.

The spatial distribution of radon in soil gas and its exhalation was studied in detail in the area of the Ravne fault in NW Slovenia, a region of recently increased seismic activity. Results are presented in the paper "Radon concentration in soil gas and radon exhalation rate at the Ravne Fault in NW Slovenia". Radon levels at sampling points aligned in five profiles revealed highly heterogeneous distribution, mainly controlled by various levels of permeability within the deformed fault zone.

In addition to the natural environment, radon concentration and radon exhalation rate was investigated on a fly ash pile, regarding its use as a building lot. The study is presented in the paper "Radon potential of a fly ash pile – a criterion for its use as a building lot". In addition, the permeability of fly ash and gamma dose rate were measured. The degree of transport of radon from a fly ash layer to the environment is important due to the enhancement of radium content in the process of coal burning in thermal power plants. Since several disposal sites of fly ash exist in Slovenia, a question emerges as to what the radon potential of a layer of fly ash is and thus what radon risk is expected when using this layer as a building lot. The site chosen was classified as a medium radon risk, according to the German classification, and a normal radon risk, according to the Swedish one.

4.1.1 Scientific paper: "Radon concentration in soil gas and radon exhalation rate at the Ravne Fault in NW Slovenia"

Nat. Hazards Earth Syst. Sci., 10, 895–899, 2010
www.nat-hazards-earth-syst-sci.net/10/895/2010/

Natural Hazards and Earth System Sciences

Radon concentration in soil gas and radon exhalation rate at the Ravne Fault in NW Slovenia

J. Vaupotič[1], A. Gregorič[1], I. Kobal[1], P. Žvab[2], K. Kozak[3], J. Mazur[3], E. Kochowska[3], and D. Grządziel[3]

[1]Jožef Stefan Institute, Ljubljana, Slovenia
[2]Faculty of Natural Sciences and Engineering, University of Ljubljana, Ljubljana, Slovenia
[3]The Henryk Niewodniczañski Institute of Nuclear Physics, Polish Academy of Science, Kraków, Poland

Received: 30 November 2009 – Revised: 15 March 2010 – Accepted: 10 April 2010 – Published: 23 April 2010

Abstract. The Ravne tectonic fault in north-west (NW) Slovenia is one of the faults in this region, responsible for the elevated seismic activity at the Italian-Slovene border. Five measurement profiles were fixed in the vicinity of the Ravne fault, four of them were perpendicular and one parallel to the fault. At 18 points along these profiles the following measurements have been carried out: radon activity concentration in soil gas, radon exhalation rate from ground, soil permeability and gamma dose rate. The radon measurements were carried out using the AlphaGuard equipment, and GammaTracer was applied for gamma dose rate measurements. The ranges of the obtained results are as follows: 0.9–32.9 kBq m^{-3} for radon concentration (C_{Rn}), 1.1–41.9 mBq m^{-2} s^{-1} for radon exhalation rate (E_{Rn}), 0.5–7.4×10^{-13} m^2 for soil permeability, and 86–138 nSv h^{-1} for gamma dose rate. The concentrations of ^{222}Rn in soil gas were found to be lower than the average for Slovenia. Because the deformation zones differ not only in the direction perpendicular to the fault but also along it, the behaviour of either C_{Rn} or E_{Rn} at different profiles differ markedly. The study is planned to be continued with measurements being carried out at a number of additional points.

1 Introduction

Noble radon gas (^{222}Rn) originates from radioactive transformation of ^{226}Ra in the ^{238}U decay chain in the earth's crust. Only a fraction of the radon atoms so created is able to emanate from the mineral grains and enter the void space, filled either by gas or water. From here, radon moves further by diffusion and, for longer distances, by advection dissolved either in water or in carrier gases. Eventually it exhales into the atmosphere. Radon emanation depends mainly on ^{226}Ra content and mineral grain size, its transport in the earth governed by geophysical and geochemical parameters, while exhalation is controlled by hydrometeorological conditions (Etiope and Martinelli, 2002). Radon activity concentration, measured at the surface, either in a thermal spring or in soil gas is a result of a combined effect of the above mentioned parameters. Among diurnal and seasonal variations which are ascribed to the hydrometeorological parameters, sudden changes (either increase or decrease, also called radon anomalies) may be observed in the time series of radon concentration. These have been found to be related to an increase in seismic (King, 1986; Zmazek et al., 2002) or volcanic (Cigolini et al., 2007; Gasparini and Mantovani, 1978) activity of a region, or activity change of a tectonic or geologic fault (Šebela et al., 2010). On the other hand, radon anomalies in the spatial distribution of radon levels in a region have been observed to coincide with the locations of tectonic and geologic faults, either well expressed on the surface or still hidden (Burton et al., 2004; Swakoñ et al., 2005).

The Ravne fault is one of the faults in NW Slovenia responsible for elevated seismic activity along the Soča (Isonzo) river at the Slovenia-Italy border. In this paper, at various distances from the fault, radon (^{222}Rn) activity concentration in soil gas, radon exhalation rate, soil permeability and gamma dose rate were measured in order to estimate the influence of the fault on radon transport, and thus on the levels of the measured parameters.

Correspondence to: A. Gregorič
(asta.gregoric@ijs.si)

Published by Copernicus Publications on behalf of the European Geosciences Union.

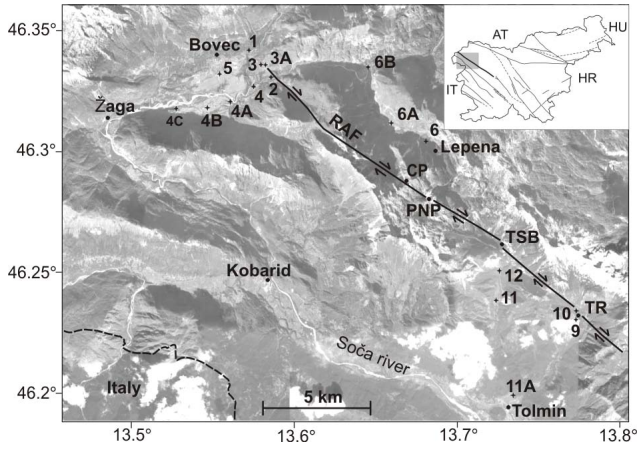

Fig. 1. Location of the Ravne fault with the measurement points indicated. CP – Čez Potoče, PNP – Planina na Polju, RAF – Ravne fault, TR – Tolminske Ravne, TSB – Tolminka Springs basin.

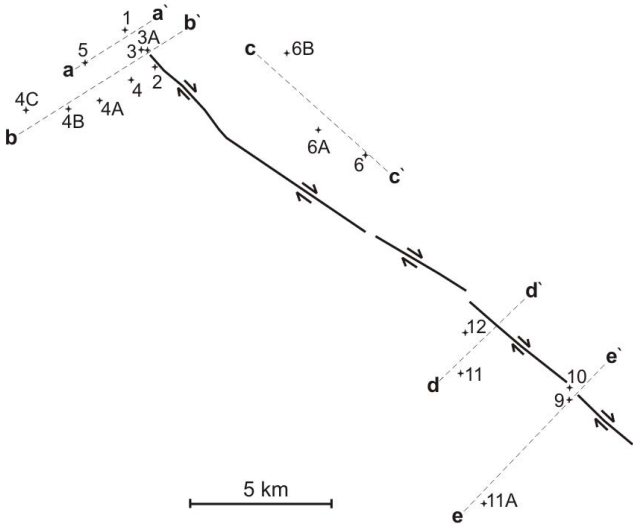

Fig. 2. Measurement profiles.

2 Description of the Ravne Fault

The Ravne Fault is an actively propagating NW-SE trending dextral strike-slip fault in the Julian Alps of NW Slovenia (Fig. 1). Strike-slip displacements on moderate-steep fault planes are responsible for the recent seismic activity that is confined to shallow crustal levels. The fault is growing by interaction of individual right stepping fault segments and breaching of local transtensional step-over zones. The fault geometry is controlled by the original geometry of the NW-SE trending thrust zone, modified by successive faulting within the fault zone. At epicentral depths, the fault system is accommodating recent strain along newly formed fault planes, whereas in upper parts of the crust the activity is distributed over a wider deformation zone that includes reactivated brittle thrust faults. The active deformation along the Ravne fault zone is concentrated in the upper parts of the crust, which is characterized by a high density of older structural elements such as fault planes, fractures and cleavage. The fault is best exposed in its central part around the Tolminka Springs basin over a length of approximately 11 km from the Čez Potoče pass in the NW to the Tolminske Ravne in the SE (Fig. 1) (Kastelic et al., 2008). The Bovec basin, at the north-western end of Ravne fault, is characterised by Triassic and Jurassic carbonates and Cretaceous flysch, covered by fluvio-glacial deposits. The Ravne fault is less exposed to the SE of the Tolminka Springs basin, where it is covered by grass and forested terrain. There are no individual fault planes outcropping between the Tolminka Springs basin and areas SE of Tolminske Ravne. Along that part of the fault trace, the fault exhibits a right-stepping fault segmentation pattern and both segments overstep in the area of Tolminske Ravne.

3 Experimental

3.1 Measurement points

In principle, measurement points were selected on the basis of geology and tectonics of the area. The number of chosen points had to be limited because of mountainous terrain with scarce roads. Some points were not accessible by car, which was necessary to transport equipment. Thus, in total, measurements were performed at 18 points, grouped in five profiles, four perpendicular and one parallel to the fault (Fig. 2).

3.2 Radon in soil gas

The measurement set-up to analyse radon concentration in soil gas C_{Rn} (Bq m^{-3}) consisted of an AlphaGuard PQ 2000 PRO (AG) radon monitor, a soil-gas probe and an Alpha-Pump (AP) (Genitron, Germany) (Fig. 3). Soil gas was pumped through the AG ionization chamber at a flow rate of 0.3 dm^3 min^{-1}. The temporary radon (^{222}Rn) concentrations were registered in one-min intervals over approximately a 20-min period. After initial growth, the concentration became stabilised. The average of the last few stabilised values was taken as the radon concentration in soil gas. At this low flow rate, contribution of thoron (^{220}Rn, half-life 55 s) was negligible (Žunić et al., 2006).

3.3 Radon exhalation from soil

The radon exhalation rate E_{Rn} (Bq m^{-2} s^{-1}) from soil was measured using the Exhalation Box (EB) and the same AG monitor and AP pump as in the previous section (Fig. 4). The air was circulated in the closed circuit for about 90 min and the concentration of radon accumulated in EB was recorded

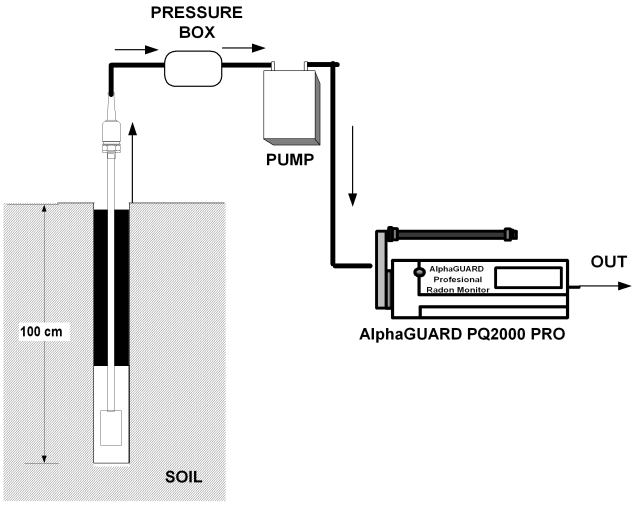

Fig. 3. Soil gas radon measurement.

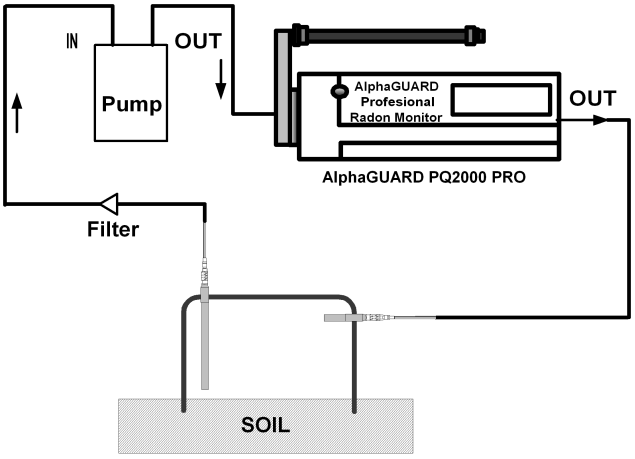

Fig. 4. Radon exhalation measurement.

every 10 min. The exhalation rate was calculated according to the formula:

$$E_{\mathrm{Rn}} = B \cdot \frac{V}{F}$$

where: B – slope of the straight line fixed to the increasing radon concentration points in the EB, V – volume of the EB (m^3), F – surface area covered by EB (m^2) (Žunić et al., 2006).

3.4 Soil permeability

The system to measure soil permeability k_{soil} (m^2) consisted of a Multisensor Unit D/D device (Genitron, Germany) and the same AG monitor, AP pump and soil-gas probe as in Sect. 3.1 (Fig. 5). Soil gas was sucked from soil by soil-gas probe and pumped through the AG and Multisensor. The pressure difference between soil air and open air (ΔP) and flow rate (Q) were measured by the Multisensor D/D. The soil permeability was calculated using a modified equation of Fick's law of diffusion (Janik, 2005):

$$k_{\mathrm{soil}} = \mu \frac{Q}{W \cdot \Delta P}, \quad (1)$$

in which: k_{soil} is soil permeability (m^2), μ is dynamic viscosity of air (Pa s), W is shape parameter of the soil-gas probe (m), Q is soil gas flow rate ($m^3\,min^{-1}$), and ΔP is pressure difference measured (Pa) (Žunić et al., 2006).

3.5 Gamma dose rate

Gamma dose rate $\dot{H}_\gamma$ (nSv h^{-1}) was measured in outdoor air at the height of 1 m above the ground using a GammaTracer TM Wide Type E probe (Genitron, Germany). The values of gamma dose rate were registered in 5-min intervals. The average value of 12–15 records was taken as a final result.

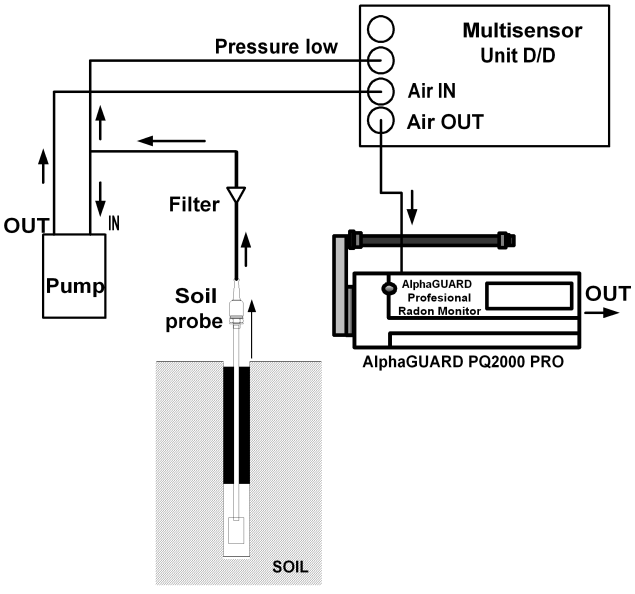

Fig. 5. Soil permeability measurement (Genitron Manual Multisensor D/D).

4 Results and discussion

The results are shown in Table 1. The coordinates and elevations above sea level (a.s.l.) of measurement points together with the dates of measurements are also presented. The measurement points lie from about 350 m to almost 900 m a.s.l. The values of radon concentration in soil gas C_{Rn} were in the range 0.9–22.9 kBq m^{-3} and are lower than the average of 40.1 kBq m^{-3} obtained at 70 points all over Slovenia (Vaupotič, 2009). Also radon exhalation rate E_{Rn} varied substantially from point to point, i.e., from about 1 mBq $m^{-2}\,s^{-1}$ to about 42 mBq $m^{-2}\,s^{-1}$. Soil permeability was found in the range $0.5–7.4\times10^{-13}$ m^2 and may be thus considered as

Table 1. Radon activity concentration in soil gas (C_{Rn}), radon exhalation rate (E_{Rn}), soil permeability (k_{soil}) and gamma dose rate ($\dot{H}_\gamma$) at the Ravne fault.

No	N	E	a.s.l. m	Date in 2008	C_{Rn} kBq m^{-3}	E_{Rn} mBq m^{-2} s^{-1}	k_{soil} m^2	$\dot{H}_\gamma$ nSv h^{-1}
1	20.536	34.414	447	27 Aug	8.4±0.9	15.6±5.0	3.6×10^{-13}	119±6
2	19.853	35.299	894	27 Aug	2.1±0.5	41.9±7.3	3.0×10^{-13}	96±5
3	20.183	34.863	454	27 Aug	16.7±1.2	14.2±4.1	7.4×10^{-13}	110±6
3A	20.155	35.017	459	3 Sep	22.9±3.0	3.0±5.3	7.2×10^{-13}	105±6
4	19.606	34.554	407	27 Aug	9.8±0.7	13.3±4.8	0.5×10^{-13}	104±6
4’	19.646	34.608	400	3 Sep	16.0±2.9	1.1±1.9	4.5×10^{-13}	122±6
4A	19.268	33.756	384	1 Sep	5.0±0.4		3.4×10^{-13}	87±4
4B	19.075	32.907	367	1 Sep	1.8±0.2	8.8±3.5	3.5×10^{-13}	113±6
4C	19.069	31.754	374	1 Sep	4.8±0.5	1.9±2.6	3.5×10^{-13}	114±6
5	19.935	32.290	450	1 Sep	14.8±1.0	40.3±7.1	3.5×10^{-13}	128±6
6	18.249	40.827	648	2 Sep	1.9±0.7	2.2±1.6	4.0×10^{-13}	86±4
6A	18.727	39.577	528	2 Sep	14.7±2.8	15.3±3.3	3.8×10^{-13}	111±6
6B	20.091	38.716	452	3 Sep	2.0±1.0	1.5±1.2	3.7×10^{-13}	86±4
9	13.803	46.292	897	28 Aug	18.9±1.2	9.5±2.9	3.9×10^{-13}	91±5
10	13.998	46.313		28 Aug	8.9±0.8	8.3±3.6	3.8×10^{-13}	87±4
11	14.287	43.385	410	29 Aug	0.9±0.2	7.0±2.3	3.7×10^{-13}	94±5
11A	11.903	44.029	340	29 Aug	9.2±0.7		3.6×10^{-13}	138±7
12	15.027	43.497	509	29 Aug	2.0±0.2	11.7±3.9	6.6×10^{-13}	87±4

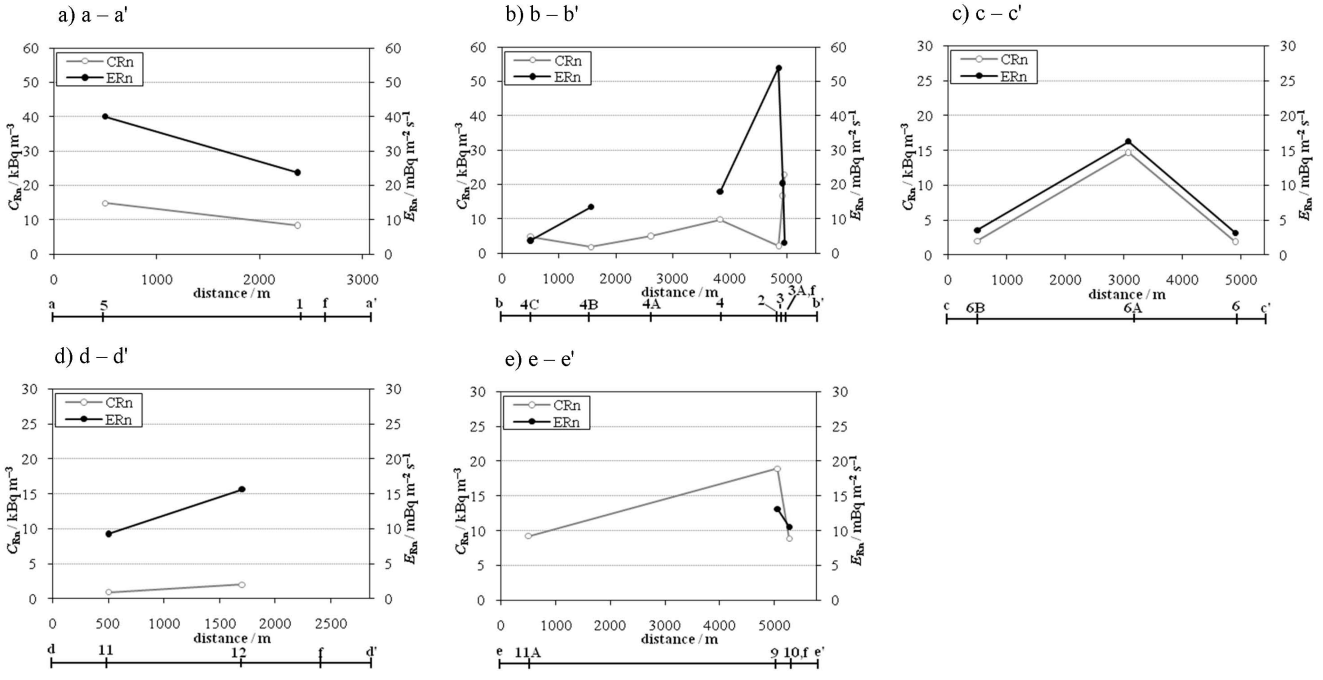

Fig. 6. Radon activity concentrations in soil gas (C_{Rn}) and radon exhalation rate (E_{Rn}) at profile (f – fault): **(a)** a–a’, **(b)** b–b’, **(c)** c–c’, **(d)** d-d’, and **(e)** e–e’.

medium. Gamma dose rate in the range 86–138 nSv h^{-1} is close to the average value obtained for the central part of Slovenia of 118 nSv h^{-1} (Brajnik et al., 1992).

Gas-bearing properties of faults depend on the enhanced permeability of fracture systems. However such permeability is not continuous leading to spotted distribution of soil-gas

anomalies, as shown by Ciotoli et al. (1999). Furthermore, C_{Rn} and E_{Rn} depend also on local characteristics such as thickness of soil covering the underlying deformed rocks. Thus, close to the fault both C_{Rn} and E_{Rn} are lower at the a–a' profile (Fig. 6a) and higher at the d-d' profile (Fig. 6d). The contribution of different stages of rock deformation along the Ravne fault depends locally on the width of the fault deformation zone. Rock fractures could increase radon exhalation from deeper layers and its accumulation in soil (point 5 in the a–a' profile, point 12 in d-d' profile), whereas in the area of intensely deformed rocks, the process of cementation could reduce radon exhalation from deeper layers (point 1 in the a–a' profile and point 10 in the e–e' profile). However deformation zones not only differ in perpendicular direction to the fault but also along its length. Therefore interpretation of radon results is not always possible.

At the b–b' profile (Fig. 6b), where a flat terrain enabled measurements at several distances from the fault, at least on one side of the fault, both C_{Rn} and E_{Rn} appear to be constant in approaching the fault until about 1 km before the fault, where E_{Rn} increases substantially, with a concomitant reduction of C_{Rn} (measurement point 2). The reason for such deviation at measurement point 2 is not understood. At the same time light soil mixed with gravel could also contribute to radon exhalation from the measuring well to the air during the measurement. In close proximity to the fault E_{Rn} is very low, thus enhancing accumulation of radon in soil and consequently increasing C_{Rn}.

The c–c' profile (Fig. 6c) lies along the Lepena valley, parallel to the fault. Higher C_{Rn} and E_{Rn} could be explained by local characteristics of rock deformation and thickness of soil.

5 Conclusions

The results of measurements of radon activity concentration in soil gas, radon exhalation rate from ground, soil permeability and gamma dose rate in the vicinity of Ravne fault in NW Slovenia are presented. The study area was chosen using geological data and the knowledge of fault course.

The concentrations of ^{222}Rn in soil gas were found to be lower than the average for Slovenia. Unlike to the results of similar study (Swakoñ et al., 2005) there was no rapid increase of radon concentration in soil near the fault. Because the deformation zones differ not only in the direction perpendicular to the fault but also along it, the behaviour of either C_{Rn} or E_{Rn} at different profiles differ markedly. Therefore, a full interpretation is very difficult based on the current database. The study is planned to be continued with measurements being carried out at a number of additional points, to build a more complete database to aid interpretation of results. More precise identification of physical characteristics of the ground as well as determination of radium ^{226}Ra in soil profiles would be needed to give a detailed interpretation.

Edited by: T. Przylibski
Reviewed by: two anonymous referees

References

Brajnik, D., Miklavžič, U., and Tomšič, J.: Map of natural radioactivity in Slovenia and its correlation to the emanation of radon, Radiat. Prot. Dosim., 45, 273–276, 1992.

Burton, M., Neri, M., and Condarelli, D.: High spatial resolution radon measurements reveal hidden active faults on Mt. Etna, Geophys. Res. Lett., 31, L07618, doi:10.1029/2003GL019181, 2004.

Cigolini, C., Laiolo, M., and Coppola, D.: Earthquake-volcano interactions detected from radon degassing at Stromboli (Italy), Earth Planet. Sc. Lett., 257, 511–525, 2007.

Ciotoli, G., Etiope, G., Guerra, M., and Lombardi, S.: The detection of concealed faults in the Ofanto Basin using the correlation between soil-gas fracture surveys, Tectonophysics, 301, 321–332, 1999.

Etiope, G. and Martinelli, G.: Migration of carrier and trace gases in the geosphere: an overview, Phys. Earth Planet. In., 129, 185–204, 2002.

Gasparini, P. and Mantovani, M. S. M.: Radon anomalies and volcanic eruptions, J. Volcanol. Geoth. Res., 3, 325–341, 1978.

Janik, M.: Radon transport model and its verification by measurements in houses, IFJ PAN, Krakow, 50–57, 2005.

Kastelic, V., Vrabec, M., Cunningham, D., and Gosar, A.: Neo-Alpine structural evolution and present-day tectonic activity of the eastern Southern Alps: The case of the Ravne Fault, NW Slovenia, J. Struct. Geol., 30, 963–975, 2008.

King, C. Y.: Gas geochemistry applied to earthquake prediction – an overview, J. Geophys. Res.-Solid, 91, 2269–2281, 1986.

Swakoñ, J., Kozak, K., Paszkowski, M., Gradziński, R., Łoskiewicz, J., Mazur, J., Janik, M., Bogacz, J., Horwacik, T., and Olko, P.: Radon concentration in soil gas around local disjunctive tectonic zones in the Krakow area, J. Environ. Radioactiv., 78, 137–149, 2005.

Šebela, S., Vaupotič, J., Koš'ták, B., and Stemberk, J.: Microdisplacements and radon air concentrations in Postojna Cave, Slovenia, J. Cave Karst Stud., in press, 2010.

Vaupotič, J.: Review of radon research in Slovenia, IAEA-TECDOC, 2009.

Zmazek, B., Živčić, M., Vaupotič, J., Bidovec, M., Poljak, M., and Kobal, I.: Soil radon monitoring in the Krško Basin, Slovenia, Appl. Radiat. Isotopes, 56, 649–657, 2002.

Žunić, Z. S., Kobal, I., Vaupotič, J., Kozak, K., Mazur, J., Birovljev, A., Janik, M., Čeliković, I., Ujićć, P., Demajo, A., Krstić, G., Jakupi, B., Quarto, M., and Bochicchio, F.: High natural radiation exposure in radon spa areas: a detailed field investigation in Niška Banja (Balkan region), J. Environ. Radioactiv., 89, 249–260, 2006.

4.1.2 Scientific paper: "Radon potential of a fly ash pile – a criterion for its use as a building lot"

Radon potential of a fly ash pile - a criterion for its use as a building lot

Radonski potencial odlagališča elektrofiltrskega pepela kot merilo za njegovo uporabo kot gradbeno zemljišče

Janja Vaupotič[1,*], Asta Gregorič[1], Krzysztof Kozak[2], Jadwiga Mazur[2], Elzbieta Kochowska[2] & Dominik Grządziel[2]

[1]Jožef Stefan Institute, Department of Environmental Sciences, Radon Center, SI-1000 Ljubljana, Slovenia
[2]Laboratory of Radiometric Expertise, Henryk Niewodniczański Institute of Nuclear Physics, Polish Academy of Sciences, 31-342 Kraków, Poland

*Corresponding author. E-mail: janja.vaupotic@ijs.si

Received: August 3, 2010 **Accepted:** October 2, 2010

Abstract: Radioactivity survey on a fly ash pile was carried out. Concentration of radon (^{222}Rn) in fly ash at a depth of 1 m was in the range of 0.3–46.9 kBq m^{-3}, with arithmetic mean of (23.8 ± 0.2) kBq m^{-3}. Radon exhalation rate was about 24 mBq m^2 s^{-1} on the part of the pile covered with grass, and about 37 mBq m^2 s^{-1} on the part with trees and bushes. Gamma dose rate was about 168 nSv h^{-1} and ash permeability around 3.9 × 10^{-13} m^2 on both parts.

Izvleček: Na odlagališču elektrofiltrskega pepela smo izvedli raziskavo radioaktivnosti. Na globini 1 m smo v elektrofiltrskem pepelu izmerili koncentracije radona (^{222}Rn) 0,3–46,9 kBq m^{-3} s povprečjem (23,8 ± 0,2) kBq m^{-3}. Na s travo poraščenem delu odlagališča smo izmerili hitrost ekshalacije radona okrog 24 mBq m^2 s^{-1}, na delu, kjer odlagališče preraščajo drevesa in grmičevje, pa okrog 37 mBq m^2 s^{-1}. Hitrost doze sevanja gama smo izmerili okrog 168 nSv h^{-1}, prepustnost pepela pa okrog 3,9 × 10^{-13} m^2 na obeh predelih.

Key words: radon, concentration, exhalation rate, gamma dose rate, fly ash
Ključne besede: radon, koncentracija, hitrost ekshalacije, hitrost doze sevanja gama, elektrofiltrski pepel

Original scientific paper

INTRODUCTION

Radon (^{222}Rn) is a radioactive noble gas (α radioactive transformation, half-life, $t_{1/2}$ = 3.82 d) originating from radioactive transformation of radium (^{226}Ra) in the natural radioactive chain of uranium (^{238}U) (NAZAROFF & NERO, 1988). Only a small fraction of radon atoms emanate from the solid and enter the space between mineral grains, from where they migrate through the medium, by both diffusion and advection, and eventually exhale into the atmosphere (ETIOPE & MARTINELLI, 2002). Radon is always accompanied by its short-lived products (^{218}Po, ^{214}Pb, ^{214}Bi and ^{214}Po) formed by its radioactive transformation and appearing in air as nano aerosols. Together, radon and radon short-lived products contribute more than half to the effective dose a member of the general public receives on the world average from all natural radioactive sources (UNSCEAR, 2000) and are a major cause of lung cancer, second only to cigarette smoking (DARBY et al., 2005). Keeping low radon levels in dwellings and at workplaces is therefore a serious social concern and a great scientific challenge.

Radon enters the indoor air mostly from the ground on which a building is standing. Other radon sources, such as outdoor air, building material, burning natural gas and using water, are usually minor if not negligible. It is therefore important where and how the building is constructed. Particularly important is the quality of the basic floor slab and parts of the walls contacting the ground. Obviously, the higher the uranium content in the ground, and, consequently, radon concentration in soil gas, the higher quality is needed to keep radon level in indoor air acceptably low. In this sense, radon concentration in soil gas together with soil permeability, as a measure of radon potential (WIEGAND, 2001; NEZNAL & ŠMARDa, 1996), should be considered when constructing a new, or remodelling an old building. In Germany, KEMSKI et al. (2001) have proposed the following ranking of radon risk with respect to radon concentration in soil: low at <10 kBq m^{-3}, medium at 10–100 kBq m^{-3}, increased at 100–500 kBq m^{-3}, and high radon risk at >500 kBq m^{-3}. In Sweden, the ranking is slightly different: low at <10 kBq m^{-3}, normal at 10–50 kBq m^{-3} and high at >50 kBq m^{-3} (EC, 2005). A classification of soil with respect to radon potential in Slovenia has not been accepted.

Radon potential varies markedly from soil to soil. It is reasonable to expect that it will be higher in the technologically enhanced naturally occurring radioactive material (TENORM). Such are wastes and by-products of technological processes

in which some members in the uranium radioactive chain are concentrated and hence their contents elevated. An example is burning coal in a thermal power plant. As in any material, also in coal, there is certain, though low, level of ^{226}Ra which, after burning, grows concentrated in the fly ash. A question emerges what is the radon potential of a layer of fly ash and thus which radon risk is expected when using this layer as a building lot.

In Slovenia, there are several fly ash disposal sites of various sizes. For this study, a small fly ash pile of well defined geometry was chosen. In addition to radon concentration in fly ash also radon exhalation rate from fly ash, permeability of fly ash and gamma dose rate were measured, and the site was classified according to radon risk. These have been the first such measurements in Slovenia, aimed only at showing as an example how radon potential for this kind of sites may be dealt with.

Materials and methods

Site description

To the site selected as an example for this study, the fly ash of a thermal power plant burning lignite had been disposed of for years. At present it is a 5–7 m thick layer of an approximate 150 m × 200 m surface area.

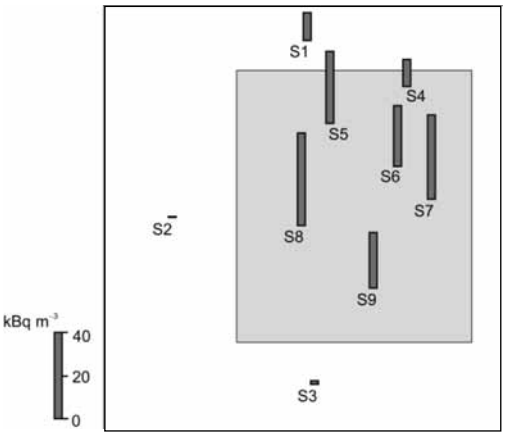

Figure 1. A schematic outline of the fly ash pile: the part covered by grass only is shadowed; measurement points are indicated, with vertical bars representing radon concentration in ash-gas.

A gamma spectrometric analysis of an averaged dry ash sample had shown the following concentrations of radionuclides (Bq kg^{-1}): ^{238}U: 200 ± 26, ^{232}Th: 37 ± 8, ^{226}Ra: 237 ± 8, ^{210}Pb: 102 ± 14, ^{40}K: 410 ± 23. For comparison, the following ranges were found in the terra rossa soil in various points in the karstic area: ^{238}U: 52–70, ^{226}Ra: 53–74, ^{40}K: 320–450, (Vaupotič et al., 2007a). A small part of the pile is a glade covered with grass only, while the rest, with dense bushes and trees (Figure 1). Complete measurements of all the parameters were carried out only in the former part because the movement of the equipment (except of scintillation cells) to the latter was practically impossible.

Radon in fly ash

To measure radon concentration (C_{Rn}/(Bq m^{-3})) in the ash-gas (gas contained in the bulk of fly ash) an AlphaGuard radon monitor and alpha scintillation cells were used. Because the cells showed similar values and are, in addition, more simple to move and use, only at two points in the part covered with grass the AlphaGuard monitor was used and the cells everywhere else.

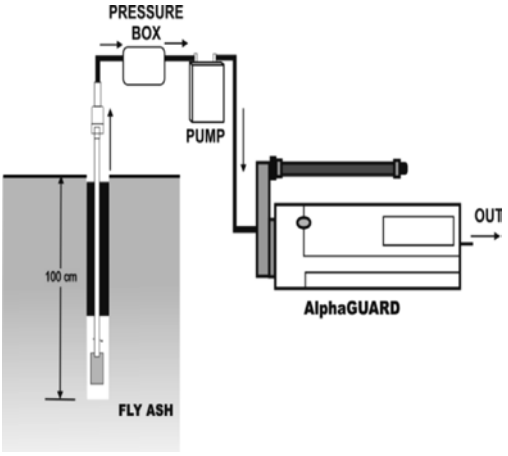

Figure 2. Schematic set-up for measuring radon concentration in ash-gas.

1. AlphaGuard

The measurement set-up to analyse radon concentration in soil gas consisted of an AlphaGuard PQ 2000 PRO (AG) radon monitor, a soil-gas probe and an AlphaPump (AP) (Genitron, Germany) (Figure 2). A borehole of 7 cm diameter was hand-drilled into the fly ash to a depth of 100 cm. The soil-gas probe was inserted to the bottom and the rubber ring around it inflated to isolate the bottom part of the borehole from the outdoor air. Soil gas was then pumped from the bottom through the AG ionization chamber at a flow rate of 0.3 dm^3 min^{-1}. The temporary radon (^{222}Rn) concentration was registered in one-minute intervals over approximately a 20-minute period. After initial growth, the concentration became stabilised. The average of the last few stabilised values was taken as the radon concentration in soil gas. At this low flow rate, contribution of thoron (^{220}Rn, half-life 55 s) was negligible (ŽUNIĆ et al., 2006).

2. Alpha scintillation cells

For this experiment, the Spanish 0.3 dm^3 alpha scintillation cells were used (QUINDOS-PONCELA et al., 2003). After the measurement with the AlphaGuard had been finished, a cell was connected to the soil-gas probe and pump, and ash-gas was flushed through the cell at a flow rate of 1 dm^3 min^{-1} for 3 minutes, necessary to exchange the air in the cell by the ash-gas sample. In a time longer than three hours, when the secular equilibrium between radon and its short-lived products had been reached, gross alpha activity of ^{222}Rn, ^{218}Po in ^{214}Po was measured in an PRM 145 α-counter (AMES, Ljubljana) (Figure 3). Cell efficiencies are from 0.000218 s^{-1} Bq^{-1} m^3 to 0.000428 s^{-1} Bq^{-1} m^3 and their background from 0.1 min^{-1} to 0.5 min^{-1}, thus assuring a lower limit of detection from 50 Bq m^{-3} to 110 Bq m^{-3} at counting times of 15 min.

Figure 3. Alpha counter with a scintillation cell.

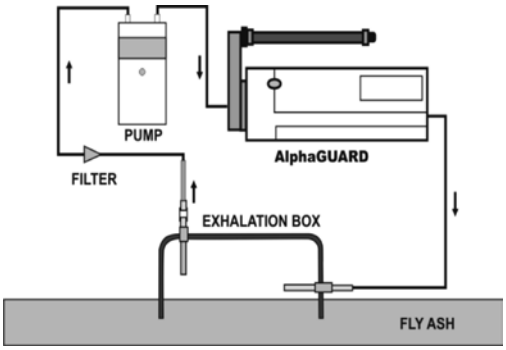

Figure 4. Schematic set-up for measuring radon exhalation rate from fly ash.

Radon exhalation from fly ash

The radon exhalation rate E_{Rn}/(Bq m^{-2} s^{-1}) from soil was measured using the Exhalation Box (EB, dimensions 0.7 m × 0.7 m × 0.2 m) and the same AG monitor and AP pump as in the previous section (Figure 4). The air was circulated in the closed circuit for about 90 min and the concentration of radon accumulated in EB was recorded every 10 min. The exhalation rate was calculated using the formula:

$$E_{Rn} = B \times \frac{V}{F} \quad (1)$$

in which: B – slope of the straight line fixed to the increasing radon concentration points in the EB, V/m^3 – volume of the EB, F/m^2 – surface area covered by EB (Žunić et al., 2006).

Fly ash permeability

The system to measure fly ash permeability k_{ash}/m^2 at 1 m depth consisted of a Multisensor Unit D/D device (Genitron, Germany) and the same AG monitor, AP pump and soil-gas probe as for measuring radon concentration (Figure 5). Ash-gas was sucked from soil by soil-gas probe and pumped through the AG and Multisensor. The pressure difference (ΔP) between ash and open air, and flow rate of ash-gas (Q) were measured by the Multisensor D/D. The fly ash permeability was calculated using a modified equation of Fick's law of diffusion (Janik, 2005):

$$k_{ash} = \mu \frac{Q}{W \times \Delta P} \quad (2)$$

in which: k_{ash}/m^2 – permeability of fly ash, μ – dynamic viscosity of air (Pa s), W/m – shape parameter of the soil-gas probe, Q/(m^3 min^{-1}) – gas flow rate and ΔP/Pa – pressure difference measured (Žunić et al., 2006).

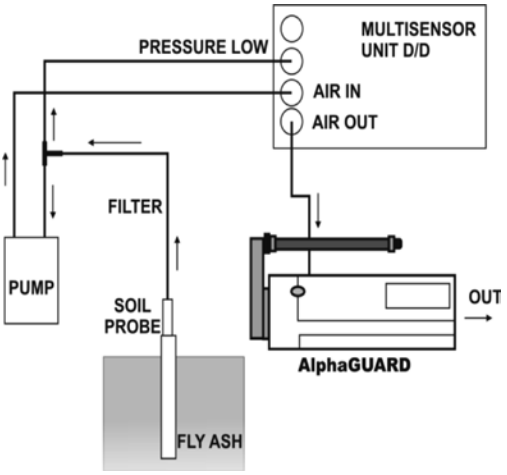

Figure 5. Schematic set-up for measuring fly ash permeability.

Gamma dose rate

Gamma dose rate $\dot{H}_\gamma$/(nSv h^{-1}) was measured in outdoor air at the height of 1 m above the ground using a Gamma-Tracer TM Wide Type E probe (Genitron, Germany). The values of gamma dose rate were registered in 5-min intervals. The average value of 12–15 records was taken as a final result.

RESULTS AND DISCUSSION

Figure 6 shows the initial increase in readings when measuring radon concentration in the ash-gas with the AlphaGuard monitor. A time of about 20 min was needed to reach the correct, saturated value, taken as the results for C_{Rn}. Accumulation of radon under the exhalation box during exhalation rate measurements is presented in Figure 7. The initial slope of the curve was used to calculate E_{Rn} (in this case (10 ± 1.2) Bq m^{-3} min^{-1}).

Values of radon concentration in ash-gas are given in Table 1, together with radon exhalation rate, fly ash permeability and gamma dose rate. Based on good agreement between radon concentrations obtained with both devices in boreholes 1 and 6 (less than 15 % difference) we decided to use the AlphaGuard monitor only at two points easily accessible for the equipment, and scintillation cells everywhere else. Except at points 2 and 3, concentrations were in the range from about 10 kBq m^{-3} to about 45 kBq m^{-3}, with an average of (23.8 ± 0.2) kBq m^{-3}. This is similar as in gravel deposits and lake sediments (38.1 kBq m^{-3} and 20.3 kBq m^{-3}, respectively) but lower than at carbonates (50.4 kBq m^{-3}) in Slovenia (VAUPOTIČ et al., 2007b; VAUPOTIČ et al., 2008), although ^{226}Ra concentration in fly ash is about four times higher, and therefore higher radon concentration would be expected, than in an ordinary soil (VAUPOTIČ et al., 2007a). The lowest two values (points 2 and 3) belong to boreholes at the very edge of the pile where the ash layer was thinner. Differences in values among points (except 2 and 3) are normal, as it is well known that even at a homogeneous distribution of ^{226}Ra, radon levels may differ markedly from borehole to borehole because of micro fractures in the ground (DURRANI

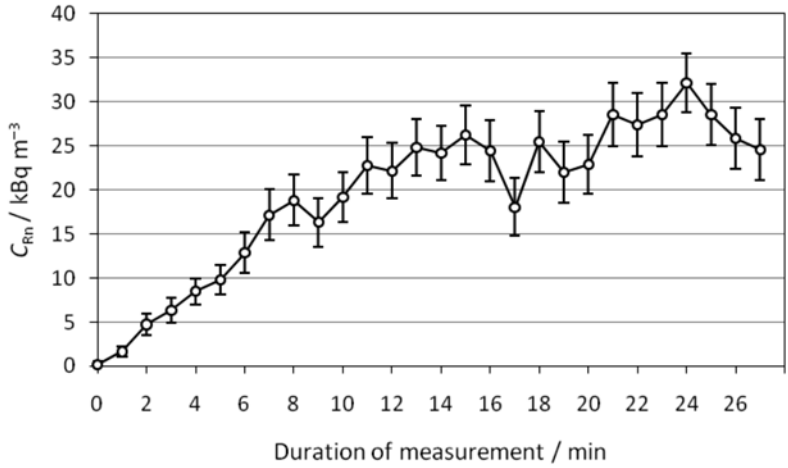

Figure 6. Initial increase in readings (S6) when measuring radon concentration in the ash-gas with the AlphaGuard monitor.

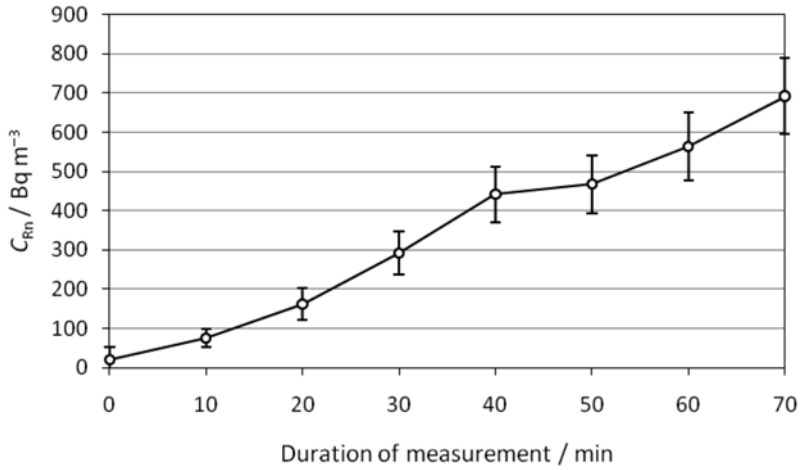

Figure 7. Accumulation of radon under the exhalation box during exhalation rate measurements (S1).

& Badr, 1995; Baixeras et al., 1996; Kemski et al., 2001; Winkler et al., 2001; Iakovleva & Ryzhakova, 2003; Vaupotič et al., 2007a). Point 4 is at the same level as other points but only 1 m or so away from the steep edge of the pile. We may speculate that atmospheric air may penetrate horizontally into the borehole, diluting the ash-gas and thus reducing radon concentration. Such a situation has not been observed at point 7 where radon concentration was second the highest. Although the radon exhalation rate is similar as

somewhere else in Slovenia (VAUPOTIČ et al., 2010; VAUPOTIČ et al., 2007b) it is higher at point 1 (36.9 mBq m^{-2} s^{-1}) than at point 8 on glade (24.2 mBq m^{-2} s^{-1}), most probably because the roots of trees and bushes here break up the bulk structure of the pile and thus enhance radon diffusion (MOLDRUP et al., 2000). Also the permeability of fly ash does not differ from that measured at other places (VAUPOTIČ et al., 2010; VAUPOTIČ et al., 2007b). It is practically the same at point 1 and 6, thus pointing out that higher exhalation rate at point 1 is due to enhanced diffusion (MOLDRUP et al., 2000) and not higher advection in the ash.

Gama dose rate of 168 nSv h^{-1} is about 50 % higher than over a nearby ground and about 15 % (27 nSv h^{-1}) lower than over the Pohorje granite (195 nSv h^{-1}) (BRAJNIK et al., 1992).

With respect to radon concentration in ash-gas (never exceeding 50 Bq m^{-3}), this fly ash pile may be considered as a building lot with a normal radon risk according to the Swedish (EC, 2005) and a medium radon risk according to the German (KEMSKI et al., 2001) classification. This classification is conservative, because the measurements were carried out in summer after a long period of dry weather when radon concentration is higher than it would be in wet condition (HOSODA et al., 2007; PAPACHRISTODOULOU et al., 2007).

CONCLUSIONS

Concentration of radon in ash-gas was in the range of 0.3–46.9 kBq m^{-3}, with arithmetic mean of (23.8 ± 0.2) kBq m^{-3}, and radon exhalation rate about 24 mBq m^2 s^{-1} on the part of the pile cov-

Table 1. Radon concentration (C_{Rn}), obtained with alpha scintillation cells and AlphaGuard monitor, radon exhalation rate (E_{Rn}), permeability of fly ash (k_{ash}) and gamma dose rate ($\dot{H}_{\gamma}$) on the fly ash pile.

Meas. point	C_{Rn}/(kBq m^{-3}) Scintillation cell	C_{Rn}/(kBq m^{-3}) AlphaGuard	E_{Rn}/(mBq m^{-2} s^{-1})	k_{ash}/m^2	$\dot{H}_{\gamma}$/(nSv h^{-1})
S1	13.6 ± 0.3	15.5 ± 2.9	36.9 ± 4.9	3.7×10^{-13}	166
S2	0.3 ± 0.05				
S3	1.2 ± 0.08				
S4	13.0 ± 0.4				
S5	37.0 ± 0.6				
S6	30.8 ± 0.6	26.5 ± 3.3		4.0×10^{-13}	169
S7	42.8 ± 0.6				
S8	46.9 ± 0.7		24.2 ± 2.5		
S9	28.9 ± 0.5				

ered with grass, and about 37 mBq m^2 s^{-1} on part with trees and bushes. According to the German classification the pile may be considered as a building lot with medium radon risk, and according to the Swedish, normal radon risk.

Acknowledgements

This work was financially supported by the Slovenian Research Agency within the project "Physico - chemical processes involved in formation of radioactive nano aerosols" (contract number J1-0745).

References

Baixeras, C., Bacmeister, G. U., Climent, H., Albarracin, D., Enge, W., Freyer, K., Treutler, H. C., Jonsson, G., Ghose, R., Monnin, M. M., Font, L., Devantier, R., Seidel, J. L., Sciocchetti, G. & Cotellessa, G. (1996): Report on the first phase activity of an EU project concerning coordinated radon measurements in five European countries. *Environ. Int.;* Vol. 22, pp. S687–S697.

Brajnik, D., Miklavžič, U. & Tomšič, J. (1992): Map of natural radioactivity in Slovenia and its correlation to the emanation of radon. *Radiat. Prot. Dosim.;* Vol. 45, pp. 273–276.

Darby, S., Hill, D., Auvinen, A., Barrios-Dios, J. M., Baysson, H., Bochicchio, F., Deo, H., Falk, R., Forastiere, F., Hakama, M., Heid, I., Kreienbrock, L., Kreuzer, M., Lagarde, F., Makelainen, I., Muirhead, C., Oberaigner, W., Pershagen, G., Ruano-Ravina, A., Ruosteenoja, E., Rosario, A. S., Tirmarche, M., Tomasek, L., Whitley, E., Wichmann, H. E. & Doll, R. (2005): Radon in homes and risk of lung cancer: collaborative analysis of individual data from 13 European case-control studies. *Br. Med. J.;* Vol. 330**,** No. 7485, pp. 223–226.

Durrani, S. A. & Badr, I. (1995): Geostatistically controlled field-study of radon levels and the analysis of their spatial variation. *Radiat. Meas.;* Vol. 25**,** No. 1–4, pp. 565–572.

EC (2005): An overview of radon surveys in Europe, European Commission.

Etiope, G. & Martinelli, G. (2002): Migration of carrier and trace gases in the geosphere: an overview. *Phys. Earth. Planet. In.;* Vol. 129**,** No. 3–4, pp. 185–204.

Hosoda, M., Shim, M., Sugino, M., Furukawa, M. & Fukushi, M. (2007): Effect of soil moisture content on radon and thoron exhalation. *J. Nucl. Sci. Technol.;* Vol. 44**,** No. 4, pp. 664–672.

Iakovleva, V. S. & Ryzhakova, N. K. (2003): Spatial and temporal variations of radon concentration in soil air. *Radiat. Meas.;* Vol. 36**,** No. 1–6, pp. 385–388.

Janik, M. (2005): Radon transport model and its verification by measurements in houses. 1966/AP, IFJ PAN, Krakow.

Kemski, J., Siehl, A., Stegemann, R. & Valdivia-Manchego, M. (2001): Mapping the geogenic radon potential in

Germany. *The Science of The Total Environment;* Vol. 272**,** No. 1–3, pp. 217–230.

Moldrup, P., Olesen, T., Gamst, J., Schjonning, P., Yamaguchi, T. & Rolston, D. E. (2000): Predicting the gas diffusion coefficient in repacked soil: Water-induced linear reduction model. *Soil Sci. Soc. Am. J.;* Vol. 64**,** No. 5, pp. 1588–1594.

Nazaroff, W. W. & Nero, A. V. (1988): *Radon and its decay products in indoor air*. New York: John Wiley & Sons.

Neznal, M. & Šmarda, J. (1996): Assessment of radon potential of soils - A five-year experience. *Environ. Int.;* Vol. 22, pp. S819–S828.

Papachristodoulou, C., Ioannides, K. & Spathis, S. (2007): The effect of moisture content on radon diffusion through soil: Assessment in laboratory and field experiments. *Health Phys.;* Vol. 92**,** No. 3, pp. 257–264.

Quindos-Poncela, L. S., Fernandez, P. L., Sainz, C., Arteche, J., Arozamena, J. G. & George, A. C. (2003): An improved scintillation cell for radon measurements. *Nuclear Instruments & Methods in Physics Research Section a-Accelerators Spectrometers Detectors and Associated Equipment;* Vol. 512**,** No. 3, pp. 606–609.

UNSCEAR (2000): Sources and effects of Ionizing radiation. UNSCEAR 2000 Report to the General assembly, with Scientific Annexes. Vol. 1.

Vaupotič, J., Barišić, D., Kobal, I. & Lulić, S. (2007a): Radioactivity and radon potential of the terra rossa soil. *Radiat. Meas.;* Vol. 42**,** No. 2, pp. 290–297.

Vaupotič, J., Gregorič, A., Kobal, I., Žvab, P., Kozak, K., Mazur, J., Kochowska, E. & Grządziel, D. (2010): Radon concentration in soil gas and radon exhalation rate at the Ravne Fault in NW Slovenia. *Nat. Hazards Earth Syst. Sci.;* Vol. 10**,** No. 4, pp. 895–899.

Vaupotič, J., Žvab, P., Gregorič, A., Kobal, I., Kocman, D., Kotnik, J. & Križman, M. (2008): Radon mapping in Slovenia based on its levels in soil gas. In: *33rd International Geological Congress;,* 6–14 August 2008, Oslo, Norway, Abstracts.

Vaupotič, J., Žvab, P., Gregorič, A., Kobal, I., Kocman, D., Kozak, K. & Mazur, J. (2007b): Soil gas radon potential on radon prone areas. Report–9694, Jožef Stefan Institute, Ljubljana.

Wiegand, J. (2001): A guideline for the evaluation of the soil radon potential based on geogenic and anthropogenic parameters. *Environ. Geol.;* Vol. 40**,** No. 8, pp. 949–963.

Winkler, R., Ruckerbauer, F. & Bunzl, K. (2001): Radon concentration in soil gas: a comparison of the variability resulting from different methods, spatial heterogeneity and seasonal fluctuations. *Sci. Total Environ.;* Vol. 272**,** No. 1–3, pp. 273–282.

Žunić, Z. S., Kobal, I., Vaupotič, J., Kozak, K., Mazur, J., Birovljev, A., Janik, M., Čeliković, I., Ujić, P., Demajo, A., Krstić, G., Jakupi, B., Quarto, M. & Bochicchio, F. (2006): High natural radiation exposure in radon spa areas: a detailed field investigation in Niška Banja (Balkan region). *J. Environ. Radioactiv.;* Vol. 89**,** No. 3, pp. 249–260.

4.2 Radon as a tracer for geophysical processes in the Earth's crust

Radon is one of many geophysical and geochemical phenomena that can be considered to be an earthquake precursor. Due to the large number of processes in the Earth's crust that control the spatial and temporal distribution of seismic events, the question about the predictability of earthquakes often arises. Nevertheless, radon has often been found as an efficient earthquake precursor and many studies report anomalous patterns of radon fluctuation prior to earthquakes. The major problem that arises with measurements in the shallow soil levels is how to eliminate the perturbing effect of atmospheric parameters on eventual radon variations caused by geophysical processes.

The basic principle of earthquake precursor studies is to learn from past observations and efficiently apply this knowledge to present data. Therefore, much energy and time has to be devoted to preliminary studies to discover the appropriate location for long-term measurements. Two measurement locations in thermal water, at Bled and Hotavlje, and their sensitivity to seismic events are presented in the paper "Radon concentration in thermal water as an indicator of seismic activity". A high radon concentration in thermal water and its fluctuation was observed at Hotavlje, showing an intensive response to weak earthquakes nearby. Although radon levels in thermal water at Bled were much lower and more stable, a significant anomalous pattern of radon fluctuation was observed during the period of increased seismic activity.

Different approaches for differentiating between those anomalies in radon time series caused by seismic activity and those caused solely by hydrometeorological parameters are combined and evaluated in the book chapter "Radon as an earthquake precursor − methods for detecting anomalies". Among four different approaches – standard deviation from the related mean value, the correlation between time gradients of barometric pressure and radon concentration, artificial neural networks and decision trees – the most promising results were achieved by using decision trees and artificial neural networks. Machine learning methods enable the simultaneous incorporation of all of the available environmental parameters, which might influence radon concentration in soil gas or water.

4.2.1 Scientific paper: "Radon concentration in thermal water as an indicator of seismic activity"

Coll. Antropol. **32** (2008) Suppl. 2: 95–98
Original scientific paper

Radon Concentration in Thermal Water as an Indicator of Seismic Activity

Asta Gregorič, Boris Zmazek and Janja Vaupotič

Radon Center, Department of Environmental Sciences, »Jožef Stefan« Institute, Ljubljana, Slovenia

A B S T R A C T

Radon concentration in thermal springs at Hotavlje and Bled has been measured from October 2005 to June 2008 and from October 2005 to September 2007, respectively. At both locations several anomalies in radon concentration were observed, that might have been caused by seismic events. In this study all earthquakes with ratio (D/R) between strain radius (D) and distance to the epicenter (R) greater than 0.5 were taken into account. Five earthquakes occurred in the vicinity of Bled in this period, the strongest at a distance of 17 km with the magnitude M_L=3.8 and four radon anomalies were observed. At Hotavlje fourteen earthquakes occurred in the vicinity with D/R ratio from 0.5 to 2.9. During this period three radon anomalies were observed.

Key words: *radon, anomalous radon level, thermal water, earthquakes*

Introduction

Earthquakes cause severe human disasters in many parts of the world. The large amount of energy released by an earthquake can lead to great loss of life and property, especially if the earthquake is located near big cities[1]. The greatest worldwide seismic hazard is the ground shaking and the greatest risk is the structural damage that results from this ground motion. On the other hand, secondary effects, such as landslides and tsunamis triggered by the ground motion, may even cause far greater loss of life and property. Therefore, earthquake precursors have been intensively sought in order to forecast increasing seismic activity – one of the precursors is radon.

Radon (^{222}Rn) can be transported effectively from deep layers of the Earth to the surface by carrier gases and by water[2–3]. This transport is affected by phenomena accompanying seismic events[4–6]. If radon in a thermal water spring is monitored for a long period, shortly before, during or after an earthquake, a radon anomaly may be observed[7–9], i.e. a sudden either increase or decrease in radon activity concentration. Radon concentrations of two standard deviations (2σ) above or below average value are considered as an anomaly. Thermal springs and ground waters in Slovenia have therefore been systematically surveyed for radon[10–12].

It is well known that a gas such as ^{222}Rn can be released by rock micro fracturing[13]. Small strains could have major effects on the generation of anomalies at pre-existing fractures and faults[14]. Toutain and Baubron[5] observed that gas transfer within the upper crust is affected by strains less than 10^{-7}, much smaller than those causing earthquakes. Anomalies in water temperature, radon concentration and gas composition are related to both hydrometeorological data and seismic events. For our purpose the radius, D, of the effective precursor manifestation zone in km (also called the »strain radius«) was calculated using Dobrovolsky's equation[15]:

$$D = 10^{0.43M} \qquad (1)$$

for an earthquake of magnitude M, corresponding to a deformation of 10^{-8}. In this study all earthquakes with ratio $D/R > 0.5$ were taken into account, where D is strain radius calculated from equation (1), R is the distance between our measurement site and the epicenter. All earthquakes were detected by the Office of Seismology at the Environmental Agency of the Republic of Slovenia.

The work presented here is a continuation of our previous radon monitoring related to seismic activity carried out on weekly analyses during 1981–82 in thermal waters of the Ljubljana basin[11]. In 1998, measurements

Received for publication July 30, 2008

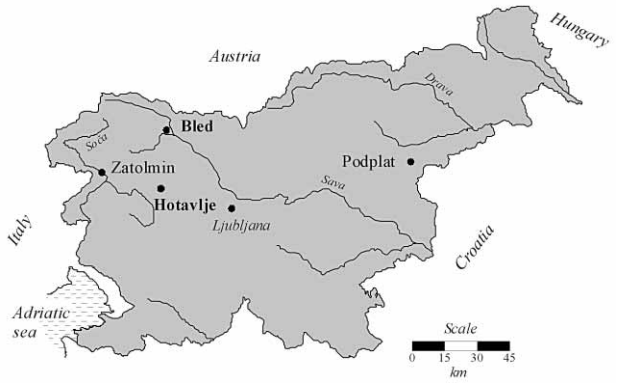

Fig. 1. Map of Slovenia.

were resumed and extended to the tectonically active region close to the Soča (Isonzo) river (north-west Slovenia) (Figure 1). Radon content, electrical conductivity and temperature were measured continuously[12] at Bled and Zatolmin, as well as at Podplat near Rogaška Slatina as a reference point. In 2003, radon measurements were started at Hotavlje village, some 30 km to the south of Bled. In this paper, we focus on radon anomalies in thermal springs at Hotavlje and Bled in the period from October 2005 to June 2008 and from October 2005 to September 2007, respectively.

Geologic setting

There are only a few thermal springs in the seismically active area along the Soča River, the closest and most easily accessible ones being at Bled and Hotavlje. In contrast, there are many thermal springs in east Slovenia, but this area exhibits lower seismic activity.

The recent geotectonic setting in Slovenia is a cumulative result of Tethyan evolution, where recent dynamics are determined by the closure of the Tethys and the collision of several lithospheric units. Slovenia lies at the junction of three tectonic plates (European, Adriatic and Tiszian), which were amalgamated during the Tertiary period[16].

The thermal spring at Bled wells on the Bled fault on the eastern side of Lake Bled (46.37N, 14.11E) which belongs to Southern Alps. Water springs from a deep Triassic carbonate reservoir and rises through Oligocene clay and shallower Quaternary Lake and glacial sediment. Thermal water is used in the swimming pool of the Toplice Hotel and is characterized by a constant temperature of 21.82 ± 0.01 °C and by active bubbling[17].

The thermal spring at Hotavlje (46.12N, 14.08E) is situated at the bank of a small stream near the Hotavlje village. Water temperature is constant at 20.22 ± 0.04 °C and wells on the fault in Main dolomite oriented along the valley of Kopačnica. The water is of meteoric origin. Meteoric water trickles through the rocks to deeper layrs, where it accumulates and warms up and is then raised again with convective flow through fault zones[18].

Materials and Methods

Radon activity concentration (shortly concentration, C_{Rn} in Bq m^{-3}) in water was measured with the Barasol probe (MC-450, ALGADE, France)[19]. The probe gives C_{Rn} based on alpha spectrometry of radon decay products in the energy range of 1.5–6 MeV, using an implanted silicon detector. The sensitivity is 50 Bq m^{-3} and sampling frequency once per hour. In addition to radon concentration, the probe also records temperature and barometric pressure. Values of all measured parameters are stored in the inner memory and later transferred to a PC for evaluation. Instruments are regularly checked using AlphaGuard radon monitor (Genitron, Germany) as a reference instrument.

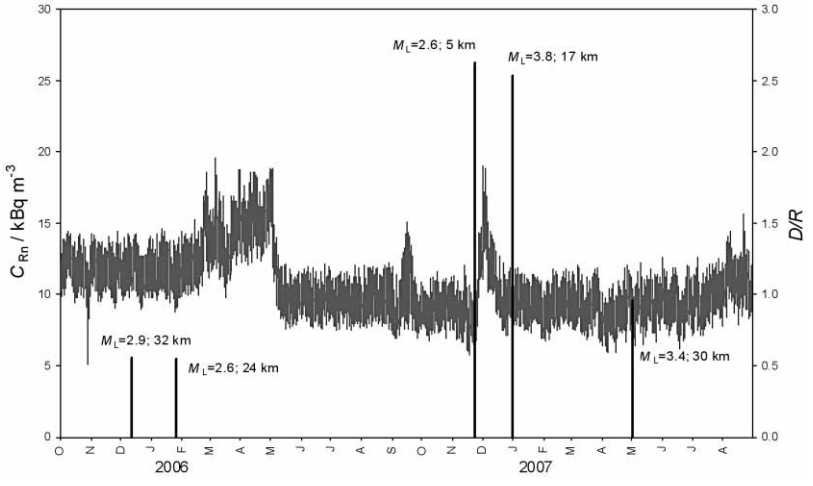

Fig. 2. Radon concentration (C_{Rn}) in thermal water at Bled and D/R ratio (ratio between the strain radius and the distance to the epicenter) for the local earthquakes during the period from October 2005 to September 2007; vertical bars present earthquakes, for which magnitude M_L and the distance between our measurement site and the epicenter are indicated.

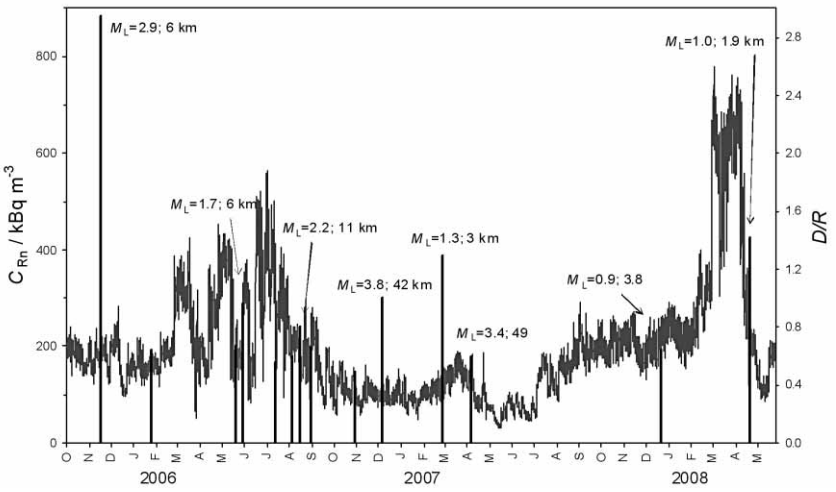

Fig. 3. Radon concentration (C_{Rn}) in thermal water at Hotavlje and D/R ratio (ratio between the strain radius and the distance to the epicenter) for the local earthquakes during the period from October 2005 to June 2008; vertical bars present earthquakes, for which magnitude M_L and the distance between our measurement site and the epicenter are indicated.

Results

The average radon concentration in thermal water at Bled in the period from October 2005 to September 2007 was 10.5 ± 2.1 kBq m^{-3} (Figure 2). Five earthquakes occurred in the vicinity in this period, with D/R ratio from 0.6 to 2.6. The strongest one at a distance of 17 km with M_L=3.8 and D/R=2.5 occurred on January 1, 2007, and the nearest one at a distance of 5 km with M_L=2.6 and D/R=2.6 on November 24, 2006. Four anomalies in radon concentration were observed.

At Hotavlje (Figure 3), the average radon concentration in water in the period from October 2005 to June 2008 was 197 ± 121 kBq m^{-3}. In this period fourteen earthquakes occurred in the vicinity, with D/R ratio from 0.5 to 2.9. The strongest one with M_L=3.8 at a distance of 42 km and D/R=1.0 occurred on January 1, 2007, and the nearest one at a distance of 1.9 km with M_L=1.0 and D/R=1.4, on May 17, 2008. The earthquake with the highest D/R ratio (D/R=2.9) occurred on December 12, 2005, only 45 days after measurements were started. In this period three radon anomalies were observed.

Discussion

The first radon anomaly at Bled was observed immediately after measurements were started, at the end of October 2005. In three days, radon concentration decreased from 11.7 to 5.2 kBq m^{-3}, being about 2.5σ below the average value. This was 45 days before the first of two earthquakes with magnitudes from 2.6 to 2.9 and epicenter distances from 24 to 32 km. A longer anomaly (about 3σ above the average value) followed from the end of February to the beginning of May 2006. The last two anomalies were observed, first one (about 2σ above the average value) in September, two months before earthquake M_L=2.6, and the second (about 3σ over the average value) in December 2006, one month before the strongest earthquake.

At Hotavlje three radon anomalies were observed from October 2005 to June 2008, as mentioned in the previous chapter. There were no anomalies in radon concentration during the short period before the first earthquake on December 12, 2005. Radon concentration raised for the first time in April 2006, however it did not exceed 2σ above the average value. The first radon anomaly was observed in June 2006. Six earthquakes followed in the period from June to September. The second anomaly (2.5σ above the average value) was observed in July 2006, five months before the strongest earthquake. After this anomaly radon concentration remained below the average value. The highest radon anomaly was observed in April 2008 (more than 4σ above the average value). Earthquake with D/R ratio 1.4 occurred on May 17, 2008 in the vicinity of Hotavlje, only few days after radon concentration dropped to the average value.

As in our previous study[19], these data will be further analyzed using machine learning statistical methods, such as decision trees and neuron networks, in order to identify anomalies that cannot be ascribed to environmental parameters, but are probably caused by seismic events.

Conclusion

Although no strong earthquakes have occurred in the period of this study, some radon anomalies were identified that might have been caused by earthquakes. At Bled, an anomaly was observed 3.5 months before the strongest earthquake with M_L=3.8. Five months before the same earthquake an anomaly was also observed at Hotavlje.

These preliminary results are based on simple statistics. Further analysis will be performed, applying decision trees and neuron networks of the machine learning approach. For that purpose, the time series of radon concentration of the whole period of measurements will be considered and not only the period limited in this paper.

Acknowledgements

This study was done within the program P1-0143 and the project PR01-575. The cooperation of personnel of the Toplice Hotel and of the owner of the nearby farm at Hotavlje is appreciated.

REFERENCES

1. LOMNITZ C, Fundamentals of Earthquake Prediction (John Wiley & Sons, New York, 1994). — 2. KRISTIANSSON K, MALMQVIST L, Geophys, 47 (1982) 1444. — 3. ETIOPE G, MARTINELLI G, Phy Earth Planet Inter, 129 (2002) 185. — 4. ULOMOV VI, MAVASHEV BZ, Izv Akad Nauk Uzb SSR, (1971) 188. — 5. TOUTAIN JP, BAUBRON JC, Tectonophys, 304 (1999) 1. — 6. UI H, MORIUCHI H, TAKEMURA Y, TSUCHIDA H, FUJII I, NAKAMURA M, Tectonophys, 152 (1988) 147. — 7. TENG TL, J Geophys Res, 85 (1980) 3089. — 8. HEINECKE J, KOCH U, HEBERT D, MARTINELLI G, Simultaneous measurements of radon and CO_2 in water as a possible tool for earthquake prediction. In: DUBOIS C (Ed) Gas Geochemistry (Science Reviews, University of France, Comté, 1995). — 9. SINGH M, KUMAR M, JAIN RK, CHATRATH RP, Radiat Meas, 30 (1999) 465. — 10. VAUPOTIČ J, KOBAL I, Radiat Prot Dosim, 97 (2001) 265. — 11. ZMAZEK B, VAUPOTIČ J, ŽIVČIĆ M, PREMRU U, KOBAL I, Fizika B, 9 (2000) 111. — 12. ZMAZEK B, ITALIANO F, ŽIVČIĆ M, VAUPOTIČ J, KOBAL I, MARTINELL G, Appl Radiat Isot, 57 (2002) 919. — 13. DONGARRA G, MARTINELLI G, Migration process of radon toward the Earth's surface: implications for the prediction of seismic and volcanic events. In: Proceedings (Scientific Meeting on Seismic Protection, Venezia, 1995). — 14. KING CY, J Geophys Res, 91 (1986) 12269. — 15. DOBROVOLSKY IP, GERSHERZON NI, GOKHBERG MB, Phys Earth Planet Interiors, 57 (1989) 144. — 16. POLJAK M, ŽIVČIČ M, ZUPANČIČ P, Pure Appl Geophys, 157 (2000) 37. — 17. POPIT A, VAUPOTIČ J, DOLENEC T, Ann Geophys, 48 (2005) 73. — 18. POPIT A, Vpliv seizmične aktivnosti na geokemične in geofizikalne lastnosti termalnih vod v Sloveniji. PhD Thesis. In Slov (University of Ljubljana, Ljubljana, 2004). 19. ZMAZEK B, TODOROVSKI L, ŽIVČIĆ M, DŽEROSKI S, VAUPOTIČ J, KOBAL I, Appl Radiat Isot, 64 (2006) 725.

A. Gregorič

»Jožef Stefan« Institute, Jamova 39, 1000 Ljubljana, Slovenia
e-mail: asta.gregoric@ijs.si

KONCENTRACIJA RADONA U TERMALNIM VODAMA KAO INDIKATOR SEIZMIČKE AKTIVNOSTI

SAŽETAK

Koncentracija radona u termalnim izvorima mjerena je na lokacijama Hotavlje i Bled (Slovenija) u razdoblju od listopada 2005.g. do lipnja 2008.g., odnosno od listopada 2005.g. do rujna 2007.g. Na objema lokacijama opaženo je nekoliko odstupanja u koncentraciji radona, koje bi mogle biti uzrokovane seizmičkom aktivnošću. U ovom istraživanju uzeti su u obzir svi potresi u kojima je omjer udaljenosti od epicentra (D) i radijusa područja deformacije (R), D/R veći od 0,5. Pet potresa pojavilo se u okolici Bleda u navedenom periodu, najjači s udaljenošću od epicentra od 17 km, magnitude M_L=3,8, a opažene su četiri anomalije u koncentraciji radona. U okolici područja Hotavlje dogodilo se 14 potresa s omjerom D/R od 0,5 do 2,9, a tijekom ovog razdoblja opažena su tri odstupanja u koncentraciji radona.

4.2.2 Book chapter: "Radon as an earthquake precursor - methods for detecting anomalies"

9

Radon as an Earthquake Precursor – Methods for Detecting Anomalies

Asta Gregorič, Boris Zmazek, Sašo Džeroski,
Drago Torkar and Janja Vaupotič
Jožef Stefan Institute, Ljubljana
Slovenia

1. Introduction

Radon is one of many geophysical and geochemical phenomena that can be considered to be an earthquake precursor. Due to the non-linear dependence of earthquakes' initial conditions, the question about the predictability of earthquakes often arises (Geller, 1997). The successful prediction of earthquakes is yet to be accomplished, in terms of their magnitude, location and time, and much effort has been spent on this goal.

The term "earthquake precursor" is used to describe a wide variety of geophysical and geochemical phenomena that reportedly precede at least some earthquakes (Cicerone et al., 2009). The observation of these types of phenomena is one recent research activity which has aimed at reducing the effects of natural hazards. Among the different precursors, geochemistry has provided some high-quality signals, since fluid flows in the Earth's crust have a widely recognised role in faulting processes (Hickman et al., 1995). The potential of gas geochemistry in seismo-tectonics has been widely discussed by Toutain and Baubron (1999).

In the late 1960s and early 1970s, reports from seismically active countries such as the former USSR, China, Japan and the USA (Ulomov & Mavashev, 1967; Wakita et al., 1980) indicated that concentrations of radon gas in the earth apparently changed prior to the occurrence of nearby earthquakes (Lomnitz, 1994). The noble gas radon (^{222}Rn) originates from the radioactive transformation of ^{226}Ra in the ^{238}U decay chain in the Earth's crust. Since radon is a radioactive gas, it is easy and relatively inexpensive to monitor instrumentally, and its short half-life (3.82 days) means that short-term changes in radon concentration in the earth can be monitored with a very good time resolution. Radon emanation from grains depends mainly on their ^{226}Ra content and their mineral grain size, its transport in the earth being governed by geophysical and geochemical parameters (Etiope & Martinelli, 2002), while exhalation is controlled by hydrometeorological conditions. The stress-strain developed within the Earth's crust before an earthquake leads to changes in gas transport and a rise of volatiles from the deep earth up to the surface (Ghosh et al., 2009; Thomas, 1988), resulting in anomalous changes in radon concentration. The mechanism of observed radon anomalies is still poorly understood, although several theories have been proposed (Atkinson, 1980; King, 1978; Lay et al., 1998; Martinelli, 1991). Over the past three decades, the occurrence of anomalous temporal

changes of radon concentrations has been studied by several authors specialising in soil gas (King, 1984, 1985; Kuo et al., 2010; Mogro-Campero et al., 1980; Planinić et al., 2001; Ramola et al., 2008; Ramola et al., 1990; Reddy & Nagabhushanam, 2011; Walia et al., 2009a; Walia et al., 2009b; Yang et al., 2005; Zmazek et al., 2005; Zmazek et al., 2002b) and groundwater (Barragán et al., 2008; Favara et al., 2001; Gregorič et al., 2008; Heinicke et al., 2010; Kuo et al., 2006; Ramola, 2010; Singh et al., 1999; Zmazek et al., 2002a; Zmazek et al., 2006). However, radon anomalies are not only controlled by seismic activity but also by meteorological parameters like soil moisture, rainfall, temperature and barometric pressure (Ghosh et al., 2009; Stranden et al., 1984). This makes it complicated and, for small earthquakes, often impossible to differentiate between those anomalies caused by seismic events and those caused solely by atmospheric changes. Therefore, the application of theoretical and empirical algorithms for removing meteorological effects is necessary (Choubey et al., 2009; Ramola et al., 2008; Ramola et al., 1988; Torkar et al., 2010; Zmazek et al., 2003). In this chapter, the different approaches to distinguishing between those anomalies in radon time series caused by seismic activity and those caused solely by hydrometeorological parameters are presented and discussed.

2. Radon migration in the Earth's crust

Only a fraction of the radon atoms created by radioactive transformation from radium are able to emanate from mineral grains and enter into the void space, filled either by gas or water. Radon ascends towards the surface mainly through cracks or faults, on a short scale by diffusion and, for longer distances, by advection - dissolved either in water or in carrier gases. Gas movement should be ascribed to the combination of both processes. Diffusive movement is driven by a concentration gradient and is described by Fick's law. Considering gas diffusion in porous media, it is necessary to take into account that the volume through which gas diffuses is reduced and the average path length between two points is increased, thus altering the diffusion coefficient (Etiope & Martinelli, 2002). Nevertheless, the velocity of radon transport in the earth is quite low ($\leq 10^{-3}$ cm/s) and the concentration of radon is reduced by radioactive decay to the background level before even 10 m are traversed (Etiope & Martinelli, 2002; Fleischer, 1981). Diffusion is only important in capillaries and small-pored rocks. On the other hand, the velocity and space scales of advective movements are much higher than those of diffusive ones. Advective transport is driven by pressure gradients, following Darcy's law. The amount of radon itself is, however, too small to form a macroscopic quantity of gas which can react to pressure gradients. Therefore, it must be carried by a macroscopic flow of carrier gases (Kristiansson & Malmqvist, 1982). A gas mixture formed by carrier gases (e.g., CO_2, CH_4, and N_2) and rare gases (e.g., He, Rn) can be referred to as "geogas" (Etiope & Martinelli, 2002; Kristiansson & Malmqvist, 1982). In dry, porous or fractured media, gas flows through an interstitial or fissure space (gas-phase advection) whereas in saturated, porous media gas can dissolve and then be transported in three ways: by groundwater (water-phase advection), by displacing water (gas-phase advection) or by forming a bubble flow by means of buoyancy in aquifers and water-filled fractures. The bubble movement has been theoretically and experimentally recognised as a fast gas migration mechanism governing the distribution of carrier and trace gases over wide areas on the Earth's surface (Vàrhegyi et al., 1992).

2.1 External effects on radon in soil gas and water

Radon concentration in soil, gas or water is not only controlled by geophysical parameters, but it also changes due to other external effects. Meteorological effects – such as soil humidity, rainfall, temperature, barometric pressure and wind – control radon concentrations in soil gas. These parameters change the physical characteristics of soil and rock, thus influencing the rate of radon transport and, consequently, perturbing eventual radon variations caused by geophysical processes originating in the deeper parts of the Earth's crust. Shallow soil levels are more affected by changing meteorological conditions than deeper ones. Radon concentrations with no larger variations present are usually observed at depths of 0.8 m or deeper. Besides the effects of meteorological parameters on radon in soil gas, considerable variations in the gas composition of thermal springs have been shown to be the result of fluctuations of local hydrologic regimes (Klusman & Webster, 1981).

The significant influence of barometric pressure has been discussed by several authors, who clearly pointed out an inverse relationship between barometric pressure and radon concentration in soil gas (Chen et al., 1995; Clements & Wilkening, 1974; Klusman & Webster, 1981). A decrease in barometric pressure, with the values of other environmental parameters remaining constant, generally causes an increase in radon exhalation from the ground, whereas during periods of rising pressure, air with low radon concentration is forced into the ground, thus diluting radon. Temperature-related fluctuations of soil gas radon concentration have also been proven to be very important. Klusman & Jaacks (1987) found an inverse relationship between soil temperature and radon concentration. They suggested that lower air temperatures as compared with soil temperatures during winter months promoted an upward movement of radon by convection, whereas during the summer, lower soil temperatures as compared with air temperatures and an inversion layer below the level of sampling reduces the upward flux and observed concentration. In general, the behaviour of soil gas migration in different types of soil is seasonally dependent (King & Minissale, 1994; Washington & Rose, 1990). In systems where gas movement is driven by diffusion or slow advection processes, radon activity in soil might be controlled by soil moisture and rainfall through the opening of cracks in the surface (Pinault & Baubron, 1996; Toutain & Baubron, 1999). On the other hand, barometric pressure has the major influence on radon concentrations in soils in advective systems, which display generally higher gas flows. However, micro-scale soil heterogeneities in permeability, porosity and lithology can cause significant heterogeneities in the response of radon concentration to changes of atmospheric parameters (King & Minissale, 1994; Neznal et al., 2004). Numerous and often divergent results in studies related to the effect of external factors on soil gas radon concentration suggest that no general predictive model for excluding meteorological effects can be proposed, and studies of radon in soil gas need a simultaneous record of meteorological parameters.

3. Anomalous radon concentration and seismicity

Both mechanisms of radon transport – diffusion and advection – depend on both soil porosity and permeability, which at the same time vary as a function of the stress field (Holub & Brady, 1981). However, migration by diffusion is negligible, where a component of advective long-distance transport exists (Etiope & Martinelli, 2002). The high permeability

of the bedrock and soil in areas of crustal discontinuities, such as fractures and fault zones, promotes intense degassing fluxes, which causes higher soil gas radon concentrations on the ground surface above active fault zones. Although several measurements, experiments and models have been performed, the understanding of the mechanism of radon anomalies and their connection to earthquakes is still inadequate (Chyi et al., 2010; King, 1978; Ramola et al., 1990). Before the earthquake stress in the Earth's crust builds up causing a change in the strain field; the formation of new cracks and pathways under the tectonic stress leads to changes in gas transport and a rise in volatiles from the deep layers to the surface. In fact, fluids play a widely recognised role in controlling the strength of crustal fault zones (Hickman et al., 1995). Anomalous changes of radon concentration are closely linked to changes in fluid flow and, therefore, also to highly permeable areas along fault zones. Large faults are not discrete surfaces but rather a braided array of slip surfaces encased in a highly fractured and often hydrothermally altered transition – or "damage" – zone. Episodic fracturing and brecciation are followed by cementation and crack healing, leading to cycles of permeability enhancement and reduction along faults (Hickman et al., 1995).

Several mechanisms have been proposed, which could explain the relationship between radon anomalies and earthquake. Two models of earthquake precursors are discussed by Mjachkin et al. (1975), with a common principle: at a certain preparation stage, a region of many cracks is formed. According to the dilatancy-diffusion model (Martinelli, 1991; Mjachkin et al., 1975), the increase in tectonic stress causes the extension and opening of favourably-oriented cracks in a porous, cracked, saturated rock. Water flows into the opened cracks, drying the rock near each pore and finally resulting in a decrease of pore pressure in the total earthquake preparation zone. Water from the surrounding medium diffuses into the zone. The increased water-rock surface area, due to cracking, leads to an increase in radon transfer from the rock matrix to the water. At the end of the diffusion period, the appearance of pore pressure and the increased number of cracks leads to the main rupture. According to the crack-avalanche model (Mjachkin et al., 1975), the increasing tectonic stress leads to the formation of a cracked focal rock zone, with slowly altering volume and shape. At a certain stage – when the whole focal zone becomes unstable – the cracks quickly concentrate near the fault surface, triggering the main rupture. An alternate mechanism for earthquake precursory study, based on stress-corrosion theory, has been proposed by Anderson and Grew (1977). According to them, the observed radon anomalies are due to slow crack growth controlled by stress corrosion in a rock matrix saturated by ground waters. King (1978) has proposed a compression mechanism for radon release, whereby anomalous high radon release may be due to an increase of crustal compression before an impending earthquake, that squeezes out soil gas into the atmosphere at an increasing rate.

Toutain and Baubron (1999) observed that gas transfer within the upper crust is affected by strains less than 10^{-7}, much smaller than those causing earthquakes. According to Dobrovolsky (1979), the radius of the effective precursory manifestation zone depends on the earthquake magnitude and can be calculated using the empirical equation:

$$R_D = 10^{0.43 \times M_L} \tag{1}$$

Where R_D is the strain radius in km and M_L is the magnitude of the earthquake. Considering the Earth's crust to be an anisotropic medium, this law can be modified according to the

effective sensitivity to the impending earthquake. The ideal circle with its theoretical radius can be transformed into an ellipse or characterised by shadow areas where no precursory phenomena are observable due to crustal anisotropy, discontinuities or loose contacts along some faults, which prevent further stress transfer (İnan & Seyis, 2010; Martinelli, 1991).
Although radon anomalies can be studied in soil gas and thermal waters, thermal waters could be much more representative of the geologic environment and could be more reactive to stress/strain changes acting at depth than soil gases. The disadvantage of soil gases lie in weak gas concentrations, generally due to the thickness of the sedimentary cover and the high level of atmospheric perturbations (Toutain & Baubron, 1999).

4. Methods for detecting anomalies in radon time series

An anomaly in radon concentration is defined as a significant deviation from the mean value. Due to the high background noise of radon time series, it is often impossible to distinguish an anomaly caused solely by a seismic event from one resulting from meteorological or hydrological parameters. For this reason, the implementation of more advanced statistical methods in data evaluation is important (Belyaev, 2001; Cuomo et al., 2000; Negarestani et al., 2003; Sikder & Munakata, 2009; Steinitz et al., 2003). In our research, radon has been monitored in several thermal springs (Gregorič et al., 2008; Zmazek et al., 2002a; Zmazek et al., 2006) and in soil gas (Zmazek et al., 2002b) and different approaches to distinguishing radon anomalies were applied.

4.1 Standard deviation

A very common practice in determining radon anomalies is the use of standard deviation. The average radon concentration is calculated for different periods with regard to the nature of yearly cycles of radon concentration. In the case of radon in soil gas, the mean value of radon concentration is calculated separately for four seasons (spring, summer, autumn and winter) based on the air and soil temperature.

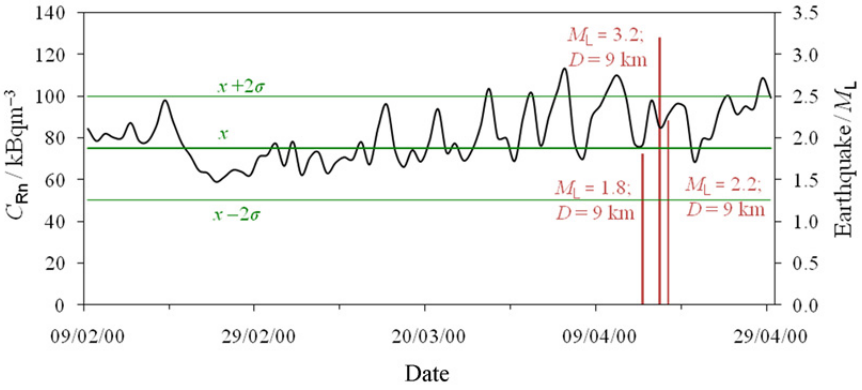

Fig. 1. Continuous radon concentration recorded in soil gas at Krško basin. Straight lines represent the mean value and two standard deviations of the radon concentration. Local seismicity is expressed in terms of local magnitude (M_L) and the distance between the measuring location and the earthquake epicentre (D). Radon anomalies are C_{Rn} values outside the ±2σ region.

In contrast to soil gas, radon in ground or spring water is greatly influenced by the hydrologic cycle, which has to be considered during the data analysis. To define the mean and standard deviation, anomalously high and low values – which may cause unnecessary high deviation and perturb the real anomalies – have to be neglected. The periods when radon concentration deviates by more than ±2σ from the related seasonal value are considered as radon anomalies that are possibly caused by earthquake events and not by meteorological parameters (Ghosh et al., 2007; Gregorič et al., 2008; Virk et al., 2002; Zmazek et al., 2002b). Fig. 1 shows an anomalous radon concentration, exceeding 2σ above the average value, which appeared approximately 10 days before the occurrence of three earthquakes with magnitudes from 1.8 to 3.2.

4.2 Relationship between radon exhalation and barometric pressure

An inverse relationship exists between the time derivative of radon concentration in soil gas and the time derivative of barometric pressure (as was discussed previously in section 2.1). A decrease in barometric pressure causes an increase in radon exhalation from the ground, whereas during periods of rising pressure, air with low radon concentration is forced into

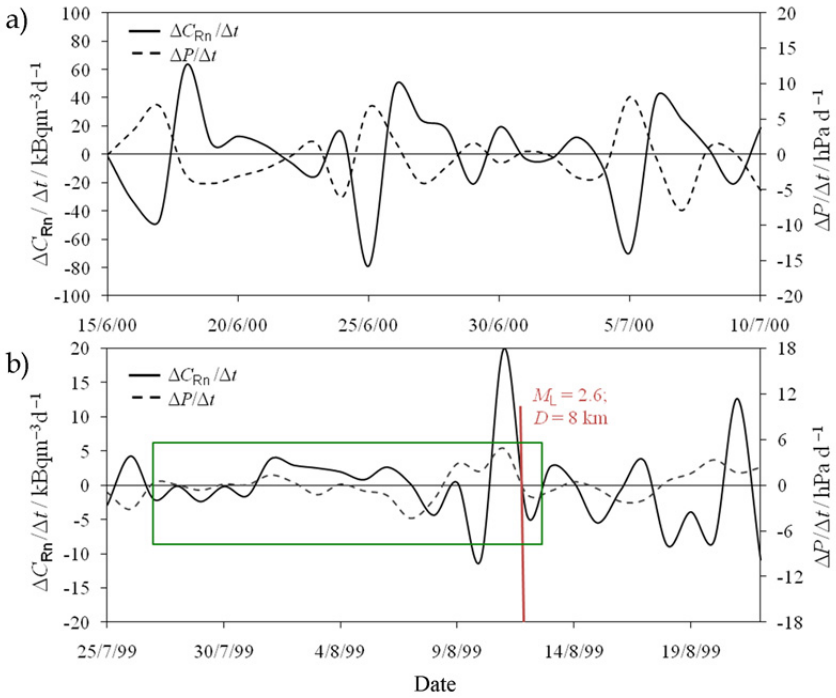

Fig. 2. The time gradient of radon concentration in soil gas and the time gradient of barometric pressure during two periods at the Krško basin: a) the period without local seismic activity, b) the seismically active period, whereby the radon anomaly 14 days before the earthquake is marked by the green rectangle. The earthquake is expressed in terms of local magnitude (M_L) and the distance between the measuring location and the earthquake epicentre (D).

the ground, thus diluting the radon concentration. Therefore, deviations from this rule during these periods – when the time gradient of barometric pressure, $\Delta P/\Delta t$, and the time gradient of radon concentration, $\Delta C_{Rn}/\Delta t$, in soil gas have the same sign – can be considered to be radon anomalies (Zmazek et al., 2002b). A clear negative correlation between the time gradient of radon concentration and the time gradient of barometric pressure can be seen in Fig. 2a, when no seismic activity is present. The radon anomaly, characterised by positive correlation of time gradients, is marked in Fig. 2b. Anomalous behaviour in radon concentration started 14 days before the earthquake with a local magnitude of 2.6, and ended a few days after the earthquake.

4.3 Machine learning methods

Machine learning methods have been successfully applied to many problems in the environmental sciences (Džeroski, 2002). In the case of radon as an earthquake precursor, it must be considered – as discussed in section 2.1 – that the variation in radon concentration is controlled not only by geophysical phenomena in the Earth's crust, but also by the environmental parameters associated with the radon monitoring sites. With machine learning methods, a model for the prediction of radon concentration can be built, taking into account various environmental parameters (e.g., barometric pressure, rainfall, and air and soil temperature). The aim is to identify radon anomalies which might be caused by seismic events. The application of artificial neural networks (Negarestani et al., 2002, 2003; Torkar et al., 2010), regression and model trees (Džeroski et al., 2003; Sikder & Munakata, 2009; Zmazek et al., 2003; Zmazek et al., 2006) and some other methods (Sikder & Munakata, 2009; Steinitz et al., 2003) have proven to be useful means of extracting radon anomalies caused by seismic events.

4.3.1 Artificial neural networks

An artificial neural network (ANN) is a well-known computational structure inspired by the operation of the biological neural system (Jain et al., 1996) and it is a well-established tool, being used widely in signal processing, pattern recognition and other applications. An ANN consists of a set of units (neurons, nodes), and a set of weighted interconnections among them (links). The organisation of neurons and their interconnections defines the net topology. The inputs are grouped in an input layer, the outputs in an output layer and all the other units in so-called hidden layers. The algorithm repeatedly adjusts the weights to minimise the mean square error between the actual output vector and the desired network output vector. The universal approximator functional form of ANNs is well-suited for the requirements of modelling the non-linear dependency of radon concentrations on multiple variables. Among a number of various topologies, training algorithms and architectures of ANNs, the traditional multilayer perceptron (MLP) with a conjugate gradient learning algorithm was chosen in the case of analysing the soil gas radon concentration time series at the Krško basin (Torkar et al., 2010). The series was first split into seismically non-active periods (NSA) and seismically active periods (SA), adjusting the duration of the seismic window from 0 to 10 days before and after the earthquake and with the purpose of investigating the influence of a complete earthquake event on radon concentration (the preparation phase, the earthquake itself and aftershocks). The ANN of the MLP type was trained with each of the NSA datasets, which were divided into three sets: the training set (60%), the cross-validation set (15%) and the test set (25%). The ANN was trained with the

training and cross-validation set, while the test set was used to verify its performance. The topology of the ANN generated for each NSA dataset is shown in Fig. 3.

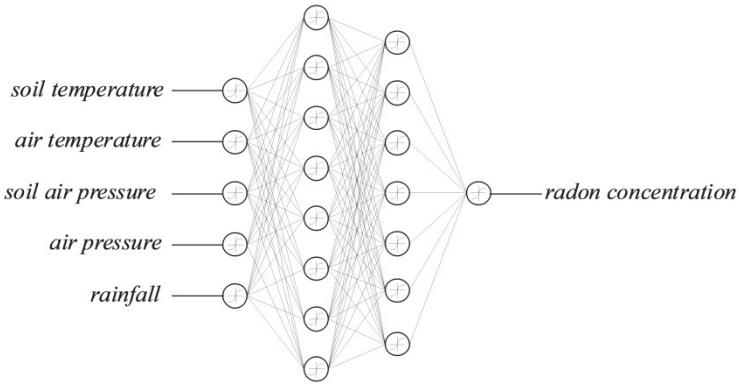

Fig. 3. The ANN topology for learning radon concentration dependency on environmental parameters.

In the testing phase, the correlation between the measured (m-C_{Rn}) and predicted (p-C_{Rn}) radon concentration in NSA periods was compared to the correlation between the measured and predicted radon concentration in the entire dataset (NSA and SA). The difference between the correlation coefficients might indicate a period of seismically induced radon anomaly. The ratio between the measured and predicted values (m-C_{Rn}/p-C_{Rn})–1 represents the discrepancy between both values (Fig. 4).

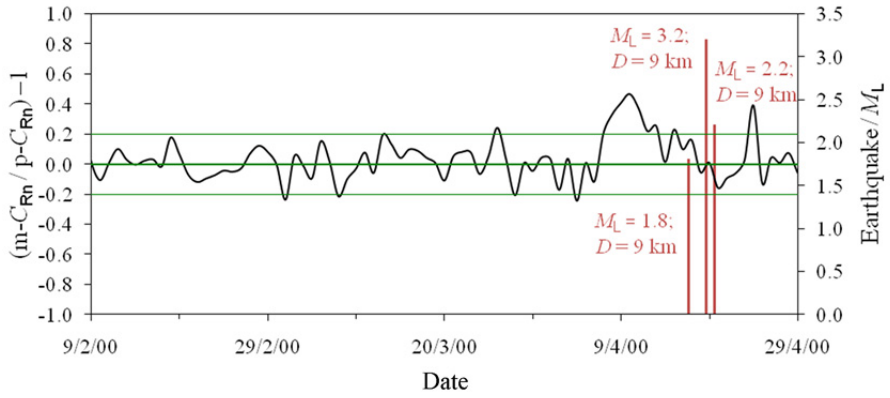

Fig. 4. The ratio between the measured and predicted radon concentration (m-C_{Rn}/p-C_{Rn})–1 using an ANN in the case of soil gas radon in the Krško basin for a seismic window of ±7 days. A radon anomaly, possibly caused by a seismic event, is observed when the signal exceeds the threshold value of 0.2.

A radon anomaly is held to be when the absolute value of signal (m-C_{Rn}/p-C_{Rn})–1 exceeds the predefined threshold of 0.2. The ANN in this case performed the best in the case of a seismic window of ±7 days (indicating the length of the period of pre- and post-seismic changes).

4.3.2 Decision trees

Decision trees are machine-learning methods for constructing prediction models from data. The models are obtained by recursively partitioning the data space and fitting a simple prediction model within each partition. As a result, the partitioning can be represented graphically as a decision tree, where each internal node contains a test on an attribute, each branch corresponds to an outcome of the test, and each leaf node gives a prediction for the value of the class variable (Džeroski, 2001; Loh, 2011). Regression trees are designed for dependent variables that take continuous or ordered discrete values. Like classical regression equations, they predict the value of a dependent variable (called the class) from the values of a set of independent variables (called attributes).

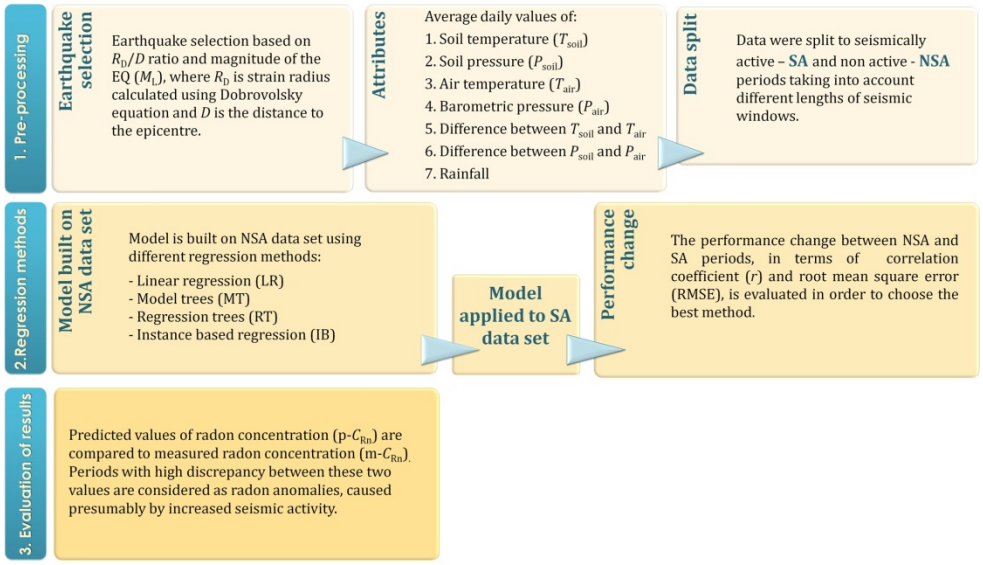

Fig. 5. A schematic description of the different stages of radon data series analysis with machine learning methods.

The model in each leaf can be either a linear equation or just a constant; trees with linear equations in the leaves are also called model trees. Tree construction proceeds recursively, starting with the entire set of training examples. At each step, the most discriminating attribute is selected as the root of the sub-tree and the current training set is split into subsets according to the values of the selected attribute. For continuous attributes, a threshold is selected and two branches are created, based on that threshold. The attributes that appear in the training set are considered to be thresholds. Tree construction stops when the variance of the class values of all examples in a node is small enough. These nodes are called leaves and are labelled with a model for predicting the class value. An important mechanism used to prevent the tree from over-fitting data is tree pruning.

Regression (RT) and model trees (MT), as implemented with the WEKA data mining suite (Witten & Frank, 1999), were used for predicting radon concentration from meteorological parameters in the case of radon time series in soil gas at the Krško basin (Zmazek et al., 2003; Zmazek et al., 2005) and in the thermal spring water in Zatolmin (Zmazek et al., 2006).

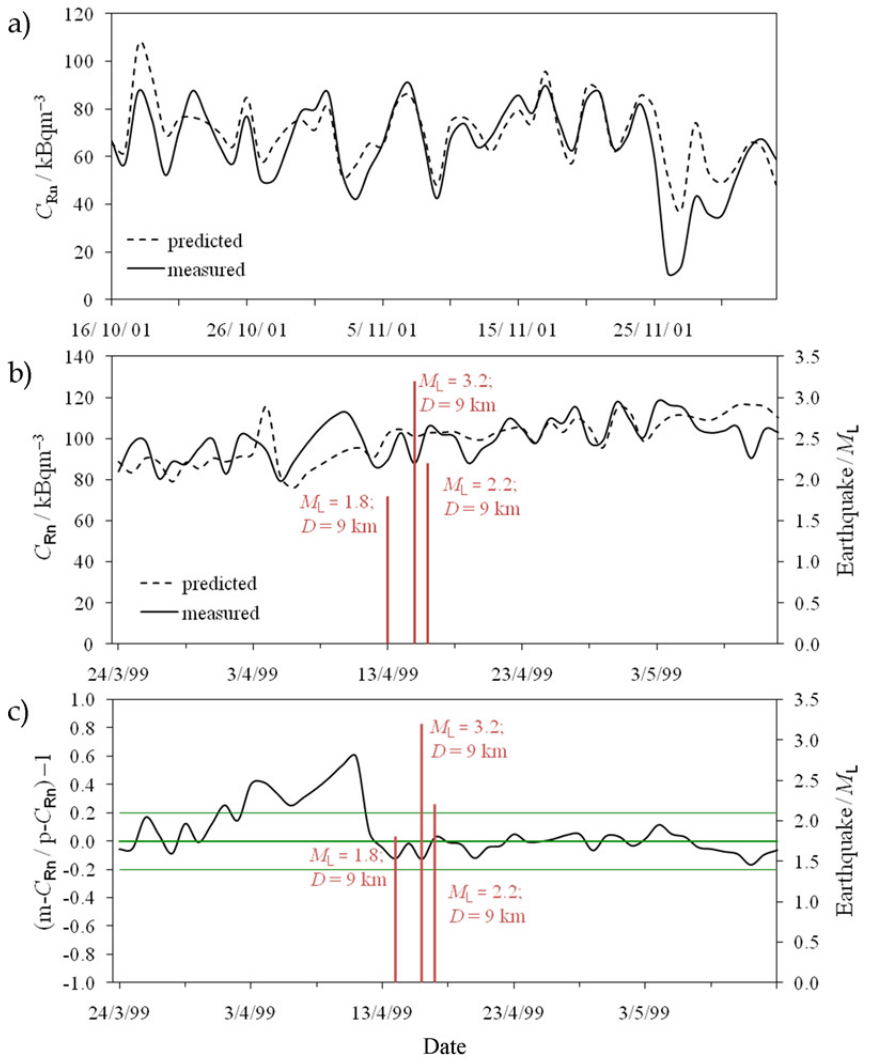

Fig. 6. Measured and predicted radon concentration using model trees in the case of soil gas radon at the Krško basin for a seismic window ±7 days; a) low discrepancy in the period without seismic activity; b) high discrepancy starting 10 days before a group of earthquakes; c) the ratio between the measured and predicted radon concentration (m-C_{Rn}/ p-C_{Rn})–1 for the same SA period. A radon anomaly, possibly caused by earthquakes, is observed when the signal exceeds the threshold value of 0.2 (marked by the green lines).

As presented in Fig. 5 the first stage of data analysis comprises the selection of attributes – i.e. environmental parameters – and the partitioning of the whole data set to the periods with and without seismic activity, SA and NSA respectively. After inspecting the correlation changes between radon concentration and barometric pressure, a seismic window of ±7

days was chosen. The performance was estimated with 10-fold cross-validation in order to evaluate the predictability of the radon concentration in the NSA periods. The model built on the NSA data set was then applied to the SA data set and the performance change was determined using two different measures, the correlation coefficient (r) and the root mean square error (RMSE). For the purposes of prediction, the measured performance in NSA periods should be higher than the performance in SA periods. In these periods, when the discrepancy between the measured and predicted radon concentration is low, no seismic activity is anticipated (Fig. 6a), while in the periods with a higher discrepancy, a radon anomaly can be ascribed to increased seismic activity, rather than to the effect of atmospheric parameters (Fig. 6b). This discrepancy is clearly shown in form of the ratio between both values (m-C_{Rn}/p-C_{Rn})–1, as shown in Fig. 6c. A radon anomaly is held to be when the absolute value of the signal (m-C_{Rn}/p-C_{Rn})–1 exceeds the predefined threshold of 0.2. Besides regression trees, other machine learning methods were also tested (e.g., linear regression and instance-based regression). However, model trees have been shown to outperform other approaches.

4.4 Comparison of the results

The results of all of the approaches used for the identification of radon anomalies caused by seismic events in the case of soil gas radon at the Krško basin are shown in Fig. 7 for the period of 1/9 – 30/12/2000. Among all of the approaches – and although not very exact – the ±xσ method (I) is the most frequently used. The threshold of anomalous concentrations (e.g., ±1σ, ±2σ, ±3σ) should be chosen in order to minimise the number of false anomalies (FA: anomalies in seismically non-active periods) and so as not to miss the correct ones (CA). Generally, a range of ±2σ from the related seasonal mean value is chosen. Furthermore, a cyclic behaviour of radon concentration has to be taken into account in order to accurately define the period of standard deviation and the calculation of the mean value. For this purpose different methods of time series analyses – for example, Fourier transform (Ramola, 2010) – can be applied.

In the case shown in Fig. 7a, three radon anomalies exceeding 2σ above the mean value may be noticed. The first, in the beginning of September, cannot be assigned to a seismic event (FA). About a week before a weak earthquake of local magnitude M_L=1.1, 5 km away from the measurement location – which is the first of five earthquakes over a period of 2 months – the second anomaly is observed. And finally, the third one can be noticed soon after a weak earthquake 6 km away (M_L=1).

The first of the anomalies mentioned above as FA is also visible by applying the method of pressure gradients (II) (Fig. 7b). A positive correlation between the time gradient of radon concentration and the time gradient of barometric pressure is considered to be a radon anomaly, and corresponds to the anomaly observed through method (I) which preceded the first earthquake (M_L=1.1). A radon anomaly can also be noticed a few days before the last earthquake, as with the analysis of method (I). Additionally, the anomalous behaviour of the radon concentration as regards the gradient approach is observed during the period starting a few days before the earthquake with M_L=2.7 and lasting until the earthquake with M_L=1.

More often than not, swarms of anomalies are observed over longer periods, with a higher number of anomalies in a swarm observed for approach (II) than for approach (I). As an additional criterion, a threshold of $\Delta P/\Delta t > 2$ hPa d^{-1} is introduced by this approach in order to optimise the identification of anomalies caused by seismic events. However, by increasing the threshold value above 2 hPa d^{-1}, the ratio between correct and false anomalies cannot be significantly improved (Zmazek et al., 2005).

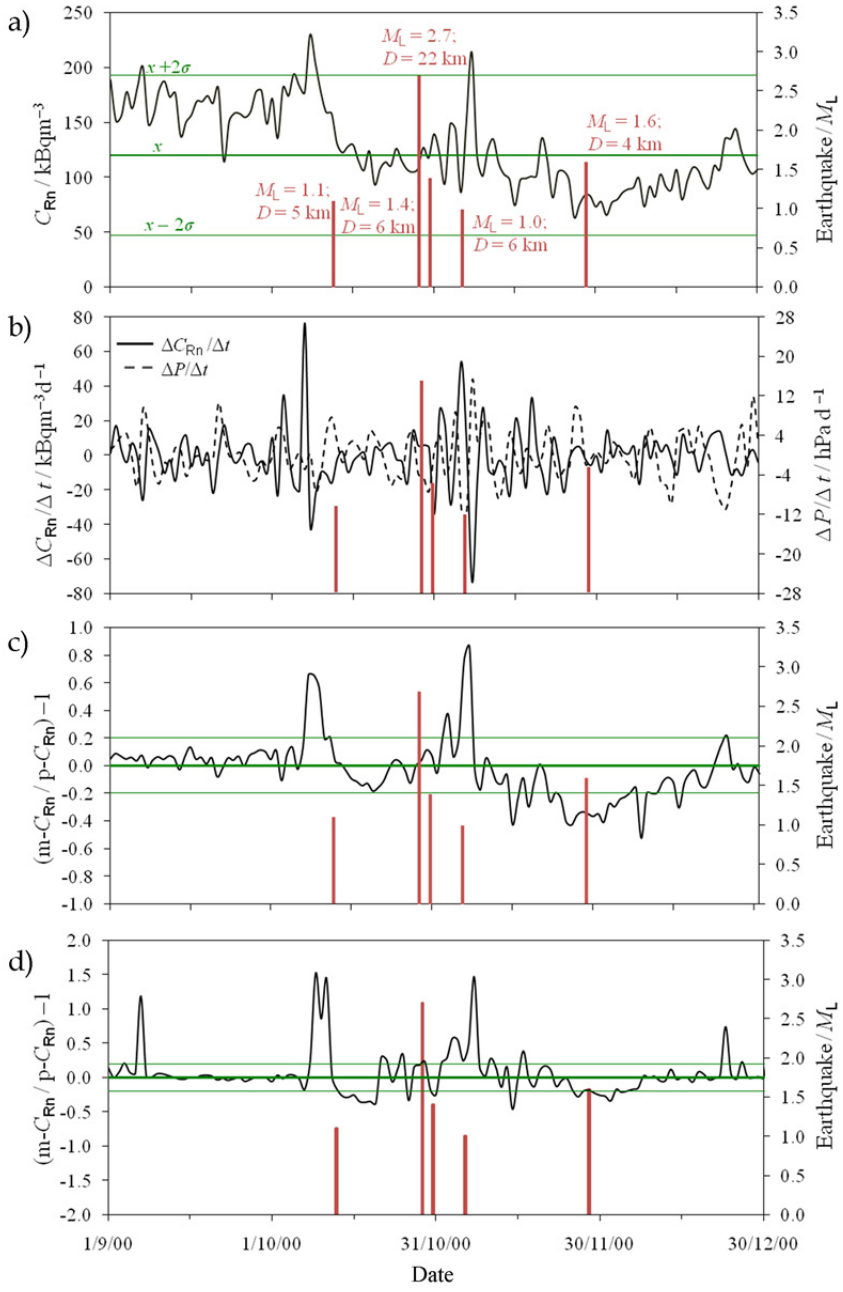

Fig. 7. A comparison of different approaches for the identification of radon anomalies: a) standard deviation (I); b) the relationship between radon exhalation and barometric pressure (II); c) artificial neural networks (III); and d) model trees (IV).

Both machine learning approaches, artificial neural networks (III) and decision trees (IV) give promising results, with a low number of false anomalies. The two distinctive anomalies – observed in Fig. 7c and Fig. 7d, for ANN and MT, respectively – confirm the anomalies identified by approaches (I) and (II). Additionally, a relatively long negative anomaly was observed using the ANN approach at the end of November, accompanying the earthquake with M_L=1.6. On the other hand, the same negative anomaly is only weakly expressed using the MT approach. A FA observed at the beginning of September using approaches (I) and (II) was also noticed using the MT approach but not by the ANN approach. Approaches (III) and (IV) do not appear to greatly depend upon the choice for the threshold of (m-C_{Rn}/p-C_{Rn})–1 and can, therefore, be used with less hesitation.

5. Conclusion

Since the appropriate interpretation of field measurements plays an important role in any research, the purpose of this work was to combine and evaluate the different approaches applied by our research group for differentiating the radon anomalies caused by increased seismic activity from those caused solely by environmental parameters. The application of four different approaches – standard deviation from the related mean value (I), the correlation between time gradients of barometric pressure and radon concentration (II), artificial neural networks (III) and decision trees (IV) – was presented. Radon anomalies based on approach (I) have been less successful in predicting earthquakes than those based on the other three approaches. Secondly, approaches (I) and (II) greatly depend upon the values of the ±xσ and $\Delta P/\Delta t$ thresholds, respectively, while the dependence of approaches (III) and (IV) on the threshold of (m-C_{Rn}/p-C_{Rn})–1 is very weak. The number of false anomalies for approach (II) points to the disturbance of radon exhalation by other environmental parameters and not just by barometric pressure. The assumption that radon exhalation is only directly influenced by barometric pressure is further suggested by different forms of radon transport at compression and dilatation zones (Ghosh et al., 2009). Promising results are achieved by applying approaches (III) and (IV), which make it possible to simultaneously incorporate all of the available environmental parameters. Furthermore, in using these techniques, the relation between radon concentration and environmental parameters does not necessarily have to be presumed linear. And finally, in taking into account the scale of the earthquake magnitudes observed during the time of radon measurements, one may speculate that the performance of the applied approaches would be better in the case of stronger earthquakes.

6. Acknowledgement

This study was done within the program P1-0143: Cycling of substances in the environment, mass balances, modelling of environmental processes and risk assessment.

7. References

Anderson, O.L., & Grew, P.C. (1977). Stress-corrosion theory of crack-propagation with applications to geophysics. *Reviews of Geophysics,* Vol. 15, No. 1, pp. 77–104

Atkinson, B.K. (1980). Stress corrosion and the rate-dependent tensile failure of a fine-grained quartz rock. *Tectonophysics,* Vol. 65, No. 3–4, pp. 281–290

Barragán, R.M., Arellano, V.M., Portugal, E., & Segovia, N. (2008). Effects of changes in reservoir thermodynamic conditions on ^{222}Rn composition of discharged fluids: study for two wells at Los Azufres geothermal field (Mexico). *Geofluids,* Vol. 8, No. 4, pp. 252–262

Belyaev, A.A. (2001). Specific features of radon earthquake precursors. *Geochemistry International,* Vol. 39, No. 12, pp. 1245–1250

Chen, C., Thomas, D.M., & Green, R.E. (1995). Modeling of radon transport in unsaturated soil. *Journal of Geophysical Research-Solid Earth,* Vol. 100, No. B8, pp. 15517–15525

Choubey, V.M., Kumar, N., & Arora, B.R. (2009). Precursory signatures in the radon and geohydrological borehole data for M4.9 Kharsali earthquake of Garhwal Himalaya. *Science of the Total Environment,* Vol. 407, No. 22, pp. 5877–5883

Chyi, L.L., Quick, T.J., Yang, T.F., & Chen, C.H. (2010). The experimental investigation of soil gas radon migration mechanisms and its implication in earthquake forecast. *Geofluids,* Vol. 10, No. 4, pp. 556–563

Cicerone, R.D., Ebel, J.E., & Britton, J. (2009). A systematic compilation of earthquake precursors. *Tectonophysics,* Vol. 476, No. 3–4, pp. 371–396

Clements, W.E., & Wilkening, M.H. (1974). Atmospheric-pressure effects on Rn-222 transport across earth-air interface. *Journal of Geophysical Research,* Vol. 79, No. 33, pp. 5025–5029

Cuomo, V., Di Bello, G., Lapenna, V., Piscitelli, S., Telesca, I., Macchiato, M., & Serio, C. (2000). Robust statistical methods to discriminate extreme events in geoelectrical precursory signals: Implications with earthquake prediction. *Natural Hazards,* Vol. 21, No. 2–3, pp. 247–261

Dobrovolsky, I.P., Zubkov, S.I., & Miachkin, V.I. (1979). Estimation of the size of earthquake preparation zones. *Pure and Applied Geophysics,* Vol. 117, No. 5, pp. 1025–1044

Džeroski, S. (2001). Data mining in a nutshell, In: *Relational data mining*, Džeroski, S., Lavrač, N. (Eds.), pp. 3–27, Springer, Berlin

Džeroski, S. (2002). Environmental sciences, In: *Handbook of data mining and knowledge discovery*, Klösgen, W., Żytkow, J. (Eds.), pp. 817–830, Oxford University Press, Oxford

Džeroski, S., Todorovski, L., Zmazek, B., Vaupotič, J., & Kobal, I. (2003). Modelling soil radon concentration for earthquake prediction. *Discovery Science, Proceedings,* Vol. 2843, pp. 87–99

Etiope, G., & Martinelli, G. (2002). Migration of carrier and trace gases in the geosphere: an overview. *Physics of the Earth and Planetary Interiors,* Vol. 129, No. 3–4, pp. 185–204

Favara, R., Grassa, F., Inguaggiato, S., & Valenza, M. (2001). Hydrogeochemistry and stable isotopes of thermal springs: earthquake-related chemical changes along Belice Fault (Western Sicily). *Applied Geochemistry,* Vol. 16, No. 1, pp. 1–17

Fleischer, R.L. (1981). Dislocation model for radon response to distant earthquakes. *Geophysical Research Letters,* Vol. 8, No. 5, pp. 477–480

Geller, R.J. (1997). Earthquake prediction: a critical review. *Geophysical Journal International,* Vol. 131, No. 3, pp. 425–450

Ghosh, D., Deb, A., & Sengupta, R. (2009). Anomalous radon emission as precursor of earthquake. *Journal of Applied Geophysics,* Vol. 69, No. 2, pp. 67–81

Ghosh, D., Deb, A., Sengupta, R., Patra, K.K., & Bera, S. (2007). Pronounced soil-radon anomaly - Precursor of recent earthquakes in India. *Radiation Measurements,* Vol. 42, No. 3, pp. 466–471

Gregorič, A., Zmazek, B., & Vaupotič, J. (2008). Radon concentration in thermal water as an indicator of seismic activity. *Collegium Antropologicum,* Vol. 32, pp. 95–98

Heinicke, J., Italiano, F., Koch, U., Martinelli, G., & Telesca, L. (2010). Anomalous fluid emission of a deep borehole in a seismically active area of Northern Apennines (Italy). *Applied Geochemistry,* Vol. 25, No. 4, pp. 555–571

Hickman, S., Sibson, R., & Bruhn, R. (1995). Introduction to special section: Mechanical involvement of fluids in faulting. *Journal of Geophysical Research,* Vol. 100, No. B7, pp. 12831–12840

Holub, R.F., & Brady, B.T. (1981). The effect of stress on radon emanation from rock. *Journal of Geophysical Research,* Vol. 86, No. NB3, pp. 1776–1784

İnan, S., & Seyis, C. (2010). Soil radon observations as possible earthquake precursors in Turkey. *Acta Geophysica,* Vol. 58, No. 5, pp. 828–837

Jain, A.K., Jianchang, M., & Mohiuddin, K.M. (1996). Artificial Neural Networks: A Tutorial. *Computer,* Vol. 29, No. 3, pp. 31–44

King, C.Y. (1978). Radon emanation on San Andreas Fault. *Nature,* Vol. 271, No. 5645, pp. 516–519

King, C.Y. (1984). Impulsive radon emanation on a creeping segment of the San-Andreas fault, California. *Pure and Applied Geophysics,* Vol. 122, No. 2–4, pp. 340–352

King, C.Y. (1985). Radon monitoring for earthquake prediction in China. *Earthquake Prediction Research,* Vol. 3, No. 1, pp. 47–68

King, C.Y., & Minissale, A. (1994). Seasonal variability of soil-gas radon concentration in central California. *Radiation Measurements,* Vol. 23, No. 4, pp. 683–692

Klusman, R.W., & Jaacks, J.A. (1987). Environmental influences upon mercury, radon and helium concentrations in soil gases at a site near Denver, Colorado. *Journal of Geochemical Exploration,* Vol. 27, No. 3, pp. 259–280

Klusman, R.W., & Webster, J.D. (1981). Preliminary analysis of meteorological and seasonal influences on crustal gas emission relevant to earthquake prediction. *Bulletin of the Seismological Society of America,* Vol. 71, No. 1, pp. 211–222

Kristiansson, K., & Malmqvist, L. (1982). Evidence for nondiffusive transport of $^{222}_{86}$Rn in the ground and a new physical model for the transport. *Geophysics,* Vol. 47, No. 10, pp. 1444–1452

Kuo, T., Fan, K., Kuochen, H., Han, Y., Chu, H., & Lee, Y. (2006). Anomalous decrease in groundwater radon before the Taiwan M6.8 Chengkung earthquake. *Journal of Environmental Radioactivity,* Vol. 88, No. 1, pp. 101–106

Kuo, T., Su, C., Chang, C., Lin, C., Cheng, W., Liang, H., Lewis, C., & Chiang, C. (2010). Application of recurrent radon precursors for forecasting large earthquakes (Mw > 6.0) near Antung, Taiwan. *Radiation Measurements,* Vol. 45, No. 9, pp. 1049–1054

Lay, T., Williams, Q., & Garnero, E.J. (1998). The core-mantle boundary layer and deep Earth dynamics. *Nature,* Vol. 392, pp. 461–468

Loh, W.-Y. (2011). Classification and regression trees. *Wiley Interdisciplinary Reviews: Data Mining and Knowledge Discovery,* Vol. 1, No. 1, pp. 14–23

Lomnitz, C. (1994). *Fundamentals of Earthquake Prediction*, John Wiley & Sons, New York

Martinelli, G. (1993). Fluidodynamical and chemical features of radon 222 related to total gases: implications for earthquake predictions, *Proceedings of IAEA Meeting on isotopic and geochemical precursors of earthquakes and volcanic eruptions*, Vienna, September 1991

Mjachkin, V.I., Brace, W.F., Sobolev, G.A., & Dieterich, J.H. (1975). Two models for earthquake forerunners. *Pure and Applied Geophysics,* Vol. 113, No. 1, pp. 169–181

Mogro-Campero, A., Fleischer, R.L., & Likes, R.S. (1980). Changes in subsurface radon concentration associated with earthquakes. *Journal of Geophysical Research,* Vol. 85, No. NB6, pp. 3053–3057

Negarestani, A., Setayeshi, S., Ghannadi-Maragheh, M., & Akashe, B. (2002). Layered neural networks based analysis of radon concentration and environmental parameters in earthquake prediction. *Journal of Environmental Radioactivity,* Vol. 62, No. 3, pp. 225–233

Negarestani, A., Setayeshi, S., Ghannadi-Maragheh, M., & Akashe, B. (2003). Estimation of the radon concentration in soil related to the environmental parameters by a modified Adaline neural network. *Applied Radiation and Isotopes,* Vol. 58, No. 2, pp. 269–273

Neznal, M., Matolin, M., Just, G., & Turek, K. (2004). Short-term temporal variations of soil gas radon concentration and comparison of measurement techniques. *Radiation Protection Dosimetry,* Vol. 108, No. 1, pp. 55–63

Pinault, J.L., & Baubron, J.C. (1996). Signal processing of soil gas radon, atmospheric pressure, moisture, and soil temperature data: A new approach for radon concentration modeling. *Journal of Geophysical Research-Solid Earth,* Vol. 101, No. B2, pp. 3157–3171

Planinić, J., Radolić, V., & Lazanin, Ž. (2001). Temporal variations of radon in soil related to earthquakes. *Applied Radiation and Isotopes,* Vol. 55, No. 2, pp. 267–272

Ramola, R.C. (2010). Relation between spring water radon anomalies and seismic activity in Garhwal Himalaya. *Acta Geophysica,* Vol. 58, No. 5, pp. 814–827

Ramola, R.C., Prasad, Y., Prasad, G., Kumar, S., & Choubey, V.M. (2008). Soil-gas radon as seismotectonic indicator in Garhwal Himalaya. *Applied Radiation and Isotopes,* Vol. 66, No. 10, pp. 1523–1530

Ramola, R.C., Singh, M., Sandhu, A.S., Singh, S., & Virk, H.S. (1990). The use of radon as an earthquake precursor. *Nuclear Geophysics,* Vol. 4, No. 2, pp. 275–287

Ramola, R.C., Singh, S., & Virk, H.S. (1988). A model for the correlation between radon anomalies and magnitude of earthquakes. *Nuclear Tracks and Radiation Measurements,* Vol. 15, No. 1–4, pp. 689–692

Reddy, D.V., & Nagabhushanam, P. (2011). Groundwater electrical conductivity and soil radon gas monitoring for earthquake precursory studies in Koyna, India. *Applied Geochemistry,* Vol. 26, No. 5, pp. 731–737

Sikder, I.U., & Munakata, T. (2009). Application of rough set and decision tree for characterization of premonitory factors of low seismic activity. *Expert Systems with Applications,* Vol. 36, No. 1, pp. 102–110

Singh, M., Kumar, M., Jain, R.K., & Chatrath, R.P. (1999). Radon in ground water related to seismic events. *Radiation Measurements,* Vol. 30, No. 4, pp. 465–469

Steinitz, G., Begin, Z.B., & Gazit-Yaari, N. (2003). Statistically significant relation between radon flux and weak earthquakes in the Dead Sea rift valley. *Geology,* Vol. 31, No. 6, pp. 505–508

Stranden, E., Kolstad, A.K., & Lind, B. (1984). Radon exhalation - moisture and temperature dependence. *Health Physics,* Vol. 47, No. 3, pp. 480–484

Thomas, D. (1988). Geochemical precursors to seismic activity. *Pure and Applied Geophysics,* Vol. 126, No. 2, pp. 241–266

Torkar, D., Zmazek, B., Vaupotič, J., & Kobal, I. (2010). Application of artificial neural networks in simulating radon levels in soil gas. *Chemical Geology,* Vol. 270, No. 1–4, pp. 1–8

Toutain, J.P., & Baubron, J.C. (1999). Gas geochemistry and seismotectonics: a review. *Tectonophysics,* Vol. 304, No. 1–2, pp. 1–27

Ulomov, V.I., & Mavashev, B.Z. (1967). On forerunners of strong tectonic earthquakes. *Doklady Akademii Nauk SSSR*, No. 176, pp. 319–322

Vàrhegyi, A., Hakl, J., Monnin, M., Morin, J.P., & Seidel, J.L. (1992). Experimental study of radon transport in water as test for a transportation microbubble model. *Journal of Applied Geophysics,* Vol. 29, No. 1, pp. 37–46

Virk, H.S., Sharma, A.K., & Sharma, N. (2002). Radon and helium monitoring in some thermal springs of North India and Bhutan. *Current Science,* Vol. 82, No. 12, pp. 1423–1424

Wakita, H., Nakamura, Y., Notsu, K., Noguchi, M., & Asada, T. (1980). Radon anomaly - possible precursor of the 1978 Izu-Oshima-Kinkai earthquake. *Science,* Vol. 207, No. 4433, pp. 882–883

Walia, V., Lin, S.J., Hong, W.L., Fu, C.C., Yang, T.F., Wen, K.L., & Chen, C.H. (2009a). Continuous temporal soil-gas composition variations for earthquake precursory studies along Hsincheng and Hsinhua faults in Taiwan. *Radiation Measurements,* Vol. 44, No. 9–10, pp. 934–939

Walia, V., Yang, T.F., Hong, W.L., Lin, S.J., Fu, C.C., Wen, K.L., & Chen, C.H. (2009b). Geochemical variation of soil-gas composition for fault trace and earthquake precursory studies along the Hsincheng fault in NW Taiwan. *Applied Radiation and Isotopes,* Vol. 67, No. 10, pp. 1855–1863

Washington, J.W., & Rose, A.W. (1990). Regional and temporal relations of radon in soil gas to soil-temperature and moisture. *Geophysical Research Letters,* Vol. 17, No. 6, pp. 829–832

Witten, I.H., & Frank, E. (1999). *Data Mining: Practical Machine Learning Tools and Techniques with Java Implementations.*, Morgan Kaufmann, San Francisco

Yang, T.F., Walia, V., Chyi, L.L., Fu, C.C., Chen, C.H., Liu, T.K., Song, S.R., Lee, C.Y., & Lee, M. (2005). Variations of soil radon and thoron concentrations in a fault zone and prospective earthquakes in SW Taiwan. *Radiation Measurements,* Vol. 40, No. 2–6, pp. 496–502

Zmazek, B., Italiano, F., Živčić, M., Vaupotič, J., Kobal, I., & Martinelli, G. (2002a). Geochemical monitoring of thermal waters in Slovenia: relationships to seismic activity. *Applied Radiation and Isotopes,* Vol. 57, No. 6, pp. 919–930

Zmazek, B., Todorovski, L., Džeroski, S., Vaupotič, J., & Kobal, I. (2003). Application of decision trees to the analysis of soil radon data for earthquake prediction. *Applied Radiation and Isotopes,* Vol. 58, No. 6, pp. 697–706

Zmazek, B., Todorovski, L., Živčić, M., Džeroski, S., Vaupotič, J., & Kobal, I. (2006). Radon in a thermal spring: Identification of anomalies related to seismic activity. *Applied Radiation and Isotopes,* Vol. 64, No. 6, pp. 725–734

Zmazek, B., Živčić, M., Todorovski, L., Džeroski, S., Vaupotič, J., & Kobal, I. (2005). Radon in soil gas: How to identify anomalies caused by earthquakes. *Applied Geochemistry,* Vol. 20, No. 6, pp. 1106–1119

Zmazek, B., Živčić, M., Vaupotič, J., Bidovec, M., Poljak, M., & Kobal, I. (2002b). Soil radon monitoring in the Krško Basin, Slovenia. *Applied Radiation and Isotopes,* Vol. 56, No. 4, pp. 649–657

4.3 Radon as a tracer for cave ventilation

While a number of radon measurements have been performed in the last few decades in Slovenian caves, they were mainly devoted to dosimetry studies, whereas the processes governing the spatial and temporal distribution of radon levels were left aside. A rising number of different studies that have been taking place in Postojna Cave have emphasised the question about the ventilation characteristics of cave passages. At this point, a long radon database (Figure 17) in Postojna Cave was found to be useful for this application. Along with ventilation studies, a chance to study radon transport from the Earth's crust to the atmosphere arose, since caves can be considered somehow a boundary layer between the lithosphere and the atmosphere.

The general ventilation characteristics of Postojna Cave and the influence of outside temperature on radon levels in the cave is presented in the paper "Dependence of radon levels in Postojna Cave on outdoor air temperature". Within this study a model was built, which helps to predict the radon concentration at a specific location in the cave on the basis of outside temperature. Although measurements cannot be avoided, the model could markedly reduce their number without diminishing the level of reliability of the data needed for dose estimates for personnel working in the cave.

The influence of geomorphology of cave passages on radon levels and the reasons for an extremely high radon concentration in the Pisani Rov part of Postojna Cave are presented and discussed in the paper "Reasons for large fluctuations of radon and CO_2 levels in a dead-end passage of a karst cave (Postojna Cave, Slovenia)". CO_2 was used as an additional parameter to interpret the contribution of different sources to radon concentration. The comparison of radon fluctuation at three different locations revealed airflow patterns and differences in the degree of ventilation of different passages.

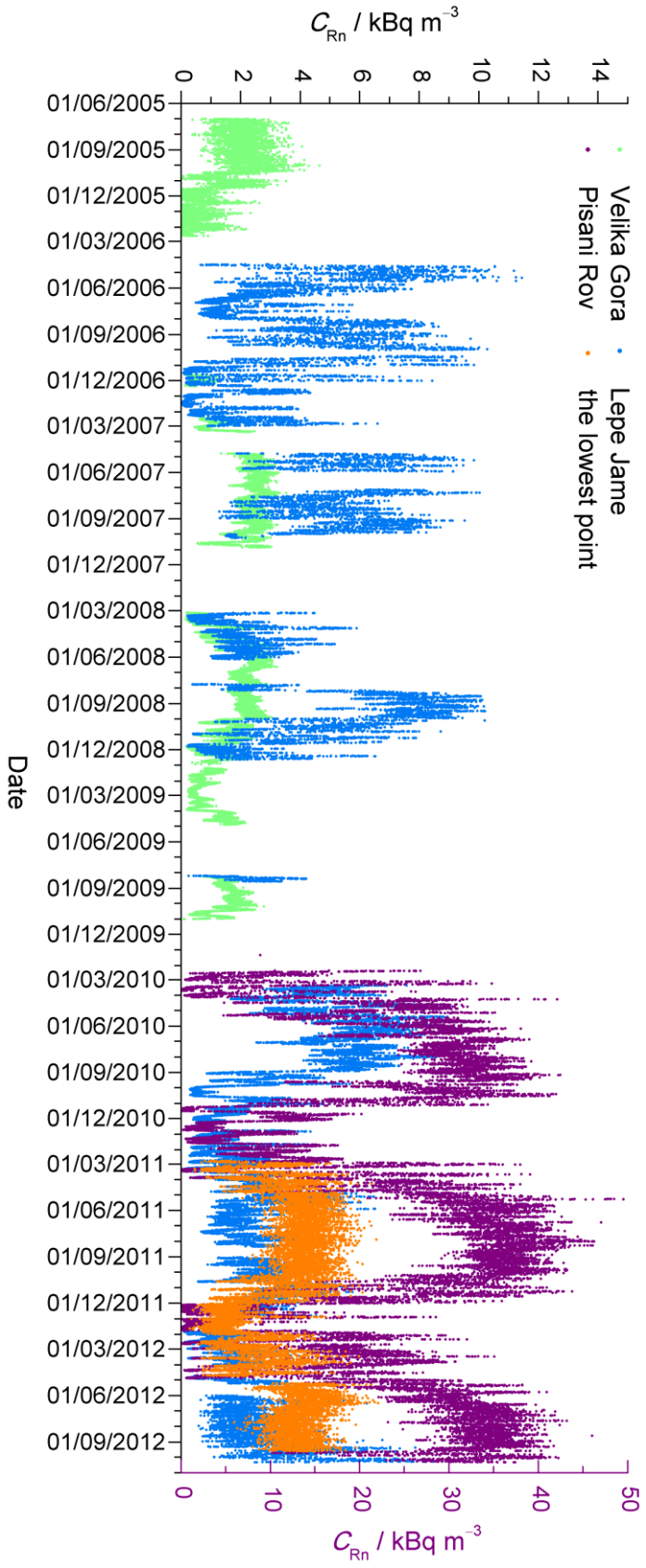

Figure 17: *Time series of radon concentration at four locations in Postojna Cave: Lepe Jame, the lowest point, Velika Gora and Pisani Rov*.

4.3.1 Scientific paper: "Dependence of radon levels in the Postojna Cave on outdoor air temperature"

Nat. Hazards Earth Syst. Sci., 11, 1523–1528, 2011
www.nat-hazards-earth-syst-sci.net/11/1523/2011/
doi:10.5194/nhess-11-1523-2011

Natural Hazards and Earth System Sciences

Dependence of radon levels in Postojna Cave on outside air temperature

A. Gregorič, A. Zidanšek, and J. Vaupotič

Jožef Stefan Institute, Ljubljana, Slovenia

Received: 20 December 2010 – Revised: 20 April 2011 – Accepted: 21 April 2011 – Published: 23 May 2011

Abstract. Postojna Cave is the largest of 21 show caves in Slovenia. The radon concentration there was measured continuously in the Great Mountain hall from July 2005 to October 2009 and ranged from about 200 Bq m^{-3} in winter to about 3 kBq m^{-3} in summer. The observed seasonal pattern of radon concentration is governed by air movement due to the difference in external and internal air densities, controlled mainly by air temperature. The cave behaves as a large chimney and in the cold period, the warmer cave air is released vertically through cracks and fissures to the colder outside atmosphere, enabling the inflow of fresh air with low radon levels. In summer the ventilation is minimal or reversed and the air flows from the higher to the lower openings of the cave. Our calculations have shown that the effect of the difference between outside and cave air temperatures on radon concentration is delayed for four days, presumably because of the distance of the measurement point from the lower entrance (ca. 2 km). A model developed for predicting radon concentration on the basis of outside air temperature has been checked and found to be successful.

1 Introduction

Radon (^{222}Rn), a radioactive gas with a half-life of 3.82 days, is released from minerals into the pore space of rocks and subsequently into the atmosphere (Nazaroff, 1992). It is well known that high concentrations of radon are common in mines (Cohen, 1982; Sevc et al., 1976). The existence of similar radiation in underground cavities was found in the 1970s, since when research on radon concentration in natural caves has taken two directions. The first is the aspect of radiation protection (Duenas et al., 1999; Fernandez et al., 1984; Kávási et al., 2010; Vaupotič, 2008) and the second that of radon as a tracer for air movement within a cave (Cunningham and Larock, 1991; Hakl et al., 1996; Kies and Massen, 1997; Kowalczk and Froelich, 2010; Perrier et al., 2004; Przylibski, 1999). Minute quantities of uranium (^{238}U) present in limestone result in relatively high values of radon in karstic caves (Cigna, 2005; Gillmore et al., 2002; Hakl et al., 1997) due to the low natural ventilation of the underground cavities. Tectonic faults constitute an additional source of radon (Ball et al., 1991; Gillmore et al., 2000; Šebela et al., 2010). Variations of radon concentration in cave air arise from a balance of the emission from cave surfaces and drip waters, decay in cave air, and exchange with the outside atmosphere (Wilkening and Watkins, 1976). Seasonal changes in natural ventilation often cause large temporal variation in radon levels, most commonly characterised by high summer and low winter concentrations (Kowalczk and Froelich, 2010; Perrier and Richon, 2010; Przylibski, 1999; Tanahara et al., 1997; Wilkening and Watkins, 1976). However, other atypical patterns have also been documented, such as maximum concentrations during autumn and minimum during summer in Mammoth Cave, Kentucky (Eheman et al., 1991) or in Moestroff Cave (Luxembourg), where the lowest concentrations are observed in the summer (Kies and Massen, 1997). As a result of elevated radon concentrations, Postojna Cave as well has been under permanent radon survey since 1995 (Vaupotič et al., 2001; Vaupotič, 2008). In this study, radon was monitored in the Great Mountain hall of the Postojna Cave from July 2005 to October 2009. Our intention was to establish a model of radon concentration in the cave air on the basis of temperature differences between the cave air and the outside air. Such a model could reduce the number of measurements in the cave needed for dose estimates for the personnel working there.

Correspondence to: A. Gregorič
(asta.gregoric@ijs.si)

Published by Copernicus Publications on behalf of the European Geosciences Union.

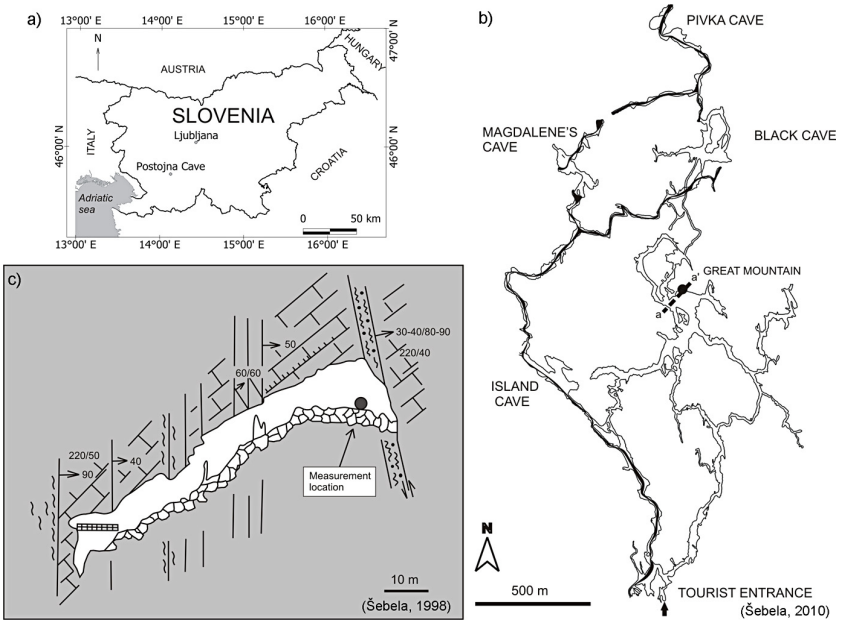

Fig. 1. (a) Slovenia with the Postojna Cave indicated. **(b)** The passages of Postojna Cave with the monitoring site in the Great Mountain hall and the cross section a–a′ indicated. **(c)** Cross section of the Great Mountain hall with the measurement point and tectonic structure.

2 Site description

Postojna Cave, with 20 km of galleries, is the longest known cave system and the largest of 21 show caves in Slovenia (Fig. 1a). It is one of the most visited show caves in the world. The vertical extent of the system is 115 m. The height above sea level of the river Pivka where it enters the cave is 511 m and that of the platform in front of the cave entrance 529 m. The cave passages have been developed in approximately 800 m of Upper Cretaceous bedded limestone situated between two important Dinaric faults (Šebela et al., 2010). This cave is a typical horizontal cave (Fig. 1b) (Šebela, 1998) with the tourist entrance being a large natural entrance with a diameter of several meters. An electric train takes visitors through 2 km long galleries and passages to the station in the cave, from where they start a walking route. Besides the part of the cave open to visitors, the Postojna Cave system is composed of several halls, named Island Cave, Magdalene's Cave and Black Cave, connected to each other by narrow passages. Some of them can be accessed from the surface through their own entrances (Fig. 1b). There is no forced ventilation in the cave and air is exchanged only by natural air draught through the numerous cracks, corridors and breathing halls (Gams, 1974) connecting the cave with the outside atmosphere. The measurement site is located in the Great Mountain hall (Fig. 1c), which is the biggest collapse chamber in Postojna Cave and lies about 2 km from the tourist entrance.

3 Methodology

3.1 Measurement methods

Radon was monitored continuously in the Great Mountain hall from July 2005 to October 2009. During the first year, a Barasol probe (MC-450, ALGADE, France) was used, which was then replaced by a Radim 5 WP monitor (SMM Company, Prague, Czech Republic). Data for some months in 2006, at the end of 2007, and in summer 2009 are missing because of high air humidity, which damaged the measuring devices. The Barasol probe is designed primarily for radon measurements in soil gas. The probe gives radon concentration, based on alpha spectrometry of radon decay products in the energy range of 1.5 MeV to 6 MeV using an implanted silicon detector. The detector sensitivity is 50 Bq m^{-3} and a sampling frequency was set at once an hour. In addition to radon concentration, the probe also recorded temperature and barometric pressure. The Radim 5 monitor determines radon concentration by measuring gross alpha activity of the decay products ^{218}Po and ^{214}Po, collected electrostatically on the surface of a semiconductor detector. The sensitivity is about 50 Bq m^{-3} and the sampling frequency was twice an hour. The data have been stored in the internal memory of both instruments and then transferred to a personal computer for further evaluation. The daily averages of radon concentration were calculated from raw measurements.

Hourly values and daily averages of outside air temperature at the Postojna meteorological station were obtained from the Office of Meteorology of the Environmental Agency of the Republic of Slovenia.

3.2 Radon modelling

Fluctuations in cave air radon concentration are a balance between the net exhalation of radon from the surfaces within the cave, decay in cave air, and the degree of mixing of outside air with cave air (Wilkening and Watkins, 1976) as described by mass balance Eq. (1):

$$\frac{\mathrm{d}C_{\mathrm{cave}}}{\mathrm{d}t} = E_{\mathrm{Rn}}\frac{S}{V} - \lambda C_{\mathrm{cave}} - \frac{Q}{V}(C_{\mathrm{cave}} - C_{\mathrm{out}}) \quad (1)$$

where C_{cave} and C_{out} represent radon concentration in the cave and outside, E_{Rn} is a net flux of radon atoms from the material surrounding the cavity into the open volume, S and V are surface area and volume of the cavity, λ is the radon decay constant and Q the natural flow rate of cave air. Since the exact volume of the cave and the natural flow rate are not known because of the complex morphology of the Postojna cave passages, radon mass balance Eq. (1) can be simplified to Eq. (2),

$$\frac{\mathrm{d}C_{\mathrm{cave}}}{\mathrm{d}t} \approx \Phi - \lambda C_{\mathrm{cave}} - \frac{k_i|\Delta T|C_{\mathrm{cave}}}{L} \quad (2)$$

where Φ (Bq m^{-3}s^{-1}) is the radon source term, ΔT (K) is the difference between outside and cave temperatures, L (m) is distance of the measuring location from the entrance and t (s) is time. The outside radon concentration is set at zero, since it is much less than the value in the cave. The radon source term, Φ, is calculated from Eq. (3) in the case of no ventilation, when radon concentration reaches its maximum

$$\Phi = \lambda C_{\mathrm{cave}}^{\mathrm{max}}. \quad (3)$$

Values of k can be calculated from existing data for every single day according to Eq. (4),

$$k_i = \frac{\Phi L}{|\Delta T|C_n} - \frac{\lambda L}{|\Delta T|} - \frac{(C_{n+1} - C_n)L}{\mathrm{d}t|\Delta T|C_n} \quad \left[\mathrm{ms^{-1}K^{-1}}\right] \quad (4)$$

where C_n and C_{n+1} represent average daily radon concentrations for two consecutive days and dt is 1 day.

4 Results and discussion

Radon concentration in the Great Mountain hall was found to be in the range from about 200 Bq m^{-3} to about 3 kBq m^{-3}. The lowest average monthly radon concentration between 2005 and 2009 occurred in March (600 Bq m^{-3}) and the highest in June (2500 Bq m^{-3}) (Fig. 2). The seasonal pattern is mainly the result of air movements caused by differences between external and internal air densities, controlled to a large extent by air temperature; this corresponds well with the processes characteristics of horizontal caves (Hakl et al., 1996). The cave temperature varies from 9 to 10 °C only, the whole year round. Radon concentrations can vary substantially from place to place in the cave (Kobal et al., 1987, 1988), depending on the distance from the entrance,

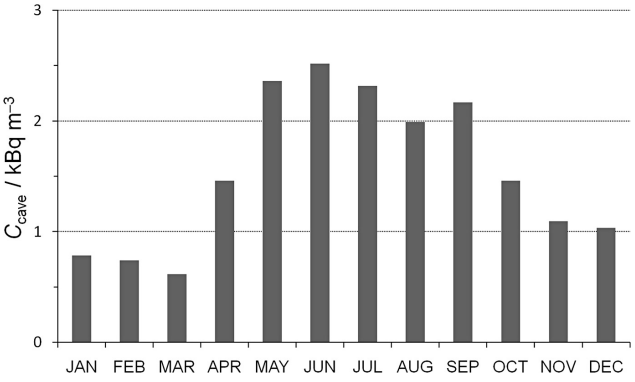

Fig. 2. Average monthly radon concentrations in the Great Mountain hall from 2005 to 2009.

the shapes of the various halls and corridors and the presence of vertical cracks and breathing halls that affect the ventilation of the cave. In addition to seasonal variation, diurnal variations were also observed at some points in the cave, usually in summer (Kobal et al., 1988; Vaupotič, 2008). However, this is not the case in the Great Mountain hall, presumably because of its huge volume; it is open on all sides and thus intensively aerated. This has a smoothing effect on radon concentration and thus reduces its diurnal variation.

4.1 Cave air ventilation and seasonal radon behaviour

During the cold winter months, air temperature in the cave is higher than outside and this temperature difference causes a natural draught of less dense, radon-rich cave air upwards through vertical cracks and channels into the outside atmosphere, thus allowing the entry of cold denser outside air into the cave through the tourist entrance (chimney effect). This continuous ventilation significantly lowers the radon concentration. As can be seen in Fig. 3a, radon concentration and outside temperature follow a linear relationship, with a correlation coefficient (R) of 0.62, as long as the outside temperature is lower than the cave temperature. However, when the daily outside temperature drops below −6 °C, radon concentration increases, presumably due to ice and snow covering the smaller breathing holes from above, thus preventing the "chimney" effect. Radon concentration reaches its maximum when ventilation stops or is minimal. This happens at outside temperatures approximately the same as the cave temperature (10 °C), as seen in Fig. 3a. Small black dots on Fig. 3a at temperatures above 10 °C and radon concentrations below 1500 Bq m^{-3}, reflect the influence of some other parameters and were not included in the analysis.

The influence of atmospheric changes on radon concentration in the Great Mountain hall was observed only after 114 h. The reason for this time lag is the geomorphology of Postojna Cave and the long distance from the tourist entrance (2 km). This shifted influence of the outdoor temperature is most clearly noticed in spring (Fig. 4a), when the cross

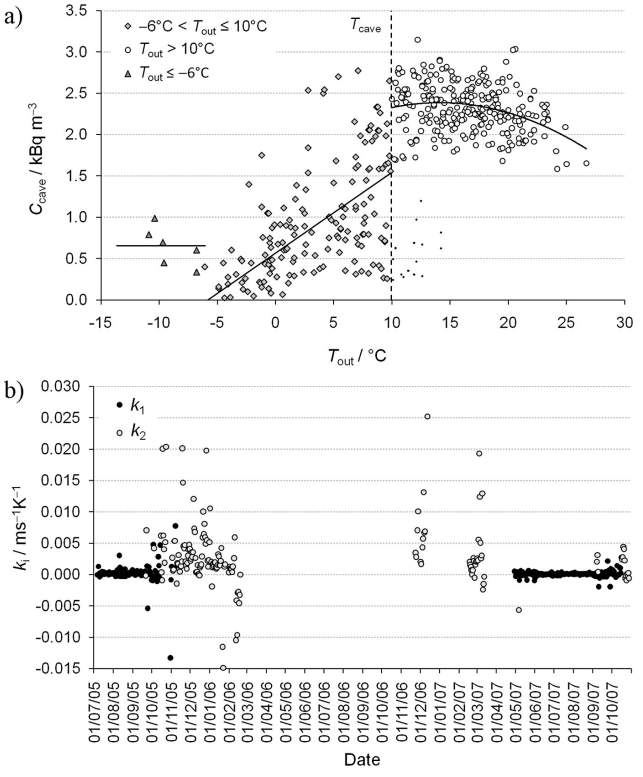

Fig. 3. **(a)** Correlation between daily average radon concentration (C_{cave}) in the Great Mountain hall and daily average outside air temperature (T_{out}) with a time lag of 4 days between temperature and radon concentration. **(b)** Calculated values of k_1 and k_2 for the period from July 2005 to October 2007.

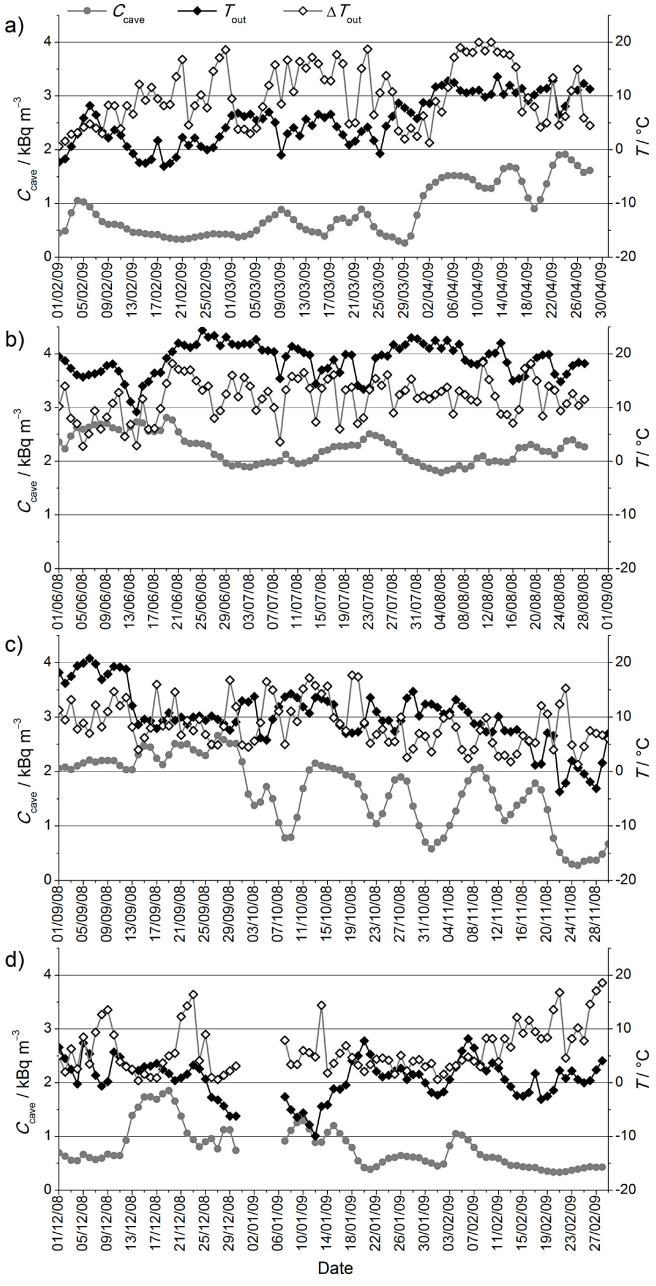

Fig. 4. Average daily radon concentrations (C_{cave}), average daily outside temperatures (T_{out}) and the difference between maximum and minimum outside temperatures (ΔT_{out}) for different seasons: **(a)** winter/spring 2009 (February, March, April), **(b)** summer 2008 (June, July, August), **(c)** autumn 2008 (September, October, November) and **(d)** winter 2008/2009 (December, January, February).

correlation between radon concentration and outside air temperatures points to 114 h lag time (Fig. 5)

In summer the ventilation is reversed and air flows from higher to lower openings of the cave. The temperature difference between outside air and cave air creates a pressure difference which causes a draught of air out of the cave and consequently lower radon concentrations over time (Fig. 3a). However this process is observed in the Great Mountain hall only when the temperature difference between outside and cave air is high enough. The effect of lowering the radon concentration could be observed during two periods of hot summer days with average daily temperatures above 20 °C in July and August 2008 (Fig. 4b).

The transition periods in spring and autumn are characterised by a large range of ventilation rates caused by diurnal variability in the temperature difference between cave and outside air. In spring, radon concentration rises only after some days of higher daily temperatures (Fig. 4a), since the increased ventilation during the cold nights prevents the accumulation of radon in the cave air. On the other hand, a sudden drop in radon concentration below 500 Bq m^{-3} can be observed as soon as one or two days after the first cold front on 19 November 2008 (Fig. 4c).

In winter, with constantly low outside temperatures (14 to 18 December 2008, Fig. 4d), continuous ventilation leads to low radon levels in the cave. In contrast, the effect of decreasing ventilation can be observed during the sunny days from 8 to 12 December 2008 (Fig. 4d), characterised by

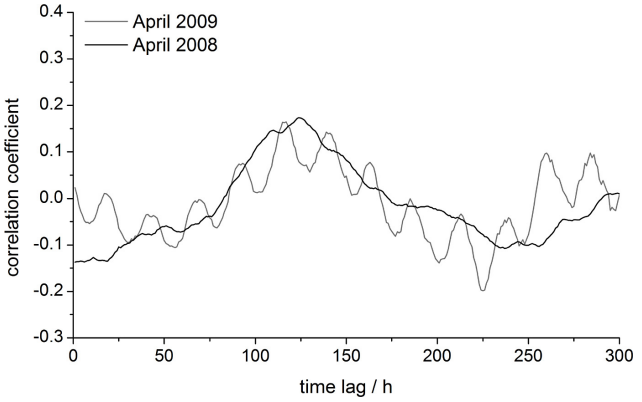

Fig. 5. Cross correlation between radon concentration and outside temperature in the period of April 2008 and April 2009 shows a common maximum at a time lag of 114 h.

high daytime temperatures around 10 °C, which caused the ventilation to slow down during daytime, thus allowing radon accumulation in the cave.

4.2 Radon modelling

The radon concentration measured from July 2005 to October 2007 was used to establish a model, while the other part of the dataset (November 2007 to November 2009) was used for testing the model. The radon source term, calculated from Eq. (3), is $(5.9 \pm 0.6) \times 10^{-3}$ Bq m^{-3} s^{-1} in the case of no ventilation, when radon concentration reaches its maximum at the confidence level of 97.5 % ($C_{cave}^{max} = 2800 \pm 280$ Bq m^{-3}). For this purpose, the time shift of 4 days between outside temperature and radon concentration was taken into account.

Constant k was calculated for every T_{out}–C_{cave} pair (daily averages) in the period from July 2005 to October 2007 and average values were determined separately for summer and winter, according to different ventilation regimes (Fig. 3b). Taking into account the different behaviour of radon concentration at temperatures below −6 °C (Fig. 3a), the average radon concentration of 0.64 ± 0.23 kBq m^{-3} was calculated. The results are collected in Table 1. Average k values were used for predicting radon concentration using Eq. (2) according to the rules described in Table 1. Constant k_1 was used for days with an average daily temperature above 10 °C and k_2 for days with an average daily temperature between −6 and 10 °C. When the average daily temperature dropped below −6 °C, radon concentration was set to 0.64 kBq m^{-3} (Table 1). The time series of predicted and measured radon concentrations are presented in Fig. 6. Radon concentration is more stable in summer than in winter (Fig. 3b), causing a higher dispersion of k_2 values and eventually also a larger discrepancy between measured and predicted radon concentrations in winter.

Table 1. Average values of k for summer (k_1) and winter (k_2) and estimated radon concentrations at daily temperatures below −6 °C.

k_i	T_{out}	k (mm s^{-1} K^{-1})	C_{cave} (kBq m^{-3})
k_1	$T_{out} > 10$ °C	0.2 ± 1.1	
k_2	-6 °C $< T_{out} \leq 10$ °C	2 ± 31	
	$T_{out} < -6$ °C		0.64 ± 0.23

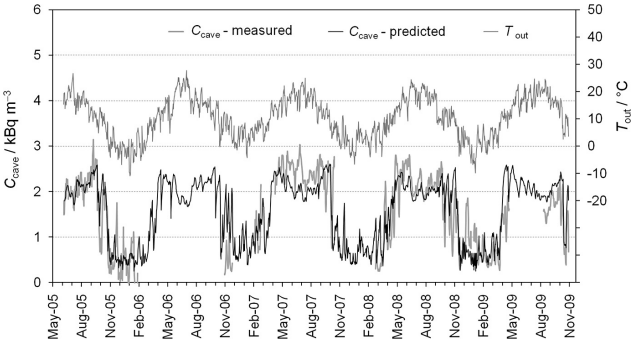

Fig. 6. Comparison of predicted and measured radon concentration (C_{cave}) and outside air temperature (T_{out}) from July 2005 to October 2009.

The correlation coefficient of 0.76 between measured and predicted radon concentrations on the validation dataset, from November 2007 to October 2009, is high. As expected, the correlation is poorer in the transitional periods of spring and autumn.

5 Conclusions

Two major ventilation regimes have been identified in the Postojna Cave that have a direct influence on radon concentration in the cave. In cold periods the cave behaves as a large chimney and the warmer, radon-rich cave air is released to the colder outside atmosphere, driving an inflow of fresh air with low radon levels. Radon levels in the cave are highest when the outside temperature is similar to or lower than the cave temperature (10 °C) and, hence, air movement is very low. Calculations have shown that the effect of the difference between outside and cave temperature on radon concentration was delayed by four days, presumably because of the distance of the Great Mountain from the tourist entrance (ca. 2 km). When the daily outside temperature drops below −6 °C, radon concentration increases. It is assumed that ice and snow on the surface above the cave prevent the cave air from leaving the cave. In summer, the ventilation is minimal or reversed and the air flows from higher to lower openings of the cave. When the temperature difference between cave and outside air is high enough to overcome the barrier

of the long distance to the cave entrance, the subsequent air pressure difference causes a draught of air out of the cave and consequently lowers radon concentration.

This model, developed on the basis of the results of our previous long-term radon monitoring in Postojna Cave, provides a relatively good prediction of radon concentration in the cave air, simply on the basis of the difference in air temperature between the cave and outside. Although successful, the model will not replace measurements, but could markedly reduce their number without diminishing the level of reliability of data needed for dose estimates for the personnel working in the cave.

Acknowledgements. This study was financed by the Slovenian Research Agency under the contract number J1–0745. The cooperation of the Postojna Cave management and personnel is appreciated.

Edited by: R. Crockett
Reviewed by: two anonymous referees

References

Ball, T. K., Cameron, D. G., Colman, T. B., and Roberts, P. D.: Behaviour of radon in the geological environment: a review, Q. J. Eng. Geol., 24, 169–182, 1991.

Cigna, A. A.: Radon in caves, Int. J. Speleol., 34, 1–18, 2005.

Cohen, B. L.: Radon daughter exposure to uranium miners, Health Phys., 42, 449–457, 1982.

Cunningham, K. I. and Larock, E. J.: Recognition of microclimate zones through radon mapping, Lechuguilla Cave, Carlsbad-caverns-national-park, New-Mexico, Health Phys., 61, 493–500, 1991.

Duenas, C., Fernandez, M. C., Canete, S., Carretero, J., and Liger, E.: Rn-222 concentrations, natural flow rate and the radiation exposure levels in the Nerja Cave, Atmos. Environ., 33, 501–510, 1999.

Eheman, C., Carson, B., Rifenburg, J., and Hoffman, D.: Occupational exposure to radon daughters in Mammoth-Cave-National-Park, Health Phys., 60, 831–835, 1991.

Fernandez, P. L., Quindos, L. S., Soto, J., and Villar, E.: Radiation exposure levels in Altamira Cave, Health Phys., 46, 445–447, 1984.

Gams, I.: Concentration of CO_2 in the caves in relation to the air circulation (in the case of the Postojna Cave), Acta Carsol., VI, 184–192, 1974.

Gillmore, G. K., Sperrin, M., Phillips, P., and Denman, A.: Radon hazards, geology, and exposure of cave users: A case study and some theoretical perspectives, Ecotoxicol. Environ. Saf., 46, 279–288, 2000.

Gillmore, G. K., Phillips, P. S., Denman, A. R., and Gilbertson, D. D.: Radon in the Creswell Crags Permian limestone caves, J. Environ. Radioactiv., 62, 165–179, 2002.

Hakl, J., Csige, I., Hunyadi, I., Várhegyi, A., and Géczy, G.: Radon transport in fractured porous media – Experimental study in caves, Environ. Int., 22, 433–437, 1996.

Hakl, J., Hunyadi, I., Csige, I., Géczy, G., Lénárt, L., and Várhegyi, A.: Radon transport phenomena studied in Karst caves – international experiences on radon levels and exposures, Radiat. Meas., 28, 675–684, 1997.

Kávási, N., Somlai, J., Szeiler, G., Szabó, B., Schafer, I., and Kovács, T.: Estimation of effective doses to cavers based on radon measurements carried out in seven caves of the Bakony Mountains in Hungary, Radiat. Meas., 45, 1068–1071, 2010.

Kies, A. and Massen, F.: Radon generation and transport in rocks and soil, in: The Moestroff Cave – a study on the geology and climate of Luxemburg's largest Maze Cave, edited by: Massen, F., Centre de Recherche Public – Centre Universitaire, 159–183, 1997.

Kobal, I., Smodiš, B., Burger, J., and Škofljanec, M.: Atmospheric ^{222}Rn in tourist caves of Slovenia, Yugoslavia, Health Phys., 52, 473–479, 1987.

Kobal, I., Ančik, M., and Škofljanec, M.: Variations of ^{222}Rn air concentration in Postojna Cave, Radiat. Prot. Dosim., 25, 207–211, 1988.

Kowalczk, A. J. and Froelich, P. N.: Cave air ventilation and CO_2 outgassing by radon-222 modeling: How fast do caves breathe?, Earth. Planet. Sci. Lett., 289, 209–219, 2010.

Nazaroff, W. W.: Radon transport from soil to air, Rev. Geophys., 30, 137–160, 1992.

Perrier, F. and Richon, P.: Spatiotemporal variation of radon and carbon dioxide concentrations in an underground quarry: coupled processes of natural ventilation, barometric pumping and internal mixing, J. Environ. Radioactiv., 101, 279–296, 2010.

Perrier, F., Richon, P., Crouzeix, C., Morat, P., and Le Mouel, J. L.: Radon-222 signatures of natural ventilation regimes in an underground quarry, J. Environ. Radioactiv., 71, 17–32, 2004.

Przylibski, T. A.: Radon concentration changes in the air of two caves in Poland, J. Environ. Radioactiv., 45, 81–94, 1999.

Šebela, S.: Tectonic structure of Postojnska jama cave system, ZRC Publishing (Scientific Research Centre), Ljubljana, 112 pp., 1998.

Šebela, S., Vaupotič, J., Koš'ták, B., and Stemberk, J.: Direct measurement of present-day tectonic movement and associated radon flux in Postojna Cave, Slovenia, J. Cave Karst Stud., 72, 21–34, 2010.

Sevc, J., Kunz, E., and Placek, V.: Lung-cancer in uranium miners and long-term exposure to radon daughter products, Health Phys., 30, 433–437, 1976.

Tanahara, A., Taira, H., and Takemura, M.: Radon distribution and the ventilation of a limestone cave on Okinawa, Geochem. J., 31, 49–56, 1997.

Vaupotič, J., Csige, I., Radolić, V., Hunyadi, I., Planinić, J., and Kobal, I.: Methodology of radon monitoring and dose estimates in Postojna Cave, Slovenia, Health Phys., 80, 142–147, 2001.

Vaupotič, J.: Nanosize radon short-lived decay products in the air of the Postojna Cave, Sci. Total Environ., 393, 27–38, 2008.

Wilkening, M. H. and Watkins, D. E.: Air exchange and Rn-222 concentrations in Carlsbad Caverns, Health Phys., 31, 139–145, 1976.

4.3.2 Scientific paper: "Reasons for large fluctuation of radon and CO_2 levels in a dead-end passage of a karst cave (Postojna Cave, Slovenia)"

Nat. Hazards Earth Syst. Sci., 13, 287–297, 2013
www.nat-hazards-earth-syst-sci.net/13/287/2013/
doi:10.5194/nhess-13-287-2013

Natural Hazards and Earth System Sciences
Open Access

Reasons for large fluctuation of radon and CO_2 levels in a dead-end passage of a karst cave (Postojna Cave, Slovenia)

A. Gregorič[1,*], J. Vaupotič[1], and F. Gabrovšek[2]

[1]Jožef Stefan Institute, Ljubljana, Slovenia
[2]Research Centre of the Slovenian Academy of Sciences and Arts, Karst Research Institute, Postojna, Slovenia

[*]*Invited contribution by A. Gregorič, recipient of the EGU Outstanding Student Poster (OSP) Award 2011.*

Correspondence to: A. Gregorič (asta.gregoric@ijs.si)

Received: 27 October 2012 – Published in Nat. Hazards Earth Syst. Sci. Discuss.: –
Revised: 17 December 2012 – Accepted: 4 January 2013 – Published: 8 February 2013

Abstract. Measurements of radon concentration were performed at three geomorphologically different locations in Postojna Cave, Slovenia. In the part of the cave open to visitors, annual average radon activity concentrations of $3255 \pm 1190\,\mathrm{Bq\,m^{-3}}$ and $2315 \pm 1019\,\mathrm{Bq\,m^{-3}}$ were found at the lowest point (LP) and in the Lepe jame (Beautiful Caves, BC), respectively. A much higher average of $25\,020 \pm 12\,653\,\mathrm{Bq\,m^{-3}}$ was characteristic of the dead-end passage Pisani rov (Gaily Coloured Corridor, GC), in which CO_2 concentration also reached very high values of 4689 ± 294 ppm in summer. Seasonal variations of radon and CO_2 levels in the cave are governed by convective airflow, controlled mainly by the temperature difference between the cave and the outside atmosphere. The following additional sources of radon and CO_2 were considered: (i) flux of geogas from the Earth's crust through fractured rocks (radon and CO_2 source), (ii) clay sediments inside the passage (radon source) and (iii) the soil layer above the cave (radon and CO_2 source).

1 Introduction

The karst cave environment is characterised by very high microenvironmental stability with essentially quasi-closed air masses (Badino, 2010), and may be considered stable in comparison to the outside atmosphere. Beyond this apparent stability, however, complex processes occur, which can today be brought to light thanks to advances in measurement techniques, data storage and data processing. All caves should be considered fragile systems, but show caves are particularly at risk because of anthropogenic impact. An understanding of cave microclimates is of great importance when studying the thermodynamics of karst processes, palaeoclimate proxies, hydrogeological aspects of speleothems, CO_2 build-up and cave ecosystems (Baldini et al., 2006; Faimon et al., 2011; Kowalczk and Froelich, 2010; Perrier and Richon, 2010; Spötl et al., 2005; Tremaine et al., 2011). The thermal and moisture characteristics of the cave air (Badino, 2010; De Freitas et al., 1982), as well as the concentration of gases (^{222}Rn, CO_2) and aerosols (Bezek et al., 2012) are mainly controlled by the degree of air exchange with the outside environment. Convective air circulation, driven by buoyancy forces created by the difference of air density between the external and internal air masses, is a major mechanism controlling air circulation in caves with more than one entrance at different elevations (Badino, 2010; Cigna, 1968; Hakl et al., 1996; Kowalczk and Froelich, 2010; Wigley, 1967). On the other hand so-called barometric circulation, driven by the internal–external pressure difference, can be very important for caves with large volumes connected by small passages, with one entrance or with extremely small entrances (Badino, 2010; Luetscher and Jeannin, 2004; Wigley, 1967). Therefore, in addition to outside atmosphere, cave geomorphology plays an important role in cave ventilation.

Radon (^{222}Rn, α-radioactive, half-life $t_{1/2} = 3.82$ days) has often been used as an excellent tracer for air circulation, since it is a noble gas and highly abundant in caves (Cigna, 2003; Cunningham and Larock, 1991; Hakl et al., 1996, 1997; Kies and Massen, 1997; Kowalczk and Froelich, 2010; Perrier et al., 2004; Przylibski, 1999). Its half-life, suitable for the timescales on which cave ventilation takes

place, distinguishes ^{222}Rn from the other two radon isotopes (^{220}Rn and ^{219}Rn). An additional advantage is its radioactivity, which makes it relatively easy to monitor the activity concentration of radon with a very low detection limit. Variation of radon concentration in cave air arises from a balance of radon emission from cave surfaces and drip waters, its radioactive transformation, and exchange with the outside atmosphere (Wilkening and Watkins, 1976). Radon concentration in underground cave systems is also characterised by internal mixing of air masses (Perrier and Richon, 2010). In a study of 220 caves around the world, Hakl et al. (1997) reported an annual average radon concentration of 2800 Bq m^{-3}.

The most important parameter governing dissolution and precipitation processes in carbonate karst is CO_2 (Dreybrodt, 1999), so understanding CO_2 distribution and dynamics in caves is important for palaeoclimatic research. The dynamics of CO_2 in caves is governed by the distribution and intensity of its sources and (mainly) advective transport by air currents. The main sources of CO_2 in caves are diffusion from the epikarst, decomposition of organic matter and precipitation of calcite from supersaturated solutions. Many authors therefore include cave ventilation when modelling CO_2 variation over time in order to explain seasonality and trend (Baldini et al., 2008; Fernandez-Cortes et al., 2011; Milanolo and Gabrovšek, 2009; Tanahara et al., 1997). CO_2 was used in this study as an additional tool to characterise and explain the sources and reasons of high radon concentration and its variability in a dead-end passage in Postojna Cave. However, the exact interpretation of short-term fluctuation of the CO_2 level remains outside the scope of this study.

The complexity and size of Postojna Cave, with its numerous known and unknown entrances at different levels and a long and highly ramified cave system, makes this cave a fascinating study site for a variety of physical and environmental studies (Bezek et al., 2012; Gosar et al., 2009; Gregorič et al., 2011; Kobal et al., 1988; Mulec et al., 2012; Šebela et al., 2010; Šebela and Turk, 2011; Vaupotič, 2008). In general the ventilation of Postojna Cave is characterised by convective airflow, controlled mainly by the temperature difference between the cave and the outside atmosphere, as discussed by Gregorič et al. (2011) for one measurement location in the Velika Gora (Great Mountain) chamber of Postojna Cave. Different ventilation regimes in the cold and warm periods of the year are responsible for the observed seasonal pattern of radon concentration with low winter and high summer levels, as already reported for this (Gregorič et al., 2011; Kobal et al., 1988; Vaupotič, 2008) and several other caves (Gillmore et al., 2002; Kowalczk and Froelich, 2010; Nagy et al., 2012; Perrier and Richon, 2010; Przylibski, 1999; Tanahara et al., 1997; Wilkening and Watkins, 1976).

In one passage of Postojna Cave, known as the Pisani rov, very high radon levels have been observed (annual mean 25 020 ± 12 653 Bq m^{-3}) which are comparable to the highest radon levels of 32 246 Bq m^{-3} (annual mean) measured in Castañar de Ibor karst cave in Spain (Lario et al., 2006), although the rest of the cave is characterised by radon levels similar to world average values (Hakl et al., 1997). This paper presents the results of 18 months (March 2011–September 2012) of continuous measurements of radon concentration in three passages in Postojna Cave, including Pisani rov, in which CO_2 concentration was additionally measured in two periods: 1 March–9 May and 28 June–1 September 2012. The aim of this study is to reveal the geophysical processes and geomorphological characteristics of cave passages that are responsible for very significant differences in the amplitude of fluctuations of radon and CO_2 levels.

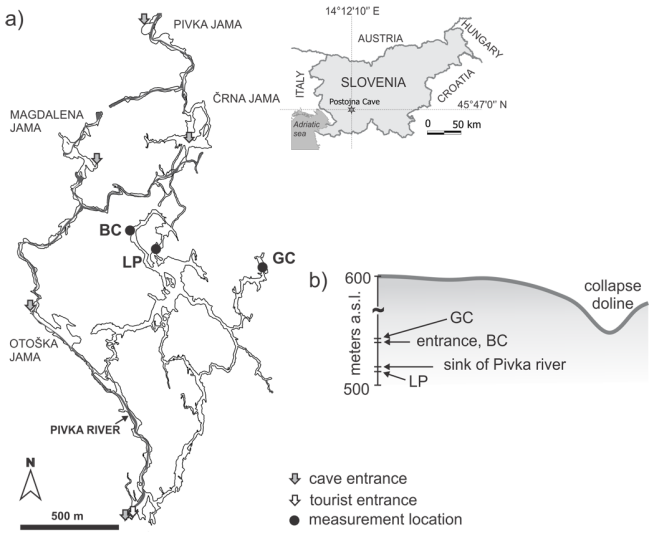

Fig. 1. Postojna Cave System. **(a)** ground plan of the Postojna Cave System with marked monitoring sites: Lepe jame (BC), the lowest point (LP) and the Pisani rov (GC); **(b)** the level of measurement locations.

2 Site and methodology

2.1 Site description

The Postojna Cave System (Fig. 1a), with its 20 570 m of known passages, is the second longest of 10 000 registered karst caves in Slovenia and one of the most visited show caves in Europe. The passages were formed at two main levels. The river Pivka sinks at the lower entrance to the cave at 511 m above sea level (m a.s.l.) (Fig. 1b) and the active river passages are mostly smaller than the higher ones. The river bed is composed mostly of gravels derived from the Eocene flysch. The entrance to the main, currently dry, passage is situated at 526.5 m a.s.l. and is 10 m high and 6 m wide. This entrance is also used as a tourist entrance. The cave passages have developed in an approximately 800 m thick layer of Upper Cretaceous bedded limestone situated

Table 1. Geomorphological characteristics of cave passages with measurement locations.

Cave passage	Abbrev.	Level/m a.s.l.	Tourist route	Geomorphological characteristics and sediments
Lepe jame (Beautiful Caves)	BC	526	15 m away	– narrow solutional fissure, created along a fault plane – loam in the fissure
Lowest point	LP	508	yes	– wide passage – thin layer of loam
Pisani rov (Gaily Coloured Corridor)	GC	529	no	– 920 m long dead-end passage – grey loam originating from weathered flysch rocks along the whole passage – 145 cm thick profile at the end of the passage: fine-grained sediments (yellowish brown silts to clays with dark stains in the upper part showing cubic to columnar disintegration with Fe stains on the fractures) covering the collapse boulders and massive flowstone

between two important Dinaric faults (Šebela et al., 2010). The cave passages are mostly horizontal. The system has six known entrances; however, unknown connections to the surface along corrosionally widened fissures undoubtedly exist. There is no forced ventilation in the cave, and air is only exchanged via natural air flow through the numerous cracks, passages and breathing holes (Gams, 1974) connecting the cave with the outside atmosphere. In the interior part the temperature is relatively stable at around 10 °C. Measurements were performed at three locations (Fig. 1a). Geomorphological characteristics of the passages are summarised in Table 1. The first location is inside a narrow solutional fissure, created along a fault plane in the Lepe jame (Beautiful Caves, BC), 526 m a.s.l. and about 15 m off the guided tourist route. The second location is situated at the lowest point (LP) of the tourist route, at 508 m a.s.l., where the passage widens significantly. The distance between the two locations is about 250 m. The third measurement location lies at the end (529 m a.s.l.) of the 920 m long Pisani rov (Gaily Coloured Corridor, GC), which deviates from the main passage to the north. This passage is not a part of the tourist route. It terminates below the slopes of a collapse doline where the bottom is filled by sediments at 535 m a.s.l. (Fig. 1b) (Šebela and Čar, 2000). Along the whole passage grey loam originating from weathered flysch rocks can be found. The roughly 145 cm thick profile of fluvial sediments situated at the end of GC consists of fine-grained sediments (yellowish brown silts to clays with dark stains in the upper part showing cubic to columnar disintegration with Fe stains on the fractures) covering the collapse boulders and massive flowstone (Zupan Hajna et al., 2008). The deepening of the collapse doline interrupted the continuation of GC towards the north (Šebela and Čar, 2000). The smallest thickness of the cave ceiling is about 30 m. Between BC and Črna jama (Black Cave) (Fig. 1a), an artificial tunnel is closed by doors that are opened only during occasional tourist visits. The ventilation from Črna jama does not have a significant impact on our monitoring locations.

2.2 Instrumentation

At all three measurement locations, radon activity concentration (C_{Rn}) was measured continuously once an hour from March 2011 to September 2012.

Radon measurements at BC were performed using a Radim 5 monitor (SMM Company, Czech Republic), which is mainly designed for radon measurements in indoor air. It determines radon concentration by measuring gross alpha activity of the radon decay products ^{218}Po and ^{214}Po, collected electrostatically on the surface of a semiconductor detector. The lower limit of detection is about 50 Bq m^{-3} and the sampling frequency is twice an hour. Hourly averages are calculated for further data evaluation in order to correspond to measurements performed using other types of measuring devices.

At the LP and GC locations, Barasol probes (MC-450, ALGADE, France) were used for radon measurements. The probe is primarily designed for radon measurements in soil gas, and it therefore has a higher lower limit of detection (about 500 Bq m^{-3}) than the Radim 5 monitor. It gives radon concentration based on alpha spectrometry of radon decay products in the energy range of 1.5 MeV to 6 MeV using an implanted silicon detector. The detector sensitivity is 50 Bq m^{-3} per 1 imp h^{-1} with a sampling frequency of once an hour. It also records temperature and relative atmospheric pressure.

In both instruments data are stored in the internal memory and are transferred to a personal computer. The instruments

are checked regularly, using a portable AlphaGuard radon monitor (Saphymo, Germany) as a reference instrument, and were calibrated in the Radon Chamber at the Henryk Niewodniczański Institute of Nuclear Physics, Polish Academy of Sciences, Kraków, Poland (Kozak et al., 2009).

Continuous measurements of CO_2 concentrations were performed in two periods, spring and summer 2012, at the GC location. CO_2 is measured along with the other microclimatic parameters within broader monitoring of cave micrometeorology. A Vaisala Carbocap CO_2 module GMM 221 with a measurement of interval 0–7000 ppm and an accuracy range of 1.5 % is used for the task. It is connected to a data logger with a sampling interval of 10 min. Probe operation is based on measurements of infrared absorption by CO_2.

Atmospheric parameters (temperature, barometric pressure and relative humidity) were measured continuously by a DL-180THP data logger (Voltcraft, Germany) in front of the tourist entrance. Daily height of rainfall was additionally provided by the Postojna weather station of the Slovenian Environment Agency (Ministry of Agriculture and Environment of the Republic of Slovenia).

3 Results

On a long timescale, radon concentration in the Postojna Cave exhibits annual cycles with high summer and low winter values (Gregorič et al., 2011), reflecting the ventilation pattern. However, amplitudes of fluctuation of radon levels differ from point to point. Annual mean radon concentration recorded at LP is $3255 \pm 1190\,\mathrm{Bq\,m^{-3}}$ and at BC, $2315 \pm 1019\,\mathrm{Bq\,m^{-3}}$, which is in the same range as values recorded at the Great Mountain location (Gregorič et al., 2011). On the other hand, radon concentration at GC is up to ten times higher than in other cave passages (Fig. 2) with the annual mean of $25\,020 \pm 12\,653\,\mathrm{Bq\,m^{-3}}$ (Table 2).

At LP radon concentration follows significant annual cycles, with average values of $1742 \pm 666\,\mathrm{Bq\,m^{-3}}$ in winter months (period D, Table 2) and constantly high summer concentrations of $4130 \pm 370\,\mathrm{Bq\,m^{-3}}$ (average of summer 2011 (B) and 2012 (F), Table 2). The biggest variations between minimum and maximum values are, as expected, characteristic of transitional periods in spring and autumn.

Situated in a side branch of the main passage, characterised by cracked and faulted rocks and possibly connected to an unknown passage, the BC location exhibits a far more variable radon concentration pattern, not only on an annual scale but also from year to year. Changes of behaviour of radon concentration were, for example, observed after floods in 2010 (Gregorič and Vaupotič, 2011). Concentration during the period discussed in this paper shows a different seasonal pattern from the LP location, with the highest values in spring and autumn, reaching up to about $5500\,\mathrm{Bq\,m^{-3}}$ (Fig. 3), whereas the concentration in summer usually remains below $4000\,\mathrm{Bq\,m^{-3}}$. Minimum radon levels are still found in the cold period of year (period D, Table 2). The radon concentration at BC exhibits high variation throughout the whole measurement period. Short periodic cycles (24 h) can be observed at BC in the transitional periods, spring and autumn, as a result of the changing ventilation regime during cold nights, when outside temperature drops below cave temperature (10 °C), and warm sunny days with outside temperature above cave temperature.

The GC location is, in contrast to LP and BC, characterised by much higher radon levels in summer, reaching up to $44\,500\,\mathrm{Bq\,m^{-3}}$, with a mean summer value of $35\,857 \pm 3259\,\mathrm{Bq\,m^{-3}}$ in 2011 and $33\,038 \pm 3015\,\mathrm{Bq\,m^{-3}}$ in 2012 (Table 1). During the cold part of the year, however, radon concentration in the periods of active ventilation drops below $500\,\mathrm{Bq\,m^{-3}}$ – the lowest of all three measurement locations (Fig. 3). The mean value in winter is $8684 \pm 7648\,\mathrm{Bq\,m^{-3}}$.

CO_2 levels at the GC location show similar seasonal characteristics in spring and summer as radon levels, with mean values of 1522 ± 614 ppm and 4689 ± 294 ppm, respectively. Higher fluctuation of CO_2 levels is observed in spring, which represents a transitional period in terms of the ventilation regime. During this period high correlation ($R^2 = 0.91$) is observed between CO_2 and ^{222}Rn concentrations, pointing to a common driving force (i.e. cave ventilation) (Fig. 4). In summer, CO_2 levels remain high, consistent with decreased ventilation. However, different behaviour of these two gases is observed, reflecting in a weaker correlation ($R^2 = 0.69$) than in spring.

3.1 Spatial differences in radon levels

Linear correlation of radon levels between the GC and LP locations, with coefficient of determination (R^2) 0.85, can be observed throughout the annual cycle, as seen in Fig. 5a and b. From Fig. 5a, where the point colour represents daily mean outside temperature, it can be noted that the lowest radon levels are usually observed at outside temperatures between 0 and 10 °C, while the highest radon levels are typical for days with daily mean outside temperatures around 15 °C. On extremely cold winter days, when T_{out} remains below 0 °C for several days, slightly higher radon levels are observed at both locations (GC and LP). Conversely, during extremely warm summer days ($T_{out} > 23$ °C), radon levels slightly below maximum are observed. Atmospheric pressure (Fig. 5b), on the other hand, does not show a significant role in controlling radon levels in the cave. Therefore, although the amplitude of fluctuation of radon concentration at GC is some orders of magnitude higher than at LP, it is obvious that both locations are subject to a similar ventilation pattern.

In contrast to GC and LP, the measurement location at BC shows slightly different behaviour, with radon levels being roughly in the same range as at the LP location. A moderate correlation ($R^2 = 0.46$) is observed between radon concentrations at BC and GC in winter months, when fresh outside

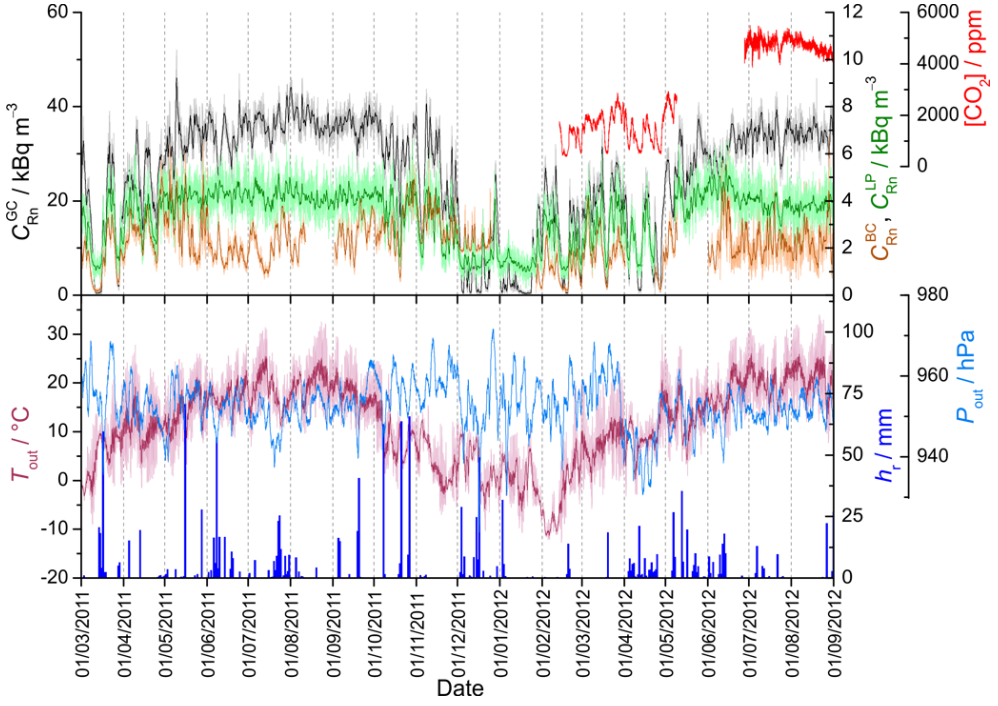

Fig. 2. Time series of radon concentration at three measurement locations (Pisani rov – C_{Rn}^{GC}, Lepe jame – $C_{Rn}^{BC}$and the lowest point – C_{Rn}^{LP}) and CO_2 concentration recorded at the GC location. Time series of main atmospheric parameters controlling radon concentration in the cave: outside air temperature (T_{out}), air pressure (P_{out}) and daily height of rainfall (h_r). Radon concentration and atmospheric parameters are expressed in hourly values, 24-h weighted average smoothing is applied to radon concentration and temperature; rainfall is expressed as absolute daily values.

air enters the cave through the large tourist entrance, and warmer cave air rises through narrow vertical cracks and channels and exits into the outside atmosphere. Radon concentration at BC (C_{Rn}^{BC}) is higher than at LP (C_{Rn}^{LP}) in autumn and lower in spring (Fig. 3). The negative correlation ($R^2 = 0.26$) observed when daily mean T_{out} exceeds 20 °C (Fig. 5c) indicates that other parameters take control of ventilation at BC and the air connection between LP and BC is cut off.

3.2 Influence of outside atmospheric parameters in governing radon levels in the cave

Correlation between radon levels at each location with outside atmospheric parameters – outside temperature (T_{out}), pressure (P_{out}) and accumulated rainfall in the last 7 days ($h_{r\text{-}7}$) (Table 2) – reveals that T_{out} has the highest influence on radon levels. The response of fluctuation of radon concentration on T_{out} is comparable at the GC and LP locations in all periods except the summer months (periods B and F), when radon concentration at BC and LP decreases with increasing T_{out}.

Correlation between P_{out} and P_{cave} (pressure in the cave) was discussed by Šebela and Turk (2011) in the study of climate characteristics of Postojna Cave, where simultaneous pressure variations at the surface and at three locations in the underground was shown. Therefore, air pressure may in this case have an influence on radon concentration only by the effect of "barometric pumping" of radon from the pore space (Perrier and Richon, 2010). However, no significant influence of P_{out} can be observed, possibly due to the obscured effect of pressure changes by airflows driven by temperature gradients.

The most sensitive measurement location for rainfall with respect to radon concentration seems to be BC, where significant changes of radon levels after heavy flooding in 2010 (Gregorič and Vaupotič, 2011) provide further evidence for high sensitivity to precipitation. Rainfall acts in two ways at this location; firstly, by reducing the air connection between the outside atmosphere and the cave atmosphere due to saturation of soil pores on the surface (thus causing an increase of radon concentration) and, secondly, by reducing radon exhalation from rock surface and cracks (decrease of radon concentration shown about a week after heavy rainfall) (Gregorič and Vaupotič, 2011). On the other hand, no significant correlation with rainfall was observed for the GC location.

3.3 Estimation of radon source

The ventilation characteristics of a cave can be reflected in the fluctuation of radon concentration provided the turnover time is shorter than about five mean lives of ^{222}Rn

Table 2. Basic statistics (min – minimum, max – maximum, AM – arithmetic mean and SD – standard deviation) of radon concentration (C_{Rn}) at locations LP, BC and GC in 6 periods (A to F) and correlation coefficient R between C_{Rn} and outside air temperature (T_{out}), C_{Rn} and atmospheric pressure (P_{out}), and C_{Rn} and cumulative height of rainfall in the last 7 days ($h_{r\text{-}7}$) for each location and time period.

		period	C_{Rn} / Bq m^{-3}						
			min	max	AM	SD	$R(C_{Rn}, T_{out})$	$R(C_{Rn}, P_{out})$	$R(C_{Rn}, h_{r\text{-}7})$
LP		Mar 2011–12 Mar 2012	1019	5030	3255	1190			
	A	Mar–May 2011	1138	4636	3370	993	0.51	0.05	0.19
	B	Jun–Aug 2011	3662	5030	4244	302	−0.30	−0.01	0.36
	C	Sep–Nov 2011	1608	4826	3653	850	0.60	−0.15	0.30
	D	Dec 2011–Feb 2012	1019	4019	1742	666	−0.55	0.18	−0.16
	E	Mar–May 2012	1275	4729	3164	980	0.57	0.31	0.26
	F	Jun–Aug 2012	2874	5389	4022	440	−0.40	−0.17	0.52
BC		Mar 2011–Mar 2012	185	4909	2315	1019			
	A	Mar–May 2011	185	4909	2430	1154	0.30	−0.06	0.09
	B	Jun–Aug 2011	937	3636	2039	654	−0.52	−0.18	0.23
	C	Sep–Nov 2011	937	4865	2925	804	−0.24	0.19	0.43
	D	Dec 2011–Feb 2012	209	3825	1543	828	0.30	−0.06	0.47
	E	Mar–May 2012	260	4059	1853	852	−0.14	−0.01	−0.27
	F	Jun–Aug 2012	1093	4428	2282	710	−0.41	−0.04	0.40
GC		Mar 2011–Mar 2012	344	44 578	25 020	12 653			
	A	Mar–May 2011	486	44 578	24 514	10 307	0.47	0.15	0.08
	B	Jun–Aug 2011	25 861	43 872	35 857	3259	0.10	0.12	−0.21
	C	Sep–Nov 2011	10 571	40 123	30 910	6884	0.64	−0.10	0.10
	D	Dec 2011–Feb 2012	344	26 666	8684	7648	−0.51	0.28	−0.31
	E	Mar–May 2012	1095	36 939	20 147	8821	0.39	0.33	0.11
	F	Jun–Aug 2012	24 373	38 776	33 038	3015	0.53	0.29	−0.27

(approximately four weeks) (Kowalczk and Froelich, 2010). Cave ventilation represents the proportion of cave air exchanged per time unit. If the cave atmosphere is just pulled back and forth due to an alternating ventilation regime during transitional periods in spring and autumn, there is no air exchange in the deeper parts of the cave. This period can be called a stagnant ventilation period and could be the reason for higher radon levels at BC in spring and autumn. By contrast, ventilation is considered active when the cave remains in one ventilation regime for long enough in comparison to the time that air is retained in the cave (i.e. residence time) (Faimon et al., 2011).

According to Wilkening and Watkins (1976) and Perrier et al. (2004), the temporal evolution of radon concentration at a given location in the cave can be described as

$$\frac{dC_{Rn}^{cave}}{dt} = \frac{S}{V}\Phi - \lambda C_{Rn}^{cave} - v(C_{Rn}^{cave} - C_{Rn}^{out}), \quad (1)$$

where S (m^2) and V (m^3) are, respectively, the total surface area and volume of the cave; Φ (Bq m^{-2} h^{-1}) represents the radon exhalation rate from the rock surface; λ (h^{-1}) is the radioactive decay constant of ^{222}Rn; v (h^{-1}) is the cave ventilation rate; and C_{Rn}^{out} (Bq m^{-3}) is the radon concentration in the outside air. Note that the radon concentration in the outside air is on the order of tens of Bq m^{-3} and thus negligible in comparison to the radon concentration in the cave air.

As the total area and volume of the cave are very hard to determine without exact measurements, we considered the radon source for different locations separately:

$$\Phi_{ch} = \frac{S_{ch}}{V_{ch}}\Phi, \quad (2)$$

where Φ_{ch} (Bq m^{-3} h^{-1}) is the radon source in a specific chamber, either GC or LP; S_{ch} (m^2) and V_{ch} (m^3) are, respectively, the surface area and volume of the chamber; and Φ (Bq m^{-2} h^{-1}) represents the radon exhalation rate from the rock surface.

The radon source can be estimated for the summer period at the GC and LP locations when radon concentration remains constantly high – around 40 kBq m^{-3} at GC and 4 kBq m^{-3} at LP location. If we consider the summer period as a stagnant ventilation period and a constant radon concentration, Eq. (1) can be transformed to

$$\Phi_{ch} = \lambda C_{Rn-max}^{ch}, \quad (3)$$

where C_{Rn-max}^{ch} (Bq m^{-3}) represents the highest radon concentration in a specific chamber. This means that in order to maintain 40 kBq m^{-3} (4 kBq m^{-3}) during stable conditions in summer at the GC (LP) location, the radon source should not be less than about 300 Bq m^{-3} h^{-1} (30 Bq m^{-3} h^{-1}).

Winter ventilation should be similar at the BC and LP locations, while during other periods of year the BC location

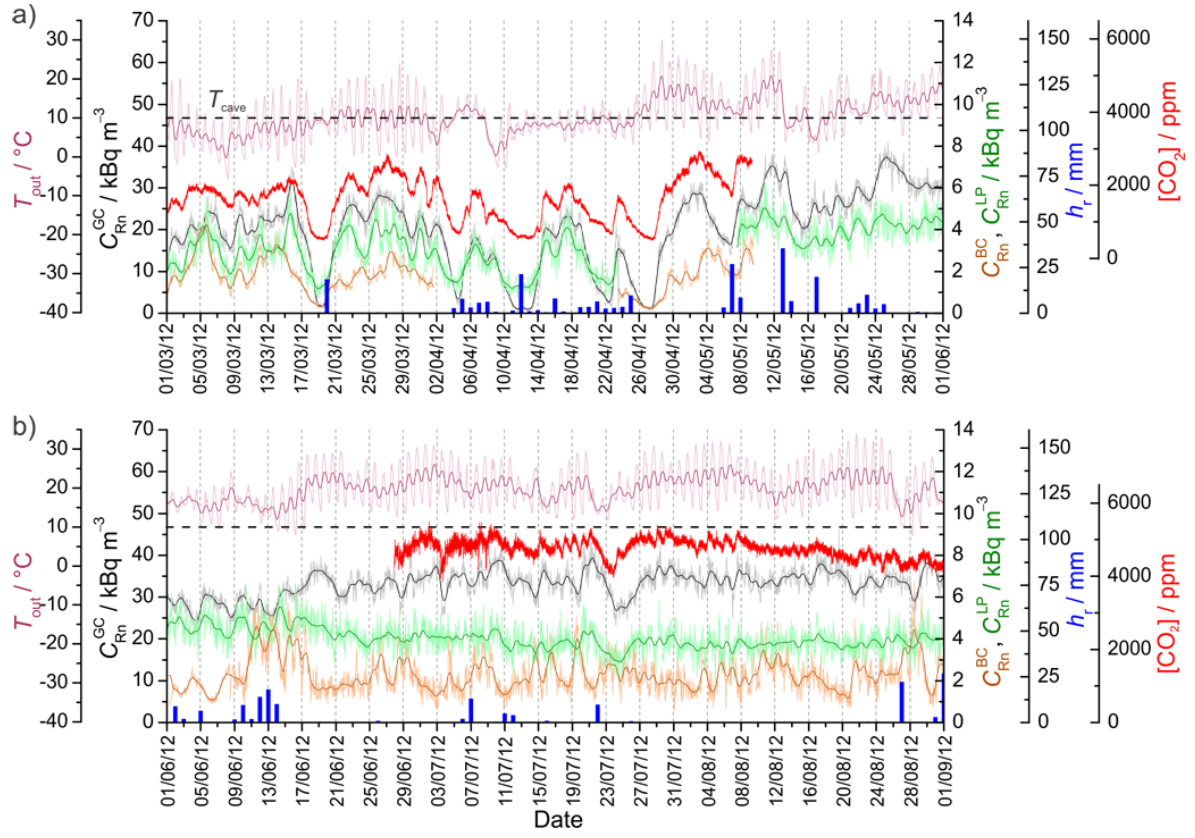

Fig. 3. Time series of radon concentration at three measurement locations (Pisani rov – C_{Rn}^{GC}, Lepe jame – $C_{Rn}^{BC}$and the lowest point – C_{Rn}^{LP}), CO_2 concentration at the GC location and atmospheric parameters: outside air temperature (T_{out}) and daily height of rainfall (h_r) in two periods: spring **(a)** and summer **(b)** 2012. Radon concentration and atmospheric parameters are expressed in hourly values; 24-h weighted average smoothing is applied to radon concentration and air temperature; rainfall is expressed as absolute daily values. CO_2 concentration is measured at 10-min intervals.

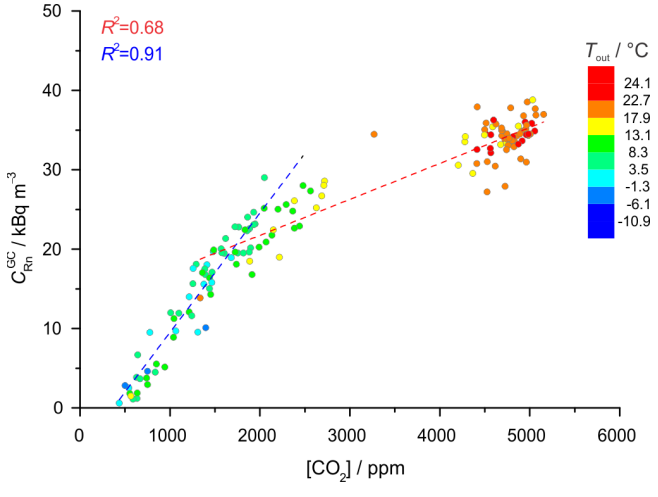

Fig. 4. Correlation between daily mean values of radon concentration (C_{Rn}^{GC}) and CO_2 concentration at GC location depending on outside air temperature (colour scale).

is subject to mixing of different air currents, carrying cave air from different passages with various radon levels. On the other hand, occasional strong winter ventilation is expected at the GC location, in order to decrease radon concentration to lower levels than at other two locations (Fig. 3a).

4 Discussion

Based on the morphology of the cave and several openings at different altitudes, we can characterise the Postojna Cave as a dynamic cave which is ventilated throughout the year. Different parts of the cave, however, exhibit different ventilation patterns based on local geomorphology. As also reported in the study of radon concentration in the Great Mountain chamber in this cave (Gregorič et al., 2011) and for several other caves (De Freitas, 2010; Spötl et al., 2005; Wilkening and Watkins, 1976), two main ventilation regimes can be distinguished in the main passage of the Postojna Cave. The measurement locations considered in this study, i.e. LP, BC and GC, have unique characteristics. Comparing the LP and BC locations, situated in the central part of the

cave in galleries extending from the main passage, LP lies at 508 m a.s.l., while BC, located at 526 m a.s.l., has a specific geomorphology and microlocation – a narrow corrosionally widened fissure, located 15 m from the central part of the passage, characterised by numerous, more or less pronounced fault planes. Significant differences can therefore be found in their ventilation pattern and radon fluctuation, while the annual mean radon concentration is roughly the same for both locations. GC, on the other hand, is situated in a dead-end passage off the main passage and is therefore characterised by a higher stability of the cave atmosphere. The entrance is located below the ceiling of the main passage, and the measurement location is situated at 529 m a.s.l.

During the winter period, the difference in density between the cold outside air and warm cave air triggers a rise of warmer cave air, which exhales to the outside atmosphere through vertical cracks and fissures, thus giving space to cold, denser outside air, which enters the cave through lower entrances. This so called "chimney effect" predominates throughout the winter and can be observed through the entire cave system. On the basis of relatively good correlation between radon concentration at all three locations (Fig. 5) in winter, as well as the good correspondence between CO_2 and radon at the GC location (Fig. 4), it may be assumed that a current of fresh outside air comes in from the tourist entrance and river entrance, is lifted upwards, and leaves the cave through vertical cracks and openings. The artificial tunnel that connects Lepe jame with Črna jama is closed off by a door, thus preventing the airflow in direction from Črna jama. Therefore, both ^{222}Rn and CO_2 concentrations at GC tend to decrease toward their atmospheric levels ($\approx$10–30 Bq m^{-3} for ^{222}Rn and $\approx$380 ppm for CO_2) during periods with an active chimney effect, whereas radon levels at LP, located lower than the tourist entrance, still remain higher than at GC. Owing to the remote location of BC, a slower increase of C_{Rn}^{BC} in comparison to C_{Rn}^{LP} is observed in spring, and a slower decrease in autumn (Fig. 3). The chimney effect is most pronounced at GC when T_{out} is lower than the cave temperature ($< 10\,°C$), but remains above 0 °C. Below that temperature, the snow layer and water freezing in the upper few centimetres of the soil layer above the cave prevent the exhalation of cave air and provoke cave air isolation. Consequently, an increase of radon concentration (and CO_2) is observed first at GC (Fig. 5a and c) and then, at lower temperatures, also at BC and LP.

Ventilation decreases in summer and is more pronounced at the beginning of the main passage, where fresh, warmer outside air enters the cave below the ceiling and cold cave air is swept out of the cave near the bottom. When the temperature difference of outside and cave air reaches the critical point, around 10 °C (at mean daily $T_{out} > 20\,°C$), warm air enters the cave system through known and unknown entrances, fissures and cracks at higher elevations and leaves the cave through lower entrances. There is frequent strong ventilation from the BC location toward the main passage

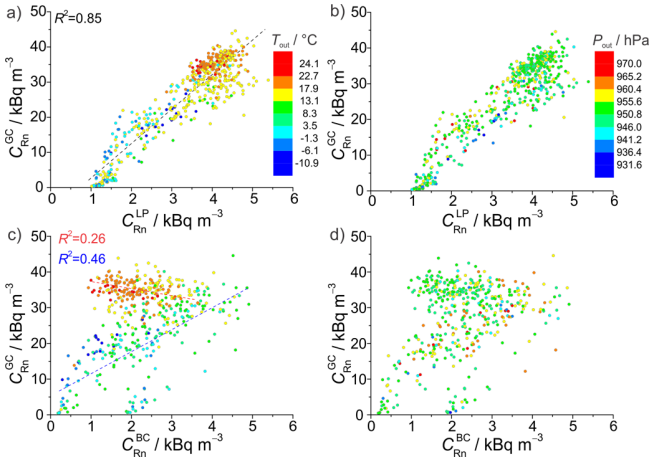

Fig. 5. Correlation between radon concentration at GC (C_{Rn}^{GC}) and LP (C_{Rn}^{LP}) depending on: **(a)** outside air temperature (colour scale) and **(b)** atmospheric pressure (colour scale) and correlation between radon concentration at GC and BC (C_{Rn}^{BC}) depending on: **(c)** outside air temperature (colour scale, R^2 for summer and winter period) and **(d)** atmospheric pressure (colour scale). Daily mean values are used.

in summer (Šebela and Turk, 2011). Behind the BC location, fresh air could enter through subvertical corrosionally widened fissures, possibly through some undiscovered cave chambers. On the other hand, summer ventilation has only a small effect on the LP location, and is almost undetectable at the GC location.

The results show that the intense winter ventilation regime takes control over the behaviour of gases in the cave, resulting in a high correlation between different locations as well as a good correspondence in the fluctuation of different gases (e.g. CO_2 and ^{222}Rn). On the other hand, together with diminishing effect of ventilation in summer, the response of gases to other processes becomes apparent (e.g. changes of radon exhalation from the rock surface and from deeper parts of the Earth's crust, and changes of the flux of CO_2 from the epikarst).

The question of high differences in the spatial distribution of gases cannot, however, be explained simply by the ventilation characteristics of the cave, although it is obvious that the atmosphere in the Pisani rov is more stable than in the main cave passages. Stable conditions are reflected additionally in cave air temperature, with the highest daily amplitude of 0.2 °C at the LP location and only 0.03 °C at the GC location. A rapid increase in both radon and CO_2 concentrations during decreased ventilation points to strong radon and CO_2 sources, which could be the sum of different contributions: (i) flux of gases from the ground in faulted rocks, (ii) cave loam sediments as a radon source and (iii) deep soil layer in the collapse doline – on the surface where the Pisani rov terminates – as a source of radon and CO_2. The process (i), known as advection of geogas (Etiope and Martinelli, 2002), is a common source of both radon and CO_2

and can act as a major radon source in fractured rocks. CO_2 (together with other gases) works as a carrier gas for radon (Kristiansson and Malmqvist, 1982). While numerous fault zones are found along the Pisani rov (Šebela, 1992), this process may have a substantial role in controlling the concentration of radon and CO_2 in this passage. The second source of radon (ii) are rock surfaces and cave sediments, from where radon diffuses to the cave air. While limestone has basically the same characteristics in all cave passages, a large amount of cave sediments at the GC location makes this part different compared to other cave passages. Clays, especially when radium is absorbed to clay minerals and ferrous oxides, may have a high emanation capacity (Miklyaev and Petrova, 2011), which determines the amount of free radon in the geologic medium. Considering the stable atmospheric conditions in the cave throughout the year, the radon emanation from clays should be constant. Process (iii) could be expressed when outside air temperature is higher than cave temperature and the chimney effect stops. Airflow in summer is decreased as the fresh outside air moves downwards through narrow fissures, soil and rock matrices. Vertical connection of the cave and outside air in summer, responsible for decreasing radon concentration at BC (and partially LP), is influenced at the GC location by the deeper soil layer in the bottom of the collapse doline. The soil in such areas on carbonate rocks (e.g. dolines, sinkholes) could become enriched with natural radionuclides (also ^{226}Ra as a radon source) due to their migration by water, as presented in the study of natural radionuclides in Slovenian soils (Gregorič et al., 2012). The soil layer on the surface can therefore have high radon potential. Furthermore, the soil layer can be also an efficient CO_2 source due to biological activity, with CO_2 entering the cave environment by degassing from percolating water and gravity seepage through rock fractures in the thin cave ceiling. The above mechanisms, with the emphasis on process (iii), are the main reason for significant difference of gas concentrations between the Pisani rov and the main cave passages during the summer ventilation regime. On the other hand, the difference in the behaviour of radon and CO_2 in summer, observed by decreased correlation between them, can be explained by processes (ii) and (iii).

5 Conclusions

Investigations of radon and CO_2 levels carried out at three geomorphologically different locations in the Postojna Cave uncovered significant differences in the spatial distribution of radon concentration, and a high amplitude of fluctuation of radon and CO_2 concentrations in the Pisani rov, a dead-end passage in the cave. Concentrations of radon measured in this passage are, according to the published data, one of the highest concentrations measured in limestone caves. This research enables better understanding not only of the ventilation characteristics of Postojna Cave, but also of radon and CO_2 sources and mechanisms leading to very high concentrations of both gases. Significant differences in radon concentration between the main passages of the cave (up to 5400 Bq m^{-3}) and the Pisani rov (up to 44 600 Bq m^{-3}), as well as high CO_2 concentration at the GC location, lead to the conclusion that ventilation itself could not be the only reason for the extremely high variability in the spatial distribution of radon and CO_2 in Postojna Cave. Taking into account the geomorphological characteristics of cave passages, a substantial contribution to radon and CO_2 concentration may be represented by the deeper soil layer above this passage, formed at the bottom of the collapse doline – this effect being additionally emphasised by the thin cave ceiling. Additional radon sources with very low variability may be the clay sediments which are present along the whole of the Pisani rov.

Acknowledgements. This work was supported by the Ministry of Education, Science, Culture and Sport of the Republic of Slovenia (Programme P1-0143: *Cycling of substances in the environment, mass balances, modelling of environmental processes and risk assessment* and Project L6-2156(B): *Measurements and analysis of selected climatic parameters in karst caves: An example of Postojnska jama (Slovenia)*).

The cooperation of the Postojna Cave management is appreciated. The authors would like to thank Stanislav Glažar for his guidance and help with measurements, and Ivan Kobal for his constructive suggestions and ideas.

Edited by: R. Crockett
Reviewed by: two anonymous referees

References

Badino, G.: Underground meteorology – "What's the weather underground?", Acta Carsol., 39, 427–448, 2010.

Baldini, J. U. L., Baldini, L. M., McDermott, F., and Clipson, N.: Carbon dioxide sources, sinks, and spatial variability in shallow temperate zone caves: Evidence from Ballynamintra Cave, Ireland, J. Cave Karst Stud., 68, 4–11, 2006.

Baldini, J. U. L., McDermott, F., Hoffmann, D. L., Richards, D. A., and Clipson, N.: Very high-frequency and seasonal cave atmosphere PCO_2 variability: Implications for stalagmite growth and oxygen isotope-based paleoclimate records, Earth. Planet. Sci. Lett., 272, 118–129, 2008.

Bezek, M., Gregorič, A., Kávási, N., and Vaupotič, J.: Diurnal and seasonal variations of concentration and size distribution of nano aerosols (10–1100 nm) enclosing radon decay products in the Postojna Cave, Slovenia, Radiat. Prot. Dosim., 152, 174–178, 2012.

Cigna, A. A.: An analytical study of air cyrculation in caves, Int. J. Speleol., 3, 41–54, 1968.

Cigna, A. A.: The distribution of radon concentration in caves, Int. J. Speleol., 32, 113–115, 2003.

Cunningham, K. I. and Larock, E. J.: Recognition of microclimate zones through radon mapping, Lechuguilla Cave, Carlsbad Cav-

erns National Park, New Mexico, Health Phys., 61, 493–500, 1991.

De Freitas, C. R.: The role and importance of cave microclimate in the sustainable use and management of show caves, Acta Carsol., 39, 477–489, 2010.

De Freitas, C. R., Littlbjohn, R. N., Clarkson, T. S., and Kristament, I. S.: Cave climate: Assessment of airflow and ventilation, J. Climatol., 2, 383–397, 1982.

Dreybrodt, W.: Chemical kinetics, speleothem growth and climate, Boreas, 28, 347–356, 1999.

Etiope, G. and Martinelli, G.: Migration of carrier and trace gases in the geosphere: an overview, Phys. Earth. Planet. Int., 129, 185–204, 2002.

Faimon, J., Troppová, D., Baldík, V., and Novotný, R.: Air circulation and its impact on microclimatic variables in the Císařská Cave (Moravian Karst, Czech Republic), Int. J. Climatol., 32, 599–623, 2011.

Fernandez-Cortes, A., Sanchez-Moral, S., Cuezva, S., Benavente, D., and Abella, R.: Characterization of trace gases' fluctuations on a "low energy" cave (Castañar de Íbor, Spain) using techniques of entropy of curves, Int. J. Climatol., 31, 127–143, 2011.

Gams, I.: Concentration of CO_2 in the caves in relation to the air circulation (in the case of the Postojna Cave), Acta Carsol., VI, 184–192, 1974.

Gillmore, G. K., Phillips, P. S., Denman, A. R., and Gilbertson, D. D.: Radon in the Creswell Crags Permian limestone caves, J. Environ. Radioactiv., 62, 165–179, 2002.

Gosar, A., Šebela, S., Koš'ták, B., and Stemberk, J.: Surface versus underground measurements of active tectonic displacements detected with TM 71 extensometers in Western Slovenia, Acta Carsol., 38, 213–226, 2009.

Gregorič, A. and Vaupotič, J.: Radon concentration and ventilation in two different passages in the Postojna Cave, EGU General Assembly, Vienna, Austria, 3–8 April 2011, EGU2011-5373-3, 2011.

Gregorič, A., Zidanšek, A., and Vaupotič, J.: Dependence of radon levels in Postojna Cave on outside air temperature, Nat. Hazards Earth Syst. Sci., 11, 1523–1528, doi:10.5194/nhess-11-1523-2011, 2011.

Gregorič, A., Kobal, I., Kovács, T., Szeiler, G., Fábián, F., Kardos, R., and Vaupotič, J.: Natural radioactivity of Slovenian soils, in: Proceedings of the11th International workshop on the geological aspects of radon risk mapping, Prague, Czech Republic, 18–20 September 2012, 116–125, 2012.

Hakl, J., Csige, I., Hunyadi, I., Várhegyi, A., and Géczy, G.: Radon transport in fractured porous media – Experimental study in caves, Environ. Int., 22, 433–437, 1996.

Hakl, J., Hunyadi, I., Csige, I., Géczy, G., Lénárt, L., and Várhegyi, A.: Radon transport phenomena studied in karst caves – international experiences on radon levels and exposures, Radiat. Meas., 28, 675–684, 1997.

Kies, A. and Massen, F.: Radon generation and transport in rocks and soil, in: The Moestroff Cave – a study on the geology and climate of Luxembourg's largest Maze Cave, edited by: Massen, F., Centre de Recherche Public – Centre Universitaire, Luxembourg, 159–183, 1997.

Kobal, I., Ančik, M., and Škofljanec, M.: Variations of ^{222}Rn air concentration in Postojna Cave, Radiat. Prot. Dosim., 25, 207–211, 1988.

Kowalczk, A. J. and Froelich, P. N.: Cave air ventilation and CO_2 outgassing by radon-222 modeling: How fast do caves breathe?, Earth. Planet. Sci. Lett., 289, 209–219, 2010.

Kozak, K., Mazur, J., Vaupotič, J., Kobal, I., Janik, M., and Kochowska, E.: Calibration of the IJS-CRn and IFJ-PAN radon measuring devices in the IFJ-KR-600 radon chamber, Jožef Stefan Institute Report IJS-DP-10103, Ljubljana, 2009.

Kristiansson, K. and Malmqvist, L.: Evidence for nondiffusive transport of ^{222}Rn in the ground and a new physical model for the transport, Geophysics, 47, 1444–1452, 1982.

Lario, J., Sánchez-Moral, S., Cuezva, S., Taborda, M., and Soler, V.: High ^{222}Rn levels in a show cave (Castañar de Ibor, Spain): Proposal and application of management measures to minimize the effects on guides and visitors, Atmos. Environ., 40, 7395–7400, 2006.

Luetscher, M. and Jeannin, P.-Y.: The role of winter air circulations for the presence of subsurface ice accumulations: an example from Monlési ice cave (Switzerland), Theor. Appl. Karstology, 17, 19–25, 2004.

Miklyaev, P. S. and Petrova, T. B.: Studies of radon emanation from clays, Water Resour., 38, 868–875, 2011.

Milanolo, S. and Gabrovšek, F.: Analysis of carbon dioxide variations in the atmosphere of Srednja Bijambarska Cave, Bosnia and Herzegovina, Bound.-Lay. Meteorol., 131, 479–493, 2009.

Mulec, J., Vaupotič, J., and Walochnik, J.: Prokaryotic and eukaryotic airborne microorganisms as tracers of microclimatic changes in the underground (Postojna Cave, Slovenia), Microb. Ecol., 64, 654–667, 2012.

Nagy, H. É., Szabó, Z., Jordán, G., Szabó, C., Horváth, Á., and Kiss, A.: Time variations of ^{222}Rn concentration and air exchange rates in a Hungarian cave, Isotopes Environ. Health Stud., 48, 464–472, 2012.

Perrier, F. and Richon, P.: Spatiotemporal variation of radon and carbon dioxide concentrations in an underground quarry: coupled processes of natural ventilation, barometric pumping and internal mixing, J. Environ. Radioactiv., 101, 279–296, 2010.

Perrier, F., Richon, P., Crouzeix, C., Morat, P., and Le Mouel, J. L.: Radon-222 signatures of natural ventilation regimes in an underground quarry, J. Environ. Radioactiv., 71, 17–32, 2004.

Przylibski, T. A.: Radon concentration changes in the air of two caves in Poland, J. Environ. Radioactiv., 45, 81–94, 1999.

Spötl, C., Fairchild, I. J., and Tooth, A. F.: Cave air control on dripwater geochemistry, Obir Caves (Austria): Implications for speleothem deposition in dynamically ventilated caves, Geochim. Cosmochim. Acta, 69, 2451–2468, 2005.

Šebela, S.: Geological characteristics of Pisani rov in Postojna Cave, Acta Carsol., 21, 97–116, 1992.

Šebela, S. and Čar, J.: Velika Jeršanova doline – a former collapse doline, Acta Carsol., 29, 201–212, 2000.

Šebela, S. and Turk, J.: Local characteristics of Postojna Cave climate, air temperature, and pressure monitoring, Theor. Appl. Climatol., 105, 371–386, 2011.

Šebela, S., Vaupotič, J., Koš'ták, B., and Stemberk, J.: Direct measurement of present-day tectonic movement and associated radon flux in Postojna Cave, Slovenia, J. Cave Karst Stud., 72, 21–34, 2010.

Tanahara, A., Taira, H., and Takemura, M.: Radon distribution and the ventilation of a limestone cave on Okinawa, Geochem. J., 31, 49–56, 1997.

Tremaine, D. M., Froelich, P. N., and Wang, Y.: Speleothem calcite farmed in situ: Modern calibration of $\delta^{18}O$ and $\delta^{13}C$ paleoclimate proxies in a continuously-monitored natural cave system, Geochim. Cosmochim. Acta, 75, 4929–4950, 2011.

Vaupotič, J.: Nanosize radon short-lived decay products in the air of the Postojna Cave, Sci. Total Environ., 393, 27–38, 2008.

Wigley, T. M. L.: Non-steady flow through a porous medium and cave breathing, J. Geophys. Res., 72, 3199–3205, 1967.

Wilkening, M. H. and Watkins, D. E.: Air exchange and Rn-222 concentrations in Carlsbad Caverns, Health Phys., 31, 139–145, 1976.

Zupan Hajna, N., Pruner, P., Mihevc, A., Schnabl, P., and Bosák, P.: Cave sediments from the Postojnska-Planinska cave system (Slovenia): evidence of multi-phase evolution in epiphreatic zone, Acta Carsol., 37, 63–68, 2008.

5 Conclusions

Radon can be used as a reliable tracer for several geophysical processes taking place either in the Earth's crust or at its surface. Radon measurements and studies were performed in different environments and under different conditions in order to improve our knowledge of radon sources and the processes governing its transport to the surface. The evaluation and detailed study of measurement data have lead to several conclusions.

a) Conclusions derived from the field of radon research in soil gas and water:

- the spatial variability of radon concentration in soil gas and its exhalation rate to the atmosphere were studied based on five profiles within the Ravne fault zone as well as on a fly ash disposal site. The results revealed high variability, which is within the same lithological type mainly controlled by various levels of rock and soil permeability. Therefore, the task of determining the appropriate measurement location for the purpose of earthquake precursory studies has to be accompanied by precise preliminary measurements,
- during two years of continuous radon measurements in the thermal water at Hotavlje and Bled, radon anomalies were identified that might have been caused by earthquakes. The different response of radon fluctuation to seismic activity was observed at these two measurement locations, which indicates a strong dependence on the geological characteristics of the aquifer,
- the comparison of four different approaches for differentiating between radon anomalies caused by seismic activity and those caused solely by hydrometeorological parameters showed the great advantage of machine learning methods, which enable the simultaneous incorporation of different environmental parameters.

b) In the case of Postojna Cave, radon concentration was found to be a reliable tracer for ventilation. Radon levels in the tourist part of the cave were found to be in the range comparable to the world average values measured in karst caves. On the other hand, significantly higher radon levels were measured in a dead-end passage – Pisani Rov. Based on the results of continuous measurements of radon concentration at four measurement locations in Postojna Cave, the following conclusions can be made:

- Seasonal characteristics of radon levels in the cave air at all measurement locations indicate that the most important parameter governing ventilation and thus radon levels in the cave is the outside air temperature. Two different ventilation regimes were identified, a summer and winter one. The ventilation rate is higher in winter due to the so-called "chimney effect" and can be observed throughout the entire cave system, thus preventing radon from accumulating in the cave. On the other hand, locally separated airflows exist in the warmer part of the year ($T_{out} > T_{cave}$), which leads to spatial differences in radon concentration, governed mainly by the geomorphological characteristics of the cave passages. The overall ventilation rate is weaker in summer, causing higher radon levels in the cave.
- For the measurement location at Velika Gora, a model was developed based on the results of the previous long-term monitoring in Postojna Cave. The model provides a relatively good prediction of radon concentration in the cave air, simply on the basis

of the difference in air temperature between the cave and outside.

- Surprisingly, a deviation from expected radon levels in the cave was observed during extremely cold winter days with average daily temperatures below 0 °C. At such atmospheric conditions, the snow layer and water freezing in the upper few centimetres of the soil layer above the cave prevent the exhalation of cave air and provoke cave air insulation.
- No significant influence of outside air pressure on radon levels in the cave was observed, possibly due to the obscured effect of pressure changes by airflows driven by temperature gradients.
- A time lag between outside atmospheric changes and an observed change in radon concentration is a function of the distance from the entrance of the outside air and of the ventilation rate. A time lag of 114 hours was observed at Velika Gora in spring 2008 and 2009. Additionally, a time lag was also observed between different measurement locations, indicating the direction of airflows.
- In Pisani Rov, both gases, radon and CO_2, are to a great extent governed by a degree of ventilation. Although CO_2 is known as a carrier gas for radon from the Earth's crust, both gases can have additional separate sources. The contribution of other sources might be observed from a lower correlation between both gases during stable summer conditions, when the effect of ventilation on the concentration of gases is much lower.
- Significant differences in radon concentration between the main passages of the cave (up to 5400 Bq m^{-3}) and Pisani Rov (up to 44600 Bq m^{-3}), as well as a high CO_2 concentration in Pisani Rov, lead to the conclusion that ventilation itself could not be the only reason for the extremely high variability in the spatial distribution of radon and CO_2 in Postojna Cave. Additional sources of radon and CO_2 in Pisani Rov were considered for the first time: (i) a substantial contribution to radon and CO_2 concentration may be represented by the deeper soil layer above this passage, formed at the bottom of a collapsed doline, this effect being additionally emphasised by the thin cave ceiling and (ii) clay sediments which are present along the whole of Pisani Rov as a source of radon with very low variability.
- A significant temporal variation of radon concentration was observed at the measurement location in Lepe Jame, which is, among all of the measurement locations, characterised by the highest variability of radon levels. A decreased radon source was observed after heavy flooding in September 2010 and was reflected by changes in the seasonal variation of radon levels in 2011.

The above mentioned conclusions indicate the high potential of the use of radon as a tracer in various fields of geophysics. Results of my doctoral dissertation have shown that the implementation of advanced tools in data analysis, such as machine learning methods, may highly improve this potential. Extensive research of radon transport in soil, thermal waters and in karst caves, has revealed the processes governing the spatial and temporal radon variability and has proved radon as a suitable indicator of changes in seismic activity and cave microclimate.

Further work in this research direction should primarily intensify the implementation of machine learning methods in radon-based modelling of cave ventilation, and add CO_2 gas as subsidiary parameter. After establishing a reliable model of radon levels in Postojna Cave, appearance of significant deviations of radon levels from the modelled values will show the anomalies potentially related to the seismic activity or tectonic movement recorded by extensometers already installed in the cave.

Additionally, reasons for high radon levels in Pisani Rov, reported in the paper entitled

"Reasons for large fluctuation of radon and CO_2 levels in a dead-end passage of a karst cave (Postojna Cave, Slovenia)" (Chapter 4.3.2) should be further supported by results of measurements of radon exhalation rate from the cave surfaces and by analysis of the ^{238}U-series radionuclides in the cave sediments and in the soil cover above the cave.

On the basis of the knowledge gained in this study, possibilities of additional application of radon as a research tool in geophysics, especially those related to the processes in the karstic environment, should be further investigated.

6 Acknowledgements / Zahvala

Ko se ob zaključku zanimivega obdobja, ki sem ga preživela kot mlada raziskovalka, ozrem nazaj, dobi moje doktorsko delo večji pomen. Ne vidim le raziskovanja, pisanja člankov in razmišljanja, ampak tudi osebno rast, nova prijateljstva in veliko novih izkušenj.

Doktorsko delo je nastalo na Odseku za znanosti o okolju Instituta "Jožef Stefan" v Ljubljani.

Najprej se zahvaljujem svoji mentorici prof. dr. Janji Vaupotič za strokovno vodstvo med študijem, pri načrtovanju raziskovalnega dela in pri izdelavi doktorske disertacije, predvsem pa za podporo in razumevanje.

Prof. dr. Ivanu Kobalu se zahvaljujem za vse nasvete, mnenja in izkušnje, ki so pripomogli k izboljšanju mojega dela.

Doc. dr. Borisu Zmazku se zahvaljujem za nasvete pri urejanju in analiziranju časovnih vrst izmerjenih podatkov v smeri iskanja anomalij radona kot možnih pokazateljev za spremembe seizmične in tektonske aktivnosti.

Prof. dr. Sašu Džeroskemu se zahvaljujem za pomoč pri uporabi metod strojnega učenja v analizi časovnih vrst koncentracije radona in hidrometeoroloških podatkov.

Prof. dr. Aleksandru Zidanšku se zahvaljujem za pomoč pri razumevanju prezračevanja Postojnske jame in izdelavi modela.

Zahvaljujem se vodji odseka prof. dr. Mileni Horvat in vsem sodelavcem, predvsem pa Mateji Bezek za spodbudno družbo in za pomoč pri meritvah.

Zahvaljujem se tudi skupini iz Krakówa (Laboratory of Radiometric Expertise, The Henryk Niewodniczański Institute of Nuclear Physics, Polish Academy of Sciences), ki so z dodatno merilno opremo in znanjem pripomogli k boljši zanesljivosti meritev radona v talnem zraku.

Za sodelovanje se zahvaljujem dr. Stanki Šebela in dr. Franciju Gabrovšku z Inštituta za raziskovanje krasa ZRC SAZU, ki sta z izrednim poznavanjem Postojnske jame in jamskih procesov zelo pripomogla pri interpretaciji rezultatov.

Hvala vodstvu Postojnske jame in Hotela Toplice na Bledu, ki sta mi omogočila meritve.

Iskreno se zahvaljujem tudi Stanislavu Glažarju za vodstvo po Postojnski jami in za pomoč pri meritvah.

Zahvaljujem se Javni agenciji za raziskovalno dejavnost Republike Slovenije, ki je v sklopu programa mladih raziskovalcev financirala moje doktorsko delo.

Posebno zahvalo namenjam svoji družini.
Borut, Enej in Lea, z vami je moje delo dobilo smisel.
Mama, hvala za vse jutranje telefonske klepete in pomoč brez kritike.
Nona in nono, naj bo ta doktorat tudi nagrada za vajino življenjsko delo; hvaležna sem vama za vse, kar sta nam omogočila.

7 References

Al-Tamimi, M. H.; Abumurad, K. M. Radon anomalies along faults in North of Jordan. *Radiation Measurements* **34**, 397–400 (2001).

Anderson, O. L.; Grew, P. C. Stress-corrosion theory of crack-propagation with applications to geophysics. *Reviews of Geophysics* **15**, 77–104 (1977).

Andjelov, M.; Brajnik, D. Map of natural radioactivity and radon emanation in Slovenia. *Environment International* **22,** 799–804 (1996).

Atkinson, B. K. Stress corrosion and the rate-dependent tensile failure of a fine-grained quartz rock. *Tectonophysics* **65**, 281–290 (1980).

Badino, G. Cave temperatures and global climatic change. *International Journal of Speleology* **33**, 103–114 (2004).

Badino, G. Underground meteorology – "What's the weather underground?" *Acta Carsologica* **39**, 427–448 (2010).

Baldini, J. U. L.; Baldini, L. M.; McDermott, F.; Clipson, N. Carbon dioxide sources, sinks, and spatial variability in shallow temperate zone caves: Evidence from Ballynamintra Cave, Ireland. *Journal of Cave and Karst Studies* **68**, 4–11 (2006).

Baldini, J. U. L.; McDermott, F.; Hoffmann, D. L.; Richards, D. A.; Clipson, N. Very high-frequency and seasonal cave atmosphere PCO_2 variability: Implications for stalagmite growth and oxygen isotope-based paleoclimate records. *Earth and Planetary Science Letters* **272**, 118–129 (2008).

Banner, J. L.; Guilfoyle, A.; James, E. W.; Stern, L. A.; Musgrove, M. Seasonal variations in modern speleothem calcite growth in central Texas, USA. *Journal of Sedimentary Research* **77**, 615–622 (2007).

Barillon, R.; Ozgumus, A.; Chambaudet, A. Direct recoil radon emanation from crystalline phases. Influence of moisture content. *Geochimica et Cosmochimica Acta* **69**, 2735–2744 (2005).

Barragán, R. M.; Arellano, V. M.; Portugal, E.; Segovia, N. Effects of changes in reservoir thermodynamic conditions on ^{222}Rn composition of discharged fluids: study for two wells at Los Azufres geothermal field (Mexico). *Geofluids* **8**, 252–262 (2008).

Baubron, J.-C.; Rigo, A.; Toutain, J.-P. Soil gas profiles as a tool to characterise active tectonic areas: the Jaut Pass example (Pyrenees, France). *Earth and Planetary Science Letters* **196**, 69–81 (2002).

Bezek, M.; Gregorič, A.; Kávási, N.; Vaupotič, J. Diurnal and seasonal variations of concentration and size distribution of nano aerosols (10–1100 nm) enclosing radon decay products in the Postojna Cave, Slovenia. *Radiation Protection Dosimetry* **152**, 174–178 (2012).

Bossew, P. The radon emanation power of building materials, soils and rocks. *Applied Radiation and Isotopes* **59**, 389–392 (2003).

Brajnik, D.; Miklavžič, U.; Tomšič, J. Map of natural radioactivity in Slovenia and its correlation to the emanation of radon. *Radiation Protection Dosimetry* **45**, 273–276 (1992).

Buser, S. *Tolmač lista Celovec, Osnovna geološka karta SFRJ, 1:100.000* (Zvezni

geološki zavod, Beograd, 1975).

Čar, J.; Šebela, S. Bedding planes, moved bedding planes, connective fissures and horizontal cave passages (examples from Postojnska Jama cave). *Acta Carsologica* **27**, 75–95 (1998).

Celik, N.; Cevik, U.; Celik, A.; Kucukomeroglu, B. Determination of indoor radon and soil radioactivity levels in Giresun, Turkey. *Journal of Environmental Radioactivity* **99**, 1349–1354 (2008).

Chen, C.; Thomas, D. M.; Green, R. E. Modeling of radon transport in unsaturated soil. *Journal of Geophysical Research-Solid Earth* **100**, 15517–15525 (1995).

Choubey, V. M.; Kumar, N.; Arora, B. R. Precursory signatures in the radon and geohydrological borehole data for M4.9 Kharsali earthquake of Garhwal Himalaya. *Science of the Total Environment* **407**, 5877–5883 (2009).

Chyi, L. L.; Quick, T. J.; Yang, T. F.; Chen, C. H. The experimental investigation of soil gas radon migration mechanisms and its implication in earthquake forecast. *Geofluids* **10**, 556–563 (2010).

Cicerone, R. D.; Ebel, J. E.; Britton, J. A systematic compilation of earthquake precursors. *Tectonophysics* **476**, 371–396 (2009).

Cigna, A. A. An analytical study of air cyrculation in caves. *International Journal of Speleology* **3**, 41–54 (1968).

Cigna, A. A. The distribution of radon concentration in caves. *International Journal of Speleology* **32**, 113–115 (2003).

Cigna, A. A. Radon in caves. *International Journal of Speleology* **34**, 1–18 (2005).

Clements, W. E.; Wilkening, M. H. Atmospheric-pressure effects on Rn-222 transport across earth-air interface. *Journal of Geophysical Research* **79**, 5025–5029 (1974).

Cuezva, S. et al. Short-term CO_2(g) exchange between a shallow karstic cavity and the external atmosphere during summer: Role of the surface soil layer. *Atmospheric Environment* **45**, 1418–1427 (2011).

Cunningham, K. I.; Larock, E. J. Recognition of microclimate zones through radon mapping, Lechuguilla Cave, Carlsbad Caverns National Park, New Mexico. *Health Physics* **61**, 493–500 (1991).

Darby, S. et al. Radon in homes and risk of lung cancer: collaborative analysis of individual data from 13 European case-control studies. *British Medical Journal* **330**, 223–226 (2005).

De Felice, P. Primary standards of radon. *Metrologia* **44**, S82–S86 (2007).

De Freitas, C. R. The role and importance of cave microclimate in the sustainable use and management of show caves. *Acta Carsologica* **39**, 477–489 (2010).

De Freitas, C. R.; Littlbjohn, R. N.; Clarkson, T. S.; Kristament, I. S. Cave climate: Assessment of airflow and ventilation. *Journal of Climatology* **2**, 383–397 (1982).

De Freitas, C. R.; Schmekal, A. Condensation as a microclimate process: measurement, numerical simulation and prediction in the Glowworm Cave, New Zealand. *International Journal of Climatology* **23**, 557–575 (2003).

Dobrovolsky, I. P.; Zubkov, S. I.; Miachkin, V. I. Estimation of the size of earthquake preparation zones. *Pure and Applied Geophysics* **117**, 1025–1044 (1979).

Dreybrodt, W. Chemical kinetics, speleothem growth and climate. *Boreas* **28**, 347–356 (1999).

Duenas, C.; Fernandez, M. C.; Canete, S.; Carretero, J.; Liger, E. Rn-222 concentrations, natural flow rate and the radiation exposure levels in the Nerja Cave. *Atmospheric Environment* **33**, 501–510 (1999).

Eheman, C.; Carson, B.; Rifenburg, J.; Hoffman, D. Occupational exposure to radon daughters in Mammoth Cave National Park. *Health Physics* **60**, 831–835 (1991).

Etiope, G.; Martinelli, G. Migration of carrier and trace gases in the geosphere: an overview. *Physics of the Earth and Planetary Interiors* **129**, 185–204 (2002).

Faimon, J.; Štelcl, J.; Sas, D. Anthropogenic CO_2-flux into cave atmosphere and its environmental impact: A case study in the Císařská Cave (Moravian Karst, Czech Republic). *Science of the Total Environment* **369**, 231–245 (2006).

Faimon, J.; Troppová, D.; Baldík, V.; Novotný, R. Air circulation and its impact on microclimatic variables in the Císařská Cave (Moravian Karst, Czech Republic). *International Journal of Climatology* **32**, 599–623 (2011).

Fairchild, I. J. et al. Modification and preservation of environmental signals in speleothems. *Earth-Science Reviews* **75**, 105–153 (2006).

Favara, R.; Grassa, F.; Inguaggiato, S.; Valenza, M. Hydrogeochemistry and stable isotopes of thermal springs: earthquake-related chemical changes along Belice Fault (Western Sicily). *Applied Geochemistry* **16**, 1–17 (2001).

Fernandez-Cortes, A.; Calaforra, J. M.; Sanchez-Martos, F. Spatiotemporal analysis of air conditions as a tool for the environmental management of a show cave (Cueva del Agua, Spain). *Atmospheric Environment* **40**, 7378–7394 (2006).

Fernandez-Cortes, A.; Sanchez-Moral, S.; Cuezva, S.; Benavente, D.; Abella, R. Characterization of trace gases' fluctuations on a 'low energy' cave (Castañar de Íbor, Spain) using techniques of entropy of curves. *International Journal of Climatology* **31**, 127–143 (2011).

Fernandez, P. L.; Quindos, L. S.; Soto, J.; Villar, E. Radiation exposure levels in Altamira Cave. *Health Physics* **46**, 445–447 (1984).

Fleischer, R. L. Dislocation model for radon response to distant earthquakes. *Geophysical Research Letters* **8**, 477–480 (1981).

Friedmann, H.; Gröller, J. An approach to improve the Austrian Radon Potential Map by Bayesian statistics. *Journal of Environmental Radioactivity* **101**, 804–808 (2010).

Gams, I. Concentration of CO_2 in the caves in relation to the air circulation (in the case of the Postojna Cave). *Acta Carsologica* **VI**, 184–192 (1974).

Ghosh, D.; Deb, A.; Sengupta, R. Anomalous radon emission as precursor of earthquake. *Journal of Applied Geophysics* **69**, 67–81 (2009).

Gillmore, G. K.; Phillips, P. S.; Denman, A. R.; Gilbertson, D. D. Radon in the Creswell Crags Permian limestone caves. *Journal of Environmental Radioactivity* **62**, 165–179 (2002).

Gospodarič, R. The Quaternary caves development between the Pivka basin and Polje of Planina (In Slovene, English Summary). *Acta Carsologica* **7**, 8–135 (1976).

Grad, K.; Ferjančič, L. *Tolmač lista Kranj. Osnovna geološka karta SFRJ, 1:100.000* (Zvezni geološki zavod, Beograd, 1968).

Gregorič, A. et al. Natural radioactivity of Slovenian soils, In: Barnet, I.; Neznal, M.; Pacherová, P. (eds.), *11th International workshop on the geological aspects of radon risk mapping*. 116–125 (Czech Geological Survey, Prague, 2012).

Hakl, J.; Csige, I.; Hunyadi, I.; Várhegyi, A.; Géczy, G. Radon transport in fractured porous media – Experimental study in caves. *Environment International* **22**, 433–437 (1996).

Hakl, J. et al. Radon transport phenomena studied in karst caves – international experiences on radon levels and exposures. *Radiation Measurements* **28**, 675–684 (1997).

Heinicke, J.; Italiano, F.; Koch, U.; Martinelli, G.; Telesca, L. Anomalous fluid emission

of a deep borehole in a seismically active area of Northern Apennines (Italy). *Applied Geochemistry* **25**, 555–571 (2010).

Hickman, S.; Sibson, R.; Bruhn, R. Introduction to special section: Mechanical involvement of fluids in faulting. *Journal of Geophysical Research* **100**, 12831–12840 (1995).

Holub, R. F.; Brady, B. T. The effect of stress on radon emanation from rock. *Journal of Geophysical Research* **86**, 1776–1784 (1981).

Humar, M. et al. Indoor and outdoor radon survey in Slovenia by etched track detectors. *Radiation Protection Dosimetry* **45**, 549–552 (1992).

İnan, S.; Seyis, C. Soil radon observations as possible earthquake precursors in Turkey. *Acta Geophysica* **58**, 828–837 (2010).

Ioannides, K.; Papachristodoulou, C.; Stamoulis, K.; Karamanis, D. Soil gas radon: a tool for exploring active fault zones. *Applied Radiation and Isotopes* **59**, 205–213 (2003).

Iskandar, D.; Yamazawa, H.; Iida, T. Quantification of the dependency of radon emanation power on soil temperature. *Applied Radiation and Isotopes* **60**, 971–973 (2004).

Jönsson, G. et al. Soil radon levels measured with SSNTD's and the soil radium content. *Radiation Measurements* **31**, 291–294 (1999).

Kastelic, V.; Vrabec, M.; Cunningham, D.; Gosar, A. Neo-Alpine structural evolution and present-day tectonic activity of the eastern Southern Alps: The case of the Ravne Fault, NW Slovenia. *Journal of Structural Geology* **30**, 963–975 (2008).

Kávási, N. et al. Estimation of effective doses to cavers based on radon measurements carried out in seven caves of the Bakony Mountains in Hungary. *Radiation Measurements* **45**, 1068–1071 (2010).

Kemski, J.; Siehl, A.; Stegemann, R.; Valdivia-Manchego, M. Mapping the geogenic radon potential in Germany. *Science of the Total Environment* **272**, 217–230 (2001).

Kies, A.; Massen, F. Radon generation and transport in rocks and soil. In: Massen, F. (ed.) *The Moestroff Cave – a study on the geology and climate of Luxembourg's largest Maze Cave*. 159–183 (Centre de Recherche Public – Centre Universitaire, Luxembourg, 1997).

King, C. Y. Radon emanation on San Andreas Fault. *Nature* **271**, 516–519 (1978).

King, C. Y. Impulsive radon emanation on a creeping segment of the San Andreas Fault, California. *Pure and Applied Geophysics* **122**, 340–352 (1984).

King, C. Y. Radon monitoring for earthquake prediction in China. *Earthquake Prediction Research* **3**, 47–68 (1985).

King, C. Y. Gas geochemistry applied to earthquake prediction: an overview. *Journal of Geophysical Research* **91**, 12269–12281 (1986).

King, C. Y.; Minissale, A. Seasonal variability of soil-gas radon concentration in central California. *Radiation Measurements* **23**, 683–692 (1994).

King, C. Y.; Zhang, W.; King, B. S. Radon anomalies on three kinds of faults in California. *Pure and Applied Geophysics* **141**, 111–124 (1993).

Klein, D.; Barillon, R.; Demongeot, S.; Tomasella, E.; Chambaudet, A. Investigative techniques for radon level characterization. *Radiation Measurements* **25**, 553–556 (1995).

Klusman, R. W.; Jaacks, J. A. Environmental influences upon mercury, radon and helium concentrations in soil gases at a site near Denver, Colorado. *Journal of Geochemical Exploration* **27**, 259–280 (1987).

Klusman, R. W.; Webster, J. D. Preliminary analysis of meteorological and seasonal

influences on crustal gas emission relevant to earthquake prediction. *Bulletin of the Seismological Society of America* **71**, 211–222 (1981).

Kobal, I.; Ančik, M.; Škofljanec, M. Variations of ^{222}Rn air concentration in Postojna Cave. *Radiation Protection Dosimetry* **25**, 207–211 (1988).

Kobal, I.; Smodiš, B.; Burger, J.; Škofljanec, M. Atmospheric ^{222}Rn in tourist caves of Slovenia, Yugoslavia. *Health Physics* **52**, 473–479 (1987).

Kobal, I. et al. Natural radioactivity of fresh waters in Slovenia, Yugoslavia. *Environment International* **16**, 141–154 (1990).

Kotrappa, P.; Dempsey, J. C.; Hickey, J. R.; Stieff, L. R. An electret passive environmental ^{222}Rn monitor based on ionization measurement. *Health Physics* **54**, 47–56 (1988).

Kovács, T. et al. Systematic survey of natural radioactivity of soil in Slovenia. *Journal of Environmental Radioactivity* (in press).

Kowalczk, A. J.; Froelich, P. N. Cave air ventilation and CO_2 outgassing by radon-222 modeling: How fast do caves breathe? *Earth and Planetary Science Letters* **289**, 209–219 (2010).

Kozak, K. et al. *Calibration of the IJS-CRn and IFJ-PAN radon measuring devices in the IFJ-KR-600 radon chamber*. Report (Jožef Stefan Institute, Ljubljana, 2009).

Kristan, J.; Kobal, I. A modified scintillation cell for the determination of radon in uranium mine atmosphere. *Health Physics* **24**, 103–104 (1973).

Kristiansson, K.; Malmqvist, L. Evidence for nondiffusive transport of ^{222}Rn in the ground and a new physical model for the transport. *Geophysics* **47**, 1444–1452 (1982).

Kunz, C.; Fisher, K.; McNulty, C.; VanOrt, S.; Papura, T. Soil characterization for indoor radon potential at eighteen schools in New York State. *Environment International* **22**, 557–561 (1996).

Kuo, T. et al. Anomalous decrease in groundwater radon before the Taiwan M6.8 Chengkung earthquake. *Journal of Environmental Radioactivity* **88**, 101–106 (2006).

Kuo, T. et al. Application of recurrent radon precursors for forecasting large earthquakes (Mw > 6.0) near Antung, Taiwan. *Radiation Measurements* **45**, 1049–1054 (2010).

Lario, J.; Sanchez-Moral, S.; Canaveras, J. C.; Cuezva, S.; Soler, V. Radon continuous monitoring in Altamira Cave (northern Spain) to assess user's annual effective dose. *Journal of Environmental Radioactivity* **80**, 161–174 (2005).

Lario, J.; Sánchez-Moral, S.; Cuezva, S.; Taborda, M.; Soler, V. High ^{222}Rn levels in a show cave (Castañar de Ibor, Spain): Proposal and application of management measures to minimize the effects on guides and visitors. *Atmospheric Environment* **40**, 7395–7400 (2006).

Lay, T.; Williams, Q.; Garnero, E. J. The core-mantle boundary layer and deep Earth dynamics. *Nature* **392**, 461–468 (1998).

Lombardi, S.; Voltattorni, N. Rn, He and CO_2 soil gas geochemistry for the study of active and inactive faults. *Applied Geochemistry* **25**, 1206–1220 (2010).

Lomnitz, C. *Fundamentals of Earthquake Prediction* (John Wiley & Sons, New York, 1994).

Luetscher, M.; Jeannin, P.-Y. Temperature distribution in karst systems: the role of air and water fluxes. *Terra Nova* **16**, 344–350 (2004).

Manning, C. E.; Ingebritsen, S. E. Permeability of the continental crust: Implications of geothermal data and metamorphic systems. *Reviews of Geophysics* **37**, 127–150 (1999).

Martinelli, G. Fluidodynamical and chemical features of radon 222 related to total gases:

implications for earthquake predictions. In: *Proceedings of the Advisory Group Meeting*. 48–62 (IAEA, Vienna, 1991).

Martinelli, G. Gas geochemistry and ^{222}Rn migration processes. *Radiation Protection Dosimetry* **78**, 77–82 (1998).

Miklyaev, P. S.; Petrova, T. B. Studies of radon emanation from clays. *Water Resources* **38**, 868–875 (2011).

Milanolo, S.; Gabrovšek, F. Analysis of carbon dioxide variations in the atmosphere of Srednja Bijambarska Cave, Bosnia and Herzegovina. *Boundary-Layer Meteorology* **131**, 479–493 (2009).

Mjachkin, V. I.; Brace, W. F.; Sobolev, G. A.; Dieterich, J. H. Two models for earthquake forerunners. *Pure and Applied Geophysics* **113**, 169–181 (1975).

Mogro-Campero, A.; Fleischer, R. L. Sub-terrestrial fluid convection – hypothesis for long-distance migration of radon within earth. *Earth and Planetary Science Letters* **34**, 321–325 (1977).

Mogro-Campero, A.; Fleischer, R. L.; Likes, R. S. Changes in subsurface radon concentration associated with earthquakes. *Journal of Geophysical Research* **85**, 3053–3057 (1980).

Morawska, L.; Phillips, C. R. Dependence of the radon emanation coefficient on radium distribution and internal structure of the material. *Geochimica et Cosmochimica Acta* **57**, 1783–1797 (1993).

Mulec, J.; Vaupotič, J.; Walochnik, J. Prokaryotic and eukaryotic airborne microorganisms as tracers of microclimatic changes in the underground (Postojna Cave, Slovenia). *Microbial Ecology* **64**, 654–667 (2012).

Nazaroff, W. W. Radon transport from soil to air. *Reviews of Geophysics* **30**, 137–160 (1992).

Nazaroff, W. W.; Moed, B. A.; Sextro, R. G. Soil as a source of indoor radon: generation, migration and entry. In: Nazaroff, W. W.; Nero, A. V. (eds.) *Radon and its decay products in indoor air*. 57–112 (John Wiley & Sons, New York, 1988).

Nero, A. V. Radon and its decay products in indoor air: an overview. In: Nazaroff, W.W.; Nero, A. V. (eds.) *Radon and its decay products in indoor air*. 1–53 (John Wiley & Sons, New York, 1988).

Neznal, M.; Matolín, M.; Just, G.; Turek, K. Short-term temporal variations of soil gas radon concentration and comparison of measurement techniques. *Radiation Protection Dosimetry* **108**, 55–63 (2004).

Neznal, M.; Neznal, M.; Šmarda, J. Assessment of radon potential of soils – A five-year experience. *Environment International* **22,** 819–828 (1996).

Papastefanou, C. An overview of instrumentantion for measuring radon in soil gas and groundwaters. *Journal of Environmental Radioactivity* **63**, 271–283 (2002).

Perrier, F.; Richon, P. Spatiotemporal variation of radon and carbon dioxide concentrations in an underground quarry: coupled processes of natural ventilation, barometric pumping and internal mixing. *Journal of Environmental Radioactivity* **101**, 279–296 (2010).

Perrier, F.; Richon, P.; Crouzeix, C.; Morat, P.; Le Mouel, J. L. Radon-222 signatures of natural ventilation regimes in an underground quarry. *Journal of Environmental Radioactivity* **71**, 17–32 (2004).

Pinault, J. L.; Baubron, J. C. Signal processing of soil gas radon, atmospheric pressure, moisture, and soil temperature data: A new approach for radon concentration modeling. *Journal of Geophysical Research-Solid Earth* **101**, 3157–3171 (1996).

Placer, L. Principles of the tectonic subdivision of Slovenia. *Geologija* **51**, 205–217 (2008).

Planinić, J.; Radolić, V.; Lazanin, Ž. Temporal variations of radon in soil related to earthquakes. *Applied Radiation and Isotopes* **55**, 267–272 (2001).

Plummer, W. T. Infrasonic resonances in natural underground cavities. *Journal of the Acoustical Society of America* **46**, 1074–1080 (1969).

Poljak, M.; Živčić, M.; Zupančič, P. The seismotectonic characteristics of Slovenia. *Pure and Applied Geophysics* **157**, 37–55 (2000).

Popit, A. *Vpliv seizmične aktivnosti na geokemične in geofizikalne lastnosti termalnih vod v Sloveniji*. Doctoral thesis (Faculty of Natural Sciences and Engineering, University of Ljubljana, Ljubljana, 2004).

Popit, A.; Vaupotič, J.; Dolenec, T. Geochemical and geophysical monitoring of thermal waters in Slovenia in relation to seismic activity. *Annals of Geophysics* **48**, 73–83 (2005).

Popit, A.; Vaupotič, J.; Kukar, N. Systematic radium survey in spring waters of Slovenia. *Journal of Environmental Radioactivity* **76**, 337–347 (2004).

Przylibski, T. A. Radon concentration changes in the air of two caves in Poland. *Journal of Environmental Radioactivity* **45**, 81–94 (1999).

Quindós-Poncela, L. S. et al. An improved scintillation cell for radon measurements. *Nuclear Instruments and Methods in Physics Research Section A: Accelerators, Spectrometers, Detectors and Associated Equipment* **512**, 606–609 (2003).

Rama; Moore, W. S. Mechanism of transport of U-Th series radioisotopes from solids into ground water. *Geochimica et Cosmochimica Acta* **48**, 395–399 (1984).

Ramola, R. C. Relation between spring water radon anomalies and seismic activity in Garhwal Himalaya. *Acta Geophysica* **58**, 814–827 (2010).

Ramola, R. C.; Prasad, Y.; Prasad, G.; Kumar, S.; Choubey, V. M. Soil-gas radon as seismotectonic indicator in Garhwal Himalaya. *Applied Radiation and Isotopes* **66**, 1523–1530 (2008).

Ramola, R. C.; Singh, M.; Sandhu, A. S.; Singh, S.; Virk, H. S. The use of radon as an earthquake precursor. *Nuclear Geophysics* **4**, 275–287 (1990).

Ramola, R. C.; Singh, S.; Virk, H. S. A model for the correlation between radon anomalies and magnitude of earthquakes. *Nuclear Tracks and Radiation Measurements* **15**, 689–692 (1988).

Reddy, D. V.; Nagabhushanam, P. Groundwater electrical conductivity and soil radon gas monitoring for earthquake precursory studies in Koyna, India. *Applied Geochemistry* **26**, 731–737 (2011).

Ribarič, V. The Idrija Earthquake of March 26, 1511. *Tectonophysics* **53**, 315–324 (1979).

Richon, P. et al. Measuring radon flux across active faults: Relevance of excavating and possibility of satellite discharges. *Radiation Measurements* **45**, 211–218 (2010).

Rogers, V. C.; Nielson, K. K. Correlations for predicting air permeabilities and ^{222}Rn diffusion coefficients of soils. *Health Physics* **61**, 225–230 (1991).

Sakoda, A. et al. First model of the effect of grain size on radon emanation. *Applied Radiation and Isotopes* **68**, 1169–1172 (2010a).

Sakoda, A. et al. Experimental and modeling studies of grain size and moisture content effects on radon emanation. *Radiation Measurements* **45**, 204–210 (2010b).

Sakoda, A.; Ishimori, Y.; Yamaoka, K. A comprehensive review of radon emanation measurements for mineral, rock, soil, mill tailing and fly ash. *Applied Radiation and*

Isotopes **69**, 1422–1435 (2011).

Sasaki, T.; Gunji, Y.; Okuda, T. Mathematical modeling of radon emanation. *Journal of Nuclear Science and Technology* **41**, 142–151 (2004).

Schmid, S. M.; Fugenschuh, B.; Kissling, E.; Schuster, R. Tectonic map and overall architecture of the Alpine orogen. *Eclogae Geologicae Helvetiae* **97**, 93–117 (2004).

Schumann, R. R.; Gundersen, L. C. S. Geologic and climatic controls on the radon emanation coefficient. *Environment International* **22,** 439–446 (1996).

Singh, M.; Kumar, M.; Jain, R. K.; Chatrath, R. P. Radon in ground water related to seismic events. *Radiation Measurements* **30**, 465–469 (1999).

Spötl, C.; Fairchild, I. J.; Tooth, A. F. Cave air control on dripwater geochemistry, Obir Caves (Austria): Implications for speleothem deposition in dynamically ventilated caves. *Geochimica et Cosmochimica Acta* **69**, 2451–2468 (2005).

Stranden, E.; Kolstad, A. K.; Lind, B. The influence of moisture and temperature on radon exhalation. *Radiation Protection Dosimetry* **7**, 55–58 (1984).

Szerbin, P. Radon concentrations and exposure levels in Hungarian caves. *Health Physics* **71**, 362–369 (1996).

Šebela, S. *Tectonic structure of Postojnska jama cave system* (ZRC Publishing, Ljubljana, 1998).

Šebela, S.; Čar, J. Velika Jeršanova doline – a former collapse doline. *Acta Carsologica* **29**, 201–212 (2000).

Šebela, S.; Turk, J. Local characteristics of Postojna Cave climate, air temperature, and pressure monitoring. *Theoretical and Applied Climatology* **105**, 371–386 (2011).

Šebela, S.; Vaupotič, J.; Košťák, B.; Stemberk, J. Direct measurement of present-day tectonic movement and associated radon flux in Postojna Cave, Slovenia. *Journal of Cave and Karst Studies* **72**, 21–34 (2010).

Tanahara, A.; Taira, H.; Takemura, M. Radon distribution and the ventilation of a limestone cave on Okinawa. *Geochemical Journal* **31**, 49–56 (1997).

Thomas, D. Geochemical precursors to seismic activity. *Pure and Applied Geophysics* **126**, 241–266 (1988).

Torkar, D.; Zmazek, B.; Vaupotič, J.; Kobal, I. Application of artificial neural networks in simulating radon levels in soil gas. *Chemical Geology* **270**, 1–8 (2010).

Toutain, J. P.; Baubron, J. C. Gas geochemistry and seismotectonics: a review. *Tectonophysics* **304**, 1–27 (1999).

Tremaine, D. M.; Froelich, P. N.; Wang, Y. Speleothem calcite farmed in situ: Modern calibration of $\delta^{18}O$ and $\delta^{13}C$ paleoclimate proxies in a continuously-monitored natural cave system. *Geochimica et Cosmochimica Acta* **75**, 4929–4950 (2011).

Ulomov, V. I.; Mavashev, B. Z. On forerunners of strong tectonic earthquakes. *Doklady Akademii Nauk SSSR*, 319–322 (1967).

United Nations. *Sources and effects of ionizing radiation. United Nations Scientific Committee on the Effects of Atomic Radiation, 2000 Report to the General Assembly, with annexes* (United Nations sales publication, New York, 2000).

Vàrhegyi, A.; Hakl, J.; Monnin, M.; Morin, J. P.; Seidel, J. L. Experimental study of radon transport in water as test for a transportation microbubble model. *Journal of Applied Geophysics* **29**, 37–46 (1992).

Vaupotič, J. Radon exposure at drinking water supply plants in Slovenia. *Health Physics* **83**, 901–906 (2002).

Vaupotič, J. Nanosize radon short-lived decay products in the air of the Postojna Cave. *Science of the Total Environment* **393**, 27–38 (2008).

Vaupotič, J. Slovenian approach in managing exposure to radon at workplace. *Nukleonika* **55**, 565–571 (2010).

Vaupotič, J.; Ančik, M.; Škofljanec, M.; Kobal, I. Alpha scintillation cell for direct measurement of indoor radon. *Journal of Environmental Science and Health - Part A Environmental Science and Engineering* **27**, 1535–1540 (1992).

Vaupotič, J.; Andjelov, M.; Kobal, I. Relationship between radon concentrations in indoor air and in soil gas. *Environmental Geology* **42**, 583–587 (2002).

Vaupotič, J.; Barišić, D.; Kobal, I.; Lulić, S. Radioactivity and radon potential of the terra rossa soil. *Radiation Measurements* **42**, 290–297 (2007).

Vaupotič, J. et al. Methodology of radon monitoring and dose estimates in Postojna Cave, Slovenia. *Health Physics* **80**, 142–147 (2001).

Vaupotič, J.; Kobal, I.; Križman, M. Background outdoor radon levels in Slovenia. *Nukleonika* **55**, 579–582 (2010).

Vaupotič, J. et al. Radon mapping in Slovenia based on its levels in soil gas. In: *33rd International Geological Congress*. (International Union of Geological Sciences, Oslo, Norway, 2008).

Vaupotič, J.; Žvab Rožič, P.; Barišić, D. Environmental aspect of radon potential in terra rossa and eutric cambisol in Slovenia. *Environmental Earth Sciences* **66**, 223–229 (2012).

Wakita, H.; Nakamura, Y.; Notsu, K.; Noguchi, M.; Asada, T. Radon anomaly – possible precursor of the 1978 Izu-Oshima-Kinkai earthquake. *Science* **207**, 882–883 (1980).

Walia, D.; Lyngdoh, A.; Saxena, A. Seismotectonic zones demarcation in the Shillong Plateau using the microearthquakes and radon emanation rate. *Acta Geophysica* **58**, 893–907 (2010).

Walia, V. et al. Continuous temporal soil-gas composition variations for earthquake precursory studies along Hsincheng and Hsinhua faults in Taiwan. *Radiation Measurements* **44**, 934–939 (2009a).

Walia, V. et al. Geochemical variation of soil-gas composition for fault trace and earthquake precursory studies along the Hsincheng fault in NW Taiwan. *Applied Radiation and Isotopes* **67**, 1855–1863 (2009b).

Washington, J. W.; Rose, A. W. Regional and temporal relations of radon in soil gas to soil-temperature and moisture. *Geophysical Research Letters* **17**, 829–832 (1990).

Whittlestone, S.; James, J.; Barnes, C. The relationship between local climate and radon concentrations in the Temple of Baal, Jenolan Caves, Australia. *Helictite* **38**, 39–44 (2003).

Wigley, T. M. L. Non-steady flow through a porous medium and cave breathing. *Journal of Geophysical Research* **72**, 3199–3205 (1967).

Wilkening, M. H. *Radon in the environment* (Elsevier science publishers B. V., Amsterdam, 1990).

Wilkening, M. H.; Watkins, D. E. Air exchange and Rn-222 concentrations in Carlsbad Caverns. *Health Physics* **31**, 139–145 (1976).

Wong, C. I.; Banner, J. L.; Musgrove, M. Seasonal dripwater Mg/Ca and Sr/Ca variations driven by cave ventilation: Implications for and modeling of speleothem paleoclimate records. *Geochimica et Cosmochimica Acta* **75**, 3514–3529 (2011).

Yang, T. F. et al. Variations of soil radon and thoron concentrations in a fault zone and prospective earthquakes in SW Taiwan. *Radiation Measurements* **40**, 496–502 (2005).

Zmazek, B. et al. Geochemical monitoring of thermal waters in Slovenia: relationships to seismic activity. *Applied Radiation and Isotopes* **57**, 919–930 (2002a).

Zmazek, B.; Todorovski, L.; Džeroski, S.; Vaupotič, J.; Kobal, I. Application of decision trees to the analysis of soil radon data for earthquake prediction. *Applied Radiation and Isotopes* **58**, 697–706 (2003).

Zmazek, B. et al. Radon in a thermal spring: Identification of anomalies related to seismic activity. *Applied Radiation and Isotopes* **64**, 725–734 (2006).

Zmazek, B. et al. Radon in soil gas: How to identify anomalies caused by earthquakes. *Applied Geochemistry* **20**, 1106–1119 (2005).

Zmazek, B. et al. Soil radon monitoring in the Krško Basin, Slovenia. *Applied Radiation and Isotopes* **56**, 649–657 (2002b).

Zupan Hajna, N.; Pruner, P.; Mihevc, A.; Schnabl, P.; Bosák, P. Cave sediments from the Postojnska-Planinska cave system (Slovenia): evidence of multi-phase evolution in epiphreatic zone. *Acta Carsologica* **37**, 63–68 (2008).

Živčić, M.; Cecić, I. Revised magnitudes of historical earthquakes in Slovenia. In: *Proceedings of the EGS XXXII General Asembly* (European Geophysical Society, Nice, France, 1998).

Index of Figures

Index of Tables

Appendix 1

Personal bibliography for the period 2005–2013

ASTA GREGORIČ [29524]

ARTICLES AND OTHER COMPONENT PARTS

1.01 Original scientific article

1. Gregorič, A.; Vaupotič, J.; Gabrovšek, F. Reasons for large fluctuation of radon and CO_2 levels in a dead-end passage of a karst cave (Postojna Cave, Slovenia). *Natural Hazards and Earth System Sciences* **13**, 287–297 (2013). (IF=1.983)
2. Bezek, M.; Gregorič, A.; Kávási, N.; Vaupotič, J. Diurnal and seasonal variations of concentration and size distribution of nanoaerosols (10–1100 nm) enclosing radon decay products in the Postojna Cave, Slovenia. *Radiation Protection Dosimetry* **152**, 174–178 (2012). (IF=0.822)
3. Gregorič, A.; Zidanšek, A.; Vaupotič, J. Dependence of radon levels in the Postojna Cave on outdoor air temperature. *Natural Hazards and Earth System Sciences* **11**, 1523–1528 (2011). (IF=1.983)
4. Vaupotič, J. et al. Radon concentration in soil gas and radon exhalation rate at the Ravne fault in NW Slovenia. *Natural Hazards and Earth System Sciences* **10**, 895–899 (2010). (IF=1.792)
5. Vaupotič, J. et al. Radon potential of a fly ash pile – a criterion for its use as a building lot = Radonski potencial odlagališča elektrofiltrskega pepela kot merilo za njegovo uporabo kot gradbeno zemljišče. *RMZ – Materials and Geoenvironment* **57**, 501–510 (2010).
6. Gregorič, A.; Zmazek, B.; Vaupotič, J. Radon concentration in thermal water as an indicator of seismic activity. *Collegium Antropologicum* **32**, 95–98 (2008). (IF=0.687)
7. Vaupotič, J.; Gregorič, A.; Kotnik, J.; Horvat, M.; Pirrone, N. Dissolved radon and gaseous mercury in the Mediterranean seawater. *Journal of Environmental Radioactivity* **99**, 1068–1074 (2008). (IF=1.114)
8. Bahtijari, M.; Vaupotič, J.; Gregorič, A.; Stegnar, P.; Kobal, I. Exposure to radon in the Gadime Cave, Kosovo. *Journal of Environmental Radioactivity* **99**, 343–348 (2008). (IF=1.114)
9. Bahtijari, M.; Vaupotič, J.; Gregorič, A.; Stegnar, P.; Kobal, I. Exposure to radon in dwellings in the Sharri community, Kosovo. *Radiation Protection Dosimetry* **130**, 244–248 (2008). (IF=0.951)

Bezek, M.; Gregorič, A.; Vaupotič, J. Radon decay products and 10–1100 nm aerosol particles in the Postojna Cave. *Natural Hazards and Earth System Sciences*. In press (2013).

Gregorič, A.; Vaupotič, J.; Šebela, S. The role of cave ventilation in governing cave air

temperature and radon levels (Postojna Cave, Slovenia). Submitted to *International Journal of Climatology* (2013).

Gregorič, A. et al. Radon emanation of soils from different lithological units. *Carpathian Journal of Earth and Environmental Sciences*. Accepted after minor revision (2013).

Kovács, T. et al. Systematic survey of natural radioactivity of soil in Slovenia. *Journal of Environmental Radioactivity*. In press (2013).

1.05 Poljudni članek

10. Vaupotič, J.; Gregorič, A. Radioaktivni žlahtni plin radon. *Didakta* **22**, 21–22 (2013).

1.08 Published scientific conference contribution

11. Gregorič, A. et al. Natural radioactivity of Slovenian soils. In: Barnet, I.; Neznal, M.; Pacherová, P. (eds.) *11th International workshop on the geological aspects of radon risk mapping*. 116–125 (Czech Geological Survey, Prague, Czech Republic, 2012).
12. Vaupotič, J. et al. Radon in soil gas at selected sites in Hokkaido, Japan. In: Barnet, I.; Neznal, M.; Pacherová, P. (eds.) *11th International workshop on the geological aspects of radon risk mapping*. 250–259 (Czech Geological Survey, Prague, 2012).
13. Gregorič, A.; Vaupotič, J.; Šebela, S. Vpliv zunanje temperature na koncentracijo radona v Postojnski jami. In: Kuhar, M. (ed.) *17. strokovno srečanje Slovenskega združenja za geodezijo in geofiziko*. 63–67 (Fakulteta za gradbeništvo in geodezijo, Ljubljana, 2012).
14. Gregorič, A. et al. Geogenic radon potential in Slovenia. In: Serafimovski, T.; Dolenec, T. (eds.) *Anthropogenic effects on the human environment in the Neogene basins in the SE Europe*. 1–8 (Faculty of Natural Sciences and Engineering, IGCP Committee, Ljubljana, 2011).
15. Gregorič, A.; Zmazek, B.; Vaupotič, J. Methods for long-term radon time-series evaluation. In: *BlackSeaHazNet Training–Seminar Workshop: Complex research of earthquake's forecasting possibilities, seismicity and climate change correlations.* 100–110 (M. Nodia Institute of Geophysics, Iv. Javakhishvili Tbilisi State University, Tbilisi, Georgia, 2011).
16. Gregorič, A.; Zmazek, B.; Kobal, I.; Vaupotič, J. Radon as earthquake precursor. In: *BlackSeaHazNet Training–Seminar Workshop: Complex research of earthquake's forecasting possibilities, seismicity and climate change correlations.* 175–180 (M. Nodia Institute of Geophysics, Iv. Javakhishvili Tbilisi State University, Tbilisi, Georgia, 2011).
17. Bezek, M.; Gregorič, A.; Vaupotič, J.; Kobal, I. Seasonal variation of nano aerosols in Postojna Cave, Slovenia. In: Somlai, J.; Kovács, T. (eds.) *VI Magyar Radon Fórum: A radon a környezetben nemzetözi workshop*. 36–48 (University of Pannonia, Veszprém, Hungary, 2011).
18. Gregorič, A.; Vaupotič, J. Diurnal variation of radon concentration in the Postojna Cave. In: Krajcar Bronić, I. (ed.) *Zbornik radova VIII. simpozija Hrvatskog društva za zaščitu od zračenja: HDZZ – CRPA.* 238–242 (Hrvatsko društvo za zaščitu od zračenja, Zagreb, Croatia, 2011).
19. Obu, K. et al. The influence of air temperature and barometric pressure on radon and carbon dioxide levels in air of a Karst cave. In: Krajcar Bronić, I. (ed.) *Zbornik radova VIII. simpozija Hrvatskog društva za zaščitu od zračenja: HDZZ –*

CRPA. 243–248 (Hrvatsko društvo za zaščitu od zračenja, Zagreb, Croatia, 2011).
20. Iskra, I.; Bezek, M.; Gregorič, A.; Vaupotič, J. Promet kot vir emisij ultrafinih delcev = Traffic emissions of ultrafine particles. In: *Slovenski kemijski dnevi 2010* (FKKT, Maribor, 2010).
21. Gregorič, A.; Vaupotič, J. Radon v talnem in zunanjem zraku = Radon in soil gas and outdoor air. In: *Slovenski kemijski dnevi 2010* (FKKT, Maribor, 2010).
22. Žvab Rožič, P.; Vaupotič, J.; Gregorič, A. Measurements of radon in soil with Alpha scintillation cells in Slovenia. In: Boev, B.; Serafimovski, T. (eds.) *Zbornik na trudovi: prvi kongres na geolozite na Republika Makedonija.* 495–502 (Makedonsko geološko društvo: Univerzitet Goce Delčev Ohrid, Ohrid, Macedonia, 2008).
23. Zmazek, B.; Gregorič, A.; Vaupotič, J.; Kobal, I. Anomalous radon levels in thermal water as an indicator of seismic activity. In: Barišić, D. (ed.) *Zbornik radova VII. simpozija Hrvatskog društva za zaščitu od zračenja: HDZZ – CRPA.* 277–281 (Hrvatsko društvo za zaščitu od zračenja, Zagreb, Croatia, 2008).

1.12 Published scientific conference contribution abstract

24. Gregorič, A.; Bezek, M.; Vaupotič, J. Radon's dual role in karst caves: tracing air movement and affecting human health. In: Lisjak, D.; Dušak, P.; Kralj, S. (eds.). *7th Young Researchers' Day 2013* (Jožef Stefan Institute, Ljubljana, 2013).
25. Gregorič, A.; Bezek, M.; Vaupotič, J. The role of natural ventilation in the exposure to radon in the Postojna Cave. In: *EGU General Assembly 2012* (European Geosciences Union, Vienna, Austria, 2012).
26. Gregorič, A.; Bezek, M.; Vaupotič, J. Radon as a tracer of cave ventilation and health hazard: the case of the Postojna Cave. In: Šebela, S. (ed.) *International Congress on "Scientific Research in Show Caves"* (Inštitut za raziskovanje krasa ZRC SAZU, Postojna, 2012).
27. Gregorič, A.; Džeroski, S.; Vaupotič, J. Radon as tracer in studying ventilation of karst caves and geophysical processes in the Earth's crust. In: Žagar, K.; Lenart, A.; Pečko, D. (eds.) *6th Young Researcher's Day 2012* (Jožef Stefan Institute, Ljubljana, 2012).
28. Bezek, M.; Gregorič, A.; Kávási, N.; Vaupotič, J. Diurnal and seasonal variations of concentration and size distribution of nanoaerosols (5–1100 nm) including radon decay products in the Postojna Cave, Slovenia. In: *NARE 2012, International Symposium on Natural Radiation Exposures and Low Dose Radiation Epidemiological Studies* (Hirosaki University, Hirosaki, Japan, 2012).
29. Vaupotič, J. et al. Radon in soil gas at selected sites in Hokkaido, Japan. In: *NARE 2012, International Symposium on Natural Radiation Exposures and Low Dose Radiation Epidemiological Studies* (Hirosaki University, Hirosaki, Japan, 2012).
30. Velišček, T.; Gregorič, A.; Vaupotič, J. Exposure to radon in wine cellars in different geological regions of Slovenia. In: *NARE 2012, International Symposium on Natural Radiation Exposures and Low Dose Radiation Epidemiological Studies* (Hirosaki University, Hirosaki, Japan, 2012).
31. Zupančič, M. et al. Dependence of radon concentration in outdoor air on meteorological conditions at different climate regions in Slovenia. In: *NARE 2012, International Symposium on Natural Radiation Exposures and Low Dose Radiation Epidemiological Studies* (Hirosaki University, Hirosaki, Japan, 2012).
32. Lekočevič, N. et al. Temporal and spatial variations of radon and carbon dioxide levels in soil gas at different geological basis in Slovenia. In: *NARE 2012, International Symposium on Natural Radiation Exposures and Low Dose*

Radiation Epidemiological Studies (Hirosaki University, Hirosaki, Japan, 2012).

33. Gregorič, A.; Vaupotič, J. Radon concentration and ventilation in two different passages in the Postojna Cave. In: *EGU General Assembly 2011* (European Geosciences Union, Vienna, Austria, 2011).
34. Žibret, L.; Žalohar, J.; Gregorič, A.; Vrabec, M. Kinematic and paleostress evolution of NW-SE trending Dinaric faults in Slovenia – A case for Neogene orogen-perpendicular extension in the External Dinaries. In: *EGU General Assembly 2011* (European Geosciences Union, Vienna, Austria, 2011).
35. Bezek, M.; Gregorič, A.; Džeroski, S.; Vaupotič, J. Continuous measurements of ultrafine particles at urban background site of Ljubljana. In: Trebše, P.; Petrič, M.; Lavtižar, V. (eds.) *The 11th European Meeting on Environmental Chemistry – EMEC 11* (University of Nova Gorica, Portorož, 2010).
36. Gregorič, A.; Zidanšek, A.; Vaupotič, J. Dependence of radon levels in the Postojna Cave on outdoor air temperature. In: *EGU General Assembly 2010* (European Geosciences Union, Vienna, Austria, 2010).
37. Gregorič, A.; Zmazek, B.; Vaupotič, J. Radon v termalni vodi kot pokazatelj seizmične aktivnosti. In: Kuščer, D.; Perc, B. (eds.) *4. Dan Mladih Raziskovalcev KMBO* (Jožef Stefan Institute, Ljubljana, 2010).
38. Gregorič, A.; Džeroski S.; Riggio, A.; Santulin, M.; Vaupotič, J. Anomalies in soil radon concentration caused by earthquakes in the Friuli region (Italy): application of machine learning methods. In: *2nd Symposium of the IGRS International Geo-Hazards Research Society: "scientific approach to Geo Hazard: a window to the future"* (International Geo-Hazards Research Society, Rosignano, Italy, 2010).
39. Gregorič, A. A model for prediction of radon concentration in the Postojna Cave. In: Kaluža, B.; Eleršič, K.; Pogorelc, B.; Šetina, B.; Vahčič, M. (eds.) *2. študentska konferenca Mednarodne podiplomske šole Jožefa Stefana = 2nd Jožef Stefan International Postgraduate School Students Conference* (Mednarodna podiplomska šola Jožefa Stefana, Ljubljana, 2010).
40. Vaupotič, J. et al. Radon in soil gas at the Ravne fault in NW Slovenia. In: *EGU General Assembly 2010* (European Geosciences Union, Vienna, Austria, 2010).
41. Vaupotič, J. et al. Radon mapping in Slovenia based on its levels in soil gas. In: *33rd International Geological Congress*. (International Union of Geological Sciences, Oslo, Norway, 2008).
42. Gregorič, A. et al. Measurements of particle size distribution in the size range 10-1100 nm. In: Mihailović, D. et al. (eds.) *Hot nano topics 2008: incorporating SLONANO 2008, 3 overlapping workshops on current hot subjects in nanoscience* (Jožef Stefan Institute, Portorož, 2008).

1.16 Independent scientific component part or a chapter in a monograph

43. Gregorič, A.; Zmazek, B.; Džeroski, S.; Torkar, D.; Vaupotič, J. Radon as an earthquake precursor – methods for detecting anomalies. In: D'amico, S. (ed.) *Earthquake research and analysis: statistical studies, observations and planning*. 179–196 (InTech, Rijeka, Croatia, 2011).
44. Kobal, I.; Vaupotič, J.; Gregorič, A.; Uralbekov, B. M. Comparison of approaches in Slovenia and Kazakhstan in managing exposure to radon. In: Burkitbayev, M.; Lehto, J. (eds.). *Environmental radioactivity in Central Asia*. 80–97 (Kazakh National University, Almaty, Kazakhstan, 2012).

MONOGRAPHS AND OTHER COMPLETED WORKS

2.11 Undergraduate thesis

45. Gregorič, A. *Analiza razvoja paleonapetosti v Dinarskem narivnem sistemu zahodne Slovenije (okolica Nove Gorice).* Diploma work (Faculty of Natural Sciences and Engineering, University of Ljubljana, Ljubljana, 2005).

2.13 Treatise, preliminary study, study

46. Vaupotič, J.; Gregorič, A.; Bezek, M.; Kobal, I. *Eradication of lung cancer caused by radon gas in Azerbaijan and Slovenia.* Report (Jožef Stefan Institute, Ljubljana, 2012).
47. Gregorič, A.; Bezek, M.; Vaupotič, J. *Radon levels in Kostanjevica Cave*. Report (Jožef Stefan Institute, Ljubljana, 2012).
48. Gregorič, A.; Kovačič, K.; Krištof, R.; Marušič, B.; Vaupotič, J. *Proposal for radon mitigation of a building at Visoko 6 with elevated radon concentration*. Report (Jožef Stefan Institute, Ljubljana, 2012).
49. Vaupotič, J. et al. *Inter-comparison measurements of radon in soil participated by IJS-CRn, IFJ-PAN and ARPA-FVG laboratories.* Report (Jožef Stefan Institute, Ljubljana, 2010).
50. Vaupotič, J. et al. *Radon concentrations in soil gas on the property of the Krka company in Krško.* Report (Jožef Stefan Institute, Ljubljana, 2009).
51. Vaupotič, J. et al. *Soil gas radon potential on radon prone areas*. Report (Jožef Stefan Institute, Ljubljana, 2007).
52. Vaupotič, J. et al. *Systematic survey of working and living environments in 2007*. Report (Jožef Stefan Institute, Ljubljana, 2007).
53. Vaupotič, J.; Dujmović, P.; Gregorič, A.; Kobal, I. *Additional radon survey and assessment of doses received by staff at the Kozina police station and the Sežana police station.* Report (Jožef Stefan Institute, Ljubljana, 2006).
54. Vaupotič, J.; Dujmović, P.; Žvab Rožič, P.; Gregorič, A.; Kobal, I. *Additional radon survey and assessment of doses received by staff at the Divača railway station*. Report (Jožef Stefan Institute, Ljubljana, 2006).

PERFORMED WORKS (EVENTS)

3.14 Invited lecture at foreign university

55. Vaupotič, J.; Gregorič, A.; Lekočevič, N. *How to obtain representative and reliable radon activity concentration in soil gas?* invited talk. Faculty of Engineering, Hokkaido University, Sapporo, Japan, 2011.
56. Gregorič, A.; Vaupotič, J. *Radon as tracer for cave air ventilation*: invited talk. Faculty of Engineering, Hokkaido University, Sapporo, Japan, 2011.
57. Vaupotič, J.; Gregorič, A.; Lekočevič, N.; Kobal, I. *Radon in soil gas in Slovenia*: invited talk. Graduate School of Engineering, Nagoya University, Nagoya, Japan, 2011.
58. Vaupotič, J. et al. *Radon potential on various grounds*: invited talk. The Henryk Niewodniczański Institute of Nuclear Physics, Polish Academy of Sciences, Kraków, Poland, 2008.

3.15 Unpublished conference contribution

59. Gregorič, A.; Vaupotič, J. Continuous radon monitoring in Postojna Cave. In: *Radon Center Seminar*. (Jožef Stefan Institute, Ljubljana, 2012).
60. Gregorič, A. Predstavitev poročila (primer – Visoko). In: *Radon v zgradbah: Ukrepi za znižanje koncentracije*. (Jožef Stefan Institute, Ljubljana, 2012).
61. Vaupotič, J.; Gregorič, A.; Bezek, M.; Abasova, G. Radon study in 400 Slovenian homes. In: *Radon Center Seminar*. (Jožef Stefan Institute, Ljubljana, 2012).
62. Gregorič, A.; Vaupotič, J. The role of cave ventilation in governing cave air temperature and radon levels. In: *Slovenian – Ukraine Scientific Seminar*. (Jožef Stefan Institute, Ljubljana, 2012).
63. Gregorič, A.; Vaupotič, J. Anomalies in soil radon concentration caused by earthquakes: application of machine learning methods. In: *Slovenian – Polish – Ukraine Scientific Seminar*. (Jožef Stefan Institute, Ljubljana, 2011).
64. Gregorič, A.; Vaupotič, J. Radon as a tracer for cave air ventilation. In: *Slovenian – Polish – Ukraine Scientific Seminar*. (Jožef Stefan Institute, Ljubljana, 2011).
65. Gregorič, A. Radon in geologija. In: *Radon v zgradbah: Ukrepi za znižanje koncentracije*. (Jožef Stefan Institute, Ljubljana, 2011).